

I hereby certify that this paper is being transmitted via the Office electronic filing system in accordance with 37 CFR § 1.6(a)(4).

Dated: October 6, 2014  
Electronic Signature for Ruth Lang: /Ruth Lang/

Docket No.: 146392023400

**IN THE UNITED STATES PATENT AND TRADEMARK OFFICE**

In re Patent of: Pablo Umaña *et al.*

Patent No.: 6,602,684

Issued: August 5, 2003

Application No: 09/294,584

For: GLYCOSYLATION ENGINEERING OF ANTIBODIES FOR IMPROVING ANTIBODY-DEPENDENT CELLULAR CYTOTOXICITY – Application for § 156 Patent Term Extension

Attorney Docket No: 146392023400

Assignee: Roche Glycart AG

Unit: Office of Patent Legal Administration

Mail Stop Hatch-Waxman PTE  
Commissioner for Patents  
P.O. Box 1450  
Alexandria, VA 22313-1450

RECEIVED  
OCT 14 2014  
PATENT EXTENSION  
OPLA

RECEIVED  
OCT 14 2014  
PATENT EXTENSION  
OPLA

**SUPPLEMENTAL PAPER**

In addition to the above-referenced application for patent term extension for U.S. Patent No. 6,602,684 based on the November 1, 2013 approval of GAZYVA<sup>®</sup>, Applicant concurrently submitted patent term extension applications for U.S. Patent Numbers 8,021,856 and 7,517,670. Thus, a total of three patent term extension applications were filed based upon the same regulatory review period for GAZYVA<sup>®</sup>. It is requested that the Office examine these three patent term extension applications concurrently so that Applicant can elect upon receipt of a Notice of Final Determination and Requirement of Election as to which patent to ultimately extend in accordance with 37 C.F.R. § 1.785.

11/14/2014 CKHLOK 00000033 031952 09294584  
01 FC:1457 1120.00 DA

pa-1658389

**Mylan v. Genentech**  
**IPR2016-00710**  
**Merck Ex. 1129, Pg. 1**

U.S. Patent No. 6,602,684

Docket No.: 146392023400

Applicant believes that no fee is due. If there is an associated fee for filing a Supplemental Paper, the Director is hereby authorized to charge the fee to our Deposit Account No. 03-1952, referencing 146392023400.

Date: October 6, 2014

Respectfully submitted,

/Shannon Reaney/

Shannon Reaney  
Registration No.: 52,285  
MORRISON & FOERSTER LLP  
755 Page Mill Road  
Palo Alto, California 94304-1018  
Phone: 650/813-5744  
Facsimile: 650/494-0792

For:

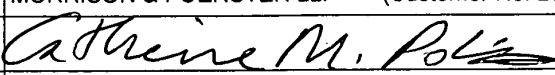
Catherine M. Polizzi  
Registration No.: 40,130  
MORRISON & FOERSTER LLP  
755 Page Mill Road  
Palo Alto, California 94304-1018  
Phone: 650/813-5651  
Facsimile: 650/494-0792


Under the Paperwork Reduction Act of 1995, no persons are required to respond to a collection of information unless it displays a valid OMB control number.

<h1>TRANSMITTAL FORM</h1> <p><i>(to be used for all correspondence after initial filing)</i></p>	Application Number	Patent#: 6,602,684	
	Filing Date	Issued: August 5, 2003	
	First Named Inventor	Pablo UMANA	
	Art Unit	1636	
	Examiner Name	W. Sandals	
Total Number of Pages in This Submission	800	Attorney Docket Number	146392023400

ENCLOSURES (Check all that apply)				
<input checked="" type="checkbox"/> Fee Transmittal Form + 4 copies (5 pages) <input type="checkbox"/> Fee Attached <input type="checkbox"/> Amendment/Reply <input type="checkbox"/> After Final <input type="checkbox"/> Affidavits/declaration(s) <input type="checkbox"/> Extension of Time Request <input type="checkbox"/> Express Abandonment Request <input type="checkbox"/> Information Disclosure Statement <input type="checkbox"/> Certified Copy of Priority Document(s) <input type="checkbox"/> Reply to Missing Parts/Incomplete Application <input type="checkbox"/> Reply to Missing Parts under 37 CFR 1.52 or 1.53	<input type="checkbox"/> Drawing(s) <input type="checkbox"/> Licensing-related Papers <input type="checkbox"/> Petition <input type="checkbox"/> Petition to Convert to a Provisional Application <input type="checkbox"/> Power of Attorney, Revocation Change of Correspondence Address <input type="checkbox"/> Terminal Disclaimer <input type="checkbox"/> Request for Refund <input type="checkbox"/> CD, Number of CD(s) _____ <input type="checkbox"/> Landscape Table on CD	<input type="checkbox"/> After Allowance Communication to TC <input type="checkbox"/> Appeal Communication to Board of Appeals and Interferences <input type="checkbox"/> Appeal Communication to TC (Appeal Notice, Brief, Reply Brief) <input type="checkbox"/> Proprietary Information <input type="checkbox"/> Status Letter <input checked="" type="checkbox"/> Other Enclosure(s) (please identify below): See Remarks		
<table border="1" style="width: 100%;"> <tr> <td style="width: 30%;">Remarks</td> <td>                     Application for Extension of Patent Term under 35 U.S.C. § 156 + 4 copies (75 pages)                      Attachment A + 4 copies (15 pages)                      Attachment B + 4 copies (80 pages)                      Attachment C + 4 copies (40 pages)                      Attachment D + 4 copies (210 pages)                      Attachment E + 4 copies (10 pages)                      Attachment F + 4 copies (20 pages)                      Attachment G + 4 copies (15 pages)                      Attachment H + 4 copies (25 pages)                      Attachment I + 4 copies (10 pages)                      Attachment J + 4 copies (65 pages)                      Attachment K + 4 copies (60 pages)                      Attachment L + 4 copies (10 pages)                      Attachment M + 4 copies (10 pages)                      Attachment N + 4 copies (30 pages)                      Attachment O + 4 copies (60 pages)                      Attachment P + 4 copies (10 pages)                      Attachment Q + 4 copies (45 pages)                      Return Receipt Post Card                 </td> </tr> </table>			Remarks	Application for Extension of Patent Term under 35 U.S.C. § 156 + 4 copies (75 pages) Attachment A + 4 copies (15 pages) Attachment B + 4 copies (80 pages) Attachment C + 4 copies (40 pages) Attachment D + 4 copies (210 pages) Attachment E + 4 copies (10 pages) Attachment F + 4 copies (20 pages) Attachment G + 4 copies (15 pages) Attachment H + 4 copies (25 pages) Attachment I + 4 copies (10 pages) Attachment J + 4 copies (65 pages) Attachment K + 4 copies (60 pages) Attachment L + 4 copies (10 pages) Attachment M + 4 copies (10 pages) Attachment N + 4 copies (30 pages) Attachment O + 4 copies (60 pages) Attachment P + 4 copies (10 pages) Attachment Q + 4 copies (45 pages) Return Receipt Post Card
Remarks	Application for Extension of Patent Term under 35 U.S.C. § 156 + 4 copies (75 pages) Attachment A + 4 copies (15 pages) Attachment B + 4 copies (80 pages) Attachment C + 4 copies (40 pages) Attachment D + 4 copies (210 pages) Attachment E + 4 copies (10 pages) Attachment F + 4 copies (20 pages) Attachment G + 4 copies (15 pages) Attachment H + 4 copies (25 pages) Attachment I + 4 copies (10 pages) Attachment J + 4 copies (65 pages) Attachment K + 4 copies (60 pages) Attachment L + 4 copies (10 pages) Attachment M + 4 copies (10 pages) Attachment N + 4 copies (30 pages) Attachment O + 4 copies (60 pages) Attachment P + 4 copies (10 pages) Attachment Q + 4 copies (45 pages) Return Receipt Post Card			

**RECEIVED**  
**DEC 17 2013**  
**PATENT EXTENSION**  
**OPLA**

SIGNATURE OF APPLICANT, ATTORNEY, OR AGENT			
Firm Name	MORRISON & FOERSTER LLP (Customer No. 25226)		
Signature			
Printed name	Catherine M. Polizzi		
Date	December 17, 2013	Reg. No.	40,130

I hereby certify that this paper is being deposited with the U.S. Postal Service as Express Mail, Airbill No. EM 021716856 US, on the date shown below in an envelope addressed to: Commissioner for Patents, P.O. Box 1450, Alexandria, VA 22313-1450.	
Dated: December 17, 2013	Signature:  (Shannon Reaney)

FEE TRANSMITTAL	Complete if known		
	Application Number	Patent #: 6,602,684	
	Filing Date	Issued: August 5, 2003	
	First Named Inventor	Pablo UMANA	
	Examiner Name	W. Sandals	
	Art Unit	1636	
<input type="checkbox"/> Applicant asserts small entity status. See 37 CFR 1.27 <input type="checkbox"/> Applicant certifies micro entity status. See 37 CFR 1.29. Form PTO/SB/15A or B or equivalent must either be enclosed or have been submitted previously		Practitioner Docket No.	146392023400
TOTAL AMOUNT OF PAYMENT		(\$)	1,120.00

**METHOD OF PAYMENT** (check all that apply)

Check   
  Credit Card   
  Money Order   
  None   
  Other (please identify): \_\_\_\_\_

Deposit Account   
 Deposit Account Number: 03-1952   
 Deposit Account Name: Morrison & Foerster LLP

For the above-identified deposit account, the Director is hereby authorized to: (check all that apply)

Charge fee(s) indicated below   
  Charge fee(s) indicated below, except for the filing fee  
 Charge any additional fee(s) or underpayment of fee(s) under 37 CFR 1.16 and 1.17   
  Credit any overpayment of fee(s)

**WARNING:** Information on this form may become public. Credit card information should not be included on this form. Provide credit card information and authorization on PTO-2038.

**FEE CALCULATION**

**1. BASIC FILING, SEARCH, AND EXAMINATION FEES (U = undiscounted fee; S = small entity fee; M = micro entity fee)**

Application Type	FILING FEES			SEARCH FEES			EXAMINATION FEES			Fees Paid (\$)
	U (\$)	S (\$)	M (\$)	U (\$)	S (\$)	M (\$)	U (\$)	S (\$)	M (\$)	
Utility	280	140*	70	600	300	150	720	360	180	
Design	180	90	45	120	60	30	460	230	115	
Plant	180	90	45	380	190	95	580	290	145	
Reissue	280	140	70	600	300	150	2,160	1,080	540	
Provisional	260	130	65	0	0	0	0	0	0	

\* The \$140 small entity status filing fee for a utility application is further reduced to \$70 for a small entity status applicant who files the application via EFS-Web.

**2. EXCESS CLAIM FEES**

Fee Description	Undiscounted Fee (\$)	Small Entity Fee (\$)	Micro Entity Fee (\$)
Each claim over 20 (including Reissues)	80	40	20
Each independent claim over 3 (including Reissues)	420	210	105
Multiple dependent claims	780	390	195

**Total Claims**      **Extra Claims**      **Fee (\$)**      **Fee Paid (\$)**      **Multiple Dependent Claims**  
 \_\_\_\_\_ - 20 or HP = \_\_\_\_\_ x \_\_\_\_\_ = \_\_\_\_\_      **Fee (\$)**      **Fee Paid (\$)**  
 HP = highest number of total claims paid for, if greater than 20.

**Indep. Claims**      **Extra Claims**      **Fee (\$)**      **Fee Paid (\$)**  
 \_\_\_\_\_ - 3 or HP = \_\_\_\_\_ x \_\_\_\_\_ = \_\_\_\_\_  
 HP = highest number of independent claims paid for, if greater than 3.

**3. APPLICATION SIZE FEE**

If the specification and drawings exceed 100 sheets of paper (excluding electronically filed sequence or computer listings under 37 CFR 1.52(e)), the application size fee due is \$400 (\$200 for small entity) (\$100 for micro entity) for each additional 50 sheets or fraction thereof. See 35 U.S.C. 41(a)(1)(G) and 37 CFR 1.16(s).

**Total Sheets**      **Extra Sheets**      **Number of each additional 50 or fraction thereof**      **Fee (\$)**      **Fee Paid (\$)**  
 \_\_\_\_\_ - 100 = \_\_\_\_\_ /50 = \_\_\_\_\_ (round up to a whole number) x \_\_\_\_\_ = \_\_\_\_\_

**4. OTHER FEE(S)**

Non-English specification, \$130 fee (no small or micro entity discount) \_\_\_\_\_

Non-electronic filing fee under 37 CFR 1.16(t) for a utility application, \$400 fee (\$200 small or micro entity) \_\_\_\_\_

Other (e.g., late filing surcharge): 1457 Extension of term of patent      1,120.00

**SUBMITTED BY**

Signature		Registration No. (Attorney/Agent)	40,130	Telephone	(650) 813-5651
Name (Print/Type)	Catherine M. Polizzi	Date	December 17, 2013		

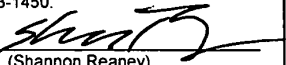
I hereby certify that this paper is being deposited with the U.S. Postal Service as Express Mail, Airbill No. EM 021716856 US, on the date shown below in an envelope addressed to:  
 Commissioner for Patents, P.O. Box 1450, Alexandria, VA 22313-1450.

Dated: December 17, 2013      Signature: (Shannon Reaney)

I hereby certify that this paper is being deposited with the U.S. Postal Service as Express Mail, Airbill No. EM 021716856 US, on the date shown below in an envelope addressed to: Mail Stop Hatch-Waxman PTE, Commissioner for Patents, P.O. Box 1450, Alexandria, VA 22313-1450.

Dated: December 17, 2013

Signature:

  
(Shannon Reaney)

Docket No.: 146392023400  
Client Ref. No.: 23437-US1

**IN THE UNITED STATES PATENT AND TRADEMARK OFFICE**

In re Patent of: Pablo Umaña *et al.*

Patent No.: 6,602,684

Issued: August 5, 2003

Application No: 09/294,584

For: GLYCOSYLATION ENGINEERING OF  
ANTIBODIES FOR IMPROVING ANTIBODY-  
DEPENDENT CELLULAR CYTOTOXICITY –  
Application for § 156 Patent Term Extension

Mail Stop Hatch-Waxman PTE  
Commissioner for Patents  
P.O. Box 1450  
Alexandria, VA 22313-1450

Attorney Docket No: 146392023400

Assignee: Roche Glycart AG

Unit: Office of Patent Legal  
Administration

**RECEIVED**  
**DEC 17 2013**  
**PATENT EXTENSION**  
**OPLA**

**APPLICATION FOR EXTENSION OF PATENT TERM UNDER 35 U.S.C. § 156**

Dear Madam:

Applicant, Genentech, Inc., hereby submits this application for extension of the term of United States Letters Patent No. 6,602,684 (the '684 Patent) under 35 U.S.C. § 156 by providing the following information in accordance with the requirements specified in 37 C.F.R. § 1.740.

A statement executed by authorized representatives of owner, Roche Glycart AG, attesting that exclusive licensee, Genentech, Inc., is authorized to act as agent for Roche Glycart AG in the submission of a patent term extension application under 35 U.S.C. § 156 for the '684 Patent is included as Attachment A.

Applicant represents that Roche Glycart AG is the assignee of the entire right, title and interest in and to United States Letters Patent No. 6,602,684 granted to Pablo Umaña, Joël Jean-Mairet, and James E. Bailey (Pablo Umaña *et al.*), by virtue of the law of Switzerland or an assignment of such patent from Pablo Umaña *et al.* to GlycArt Biotechnology GmbH, recorded February 9, 2001, at Reel 011528, Frame 0431, by virtue of company name/entity change to GlycArt Biotechnology AG, recorded May 14, 2003, at Reel 014065, Frame 0729, by virtue of an assignment from Pablo Umaña *et al.* to GlycArt Biotechnology AG, recorded April 19, 2004, at Reel 015232, Frame 0164,<sup>1</sup> and by virtue of company name change to Roche Glycart AG, recorded September 09, 2011, at Reel 026883, Frame 0831.

**1. Identification of the Approved Product [§ 1.740(a)(1)]**

The name of the approved product is GAZYVA™. The name of the active ingredient of GAZYVA™ is obinutuzumab. Obinutuzumab has also been referred to as GA101. See Klein *et al.*, *mAbs*, 2013, 5(1):22-33, abstract, provided as Attachment J. Applicant uses the nomenclature obinutuzumab, which is the same nomenclature used in the product label for GAZYVA™. Obinutuzumab is a type II, glycoengineered, humanized anti-CD20 cytolytic antibody. See Description section (page 12, section 11) and Highlights of Prescribing Information (page 1) of Obinutuzumab Product Label, provided as Attachment B and Klein *et al.*, at page 29, right-hand column, second full paragraph (Attachment J).

**2. Federal Statute Governing Regulatory Approval of the Approved Product [§ 1.740(a)(2)]**

The approved product was subject to regulatory review under, *inter alia*, the Public Health Service Act (42 U.S.C. § 201 *et seq.*) and the Federal Food, Drug and Cosmetic Act (21 U.S.C. § 355 *et seq.*).

**3. Date of Approval for Commercial Marketing [§ 1.740(a)(3)]**

GAZYVA™ was approved for commercial marketing or use under § 351 of the Public Health Service Act on **November 1, 2013**. See Obinutuzumab BLA Approval Letter, provided as Attachment C.

**4. Identification of Active Ingredient and Certifications Related to Commercial Marketing of Approved Product [§ 1.740(a)(4)]**

- (a) The name of the active ingredient of GAZYVA™ is obinutuzumab. Obinutuzumab is a type II, glycoengineered, humanized anti-CD20 cytolytic antibody. See Description section (page 12, section 11) and Highlights of Prescribing Information (page 1) of Obinutuzumab Product Label, provided as

---

<sup>1</sup> The assignment recorded at the noted location in the Office's records was originally recorded on August 18, 2003, at Reel 014405, Frame 0440. A duplicate copy was recorded at the noted date and location to correct the name of one of the Assignors in the Office's records.

Attachment B and Klein *et al.*, at page 29, right-hand column, second full paragraph (Attachment J).

- (b) Applicant certifies that obinutuzumab had not been approved for commercial marketing or use under the Federal Food, Drug and Cosmetic Act, the Public Health Service Act or the Virus-Serum-Toxin Act prior to the approval granted on November 1, 2013, to the present Applicant.<sup>2</sup>
- (c) Obinutuzumab has been approved, in combination with chlorambucil, for the treatment of patients with previously untreated chronic lymphocytic leukemia (CLL). *See* Indications and Usage section (page 2, section 1) of Obinutuzumab Product Label, provided as Attachment B.
- (d) Obinutuzumab was approved for commercial marketing pursuant to § 351 of the Public Health Service Act (42 U.S.C. § 262) under Genentech, Inc.'s existing Department of Health and Human Services (DHHS) U.S. License No. 1048. *See* Obinutuzumab BLA Approval Letter, provided as Attachment C.

**5. Statement Regarding Timeliness of Submission of Patent Term Extension Request [§ 1.740(a)(5)]**

Applicant certifies that this application for patent term extension is being timely submitted within the sixty (60) day period permitted for submission specified in 35 U.S.C. § 156(d)(1) and 37 C.F.R. § 1.720(f). The last date on which this application can be submitted is December 30, 2013.

**6. Complete Identification of the Patent for Which Extension Is Being Sought [§ 1.740(a)(6)]**

The complete identification of the patent for which an extension is being sought is as follows:

- (a) Names of the inventors: Pablo Umaña, Joël Jean-Mairet, and James E. Bailey
- (b) Patent Number: 6,602,684 (“the ‘684 Patent”)
- (c) Date of Issue: August 5, 2003
- (d) Date of Expiration: April 20, 2019

---

<sup>2</sup> The permission for the commercial marketing or use of obinutuzumab granted on November 1, 2013, to the present Applicant is also believed to be the first permitted commercial marketing or use of a product manufactured under the process claimed in the ‘684 patent.

**7. Copy of the Patent for Which an Extension Is Being Sought [§ 1.740(a)(7)]**

A copy of the '684 Patent is provided as Attachment D to the present application.

**8. Copies of Disclaimers, Certificates of Correction, Receipt of Maintenance Fee Payment, or Reexamination Certificate [§ 1.740(a)(8)]**

- (a) The '684 Patent is not subject to a Terminal Disclaimer.
- (b) No Certificate of Correction has issued with respect to the '684 Patent.
- (c) The '684 Patent issued on August 5, 2003. The first and second maintenance fees were paid on December 18, 2006 and December 28, 2010, respectively; the window for paying the third maintenance fee opens August 5, 2014. *See* Attachment E. Thus, no maintenance fee is currently due for the '684 Patent.
- (d) The '684 Patent has not been the subject of a reexamination proceeding and, thus, no re-examination certificate has been issued.

**9. Statement Regarding Patent Claims Relative to Approved Product [§ 1.740(a)(9)]**

*The statements below are made solely to comply with the requirements of 37 C.F.R. § 1.740(a)(9). Applicant notes that, as the M.P.E.P. acknowledges, § 1.740(a)(9) does not require an applicant to show whether or how the listed claims would be infringed, and that this question cannot be answered without specific knowledge concerning acts performed by third parties. As such, these comments are not an assertion or an admission of Applicant as to the scope of the listed claims, or whether or how any of the listed claims would be infringed, literally or under the doctrine of equivalents, by the manufacture, use, sale, offer for sale or the importation of any product.*

- (a) At least claims 1, 2, 3,<sup>3</sup> 5, 6, 7, 8, and 9 claim the active ingredient in the approved product or the approved product or a method that may be used to manufacture or use that ingredient or product.
- (b) Pursuant to M.P.E.P. § 2753 and 37 C.F.R. § 1.740(a)(9), the following explanation is provided which shows how at least one of the above-listed claims of the '684 Patent claims a method of manufacturing the approved product.

*(1) Description of the approved product*

The name of the approved product is GAZYVA™. The name of the active ingredient of GAZYVA™ is obinutuzumab. Obinutuzumab is a type II, glycoengineered, humanized anti-CD20 cytolytic antibody. *See* Description

---

<sup>3</sup> The approved product produced by the claimed method includes a mixture of obinutuzumab and fragments thereof.



section (page 12, section 11) and Highlights of Prescribing Information (page 1) of Obinutuzumab Product Label, provided as Attachment B and Klein *et al.*, at page 29, right-hand column, second full paragraph (Attachment J).

(2) *Explanation regarding claim 1 of the '684 Patent relative to obinutuzumab*

Claim 1 of the '684 Patent reads:

A method for producing a polypeptide having increased Fc-mediated cellular cytotoxicity in a host cell, comprising:

(a) culturing a host cell engineered to express at least one nucleic acid encoding  $\beta(1,4)$  - N - acetylglucosaminyltransferase III (GnT III) under conditions which permit the production of a polypeptide selected from the group consisting of a whole antibody molecule, an antibody fragment, and a fusion protein that includes the Fc region of an immunoglobulin, wherein said GnT III is expressed in an amount sufficient to modify the oligosaccharides in the Fc region of said polypeptide produced by said host cell and wherein said polypeptide has increased Fc-mediated cellular cytotoxicity as a result of said modification; and

(b) isolating said polypeptide having increased Fc-mediated cellular cytotoxicity.

Obinutuzumab is a humanized monoclonal antibody (which is a polypeptide) based on a human IgG<sub>1</sub>( $\kappa$ ) framework. *See* Obinutuzumab BLA, Section 3.2.S.1.2 Structure, provided as Attachment I. Thus, obinutuzumab is a polypeptide selected from the group consisting of a whole antibody molecule, an antibody fragment, and a fusion protein that includes the Fc region of an immunoglobulin.

Obinutuzumab is produced in CHO cells in suspension culture. *See* Description section (page 12, section 11) and Highlights of Prescribing Information (page 1) of Obinutuzumab Product Label, provided as Attachment B; Mössner *et al.*, *Blood*, 2010, 115:4393-4402, provided as Attachment K, at page 4396, right-hand column, second full paragraph. The CHO cells are engineered to overexpress  $\beta$ -1,4-N-acetyl-glucosaminyltransferase III (GnT III) by co-transfecting the cells with the gene (a nucleic acid) encoding GnT III. *See* Mössner *et al.*, provided as Attachment K, at page 4394, left-hand column, third paragraph and page 4396, right-hand column, second full paragraph; Obinutuzumab BLA, Section 3.2.S.2.3 Source, History, and Generation, provided as Attachment L. Obinutuzumab produced by these engineered CHO host cells is harvested, filtered, and purified. *See* Mössner *et al.*, provided as Attachment K, at page 4394, left-hand column, third paragraph; Obinutuzumab BLA, Section 3.2.S.2.2 Cell Culture and Harvest, provided as Attachment M. Thus, obinutuzumab is produced by (a) culturing a host cell engineered to express at least one nucleic acid encoding  $\beta$ -(1,4)-N-acetylglucosaminyltransferase III (GnT III) under conditions which permit the

production of the polypeptide (obinutuzumab) and (b) isolating the polypeptide (obinutuzumab).

Overexpression of the GnT III and Golgi  $\alpha$ -mannosidase II (Man-II) in the CHO cells producing obinutuzumab leads to accumulation of antibody glycoforms containing bisected, nonfucosylated oligosaccharides attached to an asparagine<sup>4</sup> in the Fc region. See Mössner *et al.*, provided as Attachment K, at page 4396, right-hand column, second full paragraph (citing Ferrara *et al.*, *J. Biol. Chem.*, 2006, 281(8):5032-5036, provided as Attachment N). GnT III overexpression alone causes the modification of oligosaccharides in the Fc regions of antibodies. See Ferrara *et al.*, *J. Biol. Chem.*, provided as Attachment N, at page 5033, right-hand column, through page 5034, left-hand column, and Figure 1; Ferrara *et al.*, *Biotechnology and Bioengineering*, 2006, 93(5):851-61, provided as Attachment O, abstract and page 854, left-hand column, third paragraph. Thus, obinutuzumab is produced in a host cell engineered to express GnT III in an amount sufficient to modify the oligosaccharides in the Fc region of the polypeptide (obinutuzumab).

The addition to obinutuzumab of a bisecting N-acetylglucosamine (bGlcNAc) (an oligosaccharide (see Ferrara *et al.*, *J. Biol. Chem.*, provided as Attachment N, at page 5033, Figure 1)) by GnT III overexpression leads to enhanced antibody dependent cellular cytotoxicity (ADCC) bioactivity. See Obinutuzumab BLA, Section 3.4.2, provided as Attachment P; Mössner *et al.*, (Attachment K), at page 4393, right-hand column, first paragraph. ADCC is Fc-mediated. See Mössner *et al.*, (Attachment K), at page 4393, right-hand column, first paragraph. Thus, obinutuzumab has increased Fc-mediated cellular cytotoxicity as a result of the modification of the oligosaccharides in the Fc region.

Thus, the limitations of claim 1 are met.

---

<sup>4</sup> The cited reference refers to this asparagine residue as asparagine (N) 297. This same residue in obinutuzumab is sometimes referred to as Asn (asparagine) 299. The difference in numbering reflects different numbering conventions (Kabat vs. sequential numbering) See Nagelkerken *et al.*, *J Immunol*, 2004; 173:993-999 (provided as Attachment Q, at page 994, left-hand column, second full paragraph, noting "Kabat nomenclature" (sometimes referred to as the EU numbering system) is being used to number asparagine residue N297, referencing, Kabat, E.A., *et al.* (1991) *Sequences of Proteins of Immunological Interest*, 3rd Ed., Vol. 1, National Institutes of Health.

**10. Relevant Dates Under 35 U.S.C. § 156 for Determination of Applicable Regulatory Review Period [§ 1.740(a)(10)]**

(a) *Patent Issue Date*

The '684 Patent was issued on August 5, 2003.

(b) *IND Effective Date [35 U.S.C. § 156(g)(1)(B)(i); 37 C.F.R. § 1.740(a)(10)(i)(A)]*

The date that an exemption under § 505(i) of the Federal Food, Drug and Cosmetic Act became effective (*i.e.*, the date that an investigational new drug application (“IND”) became effective) for obinutuzumab was March 11, 2009.<sup>5</sup> The IND was assigned number 104405. A copy of the letter from FDA acknowledging receipt of the IND and reflecting the IND number and a February 9, 2009 receipt date is attached as Attachment H.

(c) *BLA Submission Date [35 U.S.C. § 156(g)(1)(B)(i); 37 C.F.R. § 1.740(a)(10)(i)(B)]*

The BLA was submitted by Genentech, Inc., to FDA on April 19, 2013; however, FDA listed April 22, 2013 as the Date of Application (*see* BLA Acknowledgment Letter provided in Attachment F). April 22, 2013 is used herein as the BLA Submission Date. The BLA was assigned number 125486. A copy of the letter from FDA acknowledging receipt of the BLA and reflecting the BLA Application Date is provided in Attachment F.

(d) *BLA Issue Date [35 U.S.C. § 156(g)(1)(B)(ii); 37 C.F.R. § 1.740(a)(10)(i)(C)]*

FDA approved BLA 125486, authorizing the marketing of obinutuzumab, on November 1, 2013. Obinutuzumab was approved under Department of Health and Human Services (DHHS) U.S. License No. 1048. A copy of the Obinutuzumab BLA Approval Letter from FDA is provided as Attachment C.

---

<sup>5</sup> 21 C.F.R. § 312.40(b)(1). The IND was submitted to FDA on February 6, 2009 and was received by FDA on February 9, 2009. *See* Attachment H. The IND became effective on March 11, 2009, 30 days after receipt of the IND by FDA.

**11. Summary of Significant Events During Regulatory Review Period [§ 1.740(a)(11)]**

Pursuant to 37 C.F.R. § 1.740(a)(11), the following provides a brief description of the activities of Genentech, Inc., before FDA in relation to the regulatory review of obinutuzumab. The brief description lists significant events that occurred during the regulatory review period for the approved product. In several instances, communications to or from FDA are referenced. Pursuant to 37 C.F.R. § 1.740(a)(11), 21 C.F.R. § 60.20(a), and M.P.E.P. § 2753, copies of all such communications are not provided in this application, but can be obtained from records maintained by FDA.

- On February 6, 2009, Genentech, Inc., submitted to FDA an Investigational New Drug (IND) application for anti-CD20 humanized monoclonal antibody GA101 (obinutuzumab). FDA assigned the IND application number 104405. On March 11, 2009, FDA informed Genentech that BB-IND 104405 is approved and clinical trials may proceed. This IND included protocol BO21003 Version C.
- On July 7, 2009, Genentech, Inc., and FDA participated in a Type B- End of Phase II Meeting to discuss protocol BO21004/CLL11.
- On September 23, 2009, Genentech, Inc., submitted new protocol BO21004/CLL11, which formed the basis of approval for obinutuzumab in CLL.
- On November 3, 2009, Genentech, Inc., and FDA participated in a Type B End of Phase II Teleconference to discuss protocol GAO4753g.
- On September 17, 2010, Genentech, Inc., submitted new protocol GAO4779g.
- On November 15, 2010, Genentech, Inc., and FDA participated in a Type B Teleconference to discuss Protocols BO21005 and BO21223.
- On January 20, 2011, Genentech, Inc., submitted new protocol BO21005.
- On January 27, 2011, Genentech, Inc., submitted new protocol BO21223.
- On February 25, 2011, Genentech, Inc., submitted new protocol GAO4915g.
- On April 18, 2011, Genentech, Inc., submitted new protocol GAO4768g.
- On June 8, 2012, Genentech, Inc., and FDA participated in a Type C Meeting to discuss the acceptability of the proposed Statistical Analysis Plan for Protocol BO21004.
- On February 22, 2013, Genentech, Inc., and FDA participated in a Type B Pre-BLA meeting.
- On April 19, 2013, Genentech, Inc., submitted a BLA for obinutuzumab in combination with chlorambucil for the treatment of patients with previously

Patent No.: 6,602,684

Docket No.: 146392023400  
Client Ref. No.: 23437-US1

untreated chronic lymphocytic leukemia (CLL), which was given an April 22, 2013 Application Date by FDA. *See* Attachment F.

- On April 25, 2013, Genentech, Inc., submitted expanded access protocol ML28979.
- On May 2, 2013, FDA acknowledged receipt of the BLA for obinutuzumab via a communication mailed to Genentech, Inc. The letter indicated that FDA had assigned the Submission Tracking Number (STN) of BLA 125486/0 to the BLA. *See* Attachment F.
- On October 15, 2013, Genentech, Inc., and FDA participated in a Type B Pre-sBLA Meeting.
- On November 1, 2013, FDA approved BLA 125486/0, issuing marketing authorization for obinutuzumab. *See* Attachment C.

**12. Statement Concerning Eligibility for and Duration of Extension Sought Under 35 U.S.C. § 156 [37 C.F.R. § 1.740(a)(12)]**

- (a) In the opinion of the Applicant, the '684 Patent is eligible for an extension under § 156 because:
- (i) one or more claims of the '684 Patent claim the approved product or a method of manufacturing or using the approved product (35 U.S.C. § 156(a));
  - (ii) the '684 Patent has not expired before submission of this application (35 U.S.C. § 156(a)(1));
  - (iii) the term of the '684 Patent has not been previously extended on the basis of § 156 (35 U.S.C. § 156(a)(2));
  - (iv) the application for extension is submitted by an owner of record or an agent authorized to act on behalf of the owner of record in accordance with the requirements of paragraphs (1) through (4) of 35 U.S.C. § 156(d) and the rules of the Patent and Trademark Office (35 U.S.C. § 156(a)(3));
  - (v) the approved product, GAZYVA™, has been subject to a regulatory review period before its commercial marketing or use (35 U.S.C. § 156(a)(4));
  - (vi) the commercial marketing or use of the approved product, GAZYVA™, after the regulatory review period is the first permitted commercial marketing or use of the product under the provisions under the Public Health Service Act, Section 351, under which such regulatory review occurred (35 U.S.C. § 156(a)(5)(A));
  - (vii) no other patent has been extended pursuant to § 156 on the basis of the regulatory review process associated with the approved product (35 U.S.C. § 156(c)(4));
  - (viii) the applicant for marketing approval exercised due diligence within the meaning of § 156(d)(3) during the period of regulatory review;
  - (ix) the present application is being submitted within the 60-day period following the approval date of the approved product, pursuant to § 156(d); and
  - (x) this application otherwise complies with all requirements of 35 U.S.C. § 156 and applicable rules and procedures.

- (b) The period by which the term of the '684 Patent is requested by Applicant to be extended is **946 days** (35 U.S.C. § 156(c)).
- (c) The requested period of extension of term for the '684 Patent corresponds to the regulatory review period that is eligible for extension pursuant to § 156, based on the facts and circumstances of the regulatory review associated with the approved product and the issuance of the '684 Patent. The period was determined as follows.
  - (i) The relevant dates for calculating the regulatory review period, based on the events discussed in the section above, are the following:

Exemption under FDCA § 505(i) became effective	March 11, 2009
Patent was granted	August 5, 2003
Biologics License Application (BLA) under PHSA § 351 was submitted	April 22, 2013
BLA was approved	November 1, 2013
  - (ii) The '684 Patent was granted prior to the start date of the period specified in § 156(g)(1)(B)(i) (the period of 1504 days calculated from the date of the grant of the exemption under § 505(i) of the FDCA (March 11, 2009) until the date of submission of the BLA (April 22, 2013)). Pursuant to § 156(c), the calculated regulatory review period therefore includes a component of time between the date of the grant of the exemption under § 505(i) of the FDCA (March 11, 2009) and the BLA submission date (April 22, 2013) (1/2 of 1504 days or 752 days).
  - (iii) The '684 Patent was granted prior to the start of the period specified in §§ 156(g)(1)(B)(ii) (the period from the date of submission of the BLA until the date of BLA approval). The number of days which the applicant did not act with due diligence is zero (0). The regulatory review period under § 156(c) therefore includes a component of time between when the BLA was submitted and when the BLA was approved (194 days).
  - (iv) The period determined according to §§ 156(c) and (g)(1) for the approved product is 946 days.
  - (v) The '684 Patent will expire on April 20, 2019.
  - (vi) The date of approval of the approved product is November 1, 2013.

- (vii) The date that is fourteen years from the date of approval of the approved product is November 1, 2027.
- (viii) The date that is five years from the expiration date of the '684 Patent is April 20, 2024.
- (ix) The date that is provided by adding the number of days determined according to §§ 156(c) and (g)(1) for the approved product (946) to the expiration date of the '684 Patent is November 21, 2021.
- (x) The date that is fourteen years from the date of approval of the approved product (November 1, 2027) is later than the date that is provided by adding the number of days determined according to §§ 156(c) and (g)(1) for the approved product to the expiration date of the '684 Patent (November 21, 2021). As such, the period by which the patent may be extended is not limited by the fourteen-year rule of §156(c)(3).
- (xi) The date that is five years from the expiration date of the '684 Patent (April 20, 2024) is later than the date that is provided by adding the number of days determined according to §§ 156(c) and (g)(1) for the approved product to the expiration date of the '684 Patent (November 21, 2021). As such, the period by which the patent may be extended is not limited by the five-year rule of §156(g)(6)(a).
- (xii) The '684 Patent issued after the effective date of Public Law No. 98-417. As such, the two- or three-year limit of 35 U.S.C. § 156(g)(6)(C) does not apply.

**13. Statement Pursuant to 37 C.F.R. § 1.740(a)(13)**

Pursuant to 37 C.F.R. § 1.740(a)(13), Applicant acknowledges its duty to disclose to the Director of the PTO and to the Secretary of Health and Human Services any information which is material to the determination of entitlement to the extension sought, particularly as that duty is defined in 37 C.F.R. § 1.765.

**14. Applicable Fee [§ 1.740(a)(14)]**

Payment of the fee prescribed in 37 C.F.R. § 1.20(j) for a patent term extension application under 35 U.S.C. § 156 is authorized to be charged against deposit account no. 03-1952 referencing docket number 146392023400. The undersigned also authorizes any additional required fees to be deducted from, or any overpayments to be credited to, deposit account no. 03-1952.



Patent No.: 6,602,684

Docket No.: 146392023400  
Client Ref. No.: 23437-US1

**15. Name and Address for Correspondence [§ 1.740(a)(15)]**

Please direct all inquiries, questions, and communications regarding this application for term extension to:

Catherine M. Polizzi  
Registration No.: 40,130  
MORRISON & FOERSTER LLP  
755 Page Mill Road  
Palo Alto, California 94304-1018  
Phone: 650/813-5651  
Facsimile: 650/494-0792

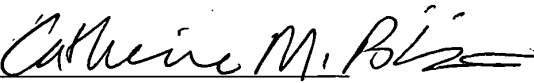
The correspondence address for U.S. Patent No. 6,602,684 is unchanged for all other purposes. Powers of Attorney granted to the Practitioners associated with Customer Number 25226 by Genentech, Inc. (*see* Attachment G) and Roche Glycart AG (*see* Attachment A), for purposes of submission of this application for term extension are provided.

Patent No.: 6,602,684

Docket No.: 146392023400  
Client Ref. No.: 23437-US1

Two additional copies of this application are enclosed, in compliance with 37 C.F.R. § 1.740(b). Applicant also provides herewith two further copies of the application for the convenience of the Office, pursuant to M.P.E.P. § 2753.

Sincerely,

By:   
Catherine M. Polizzi  
Registration No.: 40,130  
MORRISON & FOERSTER LLP  
755 Page Mill Road  
Palo Alto, California 94304-1018  
Phone: 650/813-5651  
Facsimile: 650/494-0792

Dated: December 17, 2013

### INDEX OF ATTACHMENTS

- Attachment A: Statement by Roche Glycart AG authorizing Genentech, Inc., to act as agent for Roche Glycart AG in the submission of a patent term extension application under 35 U.S.C. § 156 for the '684 Patent and conferring Power of Attorney to practitioners for this purpose
- Attachment B: Obinutuzumab Product Label
- Attachment C: Obinutuzumab Biologics License Application (BLA) Approval
- Attachment D: U.S. Patent No. 6,602,684
- Attachment E: Evidence of Maintenance Fee Schedule for U.S. Patent No. 6,602,684
- Attachment F: Letter from FDA to Genentech, Inc., acknowledging receipt of BLA
- Attachment G: Power of Attorney from Genentech, Inc., to Practitioners
- Attachment H: Letter from FDA to Genentech, Inc., acknowledging receipt of IND
- Attachment I: Obinutuzumab BLA, Section 3.2.S.1.2 Structure, redacted
- Attachment J: Klein *et al.*, *mAbs*, 2013, 5(1):22-33
- Attachment K: Mössner *et al.*, *Blood*, 2010, 115:4393-4402
- Attachment L: Obinutuzumab BLA, Section 3.2.S.2.3 Source, History, and Generation, redacted
- Attachment M: Obinutuzumab BLA, Section 3.2.S.2.2 Cell Culture and Harvest, redacted
- Attachment N: Ferrara *et al.*, *J. Biol. Chem.*, 2006, 281(8):5032-5036
- Attachment O: Ferrara *et al.*, *Biotechnology and Bioengineering*, 2006, 93(5):851-61
- Attachment P: Obinutuzumab BLA, Section 3.4.2, redacted
- Attachment Q: Nagelkerken *et al.*, *J Immunol*, 2004, 173:993-999

# **Attachment A**

**Statement by Roche Glycart AG authorizing Genentech, Inc., to act as agent for Roche Glycart AG in the submission of a patent term extension application under 35 U.S.C. § 156 for the '684 Patent and conferring Power of Attorney to practitioners for this purpose**

Docket No.: 146392023400  
Client Ref. No.: 23437-US1

**IN THE UNITED STATES PATENT AND TRADEMARK OFFICE**

In re Patent of: Umaña *et al.*

Patent No.: 6,602,684

Issued: August 5, 2003

Application No: 09/294,584

For: GLYCOSYLATION ENGINEERING OF  
ANTIBODIES FOR IMPROVING ANTIBODY-  
DEPENDENT CELLULAR CYTOTOXICITY-  
Application for § 156 Patent Term Extension

Attorney Docket No: 146392023400

Assignee: Roche Glycart AG

Unit: Office of Patent Legal  
Administration

Mail Stop Hatch-Waxman PTE  
Commissioner for Patents  
P.O. Box 1450  
Alexandria, VA 22313-1450

**AUTHORIZATION AND POWER OF ATTORNEY TO FILE APPLICATION FOR  
EXTENSION OF PATENT TERM UNDER 35 U.S.C. § 156**

As authorized representatives of Roche Glycart AG, owner of the entire right, title and interest in U.S. Patent No. 6,602,684 ("the '684 Patent"), we hereby authorize Genentech, Inc., exclusive licensee of the '684 Patent, to act as agent for Roche Glycart AG in the submission of a patent term extension application under 35 U.S.C. § 156 for the '684 Patent. We understand that counsel for Genentech, Inc., Morrison & Foerster LLP, will file and prosecute this patent term extension application and hereby grant Morrison & Foerster LLP any authorization from Roche Glycart AG necessary for Morrison & Foerster LLP to act in this capacity. In this regard, practitioners associated with Customer Number 25226 are appointed to file and prosecute the patent term extension application for the '684 Patent and to transact all business in the United States Patent and Trademark Office connected with this patent term extension application. Please direct all correspondence regarding this application for patent term extension

1

pa-1619556

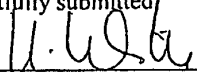
Patent No.: 6,602,684

Docket No.: 146392023400  
Client Ref. No.: 23437-US1

to Morrison & Foerster LLP, 755 Page Mill Road, Palo Alto, CA 94304-1018. The  
correspondence address for the '684 Patent is unchanged for all other purposes.

Date 13 DEC 2013

Respectfully submitted,


By: 

Name: Hubert Witte

Title: Duly Authorized Signatory

Phone: +41 (0) 61 688 51 08;

and

By: 

Name: Antonio Natoli

Title: Duly Authorized Signatory

Phone: +41 (0) 61 687 03 89

pa-1619556

# **Attachment B**

## **Obinutuzumab Product Label**

## HIGHLIGHTS OF PRESCRIBING INFORMATION

These highlights do not include all the information needed to use GAZYVA safely and effectively. See full prescribing information for GAZYVA.

GAZYVA (obinutuzumab)  
Injection, for intravenous infusion  
Initial U.S. Approval: 2013

**WARNING: HEPATITIS B VIRUS REACTIVATION AND PROGRESSIVE MULTIFOCAL LEUKOENCEPHALOPATHY**  
*See full prescribing information for complete boxed warning.*

- Hepatitis B Virus (HBV) reactivation, in some cases resulting in fulminant hepatitis, hepatic failure, and death. (5.1)
- Progressive Multifocal Leukoencephalopathy (PML) resulting in death. (5.2)

### INDICATIONS AND USAGE

GAZYVA (obinutuzumab) is a CD20-directed cytolytic antibody and is indicated, in combination with chlorambucil, for the treatment of patients with previously untreated chronic lymphocytic leukemia. (1, 14)

### DOSAGE AND ADMINISTRATION

- Premedicate with glucocorticoid, acetaminophen and anti-histamine. (2.2)
- Dilute and administer as intravenous infusion. Do not administer as an intravenous push or bolus. (2.1)
- Recommended dose for 6 cycles (28 day cycles):
  - 100 mg on day 1 Cycle 1
  - 900 mg on day 2 Cycle 1
  - 1000 mg on day 8 and 15 of Cycle 1
  - 1000 mg on day 1 of Cycles 2-6 (2.1)

### DOSAGE FORMS AND STRENGTHS

- 1000 mg/40mL (25 mg/mL) single use vial. (3)

### CONTRAINDICATIONS

None.

### WARNINGS AND PRECAUTIONS

- Infusion reactions: Premedicate patients with glucocorticoid, acetaminophen and anti-histamine. Monitor patients closely during infusions. Interrupt or discontinue infusion for reactions. (2.2, 5.3)
- Tumor Lysis Syndrome: Anticipate tumor lysis syndrome; premedicate with anti-hyperuricemics and adequate hydration especially for patients with high tumor burden and/or high circulating lymphocyte count. Correct electrolyte abnormalities, provide supportive care and monitor renal function and fluid balance. (5.4)
- Neutropenia: Monitor for infection. (5.6)
- Thrombocytopenia: Monitor platelet counts and for bleeding. Management of hemorrhage may require blood product support. (5.7)
- Immunization: Do not administer live virus vaccines prior to or during GAZYVA. (5.8)

### ADVERSE REACTIONS

The most common adverse reactions (incidence  $\geq 10\%$ ) were: infusion reactions, neutropenia, thrombocytopenia, anemia, pyrexia, cough, and musculoskeletal disorder. (6)

To report SUSPECTED ADVERSE REACTIONS, contact Genentech at 1-888-835-2555 or FDA at 1-800-FDA-1088 or [www.fda.gov/medwatch](http://www.fda.gov/medwatch).

See 17 for PATIENT COUNSELING INFORMATION

Revised: 11/2013

## FULL PRESCRIBING INFORMATION: CONTENTS\*

### WARNING: HEPATITIS B VIRUS REACTIVATION AND PROGRESSIVE MULTIFOCAL LEUKOENCEPHALOPATHY

- 1 INDICATIONS AND USAGE
- 2 DOSAGE AND ADMINISTRATION
  - 2.1 Recommended Dose Regimen
  - 2.2 Recommended Premedication
  - 2.3 Premedication for anti-microbial prophylaxis
  - 2.4 Treatment Interruption for Toxicity
  - 2.5 Preparation and Administration
- 3 DOSAGE FORMS AND STRENGTHS
- 4 CONTRAINDICATIONS
- 5 WARNINGS AND PRECAUTIONS
  - 5.1 Hepatitis B Virus Reactivation
  - 5.2 Progressive Multifocal Leukoencephalopathy
  - 5.3 Infusion reactions
  - 5.4 Tumor Lysis Syndrome
  - 5.5 Infections
  - 5.6 Neutropenia
  - 5.7 Thrombocytopenia
  - 5.8 Immunization
- 6 ADVERSE REACTIONS
  - 6.1 Clinical Trial Experience
  - 6.2 Immunogenicity
  - 6.3 Additional Clinical Trial Experience

- 7 DRUG INTERACTIONS
- 8 USE IN SPECIFIC POPULATIONS
  - 8.1 Pregnancy
  - 8.3 Nursing Mothers
  - 8.4 Pediatric Use
  - 8.5 Geriatric Use
  - 8.6 Renal Impairment
  - 8.7 Hepatic Impairment
- 10 OVERDOSAGE
- 11 DESCRIPTION
- 12 CLINICAL PHARMACOLOGY
  - 12.1 Mechanism of Action
  - 12.2 Pharmacodynamics
  - 12.3 Pharmacokinetics
- 13 NONCLINICAL TOXICOLOGY
  - 13.1 Carcinogenesis, Mutagenesis, Impairment of Fertility
- 14 CLINICAL STUDIES
  - 14.1 Chronic Lymphocytic Leukemia
- 16 HOW SUPPLIED/STORAGE AND HANDLING
  - 16.1 How Supplied/Storage
- 17 PATIENT COUNSELING INFORMATION

\*Sections or subsections omitted from the full prescribing information are not listed



## FULL PRESCRIBING INFORMATION

### **WARNING: HEPATITIS B VIRUS REACTIVATION AND PROGRESSIVE MULTIFOCAL LEUKOENCEPHALOPATHY**

- Hepatitis B Virus (HBV) reactivation, in some cases resulting in fulminant hepatitis, hepatic failure, and death, can occur in patients receiving CD20-directed cytolytic antibodies, including GAZYVA. Screen all patients for HBV infection before treatment initiation. Monitor HBV positive patients during and after treatment with GAZYVA. Discontinue GAZYVA and concomitant medications in the event of HBV reactivation [see *Warnings and Precautions (5.1)*].
- Progressive Multifocal Leukoencephalopathy (PML) including fatal PML, can occur in patients receiving GAZYVA [see *Warnings and Precautions (5.2)*].

## **1 INDICATIONS AND USAGE**

GAZYVA, in combination with chlorambucil, is indicated for the treatment of patients with previously untreated chronic lymphocytic leukemia (CLL) [see *Clinical Studies (14.1)*].

## **2 DOSAGE AND ADMINISTRATION**

### **2.1 Recommended Dosage Regimen**

- Premedicate before each infusion [see *Dosage and Administration (2.2)*].
- Administer only as an intravenous infusion through a dedicated line [see *Dosage and Administration (2.5)*].
- Do not administer as an intravenous push or bolus.
- Monitor blood counts at regular intervals.
- GAZYVA should only be administered by a healthcare professional with appropriate medical support to manage severe infusion reactions that can be fatal if they occur [see *Warnings and Precautions (5.3)*].

### **Recommended Dose:**

Each dose of GAZYVA is 1000 mg, administered intravenously, with the exception of the first infusions in cycle 1, which are administered on day 1 (100 mg) and day 2 (900 mg).

**Table 1 Dose of GAZYVA to be administered during 6 treatment cycles each of 28 days duration**

Day of treatment cycle		Dose of GAZYVA	Rate of infusion (in the absence of infusion reactions/ hypersensitivity during previous infusions)
Cycle 1	Day 1	100 mg	Administer at 25 mg/hr over 4 hours. Do not increase the infusion rate.
	Day 2	900 mg	Administer at 50 mg/hr. The rate of the infusion can be escalated in increments of 50 mg/hr every 30 minutes to a maximum rate of 400 mg/hr.
	Day 8	1000 mg	Infusions can be started at a rate of 100 mg/hr and increased by 100 mg/hr increments every 30 minutes to a maximum of 400 mg/hr.
	Day 15	1000 mg	
Cycles 2 - 6	Day 1	1000 mg	

If a planned dose of GAZYVA is missed, administer the missed dose as soon as possible and adjust dosing schedule accordingly. If appropriate, patients who do not complete the Day 1 Cycle 1 dose may proceed to the Day 2 Cycle 1 dose.

If a patient experiences an infusion reaction of any grade during infusion, adjust the infusion as follows [see *Warnings and Precautions (5.3)*]:

- Grade 4 (life threatening): Stop infusion immediately and permanently discontinue GAZYVA therapy.
- Grade 3 (severe): Interrupt infusion and manage symptoms. Upon resolution of symptoms, consider restarting GAZYVA infusion at no more than half the previous rate (the rate being used at the time that the infusion reaction occurred) and, if patient does not experience any further infusion reaction symptoms, infusion rate escalation may resume at the increments and intervals as appropriate for the treatment cycle dose. Permanently discontinue treatment if patients experience a Grade 3 infusion related symptom at re-challenge.
- Grade 1-2 (mild to moderate): Reduce infusion rate or interrupt infusion and treat symptoms. Upon resolution of symptoms, continue or resume infusion and, if patient does not experience any further infusion reaction symptoms, infusion rate escalation may resume at the increments and intervals as appropriate for the treatment cycle dose.

## 2.2 Recommended Premedication

Premedication is recommended to reduce the risk of infusion reactions as outlined in Table 2 [see *Warnings and Precautions (5.3)*].

Hypotension may occur during GAZYVA intravenous infusions. Consider withholding antihypertensive treatments for 12 hours prior to and throughout each GAZYVA infusion and for the first hour after administration [see *Warnings and Precautions (5.3)*].

For patients with high tumor burden and/or high circulating absolute lymphocyte counts (greater than  $25 \times 10^9/L$ ), premedicate with anti-hyperuricemics (e.g., *allopurinol*) beginning 12-24 hours

prior to start of therapy and ensure adequate hydration for prophylaxis of tumor lysis syndrome [see Warnings and Precautions (5.4)].

**Table 2 Premedication for GAZYVA Infusion to Reduce Infusion-Related Reactions**

Day of Treatment Cycle	Patients requiring premedication	Premedication	Administration
Cycle 1: Day 1 Day 2	All patients	Intravenous glucocorticoid: 20 mg dexamethasone or 80 mg methylprednisolone <sup>1</sup>	Completed at least 1 hour prior to GAZYVA infusion.
		650-1000 mg Acetaminophen	At least 30 minutes before GAZYVA infusion.
		Anti- histamine (e.g., diphenhydramine 50 mg)	
Cycle 1: Day 8, Day 15	All patients	650-1000 mg Acetaminophen	At least 30 minutes before GAZYVA infusion.
	Patients with an IRR ( $\geq$ Grade 1) with the previous infusion	Anti- histamine (e.g., diphenhydramine 50 mg)	At least 30 minutes before GAZYVA infusion.
	Cycles 2-6: Day 1	Patients with a Grade 3 IRR with the previous infusion OR with a lymphocyte count $>25 \times 10^9/L$ prior to next treatment	Intravenous glucocorticoid: 20 mg dexamethasone or 80 mg methylprednisolone <sup>1</sup>

<sup>1</sup> Hydrocortisone is not recommended as it has not been effective in reducing the rate of infusion reactions.

### 2.3 Premedication for anti-microbial prophylaxis

Patients with neutropenia are strongly recommended to receive antimicrobial prophylaxis throughout the treatment period. Antiviral and antifungal prophylaxis should be considered.

### 2.4 Treatment Interruption for Toxicity

Consider treatment interruption, if patients experience an infection, Grade 3 or 4 cytopenia, or a  $\geq$  Grade 2 non-hematologic toxicity.

### 2.5 Preparation and Administration

#### Preparation

Prepare the solution for infusion, using aseptic technique, as follows:

- Inspect visually for any particulate matter and discoloration prior to administration.
- Dilute into a 0.9% sodium chloride PVC or non-PVC polyolefin infusion bag. Do not use other diluents such as dextrose (5%).

- Preparation of solution for infusion on Day 1 (100 mg) and Day 2 (900 mg) of Cycle 1:
  - Withdraw 40 mL of GAZYVA solution from the vial.
  - Dilute 4 mL (100 mg) of GAZYVA into a 100 mL 0.9% sodium chloride infusion bag for immediate administration.
  - Dilute the remaining 36 mL (900 mg) into a 250 mL 0.9% sodium chloride infusion bag at the same time for use on Day 2 and store at 2°C to 8°C (36°F to 46°F) for up to 24 hours. After allowing the diluted bag to come to room temperature, use immediately.
  - Clearly label each infusion bag.
- Preparation of solution for infusion on Day 8 and 15 of Cycle 1 and Day 1 Cycles 2-6:
  - Withdraw 40 mL of GAZYVA solution from the vial.
  - Dilute 40 mL (1000 mg) into a 250 mL 0.9% sodium chloride infusion bag.
- Mix diluted solution by gentle inversion. Do not shake or freeze.
- For microbiological stability, the diluted GAZYVA infusion solution should be used immediately. Dilute under appropriate aseptic conditions. If not used immediately, the solution may be stored in a refrigerator at 2°C to 8°C (36°F to 46°F) for up to 24 hours prior to use.

The product can be administered at a final concentration of 0.4 mg/mL to 4 mg/mL.

#### Administration

- Administer as an intravenous infusion only.
- Do not administer as an intravenous push or bolus.
- Do not mix GAZYVA with other drugs.
- No incompatibilities between GAZYVA and polyvinylchloride (PVC) or non-PVC polyolefin bags and administration sets have been observed [*see How Supplied/Storage and Handling (16.1)*].

### **3 DOSAGE FORMS AND STRENGTHS**

1000 mg/40mL (25 mg/mL) single use vial.

### **4 CONTRAINDICATIONS**

None.

## 5 WARNINGS AND PRECAUTIONS

### 5.1 Hepatitis B Virus Reactivation

Hepatitis B virus (HBV) reactivation, in some cases resulting in fulminant hepatitis, hepatic failure and death, can occur in patients treated with anti-CD20 antibodies such as GAZYVA. HBV reactivation has been reported in patients who are hepatitis B surface antigen (HBsAg) positive and also in patients who are HBsAg negative but are hepatitis B core antibody (anti-HBc) positive. Reactivation has also occurred in patients who appear to have resolved hepatitis B infection (i.e., HBsAg negative, anti-HBc positive, and hepatitis B surface antibody [anti-HBs] positive).

HBV reactivation is defined as an abrupt increase in HBV replication manifesting as a rapid increase in serum HBV DNA level or detection of HBsAg in a person who was previously HBsAg negative and anti-HBc positive. Reactivation of HBV replication is often followed by hepatitis, i.e., increase in transaminase levels and, in severe cases, increase in bilirubin levels, liver failure, and death.

Screen all patients for HBV infection by measuring HBsAg and anti-HBc before initiating treatment with GAZYVA. For patients who show evidence of hepatitis B infection (HBsAg positive [regardless of antibody status] or HBsAg negative but anti-HBc positive), consult physicians with expertise in managing hepatitis B regarding monitoring and consideration for HBV antiviral therapy.

Monitor patients with evidence of current or prior HBV infection for clinical and laboratory signs of hepatitis or HBV reactivation during and for several months following treatment with GAZYVA. HBV reactivation has been reported for other CD20-directed cytolytic antibodies following completion of therapy.

In patients who develop reactivation of HBV while receiving GAZYVA, immediately discontinue GAZYVA and any concomitant chemotherapy, and institute appropriate treatment. Resumption of GAZYVA in patients whose HBV reactivation resolves should be discussed with physicians with expertise in managing hepatitis B. Insufficient data exist regarding the safety of resuming GAZYVA in patients who develop HBV reactivation.

### 5.2 Progressive multifocal leukoencephalopathy

JC virus infection resulting in progressive multifocal leukoencephalopathy (PML), which can be fatal, was observed in patients treated with GAZYVA. Consider the diagnosis of PML in any patient presenting with new onset or changes to pre-existing neurologic manifestations. Evaluation of PML includes, but is not limited to, consultation with a neurologist, brain MRI, and lumbar puncture. Discontinue GAZYVA therapy and consider discontinuation or reduction of any concomitant chemotherapy or immunosuppressive therapy in patients who develop PML.

### 5.3 Infusion Reactions

GAZYVA can cause severe and life-threatening infusion reactions. Two-thirds of patients experienced a reaction to the first 1000 mgs infused of GAZYVA. Infusion reactions can also occur with subsequent infusions. Symptoms may include hypotension, tachycardia, dyspnea, and respiratory symptoms (e.g., bronchospasm, larynx and throat irritation, wheezing, laryngeal edema). Other common symptoms include nausea, vomiting, diarrhea, hypertension, flushing, headache, pyrexia, and chills [*see Adverse Reactions (6.1)*].

Premedicate patients with acetaminophen, antihistamine and a glucocorticoid. Institute medical management (e.g., glucocorticoids, epinephrine, bronchodilators, and/or oxygen) for infusion

reactions as needed. Closely monitor patients during the entire infusion. Infusions reactions within 24 hours of receiving GAZYVA have occurred [see *Dosage and Administration (2)*].

For patients with any Grade 4 infusion reactions, including but not limited to anaphylaxis, acute life-threatening respiratory symptoms, or other life-threatening infusion reaction: Stop the GAZYVA infusion. Permanently discontinue GAZYVA therapy.

For patients with Grade 1, 2 or 3 infusion reactions: Interrupt GAZYVA for Grade 3 reactions until resolution of symptoms. Interrupt or reduce the rate of the infusion for Grade 1 or 2 reactions and manage symptoms [see *Dosage and Administration (2)*].

For patients with pre-existing cardiac or pulmonary conditions, monitor more frequently throughout the infusion and the post-infusion period since they may be at greater risk of experiencing more severe reactions. Hypotension may occur as part of the GAZYVA infusion reaction. Consider withholding antihypertensive treatments for 12 hours prior to, during each GAZYVA infusion, and for the first hour after administration until blood pressure is stable. For patients at increased risk of hypertensive crisis, consider the benefits versus the risks of withholding their hypertensive medication as is suggested here.

#### **5.4 Tumor Lysis Syndrome**

Acute renal failure, hyperkalemia, hypocalcemia, hyperuricemia, and/or hyperphosphatemia from Tumor Lysis Syndrome (TLS) can occur within 12-24 hours after the first infusion. Patients with high tumor burden and/or high circulating lymphocyte count ( $> 25 \times 10^9/L$ ) are at greater risk for TLS and should receive appropriate tumor lysis prophylaxis with anti-hyperuricemics (e.g., allopurinol) and hydration beginning 12-24 hours prior to the infusion of GAZYVA [see *Dosage and Administration (2.2)*]. For treatment of TLS, correct electrolyte abnormalities, monitor renal function, and fluid balance, and administer supportive care, including dialysis as indicated.

#### **5.5 Infection**

Serious bacterial, fungal, and new or reactivated viral infections can occur during and following GAZYVA therapy. Do not administer GAZYVA to patients with an active infection. Patients with a history of recurring or chronic infections may be at increased risk of infection.

#### **5.6 Neutropenia**

GAZYVA in combination with chlorambucil caused Grade 3 or 4 neutropenia in 34% of patients in the trial. Patients with Grade 3 to 4 neutropenia should be monitored frequently with regular laboratory tests until resolution. Anticipate, evaluate, and treat any symptoms or signs of developing infection.

Neutropenia can also be of late onset (occurring more than 28 days after completion of treatment) and/or prolonged (lasting longer than 28 days).

Patients with neutropenia are strongly recommended to receive antimicrobial prophylaxis throughout the treatment period. Antiviral and antifungal prophylaxis should be considered.

#### **5.7 Thrombocytopenia**

GAZYVA in combination with chlorambucil caused Grade 3 or 4 thrombocytopenia in 12% of patients in the trial. In 5% of patients, GAZYVA caused an acute thrombocytopenia occurring within 24 hours after the GAZYVA infusion. In patients with Grade 3 or 4 thrombocytopenia, monitor platelet counts more frequently until resolution. Transfusion of blood products (i.e., platelet transfusion) may be necessary.

## 5.8 Immunization

The safety and efficacy of immunization with live or attenuated viral vaccines during or following GAZYVA therapy has not been studied. Immunization with live virus vaccines is not recommended during treatment and until B-cell recovery.

## 6 ADVERSE REACTIONS

The following adverse reactions are discussed in greater detail in other sections of the label:

- Hepatitis B reactivation [See *Warnings and Precautions (5.1)*]
- Progressive multifocal leukoencephalopathy [See *Warnings and Precautions (5.2)*]
- Infusion reactions [See *Warnings and Precautions (5.3)*]
- Tumor lysis syndrome [See *Warnings and Precautions (5.4)*]
- Infections [See *Warnings and Precautions (5.5)*]
- Neutropenia [See *Warnings and Precautions (5.6)*]
- Thrombocytopenia [See *Warnings and Precautions (5.7)*]

The most common adverse reactions (incidence  $\geq 10\%$ ) were: infusion reactions, neutropenia, thrombocytopenia, anemia, pyrexia, cough and musculoskeletal disorders.

### 6.1 Clinical Trial Experience

Because clinical trials are conducted under widely varying conditions, adverse reaction rates observed in the clinical trials of a drug cannot be directly compared to rates in the clinical trials of another drug and may not reflect the rates observed in practice.

The data described in Tables 3 and 4 below are based on a total of 356 previously untreated patients with CLL during treatment with GAZYVA in combination with chlorambucil or with chlorambucil alone. Patients received three 1000 mg doses of GAZYVA on the first cycle and a single dose of 1000 mg once every 28 days for 5 additional cycles in combination with chlorambucil (6 cycles of 28 days each in total). In the last 45 patients enrolled, the first dose of GAZYVA was split between day 1 (100 mg) and day 2 (900 mg) [see *Dosage and Administration (2.1)*]. In total, 81% of patients received all 6 cycles (of 28 days each) of GAZYVA based therapy.

**Table 3 Summary of Adverse Reactions Reported with  $\geq 5\%$  Incidence and  $\geq 2\%$  Greater in the GAZYVA Treated Arm**

Adverse Reactions (MedDRA <sup>a</sup> ) System Organ Class	GAZYVA + Chlorambucil n =240		Chlorambucil n =116	
	All Grades %	Grades 3-4 <sup>b</sup> %	All Grades %	Grades 3-4 <sup>b</sup> %
<b>Injury, Poisoning and Procedural Complications</b>				
Infusion related reactions	69	21	0	0
<b>Blood and lymphatic system disorders<sup>c</sup></b>				
Neutropenia	40	34	18	16
Thrombocytopenia	15	11	7	3
Anemia	12	4	10	5
Leukopenia	7	5	0	0
<b>General disorders and administration site conditions</b>				
Pyrexia	10	<1	7	0
<b>Respiratory, thoracic and mediastinal disorders</b>				
Cough	10	0	7	<1

<sup>a</sup> MedDRA coded adverse reactions as reported by investigators.

<sup>b</sup> No Grade 5 adverse reactions have been observed with a difference of  $\geq 2\%$  between the treatment arms.

<sup>c</sup> Adverse events reported under 'Blood and lymphatic system disorders' reflect those reported by investigator as clinically significant.

**Table 4 Post-Baseline Laboratory Abnormalities by CTCAE Grade with  $\geq 5\%$  Incidence and  $\geq 2\%$  Greater in the GAZYVA Treated Arm**

Investigations	GAZYVA + Chlorambucil n =240		Chlorambucil n =116	
	All Grades %	Grades 3-4 %	All Grades %	Grades 3-4 %
<b>Hematology</b>				
Neutropenia	77	46	53	27
Lymphopenia	80	40	9	2
Leukopenia	84	36	12	<1
Thrombocytopenia	47	14	50	11
<b>Chemistry</b>				
Hypocalcemia	32	3	29	<1
Hyperkalemia	31	5	17	2
Hyponatremia	29	8	11	2
AST (SGOT increased)	28	<1	12	0
Creatinine increased	28	<1	18	<1
ALT (SGPT increased)	25	<1	14	0
Hypoalbuminemia	22	<1	14	<1
Alkaline Phosphatase increased	16	0	11	0
Hypokalemia	13	1	4	<1

*Infusion reactions:* The incidence of infusion reactions was 69% with the first infusion of GAZYVA. The incidence of Grade 3 or 4 infusion reactions was 21% with 8% of patients discontinuing therapy. The incidence of reactions with subsequent infusions was 3% with the second 1000 mg and <1% thereafter. No Grade 3 or 4 infusion reactions were reported beyond the first 1000 mg infused.

Of the first 53 patients receiving GAZYVA on the trial, 47 (89%) experienced an infusion reaction. After this experience, study protocol modifications were made to require pre-medication with a corticosteroid, antihistamine, and acetaminophen. The first dose was also divided into two infusions (100 mg on day 1 and 900 mg on day 2). For the 45 patients for whom



these mitigation measures were implemented, 21 patients (47%) experienced a reaction with the first 1000 mg and <2% thereafter [see *Dosage and Administration (2)*].

*Neutropenia:* The incidence of neutropenia reported as an adverse reaction was 40% in the GAZYVA treated arm and 18% in the chlorambucil alone arm with the incidence of serious adverse events being 1% and 0%, respectively (Table 3). Cases of late onset neutropenia (occurring 28 days after completion of treatment or later) were 16% in the GAZYVA treated arm and 12% in the chlorambucil alone arm.

*Infection:* The incidence of infections was similar between arms. Thirty-eight percent of patients in the GAZYVA treated arm experienced an infection, 9% were Grade 3-4 and none were fatal.

*Thrombocytopenia:* The incidence of thrombocytopenia reported as an adverse reaction was 15% in the GAZYVA treated arm and 7% in the chlorambucil alone arm (Table 3). Five percent of patients in the GAZYVA treated arm experienced acute thrombocytopenia (occurring within 24 hours after the GAZYVA infusion).

*Tumor Lysis Syndrome:* The incidence of Grade 3 or 4 tumor lysis syndrome was 2% in the GAZYVA treated arm versus 0% in the chlorambucil arm.

*Musculoskeletal Disorders:* Adverse events related to musculoskeletal disorders, including pain (System Organ Class) have been reported with GAZYVA with higher incidence than in the comparator arm (17% vs. 13%).

## 6.2 Immunogenicity

Serum samples from patients with previously untreated CLL were tested during and after treatment for antibodies to GAZYVA. Approximately 13% (9/70) of GAZYVA treated patients tested positive for anti-GAZYVA antibodies at one or more time points during the 12 month follow-up period. Neutralizing activity of anti-GAZYVA antibodies has not been assessed.

Immunogenicity data are highly dependent on the sensitivity and specificity of the test methods used. Additionally, the observed incidence of a positive result in a test method may be influenced by several factors, including sample handling, timing of sample collection, drug interference, concomitant medication and the underlying disease. Therefore, comparison of the incidence of antibodies to GAZYVA with the incidence of antibodies to other products may be misleading. Clinical significance of anti-GAZYVA antibodies is not known.

## 6.3 Additional Clinical Trial Experience

*Progressive multifocal leukoencephalopathy:* PML has been reported with GAZYVA [see *Warnings and Precautions (5.2)*].

*Worsening of Pre-Existing Cardiac Conditions:* Fatal cardiac events have been reported in patients treated with GAZYVA.

*Hepatitis B reactivation:* Hepatitis B virus reactivation has been reported with GAZYVA [see *Warnings and Precautions (5.1)*].

## 7 DRUG INTERACTIONS

No formal drug interaction studies have been conducted with GAZYVA.

## **8 USE IN SPECIFIC POPULATIONS**

### **8.1 Pregnancy**

#### **Pregnancy Category C**

##### *Risk Summary*

There are no adequate and well-controlled studies of GAZYVA in pregnant women. Women of childbearing potential should use effective contraception while receiving GAZYVA and for 12 months following treatment. GAZYVA should be used during pregnancy only if the potential benefit justifies the potential risk to the fetus.

##### *Animal Data*

In a pre- and post-natal development study, pregnant cynomolgus monkeys received weekly intravenous doses of 25 or 50 mg/kg obinutuzumab from day 20 of pregnancy until parturition. There were no teratogenic effects in animals. The high dose results in an exposure (AUC) that is 2.4 times the exposure in patients with CLL at the recommended label dose. When first measured on Day 28 postpartum, obinutuzumab was detected in offspring and B cells were completely depleted. The B-cell counts returned to normal levels, and immunologic function was restored within 6 months after birth.

### **8.3 Nursing Mothers**

It is not known whether obinutuzumab is excreted in human milk. However, obinutuzumab is excreted in the milk of lactating cynomolgus monkeys and human IgG is known to be excreted in human milk. Because many drugs are excreted in human milk and because of the potential for serious adverse reactions in nursing infants from GAZYVA, a decision should be made whether to discontinue nursing, or discontinue drug, taking into account the importance of the drug to the mother.

### **8.4 Pediatric Use**

The safety and effectiveness of GAZYVA in pediatric patients has not been established.

### **8.5 Geriatric Use**

Of 240 previously untreated CLL patients who received GAZYVA in combination with chlorambucil, 196 patients (82%) were  $\geq 65$  years of age and 109 patients (45%) were  $\geq 75$  years of age. The median age was 74 years. Of the 109 patients  $\geq 75$  years of age, 49 (45%) experienced serious adverse events and 5 (5%) experienced adverse events leading to death. For 131 patients  $< 75$  years of age, 39 (30%) experienced a serious adverse event and 3 (2%) an adverse event leading to death. Similar rates were observed in the comparator arm. No significant differences in efficacy were observed between patients  $\geq 75$  years of age and those  $< 75$  years of age [see *Clinical Studies (14.1)*].

### **8.6 Renal Impairment**

Based on population pharmacokinetic analysis, a baseline creatinine clearance (CLcr)  $> 30$  mL/min does not affect the pharmacokinetics of GAZYVA. GAZYVA has not been studied in patients with a baseline CLcr  $< 30$  mL/min [see *Clinical Pharmacology (12.3)*].

### **8.7 Hepatic Impairment**

GAZYVA has not been studied in patients with hepatic impairment.

## 10 OVERDOSAGE

There has been no experience with overdose in human clinical trials. Doses ranging from 50 mg up to and including 2000 mg per infusion have been administered in clinical trials. For patients who experience overdose, treatment should consist of immediate interruption or reduction of GAZYVA and supportive therapy.

## 11 DESCRIPTION

GAZYVA (obinutuzumab) is a humanized anti-CD20 monoclonal antibody of the IgG1 subclass. It recognizes a specific epitope of the CD20 molecule found on B-cells. The molecular mass of the antibody is approximately 150 kDa.

GAZYVA is produced by mammalian cell (CHO) suspension culture. GAZYVA is a sterile, clear, colorless to slightly brown, preservative free liquid concentrate for intravenous administration. GAZYVA is supplied at a concentration of 25 mg/mL in 1000 mg single use vials. The product is formulated in 20 mM L-histidine/ L-histidine hydrochloride, 240 mM trehalose, 0.02 % poloxamer 188. The pH is 6.0.

## 12 CLINICAL PHARMACOLOGY

### 12.1 Mechanism of Action

Obinutuzumab is a monoclonal antibody that targets the CD20 antigen expressed on the surface of pre B- and mature B-lymphocytes. Upon binding to CD20, obinutuzumab mediates B-cell lysis through (1) engagement of immune effector cells, (2) by directly activating intracellular death signaling pathways and/or (3) activation of the complement cascade. The immune effector cell mechanisms include antibody-dependent cellular cytotoxicity and antibody-dependent cellular phagocytosis.

### 12.2 Pharmacodynamics

In clinical trials in patients with CLL, GAZYVA caused CD19 B-cell depletion (defined as CD19 B-cell counts  $< 0.07 \times 10^9/L$ ). Initial CD19 B-cell recovery was observed in some patients approximately 9 months after the last GAZYVA dose. At 18 months of follow up, some patients remain B-cell depleted.

Although the depletion of B-cells in the peripheral blood is a measurable pharmacodynamic effect, it is not directly correlated with the depletion of B-cells in solid organs or in malignant deposits. B-cell depletion has not been shown to be directly correlated to clinical response.

#### *Cardiac Electrophysiology*

The potential effects of GAZYVA on the QTc interval have not been studied.

### 12.3 Pharmacokinetics

Based on a population pharmacokinetic (pop-PK) analysis, the geometric mean (CV%) volume of distribution of obinutuzumab at steady state is approximately 3.8 (23) L.

The elimination of obinutuzumab is comprised of a linear clearance pathway and a time-dependent non-linear clearance pathway. As GAZYVA treatment progresses, the impact of the time-dependent pathway diminishes in a manner suggesting target mediated drug disposition

(TMDD). Based on a pop-PK analysis, the geometric mean (CV%) terminal obinutuzumab clearance and half-life are approximately 0.09 (46%) L/day and 28.4 (43%) days, respectively.

*Specific Populations:*

*Age:* Age did not affect the pharmacokinetics of GAZYVA.

*Body Weight:* Volume of distribution and steady state clearance both increased with body weight, however, the expected change in exposure does not warrant a dose modification.

*Renal Impairment:* Based on the population pharmacokinetic analysis, a baseline creatinine clearance (CL<sub>cr</sub>) > 30mL/min does not affect the pharmacokinetics of GAZYVA. GAZYVA has not been studied in patients with a baseline CL<sub>cr</sub> < 30mL/min.

*Hepatic impairment:* GAZYVA has not been studied in patients with hepatic impairment.

## 13 NONCLINICAL TOXICOLOGY

### 13.1 Carcinogenesis, Mutagenesis, Impairment of Fertility

No carcinogenicity or genotoxicity studies have been conducted with obinutuzumab.

No specific studies have been conducted to evaluate potential effects on fertility; however, no adverse effects on male or female reproductive organs were observed in the 26-week repeat-dose toxicity study in cynomolgus monkeys.

## 14 CLINICAL STUDIES

### 14.1 Chronic Lymphocytic Leukemia

GAZYVA was evaluated in a three arm, open-label, active control, randomized, multicenter trial (Study 1) in patients with previously untreated CD20+ chronic lymphocytic leukemia requiring treatment and had coexisting medical conditions or reduced renal function as measured by creatinine clearance (CrCl) <70 mL/min. Patients with CrCl <30 mL/min, active infections, positive hepatitis B (HBsAg or anti-HBc positive, patients positive for anti-HBc could be included if hepatitis B viral DNA was not detectable) and hepatitis C serology, or immunization with live virus vaccine within 28 days prior to randomization were excluded from the trial. Patients were treated with chlorambucil control (Arm 1), GAZYVA in combination with chlorambucil (Arm 2) or rituximab in combination with chlorambucil (Arm 3). The safety and efficacy of GAZYVA was evaluated in a comparison of Arm 1 vs. Arm 2 in 356 patients. Data comparing Arm 2 vs. Arm 3 are not available at this time.

The majority of patients received 1000 mg of GAZYVA on days 1, 8 and 15 of the first cycle, followed by treatment on the first day of 5 subsequent cycles (total of 6 cycles, 28 days each). The first dose of GAZYVA was divided between day 1 (100 mg) and day 2 (900 mg) [see *Dosage and Administration (2.1)*], which was implemented in 45 patients. Chlorambucil was given orally at 0.5 mg/kg on day 1 and day 15 of all treatment cycles (1 to 6).

In Study 1, the median age was 73 years, 60% were male, and 95% were Caucasian. Sixty-eight percent had a CrCl <70 mL/min and 76% had multiple coexisting medical conditions. Twenty-two percent of patients were Binet stage A, 42% were stage B and 36% were stage C. The median estimated CrCl was 61 mL/min. Eighty-one percent of patients treated with GAZYVA in combination with chlorambucil received all 6 cycles compared to 67% of patients in the chlorambucil alone arm.

The median progression free survival (PFS) in the GAZYVA in combination with chlorambucil arm was 23.0 months and 11.1 months in the chlorambucil alone arm (median observation time

14.2 months) as assessed by independent review and is consistent with investigator assessed PFS. Efficacy results are shown in Table 5 and the Kaplan-Meier curve for PFS is shown in Figure 1.

**Table 5 Efficacy Results for Study 1**

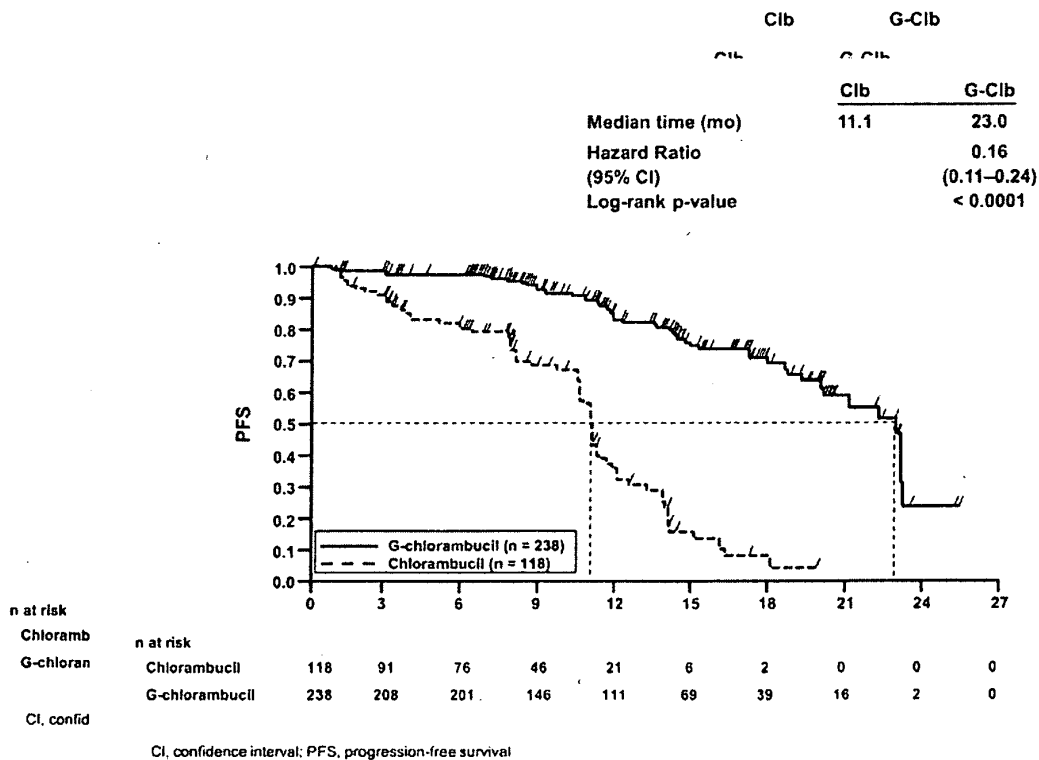
Endpoint	GAZYVA + Chlorambucil	Chlorambucil
Median Progression-Free Survival <sup>a</sup>	23.0 months (HR 0.16 [0.11; 0.24], p-value <0.0001 stratified log-rank test)	11.1 months
Overall Response Rate <sup>b</sup>	75.9%	32.1%
Complete Response	27.8%	0.9%
Median Duration of Response	15.2 months	3.5 months

<sup>a</sup> As defined by independent review. Investigator assessed PFS was consistent with data from independent review.

<sup>b</sup> As defined as best overall response rate (ORR=CR+PR)

**Figure 1**

**Kaplan-Meier Curve of Progression-Free Survival in Patients with CLL in Study 1**



## 16 HOW SUPPLIED/STORAGE AND HANDLING

### 16.1 How Supplied/Storage

GAZYVA 1000 mg/40 mL (25 mg/mL) single-use vials containing preservative-free solution (NDC 50242-070-01) are stable at 2°C to 8°C (36°F to 46°F). Do not use beyond expiration date

stamped on carton. GAZYVA vials should be protected from light. DO NOT FREEZE. DO NOT SHAKE.

For the diluted product, chemical and physical stability have been demonstrated in 0.9% NaCl at concentrations of 0.4 mg/ml to 20 mg/mL for 24 hours at 2°C to 8°C (36°F to 46°F) followed by 48 hours (including infusion time) at room temperature ( $\leq 30^\circ\text{C}/86^\circ\text{F}$ ). GAZYVA does not contain antimicrobial preservatives. Therefore care must be taken to ensure that the solution for infusion is not microbiologically compromised during preparation. The solution for infusion should be used immediately. If not used immediately, the prepared solution may be stored up to 24 hours at 2-8°C. No incompatibilities between GAZYVA and polyvinyl chloride or polyolefin infusion materials have been observed in concentration ranges from 0.4 mg/mL to 20.0 mg/mL after dilution of GAZYVA with 0.9% sodium chloride.

## 17 PATIENT COUNSELING INFORMATION

Advise patients to seek immediate medical attention for any of the following:

- Signs and symptoms of infusion reactions including dizziness, nausea, chills, fever, vomiting, diarrhea, breathing problems, or chest pain [see *Warnings and Precautions (5.3) and Adverse Reactions (6.1)*].
- Symptoms of tumor lysis syndrome such as nausea, vomiting, diarrhea and lethargy [see *Warnings and Precautions (5.4) and Adverse Reactions (6.1)*].
- Signs of infections including fever and cough [see *Warnings and Precautions (5.5) and Adverse Reactions (6.1)*].
- Symptoms of hepatitis including worsening fatigue or yellow discoloration of skin or eyes [see *Warnings and Precautions (5.1)*].
- New or changes in neurological symptoms such as confusion, dizziness or loss of balance, difficulty talking or walking, or vision problems [see *Warnings and Precautions (5.2)*].

Advise patients of the need for:

- Periodic monitoring of blood counts [see *Warnings and Precautions (5.6, and 5.7) and Adverse Reactions (6.1)*].
- Avoid vaccinations with live viral vaccines [see *Warnings and Precautions (5.8)*].
- Patients with a history of hepatitis B infection (based on the blood test) should be monitored and sometimes treated for their hepatitis [see *Warnings and Precautions (5.1)*].

---

### GAZYVA™ [obinutuzumab]

Manufactured by:

**Genentech, Inc.**

A Member of the Roche Group

South San Francisco, CA 94080-4990

U.S. License No: 1048

GAZYVA is a trademark of Genentech, Inc.

© 2013 Genentech, Inc.

# **Attachment C**

## **Obinutuzumab Biologics License Application (BLA) Approval**



BLA 125486/0

**BLA APPROVAL**

Genentech, Inc.  
Attention: Michelle H. Rohrer, Ph.D.  
Vice President, Regulatory Affairs  
1 DNA Way  
South San Francisco, CA 94080-4990

Dear Dr. Rohrer:

Please refer to your Biologics License Application (BLA) dated April 22, 2013 received on April 22, 2013 submitted under section 351(a) of the Public Health Service Act for GAZYVA (obinutuzumab).

We acknowledge receipt of your amendments dated April 25, May 15, June 3, 28, July 3, 8, 16, 18, 19, 25, 31, August 1, 2, 6, 12, 14, 15, 19, 22, 27, 30, September 3, 10, 12, 13, 17, 18, 20, 23, 24, 25, 27, October 7, 9, 15, 17, 21, 22, 23, 24, 29, 30, and 31, 2013.

**LICENSING**

We have approved your BLA for GAZYVA (obinutuzumab) effective this date. You are hereby authorized to introduce or deliver for introduction into interstate commerce, GAZYVA (obinutuzumab) under your existing Department of Health and Human Services U.S. License No. 1048. GAZYVA (obinutuzumab) is indicated for the treatment of patients with previously untreated chronic lymphocytic leukemia in combination with chlorambucil.

**MANUFACTURING LOCATIONS**

Under this license, you are approved to manufacture obinutuzumab drug substance at Roche Diagnostics GmbH in Penzberg, Germany, and obinutuzumab drug product at Roche Diagnostics GmbH in Mannheim, Germany. Drug product will be labeled and packaged at F. Hoffmann-La Roche Ltd, in Kaiseraugst, Switzerland.

You may label your product with the proprietary name, GAZYVA, and will market it in 1000 mg/40 mL (25 mg/mL) liquid single use vials.

**DATING PERIOD**

The dating period for GAZYVA (obinutuzumab) shall be 36 months from the date of manufacture when stored at 2-8°C. The date of manufacture shall be defined as [REDACTED] (b)(4)



(b) (4) The dating period for your obinutuzumab drug substance shall be (b) (4) from the date of manufacture when stored at (b) (4)

### **FDA LOT RELEASE**

You are not currently required to submit samples of future lots of GAZYVA (obinutuzumab) to the Center for Drug Evaluation and Research (CDER) for release by the Director, CDER, under 21 CFR 610.2. We will continue to monitor compliance with 21 CFR 610.1, requiring completion of tests for conformity with standards applicable to each product prior to release of each lot.

Upon review of the supporting data, the design space as proposed in BLA 125486 was found to be acceptable. The Agency would like to reiterate that in addition to the information described in the application, it is our expectation that plans for implementation of the design space for the commercial process are documented within the firm's Quality System. Such quality systems may include plans for handling movements within the design space (e.g., change control procedures, plans for updating batch records). In accordance with ICH Q8(R2), while the Agency does not expect any regulatory notification for movements within the design space, any other changes in the manufacturing, testing, packaging, or labeling or manufacturing facilities for GAZYVA (obinutuzumab) will require the submission of information to your biologics license application for our review and written approval, consistent with 21 CFR 601.12.

### **APPROVAL & LABELING**

We have completed our review of this application, as amended. It is approved, effective on the date of this letter, for use as recommended in the enclosed agreed-upon labeling text.

We note that your October 31, 2013 submission includes final printed labeling (FPL) for your package insert. We have not reviewed this FPL. You are responsible for assuring that the wording in this printed labeling is identical to that of the approved content of labeling in the structured product labeling (SPL) format.

### **CONTENT OF LABELING**

As soon as possible, but no later than 14 days from the date of this letter, submit, via the FDA automated drug registration and listing system (eLIST), the content of labeling [21 CFR 314.14(b)] in structured product labeling (SPL) format, as described at

<http://www.fda.gov/ForIndustry/DataStandards/StructuredProductLabeling/default.htm>.

Content of labeling must be identical to the enclosed labeling (text for the package insert).

Information on submitting SPL files using eLIST may be found in the guidance for industry titled "SPL Standard for Content of Labeling Technical Qs and As" at

<http://www.fda.gov/downloads/Drugs/GuidanceComplianceRegulatoryInformation/Guidances/UCM072392.pdf>.

The SPL will be accessible via publicly available labeling repositories.

**CARTON AND IMMEDIATE CONTAINER LABELS**

We acknowledge your October 18, 2013 submission containing final printed carton and container labels.

**ADVISORY COMMITTEE**

Your application for GAZYVA (obinituzumab) was not referred to an FDA advisory committee because this biologic is not the first in its class, the clinical trial design is acceptable, the application did not raise significant safety or efficacy issues that were unexpected for a drug/biologic of this class, and there were no controversial issues that would benefit from advisory committee discussion.

**REQUIRED PEDIATRIC ASSESSMENTS**

Under the Pediatric Research Equity Act (PREA) (21 U.S.C. 355c), all applications for new active ingredients, new indications, new dosage forms, new dosing regimens, or new routes of administration are required to contain an assessment of the safety and effectiveness of the product for the claimed indication(s) in pediatric patients unless this requirement is waived, deferred, or inapplicable.

Because this drug product for this indication has an orphan drug designation, you are exempt from this requirement.

**POSTMARKETING COMMITMENTS NOT SUBJECT TO THE REPORTING REQUIREMENTS UNDER SECTION 506B**

We remind you of your postmarketing commitments:

PMC #1 Perform a formal verification study of the (b)(4) hold time for (b)(4).  
Submit the final report to the Agency as a CBE-30 by February 28, 2014.

The timetable you submitted on October 16, 2013 states that you will conduct this study according to the following schedule:

Final Protocol Submission: Complete  
Study Completion: 12/2013  
Final Report Submission: 02/2014

PMC #2 Submit a protocol for (b)(4). The protocol should include bioburden and endotoxin limits to demonstrate continued microbial control over (b)(4) lifetime. The protocol should be submitted as a CBE-30 by December 2013.

Execute the approved protocol concurrently throughout the respective lifetime of the [REDACTED] (b) (4) until the claimed or planned lifetimes are reached. Provide available results in the first annual report following the approval of the CBE-30 and concurrently with subsequent annual reports.

The timetable you submitted on October 30, 2013 states that you will conduct this study according to the following schedule:

Final Protocol Submission:	12/2013
Study Completion:	concurrently throughout respective lifecycle
Final Report Submission:	Annual report 2014 and subsequent Annual reports until end of one full lifecycle for each of the included items

Submit clinical protocols to your IND 104405 for this product. Submit nonclinical and chemistry, manufacturing, and controls protocols and all postmarketing final reports to this BLA. In addition, under 21 CFR 601.70 you should include a status summary of each commitment in your annual progress report of post marketing studies to this BLA. The status summary should include expected summary completion and final report submission dates, any changes in plans since the last annual report, and, for clinical studies/trials, number of patients entered into each study/trial. All submissions, including supplements, relating to these postmarketing commitments should be prominently labeled "Postmarketing Commitment Protocol," "Postmarketing Commitment Final Report," or "Postmarketing Commitment Correspondence."

#### PROMOTIONAL MATERIALS

You may request advisory comments on proposed introductory advertising and promotional labeling. To do so, submit, in triplicate, a cover letter requesting advisory comments, the proposed materials in draft or mock-up form with annotated references, and the package insert to:

Food and Drug Administration  
Center for Drug Evaluation and Research  
Office of Prescription Drug Promotion  
5901-B Ammendale Road  
Beltsville, MD 20705-1266

As required under 21 CFR 601.12(f)(4), you must submit final promotional materials, and the package insert, at the time of initial dissemination or publication, accompanied by a Form FDA 2253. For instruction on completing the Form FDA 2253, see page 2 of the Form. For more information about submission of promotional materials to the Office of Prescription Drug Promotion (OPDP), see <http://www.fda.gov/AboutFDA/CentersOffices/CDER/ucm090142.htm>.

### **REPORTING REQUIREMENTS**

You must submit adverse experience reports under the adverse experience reporting requirements for licensed biological products (21 CFR 600.80). You should submit postmarketing adverse experience reports to:

Food and Drug Administration  
Center for Drug Evaluation and Research  
Central Document Room  
5901-B Ammendale Road  
Beltsville, MD 20705-1266

Prominently identify all adverse experience reports as described in 21 CFR 600.80.

You must submit distribution reports under the distribution reporting requirements for licensed biological products (21 CFR 600.81).

You must submit reports of biological product deviations under 21 CFR 600.14. You should promptly identify and investigate all manufacturing deviations, including those associated with processing, testing, packing, labeling, storage, holding and distribution. If the deviation involves a distributed product, may affect the safety, purity, or potency of the product, and meets the other criteria in the regulation, you must submit a report on Form FDA-3486 to:

Food and Drug Administration  
Center for Drug Evaluation and Research  
Division of Compliance Risk Management and Surveillance  
5901-B Ammendale Road  
Beltsville, MD 20705-1266

Biological product deviations, sent by courier or overnight mail, should be addressed to:

Food and Drug Administration  
Center for Drug Evaluation and Research  
Division of Compliance Risk Management and Surveillance  
10903 New Hampshire Avenue, Bldg. 51, Room 4206  
Silver Spring, MD 20903

### **MEDWATCH-TO-MANUFACTURER PROGRAM**

The MedWatch-to-Manufacturer Program provides manufacturers with copies of serious adverse event reports that are received directly by the FDA. New molecular entities and important new biologics qualify for inclusion for three years after approval. Your firm is eligible to receive copies of reports for this product. To participate in the program, please see the enrollment instructions and program description details at <http://www.fda.gov/Safety/MedWatch/HowToReport/ucm166910.htm>.

**POST APPROVAL FEEDBACK MEETING**

New molecular entities and new biologics qualify for a post approval feedback meeting. Such meetings are used to discuss the quality of the application and to evaluate the communication process during drug development and marketing application review. The purpose is to learn from successful aspects of the review process and to identify areas that could benefit from improvement. If you would like to have such a meeting with us, call the Regulatory Project Manager for this application.

**PDUFA V APPLICANT INTERVIEW**

FDA has contracted with Eastern Research Group, Inc. (ERG) to conduct an independent interim and final assessment of the Program for Enhanced Review Transparency and Communication for NME NDAs and Original BLAs under PDUFA V ('the Program'). The PDUFA V Commitment Letter states that these assessments will include interviews with applicants following FDA action on applications reviewed in the Program. For this purpose, first-cycle actions include approvals, complete responses, and withdrawals after filing. The purpose of the interview is to better understand applicant experiences with the Program and its ability to improve transparency and communication during FDA review.

ERG will contact you to schedule a PDUFA V applicant interview and provide specifics about the interview process. Your responses during the interview will be confidential with respect to the FDA review team. ERG has signed a non-disclosure agreement and will not disclose any identifying information to anyone outside their project team. They will report only anonymized results and findings in the interim and final assessments. Members of the FDA review team will be interviewed by ERG separately. While your participation in the interview is voluntary, your feedback will be helpful to these assessments.

If you have any questions, call Beatrice Kallungal, Regulatory Project Manager, at (301) 796-9304.

Sincerely,

*{See appended electronic signature page}*

Richard Pazdur, M.D.  
Director  
Office of Hematology and Oncology Products  
Center for Drug Evaluation and Research

**ENCLOSURE(S):**

Content of Labeling  
Carton and Container Labeling

-----  
**This is a representation of an electronic record that was signed electronically and this page is the manifestation of the electronic signature.**  
-----

/s/  
-----

RICHARD PAZDUR  
11/01/2013

# **Attachment D**

**U.S. Patent No. 6,602,684**



US006602684B1

(12) **United States Patent**  
**Umaña et al.**

(10) **Patent No.:** US 6,602,684 B1  
(45) **Date of Patent:** Aug. 5, 2003

- (54) **GLYCOSYLATION ENGINEERING OF ANTIBODIES FOR IMPROVING ANTIBODY-DEPENDENT CELLULAR CYTOTOXICITY**
- (75) **Inventors:** Pablo Umaña, Manchester (GB); Joël Jean-Malret, Zürich (CH); James E. Bailey, Zürich (CH)
- (73) **Assignee:** Glycart Biotechnology AG (CH)
- (\* ) **Notice:** Subject to any disclaimer, the term of this patent is extended or adjusted under 35 U.S.C. 154(b) by 0 days.

- (21) **Appl. No.:** 09/294,584
- (22) **Filed:** Apr. 20, 1999

**Related U.S. Application Data**

- (60) **Provisional application No.** 60/082,581, filed on Apr. 20, 1998.
- (51) **Int. Cl.<sup>7</sup>** ..... C12P 21/00; C12N 15/63; C12N 15/85; C07H 21/04
- (52) **U.S. Cl.** ..... 435/69.1; 435/320.1; 435/455; 536/23.1; 536/24.1
- (58) **Field of Search** ..... 435/69.1, 320.1, 435/455; 536/23.1, 24.1

(56) **References Cited**

**U.S. PATENT DOCUMENTS**

4,215,051 A	7/1980	Schroeder et al.
4,946,778 A	8/1990	Ladner et al.
5,047,335 A	9/1991	Paulson et al.
5,547,933 A	8/1996	Lin
5,736,137 A	4/1998	Anderson et al.
5,776,456 A	7/1998	Anderson et al.
5,843,439 A	12/1998	Anderson et al.
5,952,203 A *	9/1999	Withers et al. .... 435/97
5,958,403 A *	9/1999	Strom et al. .... 424/93.21

**FOREIGN PATENT DOCUMENTS**

EP	0 669 836 B1	7/1996	
EP	0 752 248 A1	1/1997	
WO	WO 95/24494 *	9/1995	..... 435/455
WO	WO 97/30087	8/1997	

**OTHER PUBLICATIONS**

- Orkin et al. Report and recommendations of the panel to assess the NIH investment in research on gene therapy, Dec. 1995.\*
- Marshall E Gene therapy's growing pains. Science vol. 269:1050-1055, Aug. 1995.\*
- Verma et al. Gene therapy—promises, problems and prospects. Nature vol. 389:239-242, Sep. 1997.\*
- Anderson WF Human gene therapy. Nature vol. 392:25-30, Apr. 1998.\*
- Fanger et al. Cytotoxicity mediated by human Fc receptors for IgG. Immunology Today. vol. 10(3):92-99, Mar. 1989.\*
- Search Report of Subject Search Conducted by Swiss Federal Institute of Intellectual Property Concerning WO 99/54342 (published international application corresponding to U.S. Appl. No. 08/294,548) dated Jul. 18, 2001.

English language abstract of Japanese Patent No. JP 09084582 A, Derwent WPI Accession No. 1997-253000 [23] (Mar. 1997).

English language abstract of German Patent No. DE 19546680 A1, Derwent WPI Accession No. 1997-321072 [30] (Jun. 1997).

English language abstract of International Patent Publication No. WO 00/52135 A2, Derwent WPI Accession No. 2000-572178 [53] (Sep. 2000).

English language abstract of International Patent Publication No. WO 00/53730 A2, Derwent WPI Accession No. 2000-594316 [56] (Sep. 2000).

English language abstract of International Patent Publication No. WO 01/29242 A2, Derwent WPI Accession No. 2001-290925 [30] (Apr. 2001).

English language abstract of European Patent Publication No. 585 083 A1, Derwent WPI Accession No. 1994-067563 [09] (1994).

English language abstract of International Patent Publication No. WO 94/12646 A1, Derwent WPI Accession No. 1994-200274 [24] (1994).

English language abstract of European Patent Publication No. 481 790 A, Derwent WPI Accession No. 1992-134048 [17] (1992).

English language abstract of International Patent Publication No. WO 95/15769 A1, Derwent WPI Accession No. 1995-224151 [29] (1995).

English language abstract of International Patent Publication No. WO 97/34632 A1, Derwent WPI Accession No. 1997-479995 [44] (Sep. 1997).

English language abstract of United States Patent No. 5,714, 350 A, Derwent WPI Accession No. 1998-129858 (Feb. 1998).

English language abstract of International Patent Publication No. WO 98/49198 A1, Derwent WPI Accession No. 1998-080758 (Nov. 1998).

English language abstract of International Patent Publication No. WO 96/13516 A1, Derwent WPI Accession No. 1996-239446 [24] (1996).

(List continued on next page.)

*Primary Examiner*—Remy Yucel  
*Assistant Examiner*—William Sandals  
(74) *Attorney, Agent, or Firm*—Sterne, Kessler, Goldstein & Fox, p.l.l.c.

(57) **ABSTRACT**

The present invention relates to the field glycosylation engineering of proteins. More particular, the present invention is directed to the glycosylation engineering of proteins to provide proteins with improved therapeutic properties, e.g., antibodies, antibody fragments, or a fusion protein that includes a region equivalent to the Fc region of an immunoglobulin, with enhanced Fc-mediated cellular cytotoxicity.

10 Claims, 16 Drawing Sheets



## OTHER PUBLICATIONS

- English language abstract of International Patent Publication No. WO 98/58964 A1, Derwent WPI Accession No. 1999-081223 [07] (Dec. 1998).
- Amslutz et al., 1993, "Production and Characterization of a Mouse/Human Chimeric Antibody Directed Against Human Neuroblastoma," *Int. J. Cancer* 53:147-152.
- Arathoon and Birch, 1986, "Large-Scale Cell Culture in Biotechnology," *Science* 232:1390-1395.
- Ausubel et al., Ed., 1987-99, *Current Protocols in Molecular Biology*, John Wiley & Sons, Inc. and *Current Protocols*, pp. 3.16.1-3.16.11, 3.17.1-3.17.10.
- Bailey, 1991, "Toward a Science of Metabolic Engineering," *Science* 252:1668-1675.
- Bailey et al., 1998, "Engineering Glycosylation in Animal Cells," *In: New Developments and New Applications in Animal Cell Technology*. Merten et al., eds. Kluwer Academic Publishers, Netherlands. pp. 5-23.
- Bailey et al., 1997, "Metabolic Engineering of N-Linked Glycoform Synthesis Systems in Chinese Hamster Ovary (CHO) Cells," *In: Animal Cell Technology*. Carrondo et al., eds. Kluwer Academic Publishers, Netherlands, pp. 489-494.
- Bibila and Flickinger, 1991, "A Model of Interorganelle Monoclonal Antibody Transport and Secretion in Mouse Hybridoma Cells," *Biotechnol. Bioeng.* 38:767-780.
- Bibila and Robinson, 1995, "In Pursuit of the Optimal Fed-Batch Process for Monoclonal Antibody Production," *Biotechnol. Prog.* 11:1-3.
- Bitter, 1987, "Heterologous Gene Expression in Yeast," *Methods in Enzymology* 152:673-684.
- Bitter, et al., 1987, "Expression and Secretion Vectors for Yeast," *Methods in Enzymology* 153:516-544.
- Breitscher and Munro, 1993, "Cholesterol and the Golgi Apparatus," *Science* 261:1280-1281.
- Briles et al., 1977, "Isolation of Wheat Germ Agglutinin resistant Clones of Chinese Hamster Ovary Cells Deficient in Membrane Sialic Acid and Galactose," *J. Biol. Chem.* 252, No. 3:1107-1116.
- Brisson et al., 1984, "Expression of a bacterial gene in plants by using a viral vector," *Nature* 310:511-514.
- Brockhausen et al., 1992, "Control of glycoprotein synthesis. Characterization of (1→4)-N-acetyl-β-D-glucosaminyltransferase acting on the α-D-(1→3)- and α-D-(1→6)-linked arms of N-linked oligosaccharides," *Carbohydrate. Res.* 236:281-299.
- Brogliè et al., 1984, "Light-Regulated Expression of a Pea Ribulose-1,5-Bisphosphate Carboxylase Small Subunit Gene in Transformed Plant Cells," *Science* 224:838-843.
- Campbell and Stanley, 1984, "A Dominant Mutation to Ricin Resistance in Chinese Hamster Ovary Cells Induces UDP-GlcNAc:Glycopeptide B-4-N-Acetylglucosaminyltransferase III Activity," *The Journal of Biological Chemistry* 261:13370-13378.
- Caruthers et al., 1980, "New chemical methods for synthesizing polynucleotides," *Nuc. Acids Res. Symp. Ser.* 7:215-223.
- Chow et al., 1981, "Synthesis of oligodeoxyribonucleotides on silica gel support," *Nuc. Acids Res.* 9:2807-2817.
- Cole et al., 1985, "The EBV-Hybridoma Techniques and Its Application to Human Lung Cancer," *In: Monoclonal Antibodies and Cancer Therapy*, Alan R. Liss, Inc., pp. 77-96.
- Cole et al., 1996, "Diffusional Mobility of Golgi Proteins in Membranes of Living Cells," *Science* 273:797-801.
- Coruzzi et al., 1984, "Tissue-specific and light-regulated expression of a pea nuclear gene encoding the small subunit of a ribulose-1,5-bisphosphate carboxylase," *EMBO J.* 3:1671-1679.
- Cote et al., 1983, "Generation of human monoclonal antibodies reactive with cellular antigens," *Proc. Natl. Acad. Sci. U.S.A.* 80:2026-2030.
- Crea and Horn, 1980, "Synthesis of oligonucleotides on cellulose by a phosphotriester method," *Nuc. Acids Res.* 8:2331-2348.
- Creighton, 1983, *Proteins Structures And Molecular Principles*, W.H. Freeman and Co., N.Y. pp. 34-60.
- Cumming, D. A., 1991, "glycosylation of recombinant protein therapeutics: control and functional implications," *Glycobiology* 1:115-129.
- Dennis et al., 1987, "β1-6 Branching of Asn-Linked Oligosaccharides Is Directly Associated with Metastasis," *Science* 236:582-585.
- Do et al., 1994, "Modification of Glycoproteins by N-Acetylglucosaminyltransferase V Is Greatly Influenced by Accessibility of the Enzyme to Oligosaccharide Acceptors," *J. Biol. Chem.* 269:23456-23464.
- Dörr, 1993, "First clinical results with the chimeric antibody chCE7 in neuroblastoma—targeting features and biodistribution data," *Eur. J. Nucl. Med.* 20:858, abstract 159.
- Dunphy and Rothman, 1983, "Compartmentation of Asparagine-linked Oligosaccharide Processing in the Golgi Apparatus," *J. Cell Biol.* 97:270-275.
- Dunphy et al., 1985, "Attachment of Terminal N-Acetylglucosamine to Asparagine-Linked Oligosaccharides Occurs in Central Cisternae of the Golgi Stack," *Cell* 40:463-472.
- Dunphy et al., 1981, "Early and late functions associated with the Golgi apparatus reside in distinct compartments," *Proc. Natl. Acad. Sci. USA* 78:7453-7457.
- Dwek, R. A., 1995, "Glycobiology: More Functions for Oligosaccharides," *Science* 269:1234-1235.
- Easton et al., 1991, "Enzymatic Amplification Involving Glycosyltransferases Forms the Basis for the Increased Size of Asparagine-linked Glycans at the Surface of NIH 3T3 Cells Expressing the N-ras Proto-oncogene," *J. Biol. Chem.* 266:21674-21680.
- Elices and Goldstein, 1988, "Ehrlich Ascites Tumor Cell UDP-Gal:N-Acetyl-D-glucosamine β(1,4)-Galactosyltransferase," *J. Biol. Chem.* 263:3354-3362.
- Field et al., 1996, "The Use of High-Performance Anion-Exchange Chromatography and Matrix-Assisted Laser Desorption/Ionization Time Mass Spectrometry to Monitor and Identify Oligosaccharide Degradation," *Analytical Biochemistry* 239:92-98.
- Fouser et al., 1992, "High Level Expression of a Chimeric Anti-Ganglioside GD2 Antibody; Genomic Kappa Sequences Improve Expression in COS and CHO Cells," *Bio/Technology* 10:1121-1127.
- Frost et al., 1997, "A Phase I/II Trial of Murine Monoclonal Anti-GD2 Antibody 14.G2a plus Interleukin-2 in Children with Refractory Neuroblastoma," *Cancer* 80:317-333.
- Glover, 1986, *DNA Cloning*, vol. II, IRL Press, Wash., D.C., Ch. 3.
- Goldberg and Kornfeld, 1983, "Evidence for Extensive Subcellular Organization of Asparagine-linked Oligosaccharide Processing and Lysosomal Enzyme Phosphorylation," *J. Biol. Chem.* 258:3159-3165.

- Gooch et al., 1992, "The Oligosaccharides of Glycoproteins: Factors Affecting Their Synthesis and Their Influence on Glycoprotein Properties," p. In: *Frontiers in Bioprocessing II*. American Chemical Society, Washington, D.C. pp. 199-240.
- Gossen et al., 1994, "Control of gene activity in higher eukaryotic cells by prokaryotic regulatory elements," *Tibtech* 12:58-62.
- Graham et al., 1996, "The polymorphic epithelial mucin: potential as an immunogen for a cancer vaccine," *Cancer Immun. Immunother.* 42:71-80.
- Grierson and Corey, 1989, "The Dynamic Nature of the Golgi Complex" *J. Cell Biol.* 108:277-297.
- Griffiths et al., 1989, "The Dynamic Nature of the Golgi Complex" *J. Cell Biol.* 108:277-297.
- Gross et al., 1990, "A Highly Sensitive Fluorometric Assay for Sialyltransferase Activity Using CMP-9-fluoresceinyl-NeuAc as Donor," *Anal Biochem.* 186:127-134.
- Gu et al., 1993, "Purification and Characterization of UDP-N-Acetylglucosamine:  $\alpha$ -6-D-Mannoside  $\beta$ 1-6N-Acetylglucosaminyltransferase (N-Acetylglucosaminyltransferase V) from a Human Lung Cancer Cell Line," *J. Biochem.* 113:614-619.
- Gurley et al., 1986, "Upstream Sequences Required for Efficient Expression of a Soybean Heat Shock Gene," *Mol. Cell. Biol.* 6:559-565.
- Haga et al., 1994, "Dose-Related Comparison of Antibody-Dependent Cellular Cytotoxicity with Chimeric and Native Monoclonal Antibody 17-1A," *International Journal of Pancreatolgy* 15:43-50.
- Harpaz and Schachter, 1980, "Control of Glycoprotein Synthesis," *J. Biol. Chem.* 255:4894-4902.
- Harvey, 1993, "Quantitative Aspects of the Matrix-assisted Laser Desorption Mass Spectrometry of Complex Oligosaccharides," *Rapid Commun. Mass Spectrom.* 7:614-619.
- Hirshberg and Snider, 1987, "Topography of Glycosylation in the Rough Endoplasmic Reticulum and Golgi Apparatus" *Annu. Rev. Biochem.* 56:63-87.
- Huse et al., 1989, "Generation of a Large Combinatorial Library of the Immunoglobulin Repertoire in Phage Lambda," *Science* 246:1275-1281.
- Jefferis et al., 1995, "Recognition sites on human IgG for Fc $\gamma$  receptors: the role of glycosylation," *Immunology Letters* 44:111-117.
- Jenkins et al., 1996, "Getting the glycosylation right: Implications for the biotechnology industry," *Nature Biotechnol.* 14:975-981.
- Jenkins, N., Curling, M. A., 1994, "Glycosylation of recombinant proteins: Problems and prospects," *Enzyme Microb. Technol.* 16:354-364.
- Kagawa et al., 1988, "Comparative Study of the Asparagine-linked Sugar Chains of Natural Human Interferon- $\beta$ 1 and Recombinant Human Interferon- $\beta$ 1 Produced by Three Different Mammalian Cells," *J. Biol. Chem.* 263:17508-17515.
- Koenig et al., 1997, "Selectin inhibition: synthesis and evaluation of novel sialylated, sulfated and fucosylated oligosaccharides, including the major capping of GlyCAM-1," *Glycobiology* 7:79-93.
- Kohler and Milstein, 1975, "Continuous cultures of fused cells secreting antibody of predefined specificity," *Nature* 256:495-497.
- Kolber et al., 1998, "Measurement of cytotoxicity by target cell release and retention of the fluorescent dye bis-carboxyethyl-carboxyfluorescein (BCECF)," *J. of Immunological Methods* 108:255-264.
- Kornfeld and Kornfeld, 1985, "Assembly of Asparagine-Linked Oligosaccharides," *Ann. Rev. Biochem.* 54:631-664.
- Küster et al., 1997, "Sequencing of N-Linked Oligosaccharides from Protein Gels: In-gel Deglycosylation Followed by Matrix-Assisted Laser Desorption/Ionization Mass Spectrometry and Normal-Phase High-Performance Liquid Chromatography," *Analytical Biochemistry* 250:82-101.
- Kozbor and Rodor, 1983, "The production of monoclonal antibodies from human lymphocytes," *Immunology Today* 4:72-79.
- Lifely et al., 1995, "Glycosylation and biological activity of CAMPATH-1H expressed in different cell lines and grown under different culture conditions," *Glycobiology* 5:813-822.
- Lis and Sharon, 1993, "Protein glycosylation: Structural and functional aspects," *Eur. J. Biochem.* 218:1-27.
- Lloyd et al., 1996, "Comparison of O-Linked Carbohydrate Chains in MUC-1 Mucin from Normal Breast Epithelial Cell Lines and Breast Carcinoma Cell Lines. Demonstration of Simpler and Fewer Glycan Chains in Tumor Cells," *J. Biol. Chem.* 271:33325-33334.
- Lund et al., 1993, "Control of IgG/Fc Glycosylation: A Comparison of Oligosaccharides from Chimeric Human/Mouse and Mouse Subclass Immunoglobulin Gs," *Molecular Immunology* 30:741-748.
- Lund et al., 1995, "Oligosaccharide-protein interactions in IgG can modulate recognition by Fc $\gamma$  receptors," *Research Communications* 9:115-119.
- Malhotra et al., 1995, "Glycosylation changes of IgG associated with rheumatoid arthritis can activate complement via the mannose-binding protein," *Nature Med.* 1:237-243.
- Matteucci and Caruthers, 1980, "The Synthesis of Oligodeoxyypyrimidines on a Polymer Support," *Tetrahedron Letters* 21:719-722.
- Misiaizu et al., 1995, "Role of Antennary Structure of N-linked Sugar Chains in Renal Handling of Recombinant Human Erythropoietin," *Blood* 86:4097-4104.
- Moreman et al., 1994, "Glycosidases of the asparagine-linked oligosaccharide processing pathway," *Glycobiology* 4:113-125.
- Morgan et al., 1995, "The N-terminal of the C $\mu$ 2 domain of chimeric human IgG1 and anti-HLA-DR is necessary for C1q, Fc $\gamma$ R1 and Fc $\gamma$ RIII binding," *Immunology* 86:319-324.
- Morrison et al., 1984, "Chimeric human antibody molecules: Mouse antigen-binding domains with human constant region domains" *Proc. Natl. Acad. Sci. U.S.A.* 81:6851-6855.
- Narasimhan, 1982, "Control of Glycoprotein Synthesis," *J. Biol. Chem.* 257:10235-10242.
- Narasimhan et al., 1985, "Control of Glycoprotein Synthesis. Bovine Milk UDPgalactose:N-Acetylglucosamine  $\beta$ -4-Galactosyltransferase Catalyzes the Preferential Transfer of Galactose to the GlcNAc $\beta$ 1,2Man $\alpha$ 1,3-Branch of both Bisected and Nonbisected Complex Biantennary Asparagine-linked Oligosaccharides," *Biochemistry* 24:1694-1700.

- Naven and Harvey, 1996, "Effect of Structure on the Signal Strength of Oligosaccharides in Matrix-assisted Laser Desorption/Ionization Mass Spectrometry on Time-of-flight and Magnetic Sector Instruments," *Rapid Communications in Mass Spectrometry* 10:1361-1366.
- Neuberger et al., 1984, "Recombinant antibodies possessing novel effector functions," *Nature* 312:604-608.
- Nilsson et al., 1993, "Overlapping Distribution of Two Glycosyltransferases in the Golgi Apparatus of HeLa Cells," *J. Cell Biol.* 120:5-13.
- Nilsson et al., 1994, "Kin recognition between medial Golgi enzymes in HeLa cells," *Embo J.* 13:562-574.
- Nilsson et al., 1996, "The role of the membrane-spanning domain and stalk region of N-acetylglucosaminyltransferase I in retention, kin recognition and structural maintenance of the Golgi apparatus in HeLa cells," *J. Cell Biol.* 109:1975-1989.
- Nishikawa et al., 1992, "Purification, cDNA cloning, and Expression of UDP-N-acetylglucosamine: $\beta$ -D-mannoside  $\beta$ -1,4N-Acetylglucosaminyltransferase III from Rat Kidney," *J. Biol. Chem.* 267:18199-18204.
- Ohno et al., 1992, "Enzymatic Basis of Sugar Structures of  $\alpha$ -Fetoprotein in Hepatoma and Hepatoblastoma Cell Lines: Correlation with Activities of  $\alpha$ 1-6 Fucosyltransferase and N-Acetylglucosaminyltransferase III and V," *Int. J. Cancer* 51:315-317.
- Pâcquet et al., 1984, "Branch Specificity of Purified Rat Liver Golgi UDP-galactose:N-Acetylglucosamine  $\beta$ -1,4-Galactosyltransferase," *J. Biol. Chem.* 259:4716-4721.
- Page and Sydenham, 1991, "High Level Expression of the Humanized Monoclonal Antibody Campath-1H in Chinese Hamster Ovary Cells," *BioTechnology* 9:64-68.
- Palcic et al., 1990, "Regulation of N-Acetylglucosaminyltransferase V Activity," *J. Biol. Chem.* 265:6759-6769.
- Paulson and Colley, 1989, "Glycosyltransferases," *J. Biol. Chem.* 264:17615-17618.
- Pels Rijcken et al., 1995, "The effect of increasing nucleotide-sugar concentrations on the incorporation of sugars into glycoconjugates in rat hepatocytes," *Biochem J.* 305:865-870.
- Rabouille et al., 1995, "Mapping the distribution of Golgi enzymes involved in the construction of complex oligosaccharides," *J. Cell Science* 108:1617-1627.
- Rao and Mendicino, 1978, "Influence of Glycopeptide Structure on the Regulation of Galactosyltransferase Activity," *Biochemistry* 17:5632-5638.
- Rearick et al., 1979, "Enzymatic Characterization of  $\beta$ -D-Galactoside  $\alpha$ 2 $\rightarrow$ 3 Sialyltransferase from Porcine Submaxillary Gland," *J. Biol. Chem.* 254:4444-4451.
- Reff et al., 1994, "Depletion of B Cells in Vivo by Chimeric Mouse Human Monoclonal Antibody to CD20," *Blood* 83:435-445.
- Riechmann et al., 1988, "Reshaping human antibodies for therapy," *Nature* 332:323-327.
- Robinson et al., 1991, "Chimeric mouse-human anti-carcinoma antibodies that mediate different anti-tumor cell biological activities," *Hum. Antibod. Hybridomas* 2:84-93.
- Rogers et al., 1988, "Gene Transfer in Plants: Production of Transformed Plants Using Ti Plasmid Vectors," *Methods for Plant Molecular Biology*, Academic Press, Inc. pp. 423-463.
- Roman, 1981, "Development of Yeast as an Experimental Organism," *The Molecular Biology of the Yeast Saccharomyces*, Cold Spring Harbor Laboratory, pp. 1-9.
- Rothman and Orci, 1992, "Molecular dissection of the secretory pathway," *Nature* 355:409-415.
- Rothman and Wieland, 1996, "Protein Sorting by Transport Vesicles," *Science* 272:227-234.
- Russo et al., 1992, " $\beta$ 1,4-Galactosyltransferase: A Short NH<sub>2</sub>-terminal Fragment That Includes the Cytoplasmic and Transmembrane Domain Is Sufficient for Golgi Retention," *J. Biol. Chem.* 267:9241-9247.
- Sambanis et al., 1991, "A Model of Secretory Protein Trafficking in Recombinant A11-20 Cells," *Biotechnol. Bioeng.* 38:280-295.
- Sambrook et al., 1989, *Molecular Cloning: A Laboratory Manual*, Cold Spring Harbor Laboratory, N.Y. 2: 8.2-9.62.
- Sburlati et al., 1997, "Novel glycoform of recombinant human IFN- $\beta$  by overexpression of N-acetyl glucosaminyltransferase III," *Glycoconjugate Journal* 14(6):781, abstract P60.
- Sburlati et al., 1998, "Synthesis of Bisected Glycoforms of Recombinant IFN- $\beta$  by Overexpression of  $\beta$ -1,4-N-Acetylglucosaminyltransferases III in Chinese Hamster Ovary Cells," *Biotechnol. Prog.* 14:189-192.
- Schachter, 1986, "Biosynthetic controls that determine the branching and microheterogeneity of protein-bound oligosaccharides," *Biochem. Cell Biol.* 64:163-181.
- Shao and Wold, 1995, "The effect of the protein matrix proximity of glycan reactivity in a glycoprotein model," *Eur. J. Biochem.* 228:79-85.
- Shao and Wold, 1988, "The Effect of the Protein Matrix on Glycan Processing in Glycoproteins," *J. Biol. Chem.* 263:5771-5774.
- Sheares and Robbins, 1986, "Glycosylation of ovalbumin in a heterologous cell: Analysis of oligosaccharide chains of the cloned glycoprotein in mouse L cells," *Proc. Natl. Acad. Sci. USA* 83:1993-1997.
- Shelikoff et al., 1983, "A Modeling Framework for the Study of Protein Glycosylation," *Biotechnol. Bioeng.* 50:73-90.
- Smith et al., 1983, "Molecular Engineering of the *Autographa californica* Nuclear Polyhedrosis Virus Genome: Deletion Mutations Within the Polyhedrin Gene," *J. Virol.* 46:584-593.
- Spellman et al., 1989, "Carbohydrate Structures of Human Tissue Plasminogen Activator Expressed in Chinese Hamster Ovary Cells," *J. Biol. Chem.* 264:14100-14111.
- Surfus et al., 1996, "Anti-Renal-Cell Carcinoma Chimeric Antibody G250 Facilitates Antibody-Dependent Cellular Cytotoxicity with In Vitro and In Vivo Interleukin-2-Activated Effectors," *Journal of Immunother.* 19:184-191.
- Tabas and Kornfeld, 1979 "Purification and Characterization of a Rat Liver Golgi  $\alpha$ -Mannosidase Capable of Processing Asparagine-linked Oligosaccharides," *J. Biol. Chem.* 254:11655-11663.
- Takamatsu et al., 1987, "Expression of bacterial chloramphenicol acetyltransferase gene in tobacco plants mediated by TMV-RNA," *EMBO J.* 6:307-311.
- Takeda et al., 1985, "Construction of chimaeric processed immunoglobulin genes containing mouse variable and human constant region sequences," *Nature* 314:452-454.
- Taniguchi et al., 1989, "Glycosyltransferase Assays Using Pyridylaminated Acceptors: N-Acetylglucosaminyltransferase III, IV, and V," *Methods Enzymol.* 179: 397-408.

- Trill et al., 1995, "Production of monoclonal antibodies in COS and CHO cells," *Current Opinion in Biotechnology* 6:553-560.
- Umana et al., 1999, "Engineered glycoforms of an antineuroblastoma IgG1 with optimized antibody-dependent cellular cytotoxic activity," *Nature Biotechnology* 17:176-180.
- Varki, A., 1993, "Biological roles of oligosaccharides: all of the theories are correct," *Glycobiology* 3:97-130.
- Velasco et al., 1993, "Cell Type-dependent Variations in the Subcellular Distribution of  $\alpha$ -Mannosidase I and II," *J. Cel Biol.* 122:39-51.
- Watson et al., 1994, "Structure determination of the intact major sialylated oligosaccharide chains of recombinant human erythropoietin expressed in Chinese hamster ovary cells," *Glycobiology* 4:227-237.
- Wiest et al., 1990, "Membrane Biogenesis during B Cell Differentiation: Most Endoplasmic Reticulum Proteins Are Expressed Coordinately," *Journal of Cell Biology* 110:1501-1511.
- Wright and Morrison, 1997, "Effect of glycosylation on antibody function: implications for genetic engineering," *Tibtech* 15: 26-31.
- Wyss and Wagner, 1996, "The structural role of sugars in glycoproteins," *Current Opinion in Biotechnology* 7:409-416.
- Yamaguchi and Fukuda, 1995, "Golgi Retention Mechanism of  $\beta$ -1,4-Galactosyltransferase," *J. Biol. Chem.* 270:12170-12176.
- Yoshimura et al., 1995, "Suppression of lung metastasis of B16 mouse melanoma by N-acetylglucosaminyltransferase III gene transfection," *Proc. Natl. Acad. Sci. USA* 92:8754-8758.
- Yu Ip et al., 1994, "Structural Characterization of the N-Glycans of a Humanized Anti-CD18 Murine Immunoglobulin G," *Arch. Biochem. Biophys.* 308:387-399.

\* cited by examiner

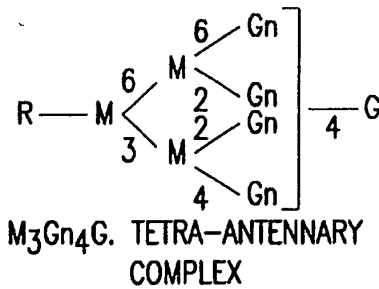
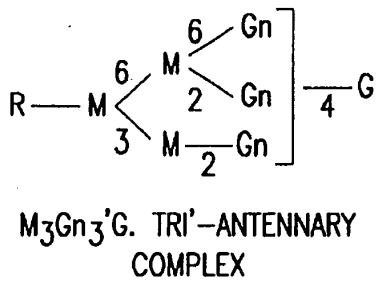
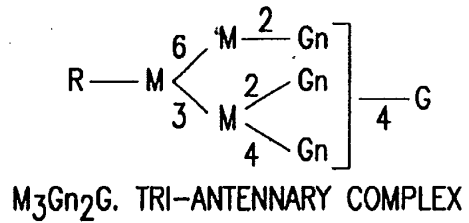
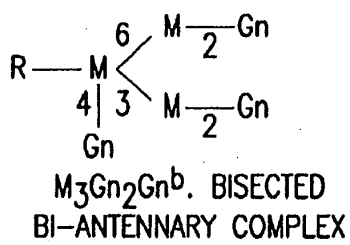
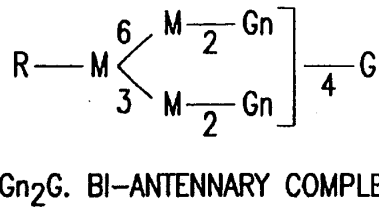
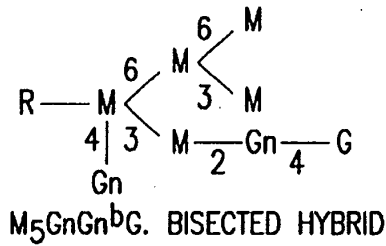
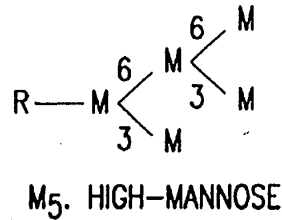
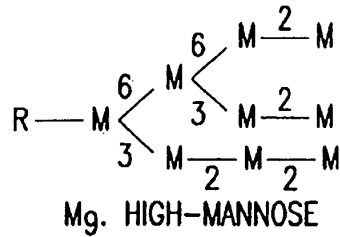


FIG. 1

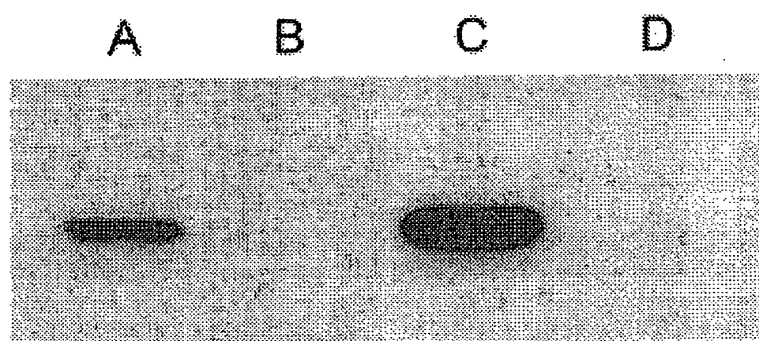


FIG. 2

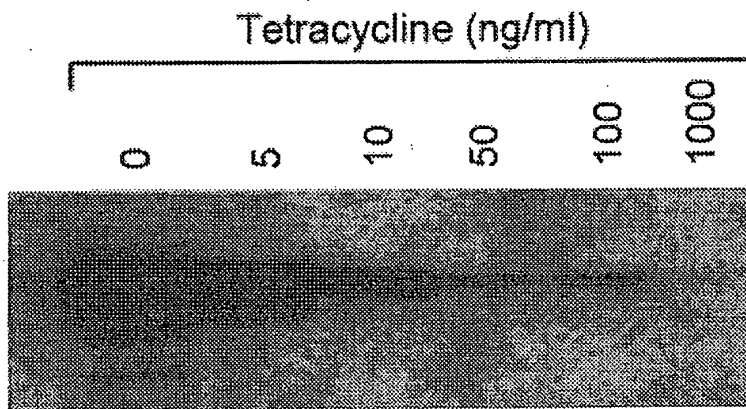


FIG. 3

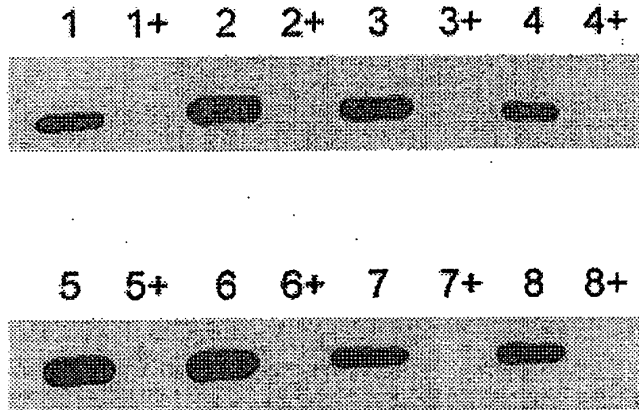


FIG. 4A

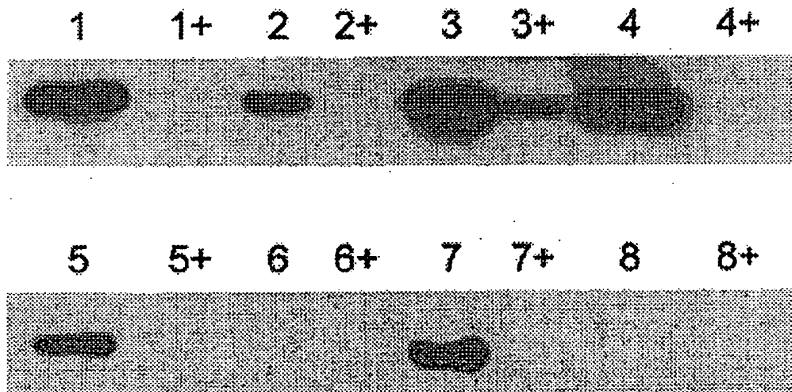


FIG. 4B



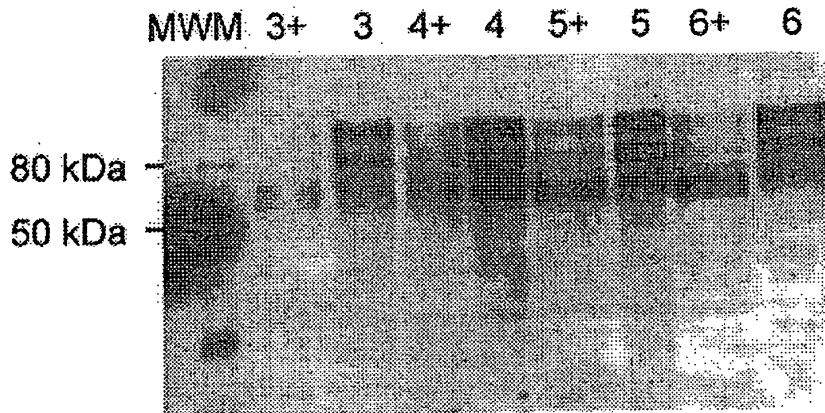


FIG. 5A

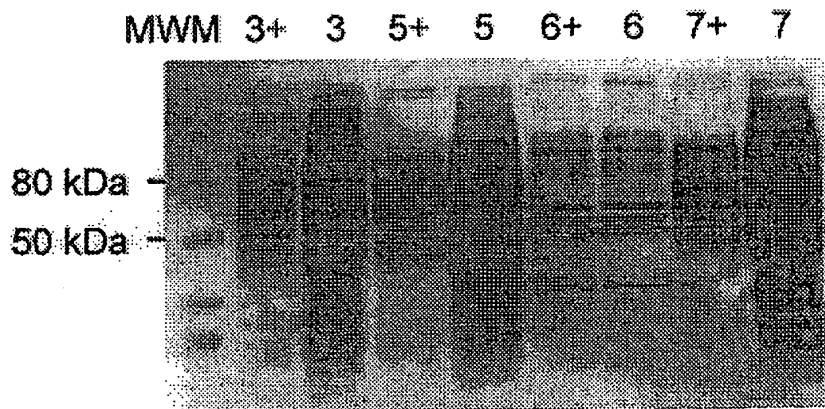


FIG. 5B

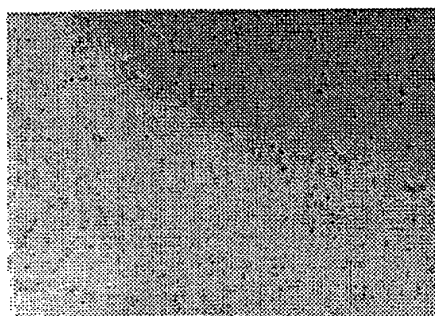


FIG. 6A

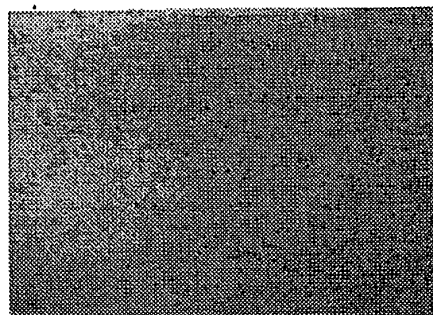


FIG. 6B

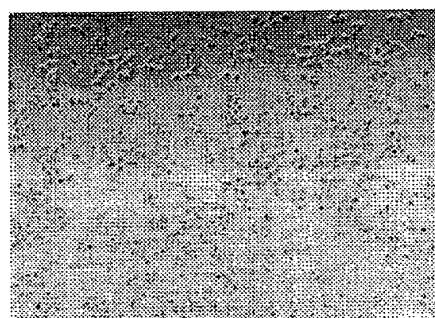


FIG. 6C

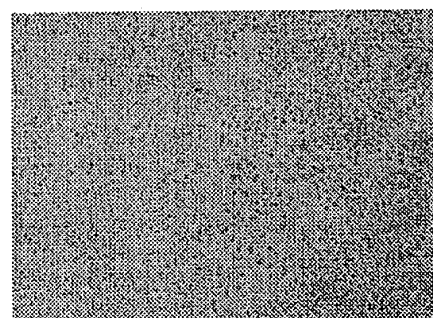


FIG. 6D

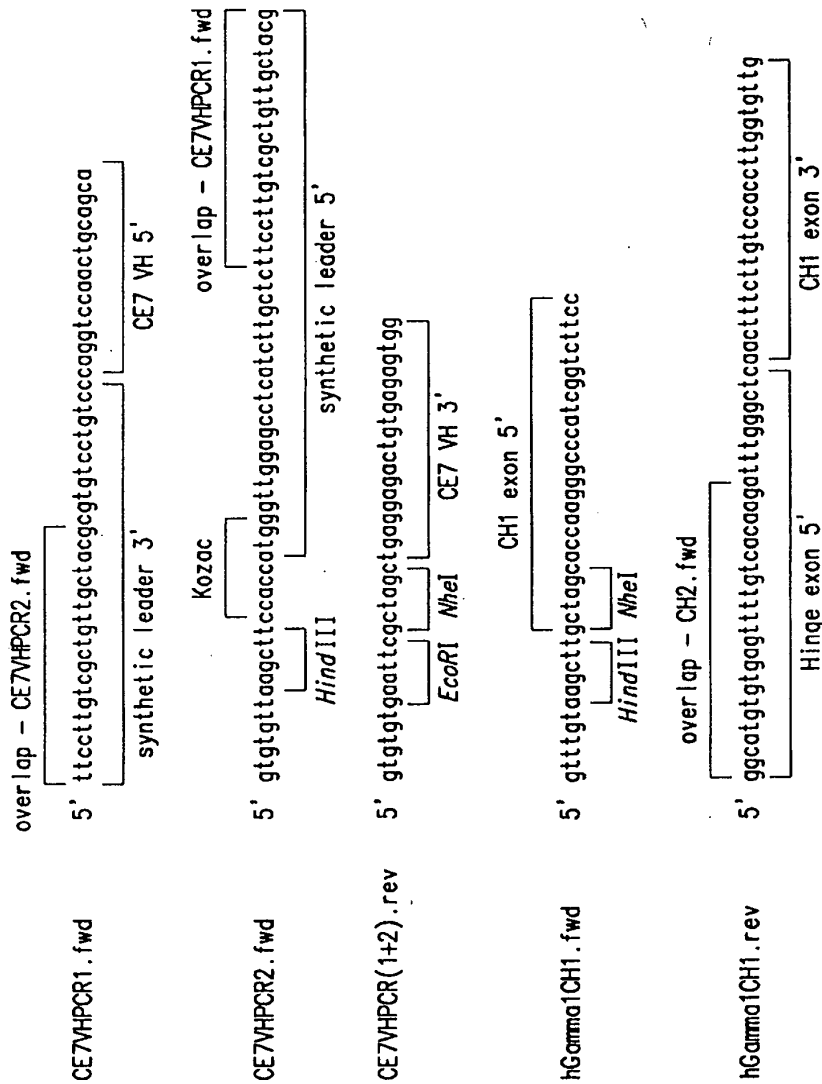


FIG.7A

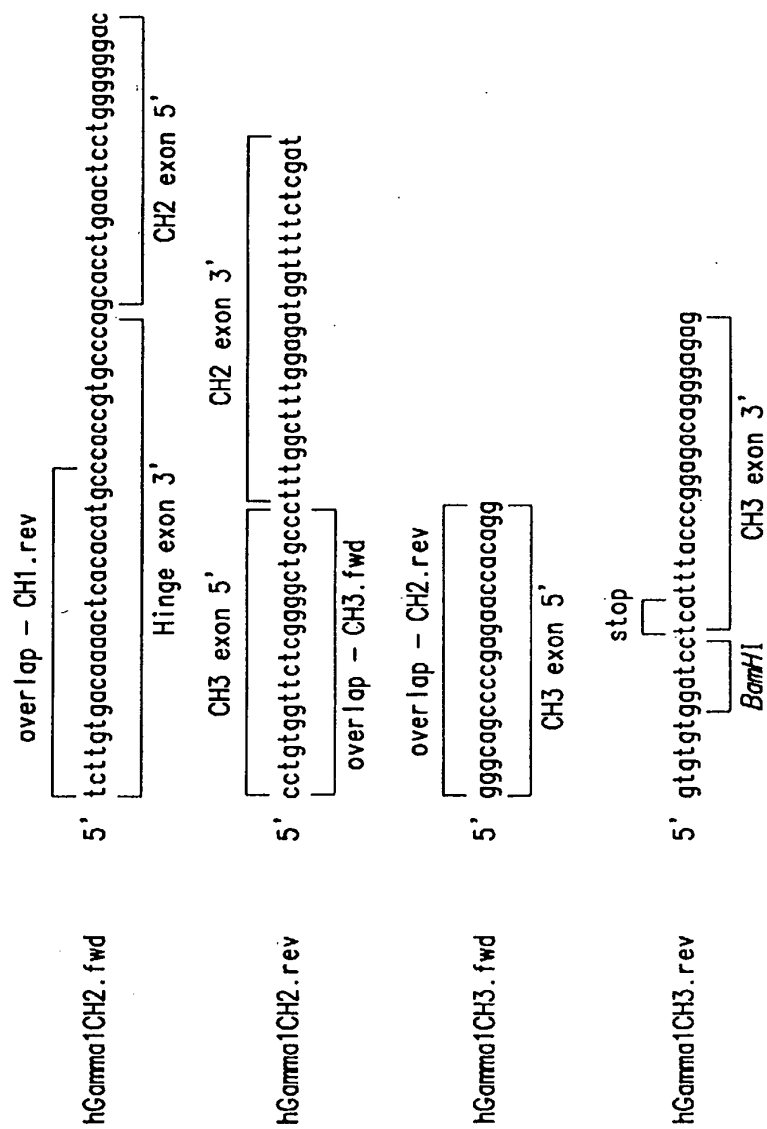


FIG.7B

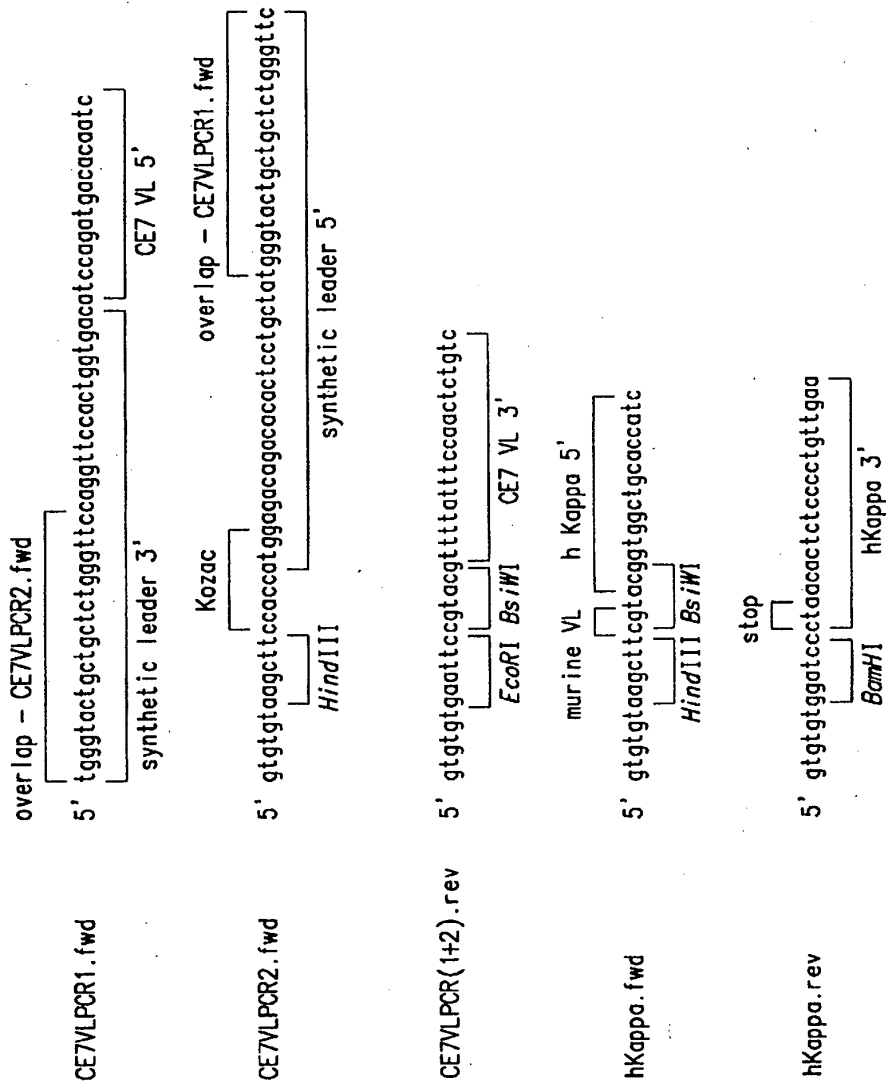


FIG.8

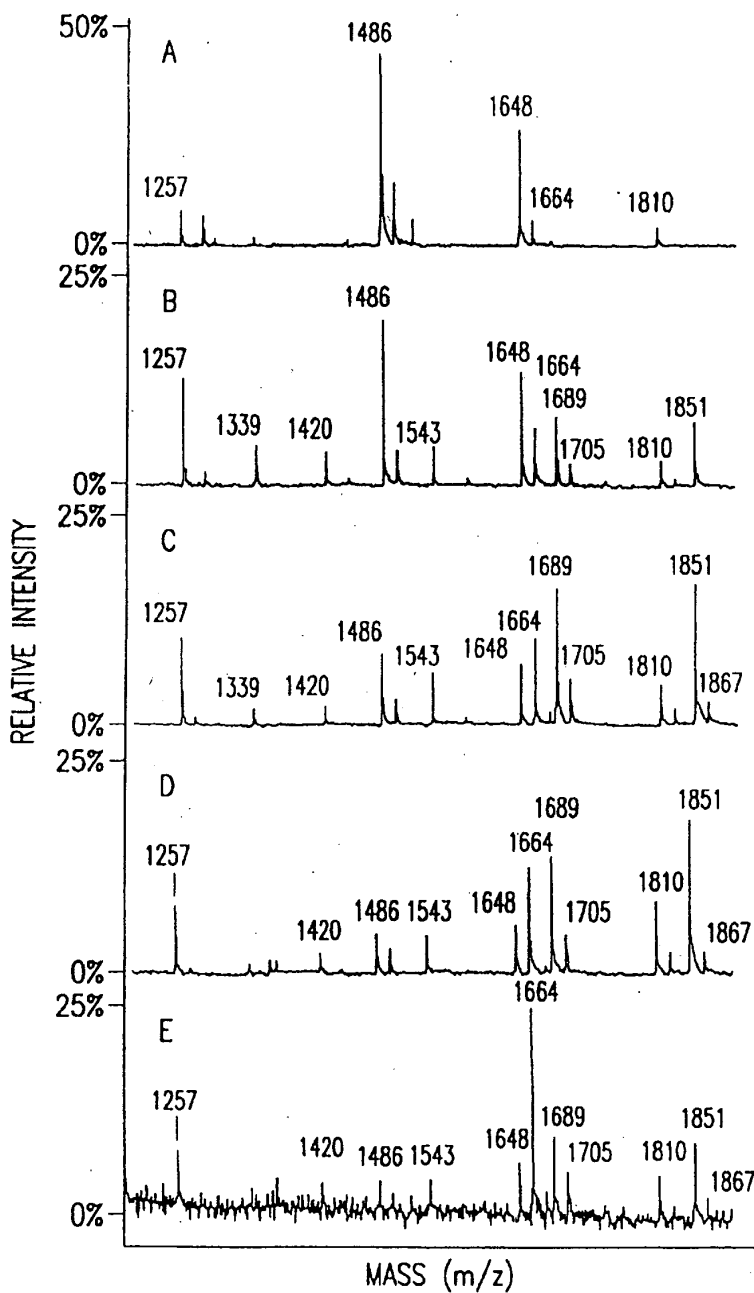


FIG.9

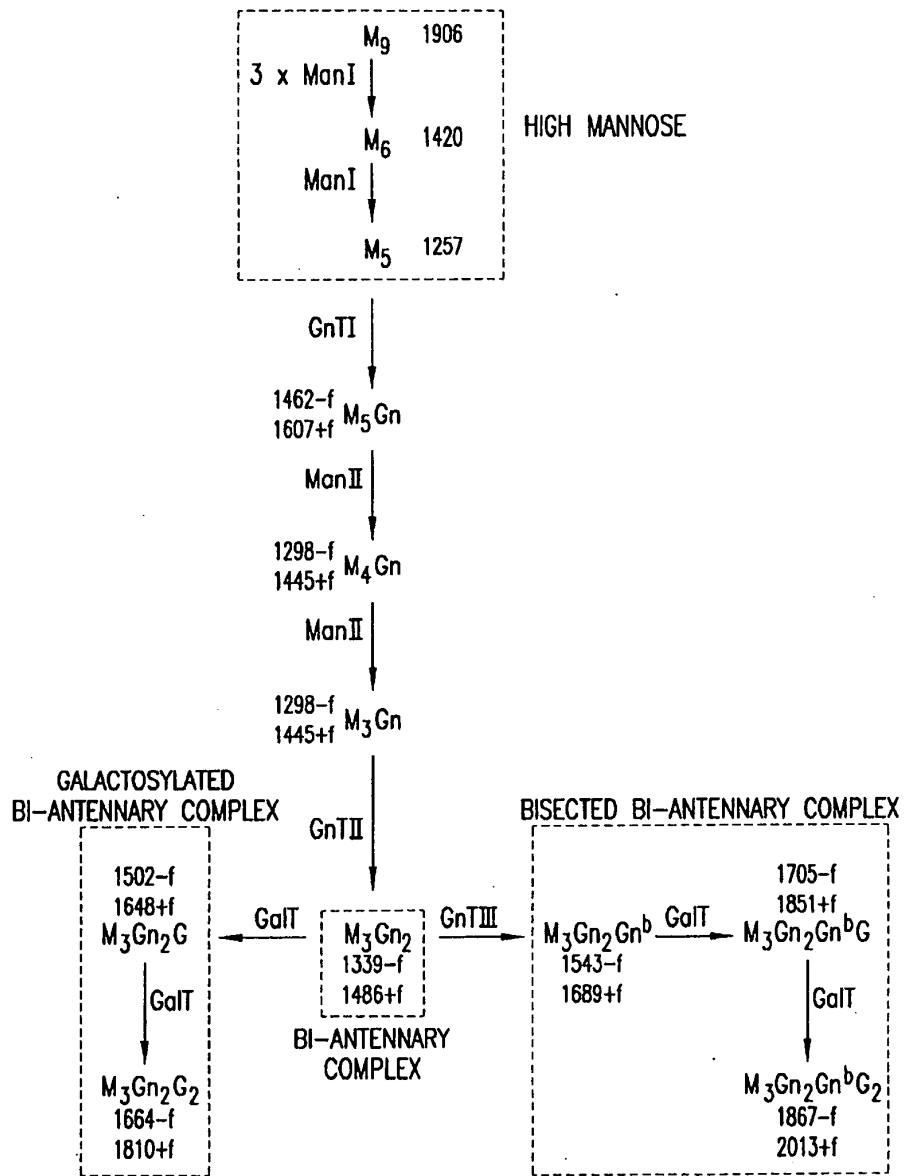


FIG.10

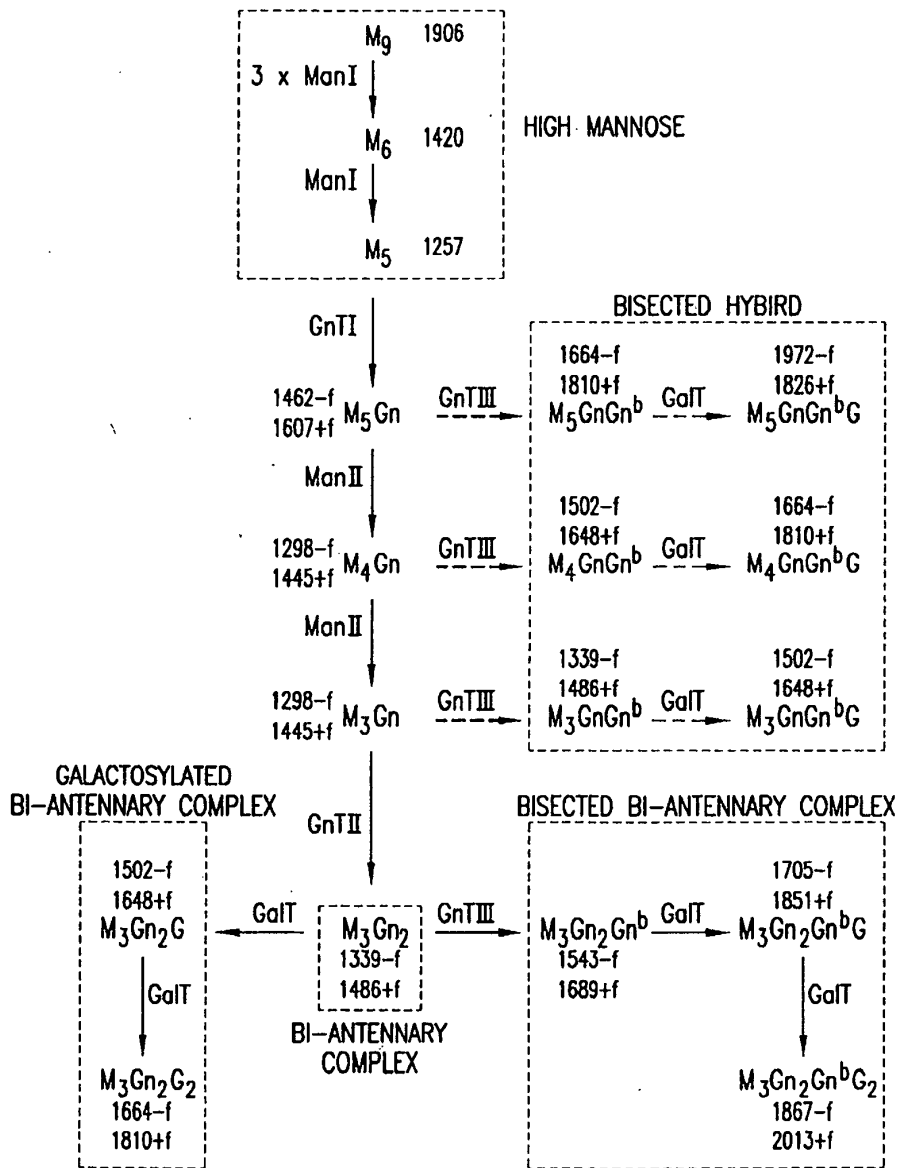


FIG.11



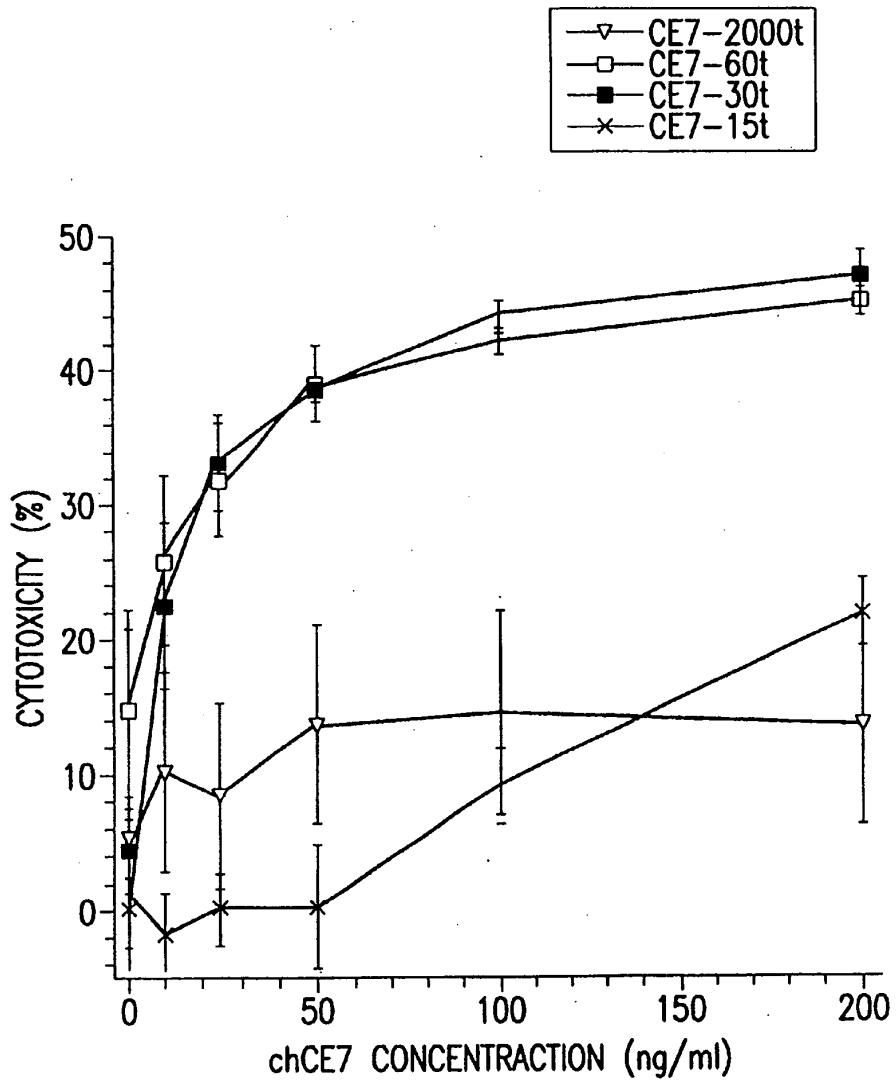


FIG.12

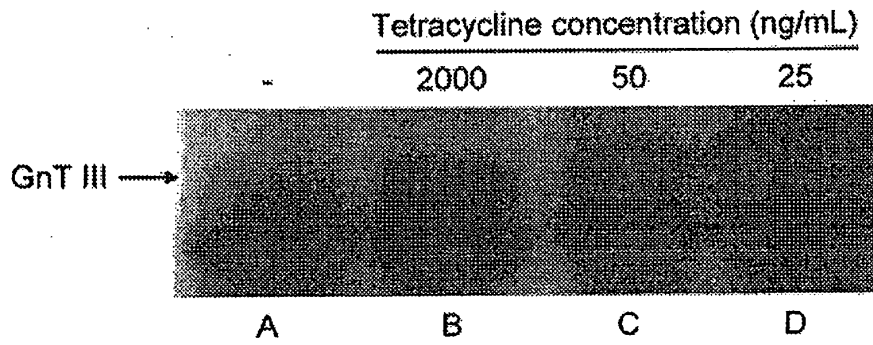


FIG. 13

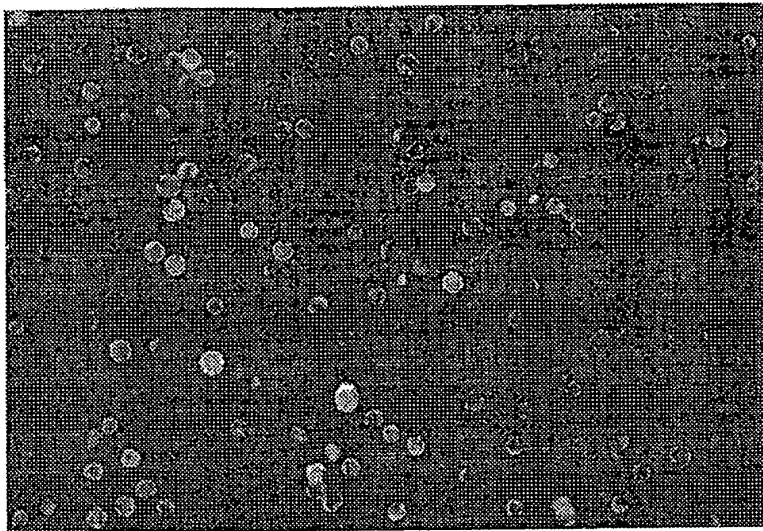


FIG. 14A

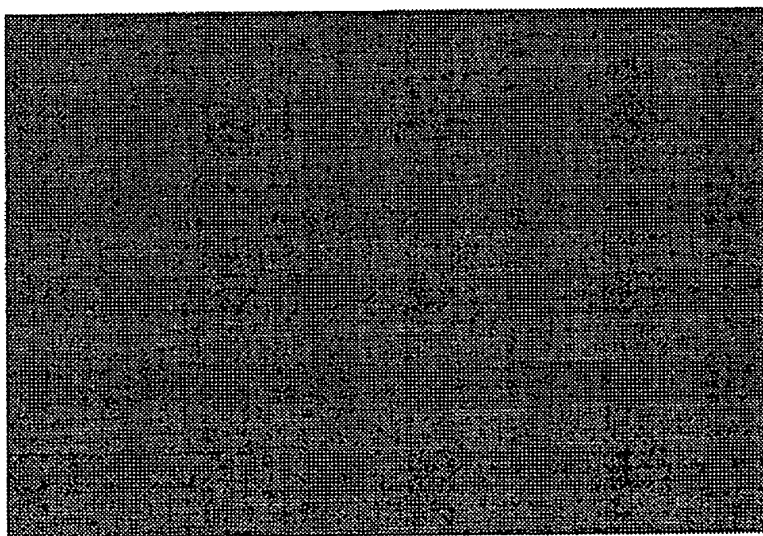


FIG. 14B

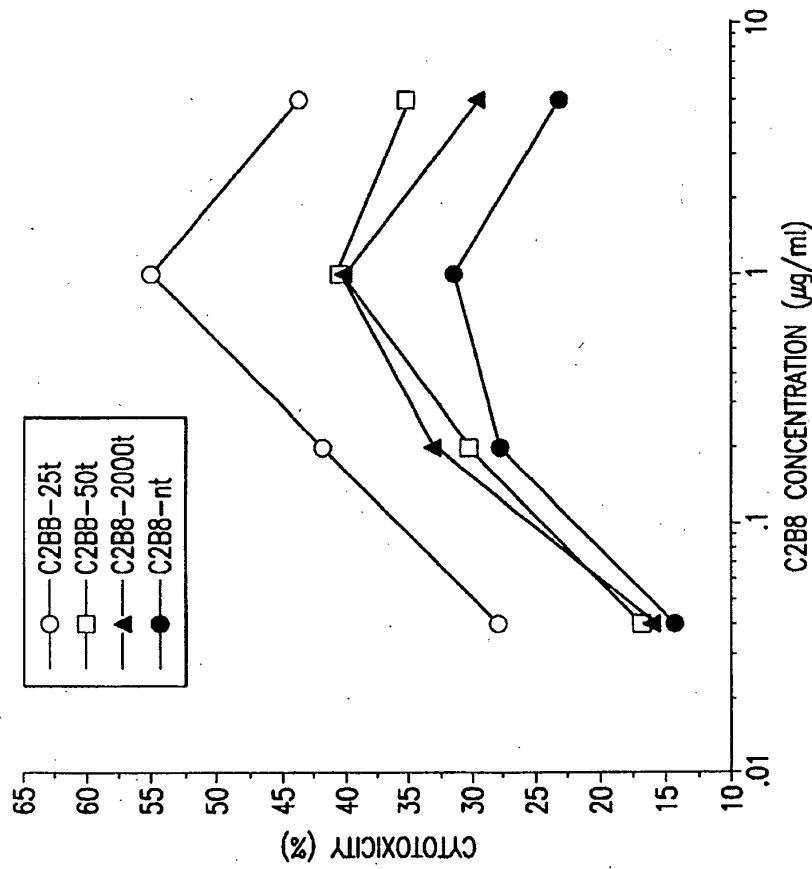


FIG.15

1

## GLYCOSYLATION ENGINEERING OF ANTIBODIES FOR IMPROVING ANTIBODY-DEPENDENT CELLULAR CYTOTOXICITY

### I. RELATION TO OTHER APPLICATIONS

This application claims priority to U.S. Provisional Application Serial No. 60/082,581, filed Apr. 20, 1998, incorporated herein by reference in its entirety.

### II. FIELD OF THE INVENTION

The present invention relates to the field of glycosylation engineering of proteins. More particularly, the present invention relates to glycosylation engineering to generate proteins with improved therapeutic properties, including antibodies with enhanced antibody-dependent cellular cytotoxicity.

### III. BACKGROUND OF THE INVENTION

Glycoproteins mediate many essential functions in human beings, other eukaryotic organisms, and some prokaryotes, including catalysis, signalling, cell-cell communication, and molecular recognition and association. They make up the majority of non-cytosolic proteins in eukaryotic organisms. Lis and Sharon, 1993, *Eur. J. Biochem.* 218:1-27. Many glycoproteins have been exploited for therapeutic purposes, and during the last two decades, recombinant versions of naturally-occurring, secreted glycoproteins have been a major product of the biotechnology industry. Examples include erythropoietin (EPO), therapeutic monoclonal antibodies (therapeutic mAbs), tissue plasminogen activator (tPA), interferon- $\beta$ , (IFN- $\beta$ ), granulocyte-macrophage colony stimulating factor (GM-CSF), and human chorionic gonadotrophin (hCG). Cumming et al., 1991, *Glycobiology* 1:115-130.

The oligosaccharide component can significantly affect properties relevant to the efficacy of a therapeutic glycoprotein, including physical stability, resistance to protease attack, interactions with the immune system, pharmacokinetics, and specific biological activity. Such properties may depend not only on the presence or absence, but also on the specific structures, of oligosaccharides. Some generalizations between oligosaccharide structure and glycoprotein function can be made. For example, certain oligosaccharide structures mediate rapid clearance of the glycoprotein from the bloodstream through interactions with specific carbohydrate binding proteins, while others can be bound by antibodies and trigger undesired immune reactions. Jenkins et al., 1996, *Nature Biotechnol.* 14:975-981.

Mammalian cells are the preferred hosts for production of therapeutic glycoproteins, due to their capability to glycosylate proteins in the most compatible form for human application. Cumming, 1991, supra; Jenkins et al., 1996, supra. Bacteria very rarely glycosylate proteins, and like other types of common hosts, such as yeasts, filamentous fungi, insect and plant cells, yield glycosylation patterns associated with rapid clearance from the blood stream, undesirable immune interactions, and in some specific cases, reduced biological activity. Among mammalian cells, Chinese hamster ovary (CHO) cells have been most commonly used during the last two decades. In addition to giving suitable glycosylation patterns, these cells allow consistent generation of genetically stable, highly productive clonal cell lines. They can be cultured to high densities in simple bioreactors using serum-free media, and permit the devel-

2

opment of safe and reproducible bioprocesses. Other commonly used animal cells include baby hamster kidney (BHK) cells, NSO- and SP2/O-mouse myeloma cells. More recently, production from transgenic animals has also been tested. Jenkins et al., 1996, supra.

The glycosylation of recombinant therapeutic proteins produced in animal cells can be engineered by overexpression of glycosyl transferase genes in host cells. Bailey, 1991, *Science* 252:1668-1675. However, previous work in this field has only used constitutive expression of the glycoprotein-modifying glycosyl transferase genes, and little attention has been paid to the expression level.

### IV. SUMMARY OF THE INVENTION

The present invention is directed, generally, to host cells and methods for the generation of proteins having an altered glycosylation pattern resulting in improved therapeutic values. In one specific embodiment, the invention is directed to host cells that have been engineered such that they are capable of expressing a preferred range of a glycoprotein-modifying glycosyl transferase activity which increases complex N-linked oligosaccharides carrying bisecting GlcNAc. In other embodiments, the present invention is directed to methods for the generation of modified glycoforms of glycoproteins, for example antibodies, including whole antibody molecules, antibody fragments, or fusion proteins that include a region equivalent to the Fc region of an immunoglobulin, having an enhanced Fc-mediated cellular cytotoxicity, and glycoproteins so generated. The invention is based, in part, on the inventors' discovery that there is an optimal range of glycoprotein-modifying glycosyl transferase expression for the maximization of complex N-linked oligosaccharides carrying bisecting GlcNAc.

More specifically, the present invention is directed to a method for producing altered glycoforms of proteins having improved therapeutic values, e.g., an antibody which has an enhanced antibody dependent cellular cytotoxicity (ADCC), in a host cell. The invention provides host cells which harbor a nucleic acid encoding the protein of interest, e.g., an antibody, and at least one nucleic acid encoding a glycoprotein-modifying glycosyl transferase. Further, the present invention provides methods and protocols of culturing such host cells under conditions which permit the expression of said protein of interest, e.g., the antibody having enhanced antibody dependent cellular cytotoxicity. Further, methods for isolating the so generated protein having an altered glycosylation pattern, e.g., the antibody with enhanced antibody dependent cellular cytotoxicity, are described.

Furthermore, the present invention provides alternative glycoforms of proteins having improved therapeutic properties. The proteins of the invention include antibodies with an enhanced antibody-dependent cellular cytotoxicity (ADCC), which have been generated using the disclosed methods and host cells.

### V. BRIEF DESCRIPTION OF THE DRAWINGS

FIG. 1 depicts the representation of typical oligosaccharide structures.

FIG. 2 depicts a Western blot analysis of tetracycline-regulated expression of GnT III in two different tTA-producing CHO clones. CHO12 (lanes A and B) and CHO17 (lanes C and D) cells were transfected with the pUDH10-3GnTIII expression vector and cultured for 36 h in the absence (lanes A and C) or presence of tetracycline, at a concentration of 400 ng/ml (lanes B and D). Cell lysates

were then prepared for western blot analysis probing with an antibody (9E10), which recognizes specifically the c-myc tag added to GnT III at its carboxy-terminus.

FIG. 3 depicts determination of the range of tetracycline concentrations where myc-tagged GnT III expression can be controlled. CHO17 cells were transfected with the pUDH10-3-GnTIII expression vector and then cultured for 48 h in the presence of the indicated concentrations of tetracycline. GnT III levels in cell lysates from these cultures were compared using western blot analysis. GnT III was detected via the c-myc tag using 9E10 antibody.

FIGS. 4A through 4B depict screening of CHO clones for stable, tetracycline-regulated expression of GnT V (FIG. 4A) or myc-tagged GnT III (FIG. 4B) glycosyltransferases by western blot analysis. CHO17 cells were co-transfected with a vector for expression of puromycin resistance (pPUR) and either pUHD10-3GnTV (FIG. 4A) or pUDH10-3GnTIII (FIG. 4B) and stable CHO clones were selected for resistance to puromycin (7.5  $\mu$ M), in the presence of tetracycline (2  $\mu$ g/ml). Eight clones (1-8) for each glycosyltransferase were cultured for 48 h in the absence or presence (+) of tetracycline (2  $\mu$ g/ml) and analysed by western blot using either an anti-GnT V antibody (FIG. 4A) or an anti-myc (9E10) antibody (FIG. 4B).

FIGS. 5A and 5B depict verification of activity of heterologous GnT V (FIG. 5A) and Gn T III (FIG. 5B) glycosyltransferases in vivo by lectin blot analysis. Cellular glycoproteins from various stable clones (numbered as in FIG. 4), cultured in the absence or presence (+) of tetracycline (2  $\mu$ g/ml), were resolved by SDS-PAGE, blotted to a membrane, and probed with either L-PHA (FIG. 5A) or E-PHA (FIG. 5B) lectins. These lectins bind with higher affinity to the oligosaccharide products of reactions catalyzed by GnT V and GnT III, respectively, than to the oligosaccharide substrates of these reactions. A molecular weight marker (MWM) was run in parallel. A comparison of lectin blots in FIGS. 5A and 5B indicates a broader range of substrates, among the endogenous CHO cell glycoproteins, for GnT III (FIG. 5B) than for GnT V (FIG. 5A).

FIGS. 6A through 6D depict inhibition of cell growth upon glycosyltransferase overexpression. CHO-tet-GnTIII cells were seeded to 5-10% confluency and cultured in the absence (FIGS. 6A and 6B) or presence (FIGS. 6C and 6D) of tetracycline. Cultures were photographed 45 (FIGS. 6A and 6C) and 85 (FIGS. 6B and 6D) hours after seeding.

FIG. 7 depicts sequences of oligonucleotide primers used in PCRs for the construction of the chCE7 heavy chain gene: CE7VHPCR1.fwd (SEQ ID NO:1), CE7VHPCR2.fwd (SEQ ID NO:2), CE7VHPCR (1+2).rev (SEQ ID NO:3), hGamma1CH1.fwd (SEQ ID NO:4), hGamma1CH1, rev (SEQ ID NO:5), hGamma1CH2.fwd (SEQ ID NO:6), hGamma1CH2.rev (SEQ ID NO:7), hGamma1CH3.fwd (SEQ ID NO:8), hGamma1CH3.rev (SEQ ID NO:9). Forward and reverse primers are identified by the suffixes "fwd" and ".rev", respectively. Overlaps between different primers, necessary to carry out secondary PCR steps using the product of a primary PCR step as a template, are indicated. Restriction sites introduced, sequences annealing to the CE7 chimeric genomic DNA, and the synthetic leader sequence introduced, are also indicated.

FIG. 8 depicts sequences of oligonucleotide primers used in PCRs for the construction of the chCE7 light chain gene: CE7VLP1.fwd (SEQ ID NO: 10), CE7VLP2.fwd (SEQ ID NO:11), CE7VLP3(1+2).rev (SEQ ID NO:12), hKappa.fwd (SEQ ID NO:13), hKappa.rev (SEQ ID NO:

14). Forward and reverse primers are identified by the suffixes "fwd" and ".rev" respectively. Overlaps between different primers, necessary to carry out secondary PCR steps using as a template the product of a primary PCR step, are indicated. Restriction sites introduced, sequences annealing to the CE7 chimeric genomic DNA, and the leader sequence introduced, are also indicated.

FIGS. 9A-E depict MALDI/TOF-MS spectra of neutral oligosaccharide mixtures from chCE7 samples produced either by SP2/0 mouse myeloma cells (FIG. 9A, oligosaccharides from 50  $\mu$ g of CE7-SP2/0), or by CHO-tetGnTIII-chCE7 cell cultures differing in the concentration of tetracycline added to the media, and therefore expressing the GnT III gene at different levels. In decreasing order of tetracycline concentration, i.e., increasing levels of GnT III gene expression, the latter samples are: CE7-2000t (FIG. 9B, oligosaccharides from 37.5  $\mu$ g of antibody), CE7-60t (FIG. 9C, oligosaccharides from 37.5  $\mu$ g of antibody), CE7-30t (FIG. 9D, oligosaccharides from 25  $\mu$ g of antibody) and CE7-15t (FIG. 9E, oligosaccharides from 10  $\mu$ g of antibody).

FIG. 10 depicts N-linked oligosaccharide biosynthetic pathways leading to bisected complex oligosaccharides via a GnT III-catalyzed reaction. M stands for Mannose; Gn, N-acetylglucosamine (G1cNAc); G, galactose; Gn<sup>b</sup>, bisecting G1cNAc; F, fucose. The oligosaccharide nomenclature consists of enumerating the M, Gn, and G residues attached to the core oligosaccharide and indicating the presence of a bisecting G1cNAc by including a Gn<sup>b</sup>. The oligosaccharide core is itself composed of 2 Gn residues and may or may not include a fucose. The major classes of oligosaccharides are shown inside dotted frames. Man I stands for Golgi mannosidase; GnT, G1cNAc transferase; and GalT, for galactosyltransferase. The mass associated with the major, sodium-associated oligosaccharide ion that is observed MALDI/TOF-MS analysis is shown beside each oligosaccharide. For oligosaccharides which can potentially be core-fucosylated, the masses associated with both fucosylated (+f) and non-fucosylated (-f) forms are shown.

FIG. 11 depicts N-linked oligosaccharide biosynthetic pathway leading to bisected complex and bisected hybrid oligosaccharides via GnT III-catalyzed reactions. M stands for mannose; Gn N-acetylglucosamine (G1cNAc); G, galactose; Gn<sup>b</sup>, bisecting G1cNAc; f, fucose. The oligosaccharide nomenclature consists of enumerating the M, Gn, and G residues attached to the common oligosaccharide and indicating the presence of bisecting G1cNAc by including a Gn<sup>b</sup>. The oligosaccharide core is itself composed of 2 Gn residues and may or not include a fucose. The major classes of oligosaccharides are shown inside dotted frames. Man I stands for Golgi mannosidase; GnT, G1cNAc transferase; and GalT, for galactosyltransferase. The mass associated with major, sodium-associated oligosaccharide ion that is observed in MALDI/TOF-MS analysis is shown beside each oligosaccharide. For oligosaccharides which can potentially be core-fucosylated, the masses associated with both fucosylated (+f) and non-fucosylated (-f) forms are shown.

FIG. 12 depicts ADCC activity of different chCE7 samples. Lysis of IMR-32 neuroblastoma cells by human lymphocytes (target:effector ratio of 1:19, 16 h incubation at 37° C.), mediated by different concentrations of chCE7 samples, was measured via retention of a fluorescent dye. The percentage of cytotoxicity is calculated relative to a total lysis control (by means of a detergent), after subtraction of the signal in the absence of antibody.

FIG. 13 depicts the GnT III expression of different cultures of CHO-tet-GnTIII grown at different tetracycline

5

concentrations used to produce distinct C2B8 antibody samples. Cell lysates from each culture grown at 2000 ng/ml (Lane C) and 25 ng/ml (Lane D) tetracycline concentrations were resolved by SDS-PAGE, blotted onto a membrane, and probed with 9E10 (see supra) and anti-mouse horseradish peroxidase as primary and secondary antibodies, respectively. Lane A depicts a negative control.

FIGS. 14A and 14B depict the specificity of antigen binding of the C2B8 anti-CD20 monoclonal antibody using an indirect immunofluorescence assay with cells in suspension. CD20 positive cells (SB cells; ATCC deposit no. ATCC CCL120) and CD20 negative cells (HSB cells; ATCC deposit no. ATCC CCL120.1), FIG. 14A and 14B respectively, were utilized. Cells of each type were incubated with C2B8 antibody produced at 25 ng/ml tetracycline as a primary antibody. Negative controls included HBSSB instead of primary antibody. An anti-human IgG Fc specific, polyclonal, FITC conjugated antibody was used for all samples as a secondary antibody.

FIG. 15 depicts the ADCC activity of different C2B8 antibody samples at different antibody concentrations (0.04–5  $\mu$ g/ml). Sample C2B8-nt represents the ADCC activity of the C2B8 antibody produced in a cell line without GnT III expression. Samples C2B8-2000t, C2B8-50t and C2B8-25t show the ADCC activity of three antibody samples produced at decreasing tetracycline concentrations (i.e., increasing GnT III expression).

#### VI. DEFINITIONS

Terms are used herein as generally used in the art, unless otherwise defined in the following:

As used herein, the term antibody is intended to include whole antibody molecules, antibody fragments, or fusion proteins that include a region equivalent to the Fc region of an immunoglobulin.

As used herein, the term glycoprotein-modifying glycosyl transferase refers to an enzyme that effects modification of the glycosylation pattern of a glycoprotein. Examples of glycoprotein-modifying glycosyl transferases include, but are not limited to glycosyl transferases such as GnT III, GnT V, GalT, and Man II.

As used herein, the term glycosylation engineering is considered to include any sort of change to the glycosylation pattern of a naturally occurring polypeptide or fragment thereof. Glycosylation engineering includes metabolic engineering of the glycosylation machinery of a cell, including genetic manipulations of the oligosaccharide synthesis pathways to achieve altered glycosylation of glycoproteins expressed in cells. Furthermore, glycosylation engineering includes the effects of mutations and cell environment on glycosylation.

As used herein, the term host cell covers any kind of cellular system which can be engineered to generate modified glycoforms of proteins, protein fragments, or peptides of interest, including antibodies and antibody fragments. Typically, the host cells have been manipulated to express optimized levels of at least one glycoprotein-modifying glycosyl transferase, including, but not limited to GnT III, GnT V, GalT, and Man II, and/or at least one glycosidase. Host cells include cultured cells, e.g., mammalian cultured cells, such as CHO cells, BHK cells, NSO cells, SP2/0 cells, or hybridoma cells, yeast cells, and insect cells, to name only a few, but also cells comprised within a transgenic animal or cultured tissue.

As used herein, the term Fc-mediated cellular cytotoxicity is intended to include antibody dependent cellular cytotoxicity

6

(ADCC), and cellular cytotoxicity directed to those cells that have been engineered to express on their cell surface an Fc-region or equivalent region of an immunoglobulin G, and cellular cytotoxicity mediated by a soluble fusion protein consisting of a target protein domain fused to the N-terminus of an Fc-region or equivalent region of an immunoglobulin G.

#### VII. DETAILED DESCRIPTION OF THE INVENTION

##### A. General Overview

The objective of the present invention is to provide glycoforms of proteins, in particular antibodies, including whole antibody molecules, antibody fragments, or fusion proteins that include a region equivalent to the Fc region of an immunoglobulin, to produce new variants of a therapeutic protein. The invention is based, in part, on the inventors' discovery that the glycosylation reaction network of a cell can be manipulated to maximize the proportion of certain glycoforms within the population, and that certain glycoforms have improved therapeutic characteristics. The invention is further based, in part, on the discovery of ways to identify glycoforms of proteins which have an improved therapeutic value, and how to generate them reproducibly. The invention is further based, in part, on the discovery that there is a preferred range of glycoprotein-modifying glycosyl transferase expression in the antibody-generating cell, for increasing complex N-linked oligosaccharides carrying bisecting GlcNAc.

As such, the present invention is directed, generally, to methods for the glycosylation engineering of proteins to alter and improve their therapeutic properties. More specifically, the present invention describes methods for producing in a host cell an antibody which has an altered glycosylation pattern resulting in an enhanced antibody dependent cellular cytotoxicity (ADCC). For the practice of the methods, the present invention provides host cells which harbor a nucleic acid encoding an antibody and at least one nucleic acid encoding a glycoprotein-modifying glycosyl transferase. Further, the present invention provides methods and protocols of culturing such host cells under conditions which permit the expression of the desired antibody having an altered glycosylation pattern resulting in an enhanced antibody dependent cellular cytotoxicity. Further, methods for isolating the so generated antibody with enhanced antibody dependent cellular cytotoxicity are described.

In more specific embodiments of the invention, two monoclonal antibodies, namely the anti-neuroblastoma antibody chCE7, and the anti-CD20 antibody C2B8, have been used as model therapeutic glycoproteins, and the target glycoforms have been those carrying a special class of carbohydrate, namely bi-antennary complex N-linked oligosaccharides modified with bisecting N-acetylglucosamine (GlcNAc). In the model system provided by the invention, CHO cells are used as host cells, although many other cell systems may be contemplated as host cell system. The glycosyl transferase that adds a bisecting GlcNAc to various types of N-linked oligosaccharides, GlcNAc-transferase III (GnT III), is not normally produced by CHO cells. Stanley and Campell, 1984, *J. Biol. Chem.* 261:13370–13378.

To investigate the effects of GnT III overexpression experimentally, a CHO cell line with tetracycline-regulated overexpression of a rat GnT III cDNA was established. Using this experimental system, the inventors discovered that overexpression of GnT III to high levels led to growth inhibition and was toxic to the cells. Another CHO cell line with tetracycline-regulated overexpression of GnT V, which is a distinct glycosyl transferase, showed the same inhibitory

effect, indicating that this may be a general feature of glycoprotein-modifying glycosyl transferase overexpression. The effect of the enzyme expression on the cell growth sets an upper limit to the level of glycoprotein-modifying glycosyl transferase overexpression and may therefore also limit the extent to which poorly accessible glycosylation sites can be modified by engineering of glycosylation pathways and patterns using unregulated expression vectors.

The production of a set of chCE7 mAb and C2B8 samples differing in their glycoform distributions by controlling GnT III expression in a range between basal and toxic levels are disclosed. Measurement of the ADCC activity of the chCE7 mAb samples showed an optimal range of GnT III expression for maximal chCE7 in vitro biological activity. The activity correlated with the level of Fc-associated bisected, complex oligosaccharides. Expression of GnT III within the practical range, i.e., where no significant growth inhibition and toxicity are observed, led to an increase of the target bisected, complex structures for this set of chCE7 samples. The pattern of oligosaccharide peaks in MALDI/TOF-mass spectrometric analysis of chCE7 samples produced at high levels of GnT III indicates that a significant proportion of potential GnT III substrates is diverted to bisected hybrid oligosaccharide by-products. Minimization of these by-products by further engineering of the pathway could therefore be valuable.

#### B. Identification And Generation Of Nucleic Acids Encoding A Protein For Which Modification Of The Glycosylation Pattern Is Desired

The present invention provides host cell systems suitable for the generation of altered glycoforms of any protein, protein fragment or peptide of interest, for which such an alteration in the glycosylation pattern is desired. The nucleic acids encoding such protein, protein fragment or peptide of interest may be obtained by methods generally known in the art. For example, the nucleic acid may be isolated from a cDNA library or genomic library. For a review of cloning strategies which may be used, see, e.g., Maniatis, 1989, *Molecular Cloning, A Laboratory Manual*, Cold Springs Harbor Press, N.Y.; and Ausubel et al., 1989, *Current Protocols in Molecular Biology*, (Green Publishing Associates and Wiley Interscience, N.Y.).

In an alternate embodiment of the invention, the coding sequence of the protein, protein fragment or peptide of interest may be synthesized in whole or in part, using chemical methods well known in the art. See, for example, Caruthers et al., 1980, *Nuc. Acids Res. Symp. Ser.* 7:215-233; Crea and Horn, 1980, *Nuc. Acids Res. USA* 9:2331; Matteucci and Caruthers, 1980, *Tetrahedron Letters* 21:719; Chow and Kempe, 1981, *Nuc. Acids Res.* 9:2807-2817. Alternatively, the protein itself could be produced using chemical methods to synthesize its amino acid sequence in whole or in part. For example, peptides can be synthesized by solid phase techniques, cleaved from the resin, and purified by preparative high performance liquid chromatography. E.g., see Creighton, 1983, *Protein Structures And Molecular Principles*, W.H. Freeman and Co., N.Y. pp. 50-60. The composition of the synthetic peptides may be confirmed by amino acid analysis or sequencing (e.g., the Edman degradation procedure; see Creighton, 1983, *Proteins, Structures and Molecular Principles*, W.H. Freeman and Co., N.Y., pp. 34-49).

In preferred embodiments, the invention provides methods for the generation and use of host cell systems for the production of glycoforms of antibodies or antibody fragments or fusion proteins which include antibody fragments with enhanced antibody-dependent cellular cytotoxicity.

Identification of target epitopes and generation of antibodies having potential therapeutic value, for which modification of the glycosylation pattern is desired, and isolation of their respective coding nucleic acid sequence is within the scope of the invention.

Various procedures known in the art may be used for the production of antibodies to target epitopes of interest. Such antibodies include but are not limited to polyclonal, monoclonal, chimeric, single chain, Fab fragments and fragments produced by an Fab expression library. Such antibodies may be useful, e.g., as diagnostic or therapeutic agents. As therapeutic agents, neutralizing antibodies, i.e., those which compete for binding with a ligand, substrate or adapter molecule, are of especially preferred interest.

For the production of antibodies, various host animals are immunized by injection with the target protein of interest including, but not limited to, rabbits, mice, rats, etc. Various adjuvants may be used to increase the immunological response, depending on the host species, including but not limited to Freund's (complete and incomplete), mineral gels such as aluminum hydroxide, surface active substances such as lysolecithin, pluronic polyols, polyanions, peptides, oil emulsions, keyhole limpet hemocyanin, dinitrophenol, and potentially useful human adjuvants such as BCG (bacille Calmette-Guerin) and *Corynebacterium parvum*.

Monoclonal antibodies to the target of interest may be prepared using any technique which provides for the production of antibody molecules by continuous cell lines in culture. These include, but are not limited to, the hybridoma technique originally described by Kohler and Milstein, 1975, *Nature* 256:495-497, the human B-cell hybridoma technique (Kosbor et al., 1983, *Immunology Today* 4:72; Cote et al., 1983, *Proc. Natl. Acad. Sci. U.S.A.* 80:2026-2030) and the EBV-hybridoma technique (Cole et al., 1985, *Monoclonal Antibodies and Cancer Therapy*, Alan R. Liss, Inc., pp. 77-96). In addition, techniques developed for the production of "chimeric antibodies" (Morrison et al., 1984, *Proc. Natl. Acad. Sci. USA.* 81:6851-6855; Neuberger et al., 1984, *Nature* 312:604-608; Takeda et al., 1985, *Nature* 314:452-454) by splicing the genes from a mouse antibody molecule of appropriate antigen specificity together with genes from a human antibody molecule of appropriate biological activity can be used. Alternatively, techniques described for the production of single chain antibodies (U.S. Pat. No. 4,946,778) can be adapted to produce single chain antibodies having a desired specificity.

Antibody fragments which contain specific binding sites of the target protein of interest may be generated by known techniques. For example, such fragments include, but are not limited to, F(ab)<sub>2</sub> fragments which can be produced by pepsin digestion of the antibody molecule and the Fab fragments which can be generated by reducing the disulfide bridges of the F(ab)<sub>2</sub> fragments. Alternatively, Fab expression libraries may be constructed (Huse et al., 1989, *Science* 246:1275-1281) to allow rapid and easy identification of monoclonal Fab fragments with the desired specificity to the target protein of interest.

Once an antibody or antibody fragment has been identified for which modification in the glycosylation pattern are desired, the coding nucleic acid sequence is identified and isolated using techniques well known in the art. See, supra. C. Generation Of Cell Lines For The Production Of Proteins With Altered Glycosylation Pattern

The present invention provides host cell expression systems for the generation of proteins having modified glycosylation patterns. In particular, the present invention provides host cell systems for the generation of glycoforms of



proteins having an improved therapeutic value. Therefore, the invention provides host cell expression systems selected or engineered to increase the expression of a glycoprotein-modifying glycosyltransferase. Specifically, such host cell expression systems may be engineered to comprise a recombinant nucleic acid molecule encoding a glycoprotein-modifying glycosyltransferase, operatively linked to a constitutive or regulated promoter system. Alternatively, host cell expression systems may be employed that naturally produce, are induced to produce, and/or are selected to produce a glycoprotein-modifying glycosyltransferase.

In one specific embodiment, the present invention provides a host cell that has been engineered to express at least one nucleic acid encoding a glycoprotein-modifying glycosyl transferase. In one aspect, the host cell is transfected or transfected with a nucleic acid molecule comprising at least one gene encoding a glycoprotein-modifying glycosyl transferase. In an alternate aspect, the host cell has been engineered and/or selected in such way that an endogenous glycoprotein-modifying glycosyl transferase is activated. For example, the host cell may be selected to carry a mutation triggering expression of an endogenous glycoprotein-modifying glycosyl transferase. This aspect is exemplified in one specific embodiment, where the host cell is a CHO loc 10 mutant. Alternatively, the host cell may be engineered such that an endogenous glycoprotein-modifying glycosyl transferase is activated. In again another alternative, the host cell is engineered such that an endogenous glycoprotein-modifying glycosyl transferase has been activated by insertion of a regulated promoter element into the host cell chromosome. In a further alternative, the host cell has been engineered such that an endogenous glycoprotein-modifying glycosyl transferase has been activated by insertion of a constitutive promoter element, a transposon, or a retroviral element into the host cell chromosome.

Generally, any type of cultured cell line can be used as a background to engineer the host cell lines of the present invention. In a preferred embodiment, CHO cells, BHK cells, NSO cells, SP2/0 cells, or a hybridoma cell line is used as the background cell line to generate the engineered host cells of the invention.

The invention is contemplated to encompass engineered host cells expressing any type of glycoprotein-modifying glycosyl transferase as defined herein. However, in preferred embodiments, at least one glycoprotein-modifying glycosyl transferase expressed by the host cells of the invention is GnT III, or, alternatively,  $\beta(1,4)$ -N-acetylglucosaminyltransferase V (GnT V). However, also other types of glycoprotein-modifying glycosyl transferase may be expressed in the host system, typically in addition to GnT III or GnT V, including  $\beta(1,4)$ -galactosyl transferase (GalT), and mannosidase II (Man II). In one embodiment of the invention, GnT III is coexpressed with GalT. In another embodiment of the invention, GnT III is coexpressed with Man II. In a further embodiment of the invention, GnT III is coexpressed with GalT and Man II. However, any other permutation of glycoprotein-modifying glycosyl transferases is within the scope of the invention. Further, expression of a glycosidase in the host cell system may be desired.

One or several nucleic acids encoding a glycoprotein-modifying glycosyl transferase may be expressed under the control of a constitutive promoter or, alternately, a regulated expression system. Suitable regulated expression systems include, but are not limited to, a tetracycline-regulated expression system, an ecdysone-inducible expression system, a lac-switch expression system, a glucocorticoid-

inducible expression system, a temperature-inducible promoter system, and a metallothionein metal-inducible expression system. If several different nucleic acids encoding glycoprotein-modifying glycosyl transferases are comprised within the host cell system, some of them may be expressed under the control of a constitutive promoter, while others are expressed under the control of a regulated promoter. The optimal expression levels will be different for each protein of interest, and will be determined using routine experimentation. Expression levels are determined by methods generally known in the art, including Western blot analysis using a glycosyl transferase specific antibody, Northern blot analysis using a glycosyl transferase specific nucleic acid probe, or measurement of enzymatic activity. Alternatively, a lectin may be employed which binds to biosynthetic products of the glycosyl transferase, for example, E<sub>4</sub>-PHA lectin. In a further alternative, the nucleic acid may be operatively linked to a reporter gene; the expression levels of the glycoprotein-modifying glycosyl transferase are determined by measuring a signal correlated with the expression level of the reporter gene. The reporter gene may be transcribed together with the nucleic acid(s) encoding said glycoprotein-modifying glycosyl transferase as a single mRNA molecule; their respective coding sequences may be linked either by an internal ribosome entry site (IRES) or by a cap-independent translation enhancer (CITE). The reporter gene may be translated together with at least one nucleic acid encoding said glycoprotein-modifying glycosyl transferase such that a single polypeptide chain is formed. The nucleic acid encoding the glycoprotein-modifying glycosyl transferase may be operatively linked to the reporter gene under the control of a single promoter, such that the nucleic acid encoding the glycoprotein-modifying glycosyl transferase and the reporter gene are transcribed into an RNA molecule which is alternatively spliced into two separate messenger RNA (mRNA) molecules; one of the resulting mRNAs is translated into said reporter protein, and the other is translated into said glycoprotein-modifying glycosyl transferase.

If several different nucleic acids encoding a glycoprotein-modifying glycosyl transferase are expressed, they may be arranged in such way that they are transcribed as one or as several mRNA molecules. If they are transcribed as a single mRNA molecule, their respective coding sequences may be linked either by an internal ribosome entry site (IRES) or by a cap-independent translation enhancer (CITE). They may be transcribed from a single promoter into an RNA molecule which is alternatively spliced into several separate messenger RNA (mRNA) molecules, which then are each translated into their respective encoded glycoprotein-modifying glycosyl transferase.

In other embodiments, the present invention provides host cell expression systems for the generation of therapeutic proteins, for example antibodies, having an enhanced antibody-dependent cellular cytotoxicity, and cells which display the IgG Fc region on the surface to promote Fc-mediated cytotoxicity. Generally, the host cell expression systems have been engineered and/or selected to express nucleic acids encoding the protein for which the production of altered glycoforms is desired, along with at least one nucleic acid encoding a glycoprotein-modifying glycosyl transferase. In one embodiment, the host cell system is transfected with at least one gene encoding a glycoprotein-modifying glycosyl transferase. Typically, the transfected cells are selected to identify and isolate clones that stably express the glycoprotein-modifying glycosyl transferase. In another embodiment, the host cell has been selected for expression of endogenous glycosyl transferase. For

example, cells may be selected carrying mutations which trigger expression of otherwise silent glycoprotein-modifying glycosyl transferases. For example, CHO cells are known to carry a silent GnT III gene that is active in certain mutants, e.g., in the mutant Lec10. Furthermore, methods known in the art may be used to activate silent glycoprotein-modifying glycosyl transferase genes, including the insertion of a regulated or constitutive promoter, the use of transposons, retroviral elements, etc. Also the use of gene knockout technologies or the use of ribozyme methods may be used to tailor the host cell's glycosyl transferase and/or glycosidase expression levels, and is therefore within the scope of the invention.

Any type of cultured cell line can be used as background to engineer the host cell lines of the present invention. In a preferred embodiment, CHO cells, BHK cells, NSO cells, SP2/0 cells. Typically, such cell lines are engineered to further comprise at least one transfected nucleic acid encoding a whole antibody molecule, an antibody fragment, or a fusion protein that includes a region equivalent to the Fc region of an immunoglobulin. In an alternative embodiment, a hybridoma cell line expressing a particular antibody of interest is used as background cell line to generate the engineered host cells of the invention.

Typically, at least one nucleic acid in the host cell system encodes GnT III, or, alternatively, GnT V. However, also other types of glycoprotein-modifying glycosyl transferase may be expressed in the host system, typically in addition to GnT III or GnT V, including GalT, and Man II. In one embodiment of the invention, GnT III is coexpressed with GalT. In another embodiment of the invention, GnT III is coexpressed with Man II. In a further embodiment of the invention, GnT III is coexpressed with GalT and Man II. However, any other permutation of glycoprotein-modifying glycosyl transferases is within the scope of the invention. Further, expression of a glycosidase in the host cell system may be desired.

One or several nucleic acids encoding a glycoprotein-modifying glycosyl transferase may be expressed under the control of a constitutive promoter, or alternately, a regulated expression system. Suitable regulated expression systems include, but are not limited to, a tetracycline-regulated expression system, an ecdysone-inducible expression system, a lac-switch expression system, a glucocorticoid-inducible expression system, a temperature-inducible promoter system, and a metallothionein metal-inducible expression system. If several different nucleic acids encoding glycoprotein-modifying glycosyl transferases are comprised within the host cell system, some of them may be expressed under the control of a constitutive promoter, while others are expressed under the control of a regulated promoter. The optimal expression levels will be different for each protein of interest, and will be determined using routine experimentation. Expression levels are determined by methods generally known in the art, including Western blot analysis using a glycosyl transferase specific antibody, Northern blot analysis using a glycosyl transferase specific nucleic acid probe, or measurement of enzymatic activity. Alternatively, a lectin may be employed which binds to biosynthetic products of glycosyl transferase, for example, E<sub>4</sub>-PHA lectin. In a further alternative, the nucleic acid may be operatively linked to a reporter gene; the expression levels of the glycoprotein-modifying glycosyl transferase are determined by measuring a signal correlated with the expression level of the reporter gene. The reporter gene may transcribed together with the nucleic acid(s) encoding said glycoprotein-modifying glycosyl transferase as a single mRNA molecule; their respec-

tive coding sequences may be linked either by an internal ribosome entry site (IRES) or by a cap-independent translation enhancer (CITE). The reporter gene may be translated together with at least one nucleic acid encoding said glycoprotein-modifying glycosyl transferase such that a single polypeptide chain is formed. The nucleic acid encoding the glycoprotein-modifying glycosyl transferase may be operatively linked to the reporter gene under the control of a single promoter, such that the nucleic acid encoding the glycoprotein-modifying glycosyl transferase and the reporter gene are transcribed into an RNA molecule which is alternatively spliced into two separate messenger RNA (mRNA) molecules; one of the resulting mRNAs is translated into said reporter protein, and the other is translated into said glycoprotein-modifying glycosyl transferase.

If several different nucleic acids encoding a glycoprotein-modifying glycosyl transferase are expressed, they may be arranged in such way that they are transcribed as one or as several mRNA molecules. If they are transcribed as single mRNA molecule, their respective coding sequences may be linked either by an internal ribosome entry site (IRES) or by a cap-independent translation enhancer (CITE). They may be transcribed from a single promoter into an RNA molecule which is alternatively spliced into several separate messenger RNA (mRNA) molecules, which then are each translated into their respective encoded glycoprotein-modifying glycosyl transferase.

#### 1. Expression Systems

Methods which are well known to those skilled in the art can be used to construct expression vectors containing the coding sequence of the protein of interest and the coding sequence of the glycoprotein-modifying glycosyl transferase and appropriate transcriptional/translational control signals. These methods include in vitro recombinant DNA techniques, synthetic techniques and in vivo recombination/genetic recombination. See, for example, the techniques described in Maniatis et al, 1989, *Molecular Cloning A Laboratory Manual*, Cold Spring Harbor Laboratory, N.Y. and Ausubel et al., 1989, *Current Protocols in Molecular Biology*, Greene Publishing Associates and Wiley Interscience, N.Y.

A variety of host-expression vector systems may be utilized to express the coding sequence of the protein of interest and the coding sequence of the glycoprotein-modifying glycosyl transferase. Preferably, mammalian cells are used as host cell systems transfected with recombinant plasmid DNA or cosmid DNA expression vectors containing the coding sequence of the protein of interest and the coding sequence of the glycoprotein-modifying glycosyl transferase. Most preferably, CHO cells, BLIK cells, NSO cells, or SP2/0 cells, or alternatively, hybridoma cells are used as host cell systems. In alternate embodiments, other eukaryotic host cell systems may be contemplated, including, yeast cells transformed with recombinant yeast expression vectors containing the coding sequence of the protein of interest and the coding sequence of the glycoprotein-modifying glycosyl transferase; insect cell systems infected with recombinant virus expression vectors (e.g., baculovirus) containing the coding sequence of the protein of interest and the coding sequence of the glycoprotein-modifying glycosyl transferase; plant cell systems infected with recombinant virus expression vectors (e.g., cauliflower mosaic virus, CaMV; tobacco mosaic virus, TMV) or transformed with recombinant plasmid expression vectors (e.g., Ti plasmid) containing the coding sequence of the protein of interest and the coding sequence of the glycoprotein-modifying glycosyl transferase; or ani-

mal cell systems infected with recombinant virus expression vectors (e.g., adenovirus, vaccinia virus) including cell lines engineered to contain multiple copies of the DNA-encoding the protein of interest and the coding sequence of the glycoprotein-modifying glycosyl transferase either stably amplified (CHO/dhfr) or unstably amplified in double-minute chromosomes (e.g., murine cell lines).

For the methods of this invention, stable expression is generally preferred to transient expression because it typically achieves more reproducible results and also is more amenable to large scale production. Rather than using expression vectors which contain viral origins of replication, host cells can be transformed with the respective coding nucleic acids controlled by appropriate expression control elements (e.g., promoter, enhancer, sequences, transcription terminators, polyadenylation sites, etc.), and a selectable marker. Following the introduction of foreign DNA, engineered cells may be allowed to grow for 1-2 days in an enriched media, and then are switched to a selective media. The selectable marker in the recombinant plasmid confers resistance to the selection and allows selection of cells which have stably integrated the plasmid into their chromosomes and grow to form foci which in turn can be cloned and expanded into cell lines.

A number of selection systems may be used, including, but not limited to, the herpes simplex virus thymidine kinase (Wigler et al., 1977, *Cell* 11:223), hypoxanthine-guanine phosphoribosyltransferase (Szybalska & Szybalski, 1962, *Proc. Natl. Acad. Sci. USA* 48:2026), and adenine phosphoribosyltransferase (Lowy et al., 1980, *Cell* 22:817) genes, which can be employed in tk<sup>-</sup>, hgpri<sup>-</sup> or aprt<sup>-</sup> cells, respectively. Also, antimetabolite resistance can be used as the basis of selection for dhfr, which confers resistance to methotrexate (Wigler et al., 1980, *Natl. Acad. Sci. USA* 77:3567; O'Hare et al., 1981, *Proc. Natl. Acad. Sci. USA* 78:1527); gpt, which confers resistance to mycophenolic acid (Mulligan & Berg, 1981, *Proc. Natl. Acad. Sci. USA* 78:2072); neo, which confers resistance to the aminoglycoside G-418 (Colberre-Garapin et al., 1981, *J. Mol. Biol.* 150:1); and hygro, which confers resistance to hygromycin (Santerre et al., 1984, *Gene* 30:147) genes. Recently, additional selectable genes have been described, namely trpB, which allows cells to utilize indole in place of tryptophan; hisD, which allows cells to utilize histinol in place of histidine (Hartman & Mulligan, 1988, *Proc. Natl. Acad. Sci. USA* 85:8047); the glutamine synthase system; and ODC (ornithine decarboxylase) which confers resistance to the ornithine decarboxylase inhibitor, 2-(difluoromethyl)-DL-ornithine, DFMO (McConlogue, 1987, in: *Current Communications in Molecular Biology*, Cold Spring Harbor Laboratory ed.).

#### 2. Identification Of Transfectants Or Transformants That Express The Protein Having A Modified Glycosylation Pattern

The host cells which contain the coding sequence and which express the biologically active gene products may be identified by at least four general approaches; (a) DNA-DNA or DNA-RNA hybridization; (b) the presence or absence of "marker" gene functions; (c) assessing the level of transcription as measured by the expression of the respective mRNA transcripts in the host cell; and (d) detection of the gene product as measured by immunoassay or by its biological activity.

In the first approach, the presence of the coding sequence of the protein of interest and the coding sequence of the glycoprotein-modifying glycosyl transferase(s) inserted in the expression vector can be detected by DNA-DNA or

DNA-RNA hybridization using probes comprising nucleotide sequences that are homologous to the respective coding sequences, respectively, or portions or derivatives thereof.

In the second approach, the recombinant expression vector/host system can be identified and selected based upon the presence or absence of certain "marker" gene functions (e.g., thymidine kinase activity, resistance to antibiotics, resistance to methotrexate, transformation phenotype, occlusion body formation in baculovirus, etc.). For example, if the coding sequence of the protein of interest and the coding sequence of the glycoprotein-modifying glycosyl transferase are inserted within a marker gene sequence of the vector, recombinants containing the respective coding sequences can be identified by the absence of the marker gene function. Alternatively, a marker gene can be placed in tandem with the coding sequences under the control of the same or different promoter used to control the expression of the coding sequences. Expression of the marker in response to induction or selection indicates expression of the coding sequence of the protein of interest and the coding sequence of the glycoprotein-modifying glycosyl transferase.

In the third approach, transcriptional activity for the coding region of the protein of interest and the coding sequence of the glycoprotein-modifying glycosyl transferase can be assessed by hybridization assays. For example, RNA can be isolated and analyzed by Northern blot using a probe homologous to the coding sequences of the protein of interest and the coding sequence of the glycoprotein-modifying glycosyl transferase or particular portions thereof. Alternatively, total nucleic acids of the host cell may be extracted and assayed for hybridization to such probes.

In the fourth approach, the expression of the protein products of the protein of interest and the coding sequence of the glycoprotein-modifying glycosyl transferase can be assessed immunologically, for example by Western blots, immunoassays such as radioimmuno-precipitation, enzyme-linked immunoassays and the like. The ultimate test of the success of the expression system, however, involves the detection of the biologically active gene products.

#### D. Generation And Use Of Proteins And Protein Fragments Having Altered Glycosylation Patterns

##### 1. Generation And Use Of Antibodies Having Enhanced Antibody-Dependent Cellular Cytotoxicity

In preferred embodiments, the present invention provides glycoforms of antibodies and antibody fragments having an enhanced antibody-dependent cellular cytotoxicity.

Clinical trials of unconjugated monoclonal antibodies (mAbs) for the treatment of some types of cancer have recently yielded encouraging results. Dillman, 1997, *Cancer Biother. & Radiopharm.* 12:223-225; Deo et al., 1997, *Immunology Today* 18:127. A chimeric, unconjugated IgG1 has been approved for low-grade or follicular B-cell non-Hodgkin's lymphoma (Dillman, 1997, supra), while another unconjugated mAb, a humanized IgG1 targeting solid breast tumors, has also been showing promising results in phase III clinical trials. Deo et al., 1997, supra. The antigens of these two mAbs are highly expressed in their respective tumor cells and the antibodies mediate potent tumor destruction by effector cells in vitro and in vivo. In contrast, many other unconjugated mAbs with fine tumor specificities cannot trigger effector functions of sufficient potency to be clinically useful. Frost et al., 1997, *Cancer* 80:317-333; Surfus et al., 1996, *J. Immunother.* 19:184-191. For some of these weaker mAbs, adjunct cytokine therapy is currently being tested. Addition of cytokines can stimulate antibody-dependent cellular cytotoxicity (ADCC) by increasing the

activity and number of circulating lymphocytes. Frost et al., 1997, supra; Surfus et al., 1996, supra. ADCC, a lytic attack on antibody-targeted cells, is triggered upon binding of lymphocyte receptors to the constant region (Fc) of antibodies. Deo et al., 1997, supra.

A different, but complementary, approach to increase ADCC activity of unconjugated IgG1s would be to engineer the Fc region of the antibody to increase its affinity for the lymphocyte receptors (FcγRs). Protein engineering studies have shown that FcγRs interact with the lower hinge region of the IgG CH2 domain. Lund et al., 1996, *J. Immunol.* 157:4963-4969. However, FcγR binding also requires the presence of oligosaccharides covalently attached at the conserved Asn 297 in the CH2 region. Lund et al., 1996, supra; Wright and Morrison, 1997, *Tibtech* 15:26-31, suggesting that either oligosaccharide and polypeptide both directly contribute to the interaction site or that the oligosaccharide is required to maintain an active CH2 polypeptide conformation. Modification of the oligosaccharide structure can therefore be explored as a means to increase the affinity of the interaction.

An IgG molecule carries two N-linked oligosaccharides in its Fc region, one on each heavy chain. As any glycoprotein, an antibody is produced as a population of glycoforms which share the same polypeptide backbone but have different oligosaccharides attached to the glycosylation sites. The oligosaccharides normally found in the Fc region of serum IgG are of complex bi-antennary type (Wormald et al., 1997, *Biochemistry* 36:130-1380), with low level of terminal sialic acid and bisecting N-acetylglucosamine (G1cNAc), and a variable degree of terminal galactosylation and core fucosylation (FIG. 1). Some studies suggest that the minimal carbohydrate structure required for FcγR binding lies within the oligosaccharide core. Lund et al., 1996, supra. The removal of terminal galactoses results in approximately a two-fold reduction in ADCC activity, indicating a role for these residues in FcγR receptor binding. Lund et al., 1996, supra.

The mouse- or hamster-derived cell lines used in industry and academia for production of unconjugated therapeutic mAbs normally attach the required oligosaccharide determinants to Fc sites. IgGs expressed in these cell lines lack, however, the bisecting G1cNAc found in low amounts in serum IgGs. Lively et al., 1995, *Glycobiology* 318:813-822. In contrast, it was recently observed that a rat myeloma-produced, humanized IgG1 (CAMPATH-1H) carried a bisecting G1cNAc in some of its glycoforms. Lively et al., 1995, supra. The rat cell-derived antibody reached a similar in vitro ADCC activity as CAMPATH-1H antibodies produced in standard cell lines, but at significantly lower antibody concentrations.

The CAMPATH antigen is normally present at high levels on lymphoma cells, and this chimeric mAb has high ADCC activity in the absence of a bisecting G1cNAc. Lively et al., 1995, supra. Even though in the study of Lively et al., 1995, supra. the maximal in vitro ADCC activity was not increased by altering the glycosylation pattern, the fact that this level of activity was obtained at relatively low antibody concentrations for the antibody carrying bisected oligosaccharides suggests an important role for bisected oligosaccharides. An approach was developed to increase the ADCC activity of IgG1s with low basal activity levels by producing glycoforms of these antibodies carrying bisected oligosaccharides in the Fc region.

In the N-linked glycosylation pathway, a bisecting G1cNAc is added by the enzyme  $\beta(1,4)$ -N-acetylglucosaminyltransferase III (GnT III). Schachter,

1986, *Biochem. Cell Biol.* 64:163-181. Lively et al., 1995, supra, obtained different glycosylation patterns of the same antibody by producing the antibody in different cell lines with different but non-engineered glycosylation machineries, including a rat myeloma cell line that expressed GnT III at an endogenous, constant level. In contrast, we used a single antibody-producing CHO cell line, that was previously engineered to express, in an externally-regulated fashion, different levels of a cloned GnT III gene. This approach allowed us to establish for the first time a rigorous correlation between expression of GnT III and the ADCC activity of the modified antibody.

As demonstrated herein, see, Example 4, infra, C2B8 antibody modified according to the disclosed method had an about sixteen-fold higher ADCC activity than the standard, unmodified C2B8 antibody produced under identical cell culture and purification conditions. Briefly, a C2B8 antibody sample expressed in CHO-11A-C2B8 cells that do not have GnT III expression showed a cytotoxic activity of about 31% (at 1  $\mu$ g/ml antibody concentration), measured as in vitro lysis of SB cells (CD20+) by human lymphocytes. In contrast, C2B8 antibody derived from a CHO cell culture expressing GnT III at a basal, largely repressed level showed at 1  $\mu$ g/ml antibody concentration a 33% increase in ADCC activity against the control at the same antibody concentration. Moreover, increasing the expression of GnT III produced a large increase of almost 80% in the maximal ADCC activity (at 1  $\mu$ g/ml antibody concentration) compared to the control at the same antibody concentration. See, Example 4, infra.

Further antibodies of the invention having an enhanced antibody-dependent cellular cytotoxicity include, but are not limited to, anti-human neuroblastoma monoclonal antibody (chCE7) produced by the methods of the invention, a chimeric anti-human renal cell carcinoma monoclonal antibody (ch-G250) produced by the methods of the invention, a humanized anti-HER2 monoclonal antibody produced by the methods of the invention, a chimeric anti-human colon, lung, and breast carcinoma monoclonal antibody (ING-1) produced by the methods of the invention, a humanized anti-human 17-1A antigen monoclonal antibody (3622W94) produced by the methods of the invention, a humanized anti-human colorectal tumor antibody (A33) produced by the methods of the invention, an anti-human melanoma antibody (R24) directed against GD3 ganglioside produced by the methods of the invention, and a chimeric anti-human squamous-cell carcinoma monoclonal antibody (SF-25) produced by the methods of the invention. In addition, the invention is directed to antibody fragment and fusion proteins comprising a region that is equivalent to the Fc region of immunoglobulins. See, infra.

2. Generation And Use Of Fusion Proteins Comprising A Region Equivalent To An Fc Region Of An Immunoglobulin That Promote Fc-Mediated Cytotoxicity

As discussed above, the present invention relates to a method for enhancing the ADCC activity of therapeutic antibodies. This is achieved by engineering the glycosylation pattern of the Fc region of such antibodies, in particular by maximizing the proportion of antibody molecules carrying bisected complex oligosaccharides N-linked to the conserved glycosylation sites in their Fc regions. This strategy can be applied to enhance Fc-mediated cellular cytotoxicity against undesirable cells mediated by any molecule carrying a region that is an equivalent to the Fc region of an immunoglobulin, not only by therapeutic antibodies, since the changes introduced by the engineering of glycosylation affect only the Fc region and therefore its interactions with

the Fc receptors on the surface of effector cells involved in the ADCC mechanism. Fc-containing molecules to which the presently disclosed methods can be applied include, but are not limited to, (a) soluble fusion proteins made of a targeting protein domain fused to the N-terminus of an Fc-region (Charnov and Ashkenazi, 1996, *TECH* 14: 52) and (b) plasma membrane-anchored fusion proteins made of a type II transmembrane domain that localizes to the plasma membrane fused to the N-terminus of an Fc region (Stabila, P. F., 1998, *Nature Biotech.* 16: 1357).

In the case of soluble fusion proteins (a) the targeting domain directs binding of the fusion protein to undesirable cells such as cancer cells, i.e., in an analogous fashion to therapeutic antibodies. The application of presently disclosed method to enhance the Fc-mediated cellular cytotoxic activity mediated by these molecules would therefore be identical to the method applied to therapeutic antibodies. See, Example 2 of U.S. Provisional Application Serial No. 60/082,581, incorporated herein by reference.

In the case of membrane-anchored fusion proteins (b) the undesirable cells in the body have to express the gene encoding the fusion protein. This can be achieved either by gene therapy approaches, i.e., by transfecting the cells in vivo with a plasmid or viral vector that directs expression of the fusion protein-encoding gene to undesirable cells, or by implantation in the body of cells genetically engineered to express the fusion protein on their surface. The later cells would normally be implanted in the body inside a polymer capsule (encapsulated cell therapy) where they cannot be destroyed by an Fc-mediated cellular cytotoxicity mechanism. However should the capsule device fail and the escaping cells become undesirable, then they can be eliminated by Fc-mediated cellular cytotoxicity. Stabila et al., 1998, *Nature Biotech.* 16: 1357. In this case, the presently disclosed method would be applied either by incorporating into the gene therapy vector an additional gene expression cassette directing adequate or optimal expression levels of GnT III or by engineering the cells to be implanted to express adequate or optimal levels of GnT III. In both cases, the aim of the disclosed method is to increase or maximize the proportion of surface-displayed Fc regions carrying bisected complex oligosaccharides.

The examples below explain the invention in more detail. The following preparations and examples are given to enable those skilled in the art to more clearly understand and to practice the present invention. The present invention, however, is not limited in scope by the exemplified embodiments, which are intended as illustrations of single aspects of the invention only, and methods which are functionally equivalent are within the scope of the invention. Indeed, various modifications of the invention in addition to those described herein will become apparent to those skilled in the art from the foregoing description and accompanying drawings. Such modifications are intended to fall within the scope of the appended claims.

## VIII. EXAMPLES

### A. Example 1

#### Tetracycline-Regulated Overexpression Of Glycosyl Transferases In Chinese Hamster Ovary Cells

To establish a cell line in which the expression of GnT III could be externally-controlled, a tetracycline-regulated expression system was used. Gossen, M. and Bujard, H., 1992, *Proc. Nat. Acad. Sci. USA*, 89: 5547-5551. The amount of GnT III in these cells could be controlled simply

by manipulating the concentration of tetracycline in the culture medium. Using this system, it was found that overexpression of GnT III to high levels led to growth inhibition and was toxic to the cells. Another CHO cell line with tetracycline-regulated overexpression of GnT V, a distinct glycoprotein-modifying glycosyl transferase, showed the same inhibitory effect, indicating that this may be a general feature of glycoprotein-modifying glycosyl transferase overexpression. This phenomenon has not been reported previously, probably due to the fact that investigators generally have used constitutive promoters for related experiments. The growth effect sets an upper limit to the level of glycoprotein-modifying glycosyl transferase overexpression, and may thereby also limit the maximum extent of modification of poorly accessible glycosylation sites.

#### 1. Materials And Methods

**Establishment Of CHO Cells With Tetracycline-Regulated Expression Of Glycosyltransferases.** In a first step, an intermediate CHO cell line (CHO-tTA) was first generated that constitutively expresses a tetracycline-controlled transactivator (tTA) at a level for the adequate for the regulation system. Using Lipofectamine reagent (Gibco, Eggenfelden, Germany), CHO (DUKX) cells were co-transfected, with pUHD15-1, a vector for constitutive expression of the tTA gene (Gossen and Bujard, 1992, *Proc. Nat. Acad. Sci. USA*, 89: 5547-5551), and pSV2Neo, a vector for constitutive expression of a neomycin resistance gene (Clontech, Palo Alto, Calif.). Stable, drug-resistant clones were selected and screened for adequate levels of tTA expression via transient transfections with a tetracycline-regulated  $\beta$ -galactosidase expression vector, pUHG16-3. C-myc epitope-encoding DNA was added to the 3' end of the rat GnT III cDNA (Nishikawa et al., 1992, *J. Biol. Chem.* 267:18199-18204) by PCR amplification. Nilsson et al., 1993, *J. Cell Biol.* 120:5-13. The product was sequenced and subcloned into pUHD10-3, a vector for tetracycline-regulated expression (Gossen and Bujard, supra) to generate the vector pUHD10-3-GnT III. The human GnT V cDNA (Saito et al., 1995, *Eur. J. Biochem.* 233:18-26), was directly subcloned into pUHD10-3 to generate plasmid vector pUHD10-3-GnT V. CHO-tTA cells were co-transfected using a calcium phosphate transfection method (Jordan and Wurm, 1996, *Nucleic Acids Res.* 24:596-601), with pPur, a vector for constitutive expression of puromycin resistance (Clontech, Palo Alto, Calif.), and either the vector pUHD10-3-GnT III or the vector pUHD10-3-GnT V. Puromycin resistant clones were selected in the presence of tetracycline, isolated and then analyzed for tetracycline-regulated expression of GnT III or GnT V via western blots analysis. See, infra.

**Western And Lectin Blotting.** For Western blot analysis of GnT III or GnT V, cell lysates were separated by SDS-PAGE and electroblotted to PVDF membranes (Millipore, Bedford, Mass.). GnT III was detected using the anti-c-myc monoclonal antibody 9E10 (Nilsson et al., 1993, *J. Cell Biol.* 120:5-13) and GnT V using with an anti-GnT V rabbit polyclonal antibody (Chen et al., 1995, *Glycoconjugate J.* 12:813-823). Anti-mouse or anti-rabbit IgG-horse radish peroxidase (Amersham, Arlington, Ill.) was used as secondary antibody. Bound secondary antibody was detected using an enhanced chemiluminescence kit (ECL kit, Amersham, Arlington, Ill.)

For lectin blot analysis of glycoproteins modified either by GnT III- or GnT V-catalyzed reactions, biotinylated E-PHA (Oxford Glycosciences, Oxford, United Kingdom) or L-PHA-digoxigenin (Boehringer Mannheim, Mannheim,

Germany), respectively, were used. Merkle and Cummings, 1987, *Methods Enzymol.* 138:232-259.

## 2. Results And Discussion

Establishment Of CHO Cell Lines With Tetracycline-Regulated Overexpression Of Glycosyl Transferases. The strategy used for establishment of glycosyl transferase over-expressing cell lines consisted of first generating an intermediate CHO cell line constitutively expressing the tetracycline-controlled transactivator (tTA) at an adequate level for the system to work. Yin et al., 1996, *Anal. Biochem.* 235:195-201. This level had to be high enough to activate high levels of transcription, in the absence of tetracycline, from the minimal promoter upstream of the glycosyl transferase genes. CHO cells were co-transfected with a vector for constitutive expression for tTA, driven by the human cytomegalovirus (hCMV) promoter/enhancer, and a vector for expression of a neomycin-resistance (Neo<sup>R</sup>) gene. An excess of the tTA-expression vector was used and neomycin-resistant clones were isolated.

In mammalian cells, co-transfected DNA integrates adjacently at random locations within the chromosomes, and expression depends to a large extent on the site of integration and also on the number of copies of intact expression cassettes. A mixed population of clones with different expression levels of the transfected genes is generated. Yin et al., 1996, supra. Selection for neomycin resistance merely selects for integration of an intact Neo<sup>R</sup> expression cassette, while the use of an excess of the tTA-expression vector increases the probability of finding clones with good expression of tTA. The mixed population of clones has to be screened using a functional assay for tTA expression. Gossen and Bujard, 1992, supra; Yin et al., 1996, supra. This was done by transfection of each clone with a second vector harboring a reporter gene, lacZ, under the control of the tet-promoter and screening for tetracycline-regulated (tet-regulated), transient expression (i.e., one to three days after transfection) of  $\beta$ -galactosidase activity. CHO117, which showed the highest level of tet-regulated  $\beta$ -galactosidase activity among twenty screened clones, was selected for further work.

CHO117 cells were tested for tet-regulated expression of GnT III by transfecting the cells with vector pUHD10-3-GnT III<sub>m</sub> and comparing the relative levels of GnT III after incubation of the cells in the presence and absence of tetracycline for 36 h. GnT III levels were compared by western blot analysis, using a monoclonal antibody (9E 10) which recognizes the c-myc peptide epitope tag at the carboxy-terminus of GnT III. The tag had been introduced through a modification of the glycosyl transferase gene using PCR amplification. Various reports have demonstrated addition of peptide epitope tags to the carboxy-termini of glycosyl transferases, a group of enzymes sharing the same topology, without disruption of localization or activity. Nilsson et al., 1993, supra; Rabouille et al., 1995, *J. Cell Science* 108:1617-1627. FIG. 2 shows that in clone CHO117 GnT III accumulation is significantly higher in the absence than in the presence of tetracycline. An additional clone, CHO12, which gave weaker activation of transcription in the  $\beta$ -galactosidase activity assay, was tested in parallel (FIG. 2). GnT III and  $\beta$ -galactosidase expression levels follow the same pattern of tetracycline-regulation for both of these clones. The range of tetracycline concentrations where GnT III expression can be quantitatively controlled was found to be from 0 to 100 ng/ml (FIG. 3). This result agrees with previous research using different cell lines and genes (Yin et al., 1996, supra).

To generate a stable cell line with tet-regulated expression of GnT III, CHO117 cells were co-transfected with vector

pU HD10-3-GnT III<sub>m</sub> and vector, pPUR, for expression of a puromycin resistance gene. In parallel, CHO117 cells were co-transfected with pUHD10-3-GnT V and pPUR vectors to generate an analogous cell line for this other glycosyl transferase. A highly efficient calcium phosphate transfection method was used and the DNA was linearized at unique restriction sites outside the eucaryotic expression cassettes, to decrease the probability of disrupting these upon integration. By using a host in which the levels of tTA expressed had first been proven to be adequate, the probability of finding clones with high expression of the glycosyl transferases in the absence of tetracycline is increased.

Stable integrants were selected by puromycin resistance, keeping tetracycline in the medium throughout clone selection to maintain glycosyl transferase expression at basal levels. For each glycosyl transferase, sixteen puromycin resistant clones were grown in the presence and absence of tetracycline, and eight of each were analysed by western blot analysis (FIG. 4). The majority of the clones showed good regulation of glycosyl transferase expression. One of the GnT III-expressing clones showed a relatively high basal level in the presence of tetracycline (FIG. 4B, clone 3), which suggests integration of the expression cassette close to an endogenous CHO-cell enhancer; while two puromycin-resistant clones showed no expression of GnT III in the absence of tetracycline (FIG. 4B, clones 6 and 8). Among the clones showing good regulation of expression, different maximal levels of glycosyl transferase were observed. This may be due to variations in the site of integration or number of copies integrated. Activity of the glycosyl transferases was verified by E-PHA and L-PHA lectin binding to endogenous cellular glycoproteins derived from various clones grown in the presence and absence of tetracycline (FIG. 5). Lectins are proteins which bind to specific oligosaccharide structures. E-PHA lectin binds to bisected oligosaccharides, the products of GnT III-catalyzed reactions, and L-PHA binds to tri- and tetra-antennary oligosaccharides produced by GnT V-catalyzed reactions (Merkle and Cummings, 1987, *Methods Enzymol.* 138:232-259). For each glycosyl transferase, a clone with high expression in the absence, but with undetectable expression in the presence, of tetracycline (clone 6, FIG. 4A, CHO-tet-GnT V, and clone 4, FIG. 4B, CHO-tet-GnT III<sub>m</sub>) was selected for further work.

## B. Example 2

### Inhibition Of Cell Growth Effected By Glycosyl Transferase Overexpression

During screening of GnT III- and GnT V-expressing clones in the absence of tetracycline, see, Example 1, supra, approximately half of each set of clones showed a strong inhibition of growth. The extent of growth-inhibition varied among clones, and comparison with expression levels estimated from western blot analysis (FIG. 4) suggested a correlation between the degree of growth-inhibition and glycosyl transferase overexpression. This correlation was firmly established by growing the final clones, CHO-tet-GnT III<sub>m</sub> and CHO-tet-GnT V, in different concentrations of tetracycline. A strong inhibition of growth was evident after two days of culture at low levels of tetracycline (FIG. 6). Growth-inhibited cells displayed a small, rounded morphology instead of the typical extended shape of adherent CHO cells. After a few days, significant cell death was apparent from the morphology of the growth-inhibited cells.

Growth-inhibition due to glycosyl transferase overexpression has not hitherto been reported in the literature, probably due to the widespread use of constitutive promoters. Those

clones giving constitutive expression of a glycosyl transferase at growth-inhibiting levels, would be lost during the selection procedure. This was avoided here by keeping tetracycline in the medium, i.e., basal expression levels, throughout selection. Prior to selection, the frequency of clones capable of expressing glycosyl transferases to growth-inhibiting levels using traditional mammalian vectors based on the constitutive hCMV promoter/enhancer would be expected to be lower. This is due to the fact that, for any given gene, the pUHD10-3 vector in CHO cell lines selected for high constitutive levels of tTA, gives significantly higher expression levels than constitutive hCMV promoter/enhancer-based vectors, as observed by others. Yin et al., 1996, supra.

Inhibition of cell growth could be due to a direct effect of overexpression of membrane-anchored, Golgi-resident glycosyl transferases independent of their *in vivo* catalytic activity, e.g., via misfolding in the endoplasmic reticulum (ER) causing saturation of elements which assist protein folding in the ER. This could possibly affect the folding and secretion of other essential cellular proteins. Alternatively, inhibition of growth could be related to increased *in vivo* activity of the glycosyl transferase leading to a change of the glycosylation pattern, in a function-disrupting fashion, of a set of endogenous glycoproteins necessary for growth under standard *in vitro* culture conditions.

Independent of the underlying mechanism, the growth-inhibition effect has two consequences for engineering the glycosylation of animal cells. First, it implies that cotransfection of constitutive glycosyl transferase expression vectors together with vectors for the target glycoprotein product is a poor strategy. Other ways of linking expression of these two classes of proteins, e.g., through the use of multiple constitutive promoters of similar strength or use of multicistronic, constitutive expression vectors, should also be avoided. In these cases, clones with very high, constitutive expression of the target glycoprotein, a pre-requisite for an economical bioprocess, would also have high expression of the glycosyl transferase and would be eliminated during the selection process. Linked, inducible expression could also be problematic for industrial bioprocesses, since the viability of the growth-arrested cells would be compromised by the overexpression of the glycosyl transferase.

The second consequence is that it imposes an upper limit on glycosyl transferase overexpression for glycosylation engineering approaches. Clearly, the conversions of many glycosyl transferase-catalyzed reactions in the cell, at the endogenous levels of glycosyl transferases, are very high for several glycosylation sites. However, glycosylation sites where the oligosaccharides are somewhat inaccessible or are stabilized in unfavorable conformations for specific glycosyl transferases also exist. For example, it has been observed that addition of bisecting GlcNAc is more restricted to the oligosaccharides attached to the Fc region than to those located on the variable regions of human IgG antibodies. Savvidou et al., 1984, *Biochemistry* 23:3736-3740. Glycosylation engineering of these restricted sites could be affected by such a limit on glycosyl transferase expression. Although this would imply aiming for an "unnatural" distribution of glycoforms, these could be of benefit for special therapeutic applications of glycoproteins.

### C. Example 3

#### Engineering The Glycosylation Of An Anti-Human Neuroblastoma Antibody In Chinese Hamster Ovary Cells

In order to validate the concept of engineering a therapeutic antibody by modifying its glycosylation pattern, a

chimeric anti-human neuroblastoma IgG1 (chCE7) was chosen which has insignificant ADCC activity when produced by SP2/0 recombinant mouse myeloma cells. ChCE7 recognizes a tumor-associated 190-kDa membrane glycoprotein and reacts strongly with all neuroblastoma tumors tested to date. It has a high affinity for its antigen ( $K_d$  of  $10^{10}M^{-1}$ ) and, because of its high tumor-specificity, it is routinely used as a diagnostic tool in clinical pathology. Amstutz et al., 1993, *Int. J. Cancer* 53:147-152. In recent studies, radiolabelled chCE7 has shown good tumor localization in human patients. Dürr, 1993, *Eur. J. Nucl. Med.* 20:858. The glycosylation pattern of chCE7, an anti-neuroblastoma therapeutic monoclonal antibody (mAb) was engineered in CHO cells with tetracycline-regulated expression of GnT III. A set of mAb samples differing in their glycoform distribution was produced by controlling Grt III expression in a range between basal and toxic levels, and their glycosylation profiles were analyzed by MALDI/TOF-MS of neutral oligosaccharides. Measurement of the ADCC activity of these samples showed an optimal range of GnT III expression for maximal chCE7 *in vitro* biological activity, and this activity correlated with the level of Fc-associated bisected, complex oligosaccharides.

#### 1. Materials And Methods

Construction Of chCE7 Expression Vectors. Plasmid vectors 10CE7VH and 98CE7VL, for expression of heavy (IgG1) and light ( $\kappa$ ) chains, respectively, of anti-human neuroblastoma chimeric antibody chCE7, which contain chimeric genomic DNA including the mouse immunoglobulin promoter/enhancer, mouse antibody variable regions, and human antibody constant regions (Amstutz et al., 1993, *Int. J. Cancer* 53:147-152) were used as starting materials for the construction of the final expression vectors, pchCE7H and pchCE7L. Chimeric heavy and light chain chCE7 genes were reassembled and subcloned into the pcDNA3.1(+) vector. During reassembly, all introns were removed, the leader sequences were replaced with synthetic ones, Reff et al., 1994, *Blood* 83:435-445, and unique restriction sites joining the variable and constant region sequences were introduced. Introns from the heavy constant region were removed by splicing with overlap-extension-PCR. Clackson et al., 1991, *General Applications of PCR to Gene Cloning and Manipulation*, p. 187-214, in: McPherson et al. (ed.), *PCR a Practical Approach*, Oxford University Press, Oxford.

Production Of ch CE7 In CHO Cells Expressing Different Levels Of Gn T III. CHO-tet-GnT III $\mu$  (see, supra) cells were co-transfected with vectors pchCE7H, pchCE7L, and pZeoSV2 (for Zeocin resistance, Invitrogen, Groningen, The Netherlands) using a calcium phosphate transfection method. Zeocin resistant clones were transferred to a 96-well cell culture plate and assayed for chimeric antibody expression using an ELISA assay specific for human IgG constant region. Lively et al, 1995, supra. Four chCE7 antibody samples were derived from parallel cultures of a selected clone (CHO-tet-GnT III $\mu$ -chCE7), grown in FMX-8 cell culture medium supplemented with 10% FCS; each culture containing a different level of tetracycline and therefore expressing GnT III at different levels. CHO-tet-GnT III $\mu$ -chCE7 cells were expanded and preadapted to a different concentration of tetracycline during 7 days. The levels of tetracycline were 2000, 60, 30, and 15 ng/ml.

Purification Of chCE7 Antibody Samples. Antibody was purified from culture medium by Protein A affinity chromatography on a 1 ml Protein A column (III-TRAP, Pharmacia Biotech, Uppsala, Sweden), using linear pH gradient elution from 20 mM sodium phosphate, 20 mM sodium citrate, 500

mM sodium chloride, 0.01% polyoxyethylenesorbitan monolaurate (TWEEN 20), 1M urea, pH 7.5 (buffer A) to buffer B (buffer A without sodium phosphate, pH 2.5). Affinity purified chCE7 samples were buffer exchanged to PBS on a 1 ml cation exchange column (RESOURCES, Pharmacia Biotech, Uppsala, Sweden). Final purity was judged to be higher than 95% from SDS-PAGE and Coomassie-Blue staining. The concentration of each sample was estimated from the absorbance at 280 nm.

Binding Of antibodies To Neuroblastoma Cells. Binding affinity to human neuroblastoma cells was estimated from displacement of <sup>125</sup>I-labeled chCE7 by the CHO-produced samples. Amstutz et al, 1993, supra.

Oligosaccharide Analysis By MALDI/TOF-MS. CE7-2000i, -60i, -30i, and -15i samples were treated with *A. urefaciens* sialidase (Oxford Glycosciences, Oxford, United Kingdom), following the manufacturer's instructions, to remove any sialic acid monosaccharide residues. The sialidase digests were then treated with peptide N-glycosidase F (PNGaseF, Oxford Glycosciences, Oxford, United Kingdom), following the manufacturer's instructions, to release the N-linked oligosaccharides. Protein, detergents, and salts were removed by passing the digests through microcolumns containing, from top to bottom, 20  $\mu$ l of C18 reverse phase matrix (SEP-PAK, Waters, Milford, Mass.), 20 ml of cation exchange matrix (DOWEX AG 50W X8, BioRad cation exchange matrix, Hercules, Calif.), and 20  $\mu$ l of AG 4x4 anion exchange matrix (BioRad, Hercules, Calif.). The microcolumns were made by packing the matrices in a gel loading pipette tip (GEL LOADER, Eppendorf, Basel, Switzerland) filled with ethanol, followed by an equilibration with water. Küster et al., 1997, *Anal. Biochem.* 250:82-101. Flow through liquid and a 300  $\mu$ l-water wash were pooled, filtered, evaporated to dryness at room temperature, and resuspended in 2 ml of deionized water. One microliter was applied to a MALDI-MS sample plate (Perceptive Biosystems, Farmingham, Mass.) and mixed with 1  $\mu$ l of a 10 mg/ml dehydrobenzoic acid (DHB, Aldrich, Milwaukee, Wis.) solution in acetonitrile. The samples were air dried and the resulting crystals were dissolved in 0.2  $\mu$ l of ethanol and allowed to recrystallize by air drying. Harvey, 1993, *Rapid Mass. Spectrom.* 7:614-619. The oligosaccharide samples were then analyzed by matrix-assisted laser desorption ionization/time-of-flight-mass spectrometry (MALDI/TOF-MS) using a mass spectrometer (ELITE VOYAGER 400, Perceptive Biosystems, Farmingham, Mass.), equipped with a delayed ion extraction MALDI-ion source, in positive ion and reflector modes, with an acceleration voltage of 20 kV. One hundred and twenty eight scans were averaged. Bisected biantennary complex oligosaccharide structures were assigned to five-HexNAc-associated peaks. Non-bisected tri-antennary-linked oligosaccharides, the alternative five HexNAc-containing isomers, have never been found in the Fc region of IgGs and their syntheses are catalyzed by glycosyltransferases discrete from GnT III.

ADCC Activity Assay. Lysis of IMR-32 human neuroblastoma cells (target) by human lymphocytes (effector), at a target:effector ratio of 1:19, during a 16 h incubation at 37° C. in the presence of different concentrations of chCE7 samples, was measured via retention of a fluorescent dye. Kolber et al, 1988, *J. Immunol. Methods* 108: 255-264. IM-32 cells were labeled with the fluorescent dye Calcein AM for 20 min (final concentration 3.3  $\mu$ M). The labeled cells (80,000 cells/well) were incubated for 1 h with different concentrations of CE7 antibody. Then, monocyte depleted mononuclear cells were added (1,500,000 cells/

well) and the cell mixture was incubated for 16 h at 37° C. in a 5% CO<sub>2</sub> atmosphere. The supernatant was discarded and the cells were washed once with HBSS and lysed in non-ionic detergent, t-octylphenoxypolyethoxyethanol (TRITON X-100 (0.1%). Retention of the fluorescent dye in IMR-32 cells was measured with a fluorometer (Perkin Elmer, Luminescence Spectrometer LS 50H, Foster City, Calif.) and specific lysis was calculated relative to a total lysis control, resulting from exposure of the target to a detergent instead of exposure to antibody. The signal in the absence of antibody was set to 0% cytotoxicity. Each antibody concentration was analyzed by triplicate, and the assay was repeated three separate times.

## 2. Results And Discussion

Production Of chCE7 In CHO Cells Expressing Different Levels Of GnT III. ChCE7 heavy and light chain expression vectors were constructed incorporating the human cytomegalovirus (hCMV) promoter, the bovine growth hormone termination and polyadenylation sequences, and eliminating all heavy and light chain introns. This vector design was based on reports of reproducible high-level expression of recombinant IgG genes in CHO cells. Reff et al., 1994, supra; Trill et al., 1995, *Current Opinion Biotechnol.* 6:553-560. In addition, a unique restriction sites was introduced in each chain, at the junction between the variable and constant regions. These sites conserve the reading frame and do not change the amino acid sequence. They should enable simple exchange of the mouse variable regions, for the production of other mouse-human chimeric antibodies. Reff et al., 1994, supra. DNA sequencing confirmed that the desired genes were appropriately assembled, and production of the chimeric antibody in transfected CHO cells was verified with a human Fc-ELISA assay.

CHO-tet-GnT III-m-chCE7 cells, with stable, tetracycline-regulated expression of GnT III and stable, constitutive expression of chCE7, were established and scaled-up for production of a set of chCE7 samples. During scale-up, four parallel cultures derived from the same CHO clone were grown, each at a different level of tetracycline and therefore only differing in the level of expression of the GnT III gene. This procedure eliminates any clonal effects from other variables affecting N-linked glycoform biosynthesis, permitting a rigorous correlation to be established between GnT III gene expression and biological activity of the glycosylated antibody. The tetracycline concentration ranged from 2000 ng/ml, i.e., the basal level of GnT III expression, to 15 ng/ml, at which significant growth inhibition and toxicity due to glycosyl transferase overexpression was observed (see, supra). Indeed, only a small amount of antibody could be recovered from the latter culture. The second highest level of GnT III expression, using tetracycline at a concentration of 30 ng/ml, produced only a mild inhibition of growth. The purified antibody yield from this culture was approximately 70% that from the remaining two lower levels of GnT III gene overexpression.

The four antibody samples, CE7-2000i, -60i, -30i, and -15i, numbers denoting the associated concentration of tetracycline, were purified by affinity chromatography on Protein A and buffer exchanged to PBS using a cation exchange column. Purity was higher than 95% as judged from SDS-PAGE with Coomassie Blue staining. Binding assays to human neuroblastoma cells revealed high affinity to the cells and no significant differences in antigen binding among the different samples (estimated equilibrium dissociation constants varied between 2.0 and 2.7x10<sup>-10</sup> M). This was as expected, since there are no potential N-linked glycosylation sites in the CE7 variable regions.



Oligosaccharide Distributions And Levels Of Bisected Complex Oligosaccharides Of Different chCE7 Samples. Oligosaccharide profiles were obtained by matrix-assisted laser desorption/ionization mass spectrometry on a time-of-flight instrument (MALDI/TOF-MS). Mixtures of neutral N-linked oligosaccharides derived from each of the four CHO-produced antibody samples and from a SP2/0 mouse myeloma-derived chCE7 (CE7-SP2/0) sample were analyzed using 2,5-dehydrobenzoic acid (2,5-DHB) as the matrix (FIG. 9). Under these conditions, neutral oligosaccharides appear essentially as single  $[M+Na]^+$  ions, which are sometimes accompanied by smaller  $[M+K]^+$  ions, depending on the potassium content of the matrix. Bergweff et al., 1995, *Glycoconjugate J.* 12:318-330.

This type of analysis yields both the relative proportions of neutral oligosaccharides of different mass, reflected by relative peak height, and the isobaric monosaccharide composition of each peak. Küster et al., 1997, supra; Naven and Harvey, 1996, *Rapid Commun. Mass Spectrom.* 10:1361-1366. Tentative structures are assigned to peaks based on the monosaccharide composition, knowledge of the biosynthetic pathway, and on previous structural data for oligosaccharides derived from the same glycoprotein produced by the same host, since the protein backbone and the cell type can have a strong influence on the oligosaccharide distribution. Field et al., 1996, *Anal. Biochem.* 239:92-98. In the case of Fc-associated oligosaccharides, only bi-antennary complex oligosaccharides have been detected in IgGs present in human serum or produced by mammalian cell cultures under normal conditions. Wormald et al., 1997, *Biochemistry* 36:1370-1380; Wright and Morrison, 1997, *Tibtech* 15:26-31. The pathway leading to these compounds is illustrated in FIG. 10, including the mass of the  $[M+Na]^+$  ion corresponding to each oligosaccharide. High mannose oligosaccharides have also been detected on antibodies produced in the stationary and death phases of batch cell cultures. Yu Ip et al., 1994, *Arch. Biochem. Biophys.* 308:387-399.

The two major peaks in the CE7-SP2/0 sample (FIG. 9A) correspond to masses of fucosylated oligosaccharides with four N-acetylhexosamines (HexNAcs) containing either three ( $m/z$  1486) or four ( $m/z$  1648) hexoses. See, FIG. 10, but note that the summarized notation for oligosaccharides in this figure does not count the two GlcNAcs of the core. This composition is consistent with core fucosylated, bi-antennary complex oligosaccharide structures carrying zero or one galactose residues, respectively, typical of Fc-associated oligosaccharides, and as previously observed in NMR analysis of Fc oligosaccharides derived from a chimeric IgG1 expressed in SP2/0 cells. Bergweff et al., 1995, supra.

GnT III-catalyzed transfer of a bisecting GlcNAc to these bi-antennary compounds, which are the preferred GnT III acceptors, would lead to oligosaccharides with five HexNAcs ( $m/z$  1689 and 1851, non- and mono-galactosylated, respectively, FIG. 10), which are clearly absent in the CE7-SP2/0 sample. The latter peaks appear when chCE7 is expressed in CHO-tet-GnTIII cells. In the CHO-expressed antibodies the four HexNAc-containing peaks are also mainly fucosylated, although a small amount of non-fucosylated structures is evident from the peak at  $m/z$  1339 (see, FIG. 10). The level of galactosylation is also not very different between the CHO- and SP2/0-derived material. At the basal level of GnT III expression (CE7-2000t sample, FIG. 9B), the molecules with five HexNAcs are present in a lower proportion than those with four HexNAcs. A higher level of GnT III expression (CE7-60t sample, FIG. 9C) led

to a reversal of the proportions in favor of oligosaccharides with five HexNAcs. Based on this trend, bisected, bi-antennary complex oligosaccharide structures can be assigned to compounds with five HexNAcs in these samples. Tri-antennary N-linked oligosaccharides, the alternative five HexNAc-containing isomers, have never been found in the Fc region of IgGs and their syntheses are catalyzed by GlcNAc-transferases discrete from GnT III.

A further increase in GnT III expression (CE7-30t sample, FIG. 9D) did not lead to any significant change in the levels of bisected complex oligosaccharides. Another peak ( $m/z$  1543) containing five HexNAcs appears at low, but relatively constant levels in the CHO-GnTIII samples and corresponds in mass to a non-fucosylated, bisected-complex oligosaccharide mass (FIG. 10). The smaller peaks at  $m/z$  1705 and 1867, also correspond to five HexNAc-containing bi-antennary complex oligosaccharides. They can be assigned either to potassium adducts of the peaks at  $m/z$  1689 and 1851 (mass difference of 16 Da with respect to sodium adducts) (Küster et al., 1997, supra) or to mono- and bi-galactosylated, bisected complex oligosaccharides without fucose (FIG. 10). Together, the bisected complex oligosaccharides amount to approximately 25% of the total in sample CE7-2000t and reach approximately 45 to 50% in samples CE7-60t and CE7-30t.

Additional information From The Oligosaccharide Profiles Of chCE7 Samples. Although the levels of bisected complex oligosaccharides were not higher in sample CE730t, increased overexpression of GnT III did continue to reduce, albeit to a small extent, the proportions of substrate bi-antennary complex oligosaccharide substrates. This was accompanied by moderate increases in two different, four HexNAc-containing peaks ( $m/z$  1664 and 1810). The latter two peaks can correspond either to galactosylated bi-antennary complex oligosaccharides or to bisected hybrid compounds (FIG. 11). A combination of both classes of structures is also possible. The relative increase in these peaks is consistent with the accumulation of bisected hybrid by-products of GnT III overexpression. Indeed, the sample produced at the highest level of GnT III overexpression, CE7-15t, showed a large increase in the peak at  $m/z$  1664, a reduction in the peak at  $m/z$  1810 and a concomitant reduction of complex bisected oligosaccharides to a level of approximately 25%. See, peaks with  $m/z$  1689 and 1851 in FIG. 9E and the corresponding structures in FIG. 11. Higher accumulation of non-fucosylated ( $m/z$  1664) bisected hybrid by-products, instead of fucosylated ones ( $m/z$  1810), would agree with the fact that oligosaccharides which are first modified by GnT III can no longer be biosynthetic substrates for core  $\alpha$ 1,6-fucosyltransferase. Schachter, 1986, *Biochem. Cell Biol.* 64:163-181.

The peak at  $m/z$  1257 is present at a level of 10-15% of the total in the CHO-derived samples and at a lower level in CE7-SP2/0 (FIG. 9). It corresponds to five hexoses plus two HexNAcs. The only known N-linked oligosaccharide structure with this composition is a five mannose-containing compound of the high-mannose type. Another high mannose oligosaccharide, a six mannose one ( $m/z$  1420), is also present at much lower levels. As mentioned above, such oligosaccharides have been detected in the Fc of IgGs expressed in the late phase of batch cell cultures. Yu Ip et al., 1994, supra.

Antibody Dependent Cellular Cytotoxicity Of ch CE7 Samples. ChCE7 shows some ADCC activity, measured as in vitro lysis of neuroblastoma cells by human lymphocytes, when expressed in CHO-tet-GnTIII cells with the minimum level of GnT III overexpression (FIG. 12,

sample CE7-2000t). Raising the level of GnT III produced a large increase in ADCC activity (FIG. 12, sample CE7-60t). Further overexpression of GnT III was not accompanied by an additional increase in activity (FIG. 12, sample CE7-30t), and the highest level of expression actually led to reduced ADCC (FIG. 12, sample CE7-15t). Besides exhibiting the highest ADCC activities, both CE7-60t and CE7-30t samples show significant levels of cytotoxicity at very low antibody concentrations. These results show that there is an optimal range of GnT III overexpression in CHO cells for ADCC activity, and comparison with oligosaccharide profiles shows that activity correlates with the level of Fc-associated, bisected complex oligosaccharides.

Given the importance of bisected complex oligosaccharides for ADCC activity, it would be useful to engineer the pathway to further increase the proportion of these compounds. Overexpression of GnT III to levels approaching that used for sample CE7-30t is within the biotechnologically practical range where no significant toxicity and growth inhibition are observed. At this level of expression, the non-galactosylated, non-bisected, bi-antennary complex oligosaccharides, i.e., the preferred, potential GnT III substrates, are reduced to less than 10% of the total. See, m/z 1486 peak, FIG. 9D. However, only 50% are converted to the desired bisected biantennary complex structures. The rest are either diverted to bisected, hybrid oligosaccharide byproducts or consumed by the competing enzyme  $\beta$ 1,4-galactosyltransferase, GalT (FIG. 11).

Resolution of the bisected hybrid and the non-bisected, galactosylated complex oligosaccharide peaks by complementary structural analyses would determine how much each potential, undesired route is consuming. The growth of the m/z 1664 and 1810 peaks at high GnT III overexpression levels suggests that at least a fraction of these peaks corresponds to bisected hybrid oligosaccharides (FIG. 11). In theory, a flux going to bisected hybrid compounds can be reduced by co-overexpression of enzymes earlier in the pathway such as mannosidase II together with GnT III. On the other hand, competition between GnT III and GalT for bisected complex oligosaccharide substrates could potentially be biased towards GnT III-catalyzed reactions, by increasing the intra-Golgi concentration of UDP-G1cNAc while overexpressing GnT III. GnT III transfers a G1cNAc from the co-substrate UDP-G1cNAc to the different oligosaccharides. Should the intra-Golgi concentration of UDP-G1cNAc co-substrate be sub-saturating for GnT III, then increasing it, either by manipulation of the culture medium composition or by genetic manipulation of sugar-nucleotide transport into the Golgi, could favor GnT III in a competition for oligosaccharides with GalT.

It remains to be determined whether the increase in ADCC activity results from the increase in both the galactosylated and non-galactosylated, bisected complex oligosaccharides, or only from one of these forms. See, peaks at m/z 1689 and 1851 in FIG. 9. If it is found that galactosylated, bisected complex bi-antennary oligosaccharides are the optimal structures for increased ADCC activity, then maximizing the fraction of these compounds on the Fc region would require overexpression of both GnT III and GalT. Given the competitive scenario discussed previously, the expression levels of both genes would have to be carefully regulated. In addition, it would be valuable to try to re-distribute overexpressed GalT as much as possible towards the TGN instead of the trans-Golgi cisterna. The latter strategy may be realized by exchanging the transmembrane region-encoding sequences of GalT with those of  $\alpha$ 2,6-sialyltransferase (Chege and Pfeiffer, 1990, *J. Cell Biol.* 111:893-899).

## D. Example 4

## Engineering The Glycosylation Of The Anti-CD20 Monoclonal Antibody C2B8

C2B8 is an anti-human CD20 chimeric antibody, Reff, M. E. et al, 1994, supra. It received FDA approval in 1997 and is currently being used, under the commercial name of Rituxan™, for the treatment of Non-Hodgkin's lymphoma in the United States. It is derived from CHO cell culture and therefore should not carry bisected oligosaccharides. See, supra. In order to produce an improved version of this antibody, the method demonstrated previously for the chCE7 anti-neuroblastoma antibody was applied. See, supra. C2B8 antibody modified according to the disclosed method had a higher ADCC activity than the standard, unmodified C2B8 antibody produced under identical cell culture and purification conditions.

## 1. Material And Methods Synthesis Of The Variable Light And Variable Heavy Chain

Regions Of Chimeric Anti-CD20 Monoclonal Antibody (C2B8). The VH and VL genes of the C2B8 antibody were assembled synthetically using a set of overlapping single-stranded oligonucleotides (primers) in a one-step process using PCR, Kobayashi et al, 1997, *Biotechniques* 23: 500-503. The sequence data coding for mouse immunoglobulin light and heavy chain variable regions (VL and VH respectively) of the anti-CD20 antibody were obtained from a published international patent application (International Publication Number: WO 94/11026). The assembled DNA fragments were subcloned into pBluescriptIIKS(+) and sequenced by DNA cycle sequencing to verify that no mutations had been introduced.

Construction Of Vectors For Expression Of Chimeric Anti-CD20 Monoclonal Antibody (C2B8). VH and VL coding regions of the C2B8 monoclonal antibody were subcloned in pchCE7H and pchCE7L respectively. In the subcloning, the sequences coding for the variable heavy and light chains of the anti-neuroblastoma CE7 (see, supra) were exchanged with the synthetically assembled variable heavy and variable light chain regions of C2B8.

Generation Of CHO-tet-GnTIII<sup>hi</sup> Cells Expressing C2B8 Antibody. The method for the generation of a CHO-tet-GnTIII<sup>hi</sup> cell line expressing C2B8 antibody was exactly the same as for CHO-tet-GnTIII<sup>hi</sup>-CE7. See, supra. The clone chosen for further work was named CHO-tet-GnTIII<sup>hi</sup>-C2B8.

Generation Of CHO-tTA Expressing C2B8 Antibody. CHO-tTA is the parental cell line of CHO-tet-GnTIII<sup>hi</sup>. See, supra. The method for the generation of a CHO-tTA cell line expressing C2B8 antibody without GnT III expression was exactly the same as for CHO-tet-GnTIII<sup>hi</sup>-C2B8 and CHO-tet-GnTIII<sup>hi</sup>-chCE7. See, supra. The clone chosen for further work was named CHO-tTA-C2B8.

Production Of C2B8 Antibody Samples. Two C2B8 antibody samples were derived from parallel CHO-tet-GnTIII<sup>hi</sup>-C2B8 cultures; each culture containing different levels of tetracycline and therefore expected to express GnTIII at different levels. The levels of tetracycline were 2000, 50, and 25 ng/ml. The C2B8 antibody samples derived from these cultures were designated as C2B8-2000t, C2B8-50t, and C2B8-25t, respectively. In parallel, one antibody sample (C2B8-nt) was made from a CHO-tTA-C2B8 culture, this cell line does not express GnT III. CHO-tTA-C2B8 cells were cultured without tetracycline.

Analysis Of GnT III Expression. For Western blot analysis of GnT III, cell lysates of each of the production cultures were resolved by SDS-PAGE and electroblotted to polyvi-

nylidene difluoride membranes. Anti-c-myc monoclonal antibody 9E 10 and anti-mouse IgG-horseradish peroxidase (Amersham, Arlington, Ill.) were used as primary and secondary antibodies respectively. Bound antibody was detected using an enhanced chemiluminescence kit (Amersham, Arlington, Ill.).

Purification Of C2B8 Antibody Samples. Antibody samples were purified using the same procedure as for the chCE7 antibody samples. See, supra. The concentration was measured using a fluorescence based kit from Molecular Probes (Leiden, The Netherlands).

Verification Of Specific C2B8 Antigen Binding. The specificity of antigen binding of the C2B8 anti-CD20 monoclonal antibody was verified using an indirect immunofluorescence assay with cells in suspension. For this study, CD20 positive cells (SB cells; ATCC deposit no. ATCC CCL120) and CD20 negative cells (HSB cells;

ATCC deposit no. ATCC CCL120.1) were utilized. Cells of each type were incubated with C2B8 antibody produced at 25 ng/ml tetracycline, as a primary antibody. Negative controls included HBSSB instead of primary antibody. An anti-human IgG Fc specific, polyclonal, FITC conjugated antibody was used for all samples as a secondary antibody (SIGMA, St. Louis, Mo.). Cells were examined using a Leica (Bensheim, Germany) fluorescence microscope.

ADCC Activity Assay. Lysis of SB cells (CD20+ target cells; ATCC deposit no. ATCC CCL120) by human monocyte depleted peripheral blood mononuclear cells (effector cells) in the presence of different concentrations of C2B8 samples was performed basically following the same procedure described in Brunner et al., 1968, *Immunology* 14:181-189. The ratio of effector cells to target cells was 100:1.

## 2. Results And Discussion

GnT III Is Expressed At Different Levels In Different Cell Lines And Cultures. The cells of the parallel CHO-tet-GnTIII-C2B8 cultures, each culture containing different levels of tetracycline (2000, 50, and 25 ng/ml) and therefore expected to express GnTIII at different levels, were lysed and the cell lysates were resolved by SDS-PAGE and detected by Western blotting. The lysates of the culture grown at 25 ng/ml tetracycline showed an intense band at the corresponding molecular weight of GnT III whereas cultures grown at 50 and at 2000 ng/ml had much less expression of GnT III as shown in FIG. 13.

Verification Of Specific C2B8 Antigen Binding. C2B8 samples produced from parallel cultures of cells expressing different levels of GnT III were purified from the culture supernatants by affinity chromatography and buffer exchanged to PBS on a cation exchange column. Purity was estimated to be higher than 95% from Coomassie Blue staining of an SDS-PAGE under reducing conditions. These antibody samples were derived from expression of antibody genes whose variable regions were synthesized by a PCR assembly method. Sequencing of the synthetic cDNA fragments revealed no differences to the original C2B8 variable region sequences previously published in an international patent application (International Publication Number WO 94/11026). Specific binding of the samples to human CD20, the target antigen of C2B8, was demonstrated by indirect immunofluorescence using a human lymphoblastoid cell line SB expressing CD20 on its surface and an HSB lymphoblastoid cell line lacking this antigen. Antibody sample C2B8-25t gave positive staining of SB cells (FIG. 14A), but not of HSB cells under identical experimental conditions (see FIG. 14B). An additional negative control consisted of SB cells incubated with PBS buffer instead of C2B8-25t antibody. It showed no staining at all.

In Vitro ADCC Activity Of C2B8 Samples. The antibody sample C2B8-nt expressed in CHO-tA-C2B8 cells that do not have GnT III expression (see, supra) showed 31% cytotoxic activity (at 1  $\mu$ g/ml antibody concentration), measured as in vitro lysis of SB cells (CD20+) by human lymphocytes (FIG. 15, sample C2B8-nt). C2B8-2000t antibody derived from a CHO-tet-GnTIII culture grown at 2000 ng/ml of tetracycline (i.e., at the basal level of cloned GnT III expression) showed at 1  $\mu$ g/ml antibody concentration a 33% increase in ADCC activity with respect to the C2B8-nt sample at the same antibody concentration. Reducing the concentration of tetracycline to 25 ng/ml (sample C2B8-25t), which significantly increased GnTIII expression, produced a large increase of almost 80% in the maximal ADCC activity (at 1  $\mu$ g/ml antibody concentration) with respect to the C2B8-nt antibody sample at the same antibody concentration (FIG. 15, sample C2B8-25t).

Besides exhibiting the highest ADCC activity, C2B8-25t showed significant levels of cytotoxicity at very low antibody concentrations. The C2B8-25t sample at 0.06  $\mu$ g/ml showed an ADCC activity similar to the maximal ADCC activity of C2B8-nt at 1  $\mu$ g/ml. This result showed that sample C2B8-25t, at a 16-fold lower antibody concentration, reached the same ADCC activity as C2B8-nt. This result indicates that the chimeric anti-CD20 antibody C2B8 produced in a cell line actively expressing GnT III was significantly more active than the same antibody produced in a cell line that did not express GnT III.

One advantage of this antibody using the methods of the invention is that (1) lower doses of antibody have to be injected to reach the same therapeutic effect, having a beneficial impact in the economics of antibody production, or (2) that using the same dose of antibody a better therapeutic effect is obtained.

### E. Example 5

#### Establishment Of CHO Cell Lines With Constitutive Expression Of Glycosyltransferase Genes At Optimal Levels Leading To Maximal ADCC Activity

In some applications of the method for enhancing the ADCC it may be desirable to use constitutive rather than regulated expression of GnT III on its own or together with other cloned glycosyltransferases and/or glycosidases. However, the inventors have demonstrated that ADCC activity of the modified antibody depends on the expression level of GnT III. See, supra. Therefore, it is important to select a clone with constitutive expression of GnT III alone or together with other glycosyltransferase and/or glycosidase genes at optimal or near optimal levels. The optimal levels of expression of GnT III, either alone or together with other glycosyl transferases such as  $\beta$ (1,4)-galactosyl transferase (GalT), are first determined using cell lines with regulated expression of the glycosyl transferases. Stable clones with constitutive expression of GnT III and any other cloned glycosyltransferase are then screened for expression levels near the optimum.

#### 1. Determination Of Near-optimal Expression Levels

Construction Of A Vector For Regulated GnT III Expression linked To GFP Expression. Each glycosyl transferase gene is linked, via an IRES sequence, to a reporter gene encoding a protein retained in the cell, e.g., green fluorescent protein (GFP) or a plasma membrane protein tagged with a peptide that can be recognized by available antibodies. If more than one glycosyl transferase is being tested, a different marker is associated with each glycosyl transferase, e.g.,

GnT III may be associated to GFP and GalT may be associated to blue fluorescent protein (BFP). An eucaryotic expression cassette consisting of the GnT III cDNA upstream of an IRES element upstream of the GFP cDNA is first assembled by standard subcloning and/or PCR steps. This cassette is then subcloned in the tetracycline regulated expression vector pUHD10-3 (see, supra), downstream of the tet-promoter and upstream of the termination and polyadenylation sequences resulting in vector pUHD10-3-GnTIII-GFP.

Establishment Of CHO Cells With Regulated GnTIII Expression Linked To GFP Expression And Constitutive chCE7Antibody Expression. CHO-(TA) cells (see, supra) expressing the tetracycline-responsive transactivator, are co-transfected with vector pUHD10-3-GnTIII-GFP and vector pPur for expression of a puromycin-resistance gene. See, supra. Puromycin resistant clones are selected in the presence of tetracycline. Individual clones are cultured by duplicate in the presence (2 µg/ml) or absence of tetracycline. Six clones that show inhibition of growth in the absence of tetracycline, due to glycosyltransferase overexpression (see, supra), are selected and analyzed by fluorescence-activated cell sorting (FACS) for detection of the GFP-associated signal. A clone giving the highest induction ratio, defined as the ratio of fluorescence in the absence of tetracycline to fluorescence in the presence of tetracycline is chosen for further work and designated as CHO-tet-GnTIII-GFP. CHO-tet-GnTIII-GFP are transfected with expression vectors for antibody chCE7 and a clone with high constitutive expression of this antibody is selected CHO-tet-GnTIII-GFP-chCE7. See, supra.

Production Of chCE7 Samples, Measurement Of ADCC Activity And Determination Of Optimal GnTIII Expression Levels. Parallel cultures of CHO-tet-GnTIII-GFP-chCE7 are grown at different levels of tetracycline, and therefore expressing GnTIII together with GFP at different levels. chCE7 antibody samples are purified from the culture supernatants by affinity chromatography. In parallel, the cells from each culture are analyzed by FACS to determine the mean level of GFP-associated fluorescence, which is correlated to the expression level of GnT III, of each culture. The in vitro ADCC activity of each chCE7 antibody sample is determined (see, supra) and the maximal in vitro ADCC activity of each sample is plotted against the mean fluorescence of the cells used to produce it.

#### 2. Establishment Of A CHO Cell Line With Constitutive GnTIII expression At Near-optimal Levels

The GnTIII-IRES-GFP cassette (see, supra) is subcloned in a constitutive expression vector. CHO cells are stably co-transfected with this vector and a vector for puromycin resistance. Puromycin resistant cells are selected. This population of stably transfected cells is then sorted via FACS, and clones are selected which express the levels of reporter GFP gene near the within the range where optimal or near-optimal ADCC activity is achieved. See, supra. This final transfection step may be done either on CHO cells already stably expressing a therapeutic antibody or on empty CHO cells, e.g., DUKX or DG44 dhfr- CHO cells. In the latter case, the clones obtained from the procedure described above will be transfected with therapeutic antibody-expression vectors in order to generate the final antibody-producing cell lines.

#### F. Example 6

##### Cell Surface Expression Of A Human IgG Fc Chimera With Optimized Glycosylation

Encapsulated cell therapy is currently being tested for a number of diseases. An encapsulated cell implant is

designed to be surgically placed into the body to deliver a desired therapeutic substance directly where it is needed. However, if once implanted the encapsulated device has a mechanical failure, cells can escape and become undesirable. One way to destroy escaped, undesirable cells in the body is via an Fc-mediated cellular cytotoxicity mechanism. For this purpose, the cells to be encapsulated can be previously engineered to express a plasma membrane-anchored fusion protein made of a type 11 transmembrane domain that localizes to the plasma membrane fused to the N-terminus of an Fc region. Stabila, P. F., 1998, supra. Cells inside the capsule are protected against Fc-mediated cellular cytotoxicity by the capsule, while escaped cells are accessible for destruction by lymphocytes which recognize the surface-displayed Fc regions, i.e., via an Fc-mediated cellular cytotoxicity mechanism. This example illustrates how this Fc-mediated cellular cytotoxicity activity is enhanced by glycosylation engineering of the displayed Fc regions.

#### 1. Establishment Of Cells Expressing The Fc Chimera On Their Surface And Expressing GnTIII

Cells to be implanted for a particular therapy, for example baby hamster kidney (BHK) cells, which already produce the surface-displayed Fc chimera and a secreted, therapeutic protein, are first stably transfected with a vector for constitutive expression of GnTIII linked via an IRES element to expression of GFP. See, supra. Stable transfectants are selected by means of a marker incorporated in the vector, e.g., by means of a drug resistance marker and selected for survival in the presence of the drug.

#### 2. Screening Of Cells Expressing Different Levels Of GnTIII And Measurement

Stable transfectants are analyzed by fluorescence-activated cell sorting (FACS) and a series of clones with different mean fluorescence levels are selected for further studies. Each selected clone is grown and reanalyzed by FACS to ensure stability of GFP, and therefore associated GnT III, expression.

#### 3. Verification Of Different Levels Of Bisected Complex Oligosaccharides On The Displayed Fc Regions

Fc regions from three clones with different levels of GFP-associated fluorescence and from the original BHK cells not transfected with the GnTIII-IRES-GFP vector are solubilized from the membrane by means of a detergent and then purified by affinity chromatography. The oligosaccharides are then removed, purified and analyzed by MALDI-TOF/MS. See, supra. The resulting MALDI-TOF/MS profiles show that the Fc-regions of the modified, fluorescent clones carry different proportions of bisected complex oligosaccharides. The MALDI profile from the unmodified cells does not show any peak associated to bisected oligosaccharides. The clone with carrying the highest levels of bisected complex oligosaccharides on the displayed Fc regions is chosen for further work.

#### 4. In vitro Fc-mediated Cellular Cytotoxicity Activity Assay

Two Fc-mediated cellular cytotoxicity activity assays are then conducted in parallel. In one assay the target cells are derived from the clone selected above. In the parallel assay the target cells are the original cells to be encapsulated and which have not been modified to express GnTIII. The assay is conducted using the procedure described previously (see, supra) but in the absence of any additional antibody, since the target cells already display Fc regions. This experiment demonstrates that the Fc-mediated cellular cytotoxicity activity against the cells expressing GnT III is higher than that against cells not expressing this glycosyltransferase.

All references cited within the body of the instant specification are hereby incorporated by reference in their entirety.

## SEQUENCE LISTING

<160> NUMBER OF SEQ ID NOS: 14

<210> SEQ ID NO 1  
 <211> LENGTH: 50  
 <212> TYPE: DNA  
 <213> ORGANISM: Artificial Sequence  
 <220> FEATURE:  
 <223> OTHER INFORMATION: PCR Oligonucleotide Primer CE7VHPCR1.fwd

<400> SEQUENCE: 1

ttccttgctg ctgttgctac gcgtgtcctg tcccaggtcc aactgcagca 50

<210> SEQ ID NO 2  
 <211> LENGTH: 63  
 <212> TYPE: DNA  
 <213> ORGANISM: Artificial Sequence  
 <220> FEATURE:  
 <223> OTHER INFORMATION: PCR Oligonucleotide Primer CE7VHPCR2.fwd

<400> SEQUENCE: 2

gtgtgttaaag cttccaccat gggttggaqc ctcactctgc tcttccttgt cgctgttget 60  
 acg 63

<210> SEQ ID NO 3  
 <211> LENGTH: 38  
 <212> TYPE: DNA  
 <213> ORGANISM: Artificial Sequence  
 <220> FEATURE:  
 <223> OTHER INFORMATION: PCR Oligonucleotide Primer CE7VHPCR(1+2).rev

<400> SEQUENCE: 3

gtgtgtgaat.tcgctagctg aggagactgt gagagtgg 38

<210> SEQ ID NO 4  
 <211> LENGTH: 40  
 <212> TYPE: DNA  
 <213> ORGANISM: Artificial Sequence  
 <220> FEATURE:  
 <223> OTHER INFORMATION: PCR Oligonucleotide Primer hGamma1CH1.fwd

<400> SEQUENCE: 4

gtttgtaagc ttgctagcac caagggccca tcggtcttcc 40

<210> SEQ ID NO 5  
 <211> LENGTH: 59  
 <212> TYPE: DNA  
 <213> ORGANISM: Artificial Sequence  
 <220> FEATURE:  
 <223> OTHER INFORMATION: PCR Oligonucleotide Primer hGamma1CH1.rev

<400> SEQUENCE: 5

ggcatgtgtg agttttgtca caagatttgg gctcaacttt cttgtccacc ttggtgttg 59

<210> SEQ ID NO 6  
 <211> LENGTH: 57  
 <212> TYPE: DNA  
 <213> ORGANISM: Artificial Sequence  
 <220> FEATURE:  
 <223> OTHER INFORMATION: PCR Oligonucleotide Primer hGamma1CH2.fwd

<400> SEQUENCE: 6

tcttgtgaca aaactcacac atgcccaccg tgcccagacc tgaactcctg gggggac 57

-continued

---

```

<210> SEQ ID NO 7
<211> LENGTH: 49
<212> TYPE: DNA
<213> ORGANISM: Artificial Sequence
<220> FEATURE:
<223> OTHER INFORMATION: hGamma1CH2.rev

<400> SEQUENCE: 7
ctctgtggttc tcgggggtgc cctttggctt tggagatggt tttctcgat          49

<210> SEQ ID NO 8
<211> LENGTH: 22
<212> TYPE: DNA
<213> ORGANISM: Artificial Sequence
<220> FEATURE:
<223> OTHER INFORMATION: PCR Oligonucleotide Primer hGamma1CH3.fwd

<400> SEQUENCE: 8
gggcagcccc gagaaccaca gg                                          22

<210> SEQ ID NO 9
<211> LENGTH: 36
<212> TYPE: DNA
<213> ORGANISM: Artificial Sequence
<220> FEATURE:
<223> OTHER INFORMATION: PCR Oligonucleotide Primer hGamma1CH2.rev

<400> SEQUENCE: 9
gtgtgtggat cctcatttac ccggagacag ggagag                          36

<210> SEQ ID NO 10
<211> LENGTH: 56
<212> TYPE: DNA
<213> ORGANISM: Artificial Sequence
<220> FEATURE:
<223> OTHER INFORMATION: PCR Oligonucleotide Primer CE7VLPCR1.fwd

<400> SEQUENCE: 10
tgggtactgc tgetctgggt tccaggttcc actggtgaca tccagatgac acaatc   56

<210> SEQ ID NO 11
<211> LENGTH: 63
<212> TYPE: DNA
<213> ORGANISM: Artificial Sequence
<220> FEATURE:
<223> OTHER INFORMATION: PCR Oligonucleotide Primer CE7VLPCR2.fwd

<400> SEQUENCE: 11
gtgtgtaagc ttccaccatg gagacagaca cactctctgct atgggtactg ctgctctggg  60
ttc                                                                    63

<210> SEQ ID NO 12
<211> LENGTH: 37
<212> TYPE: DNA
<213> ORGANISM: Artificial Sequence
<220> FEATURE:
<223> OTHER INFORMATION: PCR Oligonucleotide Primer CE7VLPCR(1+2).rev

<400> SEQUENCE: 12
gtgtgtgaat tccgtactgt ttatttccaa ctctgtc                          37

<210> SEQ ID NO 13
<211> LENGTH: 32
<212> TYPE: DNA
<213> ORGANISM: Artificial Sequence
<220> FEATURE:

```

-continued

&lt;223&gt; OTHER INFORMATION: PCR Oligonucleotide Primer hKappa.fwd

&lt;400&gt; SEQUENCE: 13

gtgtgtaagc ttctgaacgt ggtgcacca tc

32

&lt;210&gt; SEQ ID NO 14

&lt;211&gt; LENGTH: 33

&lt;212&gt; TYPE: DNA

&lt;213&gt; ORGANISM: Artificial Sequence

&lt;220&gt; FEATURE:

&lt;223&gt; OTHER INFORMATION: PCR Oligonucleotide Primer hKappa.rev

&lt;400&gt; SEQUENCE: 14

gtgtgtggat ccctaacact ctcccctggt gaa

33

What is claimed is:

1. A method for producing a polypeptide having increased Fc-mediated cellular cytotoxicity in a host cell, comprising:

(a) culturing a host cell engineered to express at least one nucleic acid encoding  $\beta(1,4)$ -N-acetylglucosaminyltransferase III (GnT III) under conditions which permit the production of a polypeptide selected from the group consisting of a whole antibody molecule, an antibody fragment, and a fusion protein that includes the Fc region of an immunoglobulin, wherein said GnT III is expressed in an amount sufficient to modify the oligosaccharides in the Fc region of said polypeptide produced by said host cell and wherein said polypeptide has increased Fc-mediated cellular cytotoxicity as a result of said modification; and

(b) isolating said polypeptide having increased Fc-mediated cellular cytotoxicity.

2. The method of claim 1, wherein in step (a), said host cell comprises at least one nucleic acid encoding a whole antibody.

3. The method of claim 1, wherein in step (a), said host cell comprises at least one nucleic acid encoding an antibody fragment.

4. The method of claim 1, wherein in step (a), said host cell comprises at least one nucleic acid encoding a fusion protein comprising a glycosylated Fc region of an immunoglobulin.

5. The method of claim 1, wherein the expression level of glycosyl transferase GnT III produces an antibody molecule, antibody fragment, or a fusion protein that includes the Fc region of an immunoglobulin having increased Fc-mediated cellular cytotoxicity at a higher level than the Fc-mediated cellular cytotoxicity obtained from a different expression level of the same glycosyl transferase GnT III gene.

6. The method of claim 1, wherein said host cell further comprises a nucleic acid encoding a glycosidase.

7. The method of claim 1, wherein the expression level of glycosyl transferase GnT III is sufficient to form bisected oligosaccharides in the Fc region of said polypeptide.

8. The method of claim 7, wherein the proportion of bisected oligosaccharides in the Fc region is at least 45 percent.

9. The method of claim 7, wherein said bisected oligosaccharides are bisected, complex oligosaccharides.

10. A method for producing a polypeptide having increased Fc-mediated cellular cytotoxicity in a host cell, comprising:

(a) culturing a host cell engineered to express at least one nucleic acid encoding  $\beta(1,4)$ -N-acetylglucosaminyltransferase III (GnT III) under conditions which permit the production of a polypeptide selected from the group consisting of a whole antibody molecule, an antibody fragment, and a fusion protein that includes a Fc region of an immunoglobulin and an antigen binding region, wherein said GnT III is expressed in an amount sufficient to modify oligosaccharides in the Fc region of said polypeptide produced by said host cell, and wherein said polypeptide has increased Fc-mediated cellular cytotoxicity as a result of said modification; and

(b) isolating said polypeptide having increased Fc-mediated cellular cytotoxicity;

wherein said increased Fc-mediated cellular cytotoxicity is determined by an increase in antibody-dependent cellular cytotoxicity as measured in the following standard in vitro assay which uses viable target cells that are known to express a target antigen recognized by the antigen-binding region of said polypeptide, and uses as effector cells human peripheral blood mononuclear cells (PBMCs), said standard in vitro assay comprising the steps of:

(i) labeling said target cells with the fluorescent dye Calcein AM as a marker for cell integrity;

(ii) obtaining a first portion of said labeled target cells and dividing said first portion into multiple equal subportions of said labeled target cells;

(iii) obtaining second and third portions of said labeled target cells having the same number of labeled target cells as said multiple equal subportions;

(iv) mixing each said multiple equal subportion of said labeled target cells with a different concentration of polypeptide in a multi-well assay plate, each concentration being tested in triplicate and said different concentrations of polypeptide chosen to give different percentages of specific lysis;

(v) mixing said second portion of said labeled target cells with a detergent that lyses said labeled target cells in said multi-well assay plate to provide a total lysis control portion;

(vi) mixing said third portion of said labeled target cells with antibody-free culture medium in said multi-well assay plate to provide a spontaneous release control portion;

(vii) incubating said multi-well assay plate containing said multiple equal subportions, total lysis control portion, and spontaneous release control portion for 1 hr;

39

- (viii) adding effector cells to each of said multiple equal subportions, total lysis control portion, and spontaneous release control portion in said multi-well assay plate to yield an effector cell: target cell ratio of 19:1 and mixing;
- (ix) incubating said multi-well assay plate in an incubator under 5% CO<sub>2</sub> atmosphere at 37° C. for 16 hrs;
- (x) discarding the cell free supernatant from each well of said multi-well assay plate;
- (xi) washing said labeled target cells in said multi-well assay plate with buffered saline solution;
- (xii) lysing said labeled target cells in nonionic detergent t-octylphenoxypolyethoxyethanol at a final concentration of 0.1% (v/v);
- (xiii) measuring the experimentally retained fluorescence (EF) of said target cells with a fluorometer;

40

wherein the percentage of specific cell lysis for each polypeptide concentration is calculated according to the formula  $(SR-EF)/(SR-MR) \times 100$ , where EF is average fluorescence measured for a given polypeptide concentration, MR is the average fluorescence measured for said total lysis control portion, and SR is the average fluorescence measured for said spontaneous release control portion, and wherein an increase in antibody-dependent cellular cytotoxicity is measured as either an increase in the maximum percentage of specific lysis observed within the polypeptide concentration range tested, and/or a reduction in the concentration of polypeptide required to achieve one half of the maximum percentage of specific lysis observed within the polypeptide concentration range tested.

\* \* \* \* \*



# **Attachment E**

**Evidence of Maintenance Fee Schedule for  
U.S. Patent No. 6,602,684**

[Return To:](#)[USPTO Home Page](#)[Finance Online Shopping Page](#)

United States  
Patent and  
Trademark Office

Patent Bibliographic Data		12/09/2013 07:40 PM	
Patent Number:	6602684	Application Number:	09294584
Issue Date:	08/05/2003	Filing Date:	04/20/1999
Title:	GLYCOSYLATION ENGINEERING OF ANTIBODIES FOR IMPROVING ANTIBODY-DEPENDENT CELLULAR CYTOTOXICITY		
Status:	12th year fee window opens: 08/05/2014		Entity: LARGE
Window Opens:	N/A	Surcharge Date:	N/A
Expiration:	N/A		
Fee Amt Due:	Window not open	Surchg Amt Due:	Window not open
Total Amt Due:	Window not open		
Fee Code:			
Surcharge Fee Code:			
Most recent events (up to 7):	12/28/2010 Payment of Maintenance Fee, 8th Year, Large Entity. 12/18/2006 Payment of Maintenance Fee, 4th Year, Large Entity. --- End of Maintenance History ---		
Address for fee purposes:	STERNE, KESSLER, GOLDSTEIN & FOX P.L.L.C 1100 NEW YORK AVENUE, N.W. WASHINGTON DC 20005		
<a href="#">Run Another Query</a>			

[Need Help?](#) | [USPTO Home Page](#) | [Finance Online Shopping Page](#) | [Alerts Page](#)

<https://ramps.uspto.gov/eram/getMaintFeesInfo.do?jsessionid=AF42E9CF1E4B9CC46B50...> 12/9/2013

# **Attachment F**

**Letter from FDA to Genentech, Inc.,  
acknowledging receipt of BLA**



DEPARTMENT OF HEALTH AND HUMAN SERVICES

RECEIVED MAY 08 2013  
FD

Food and Drug Administration  
Silver Spring MD 20993

BLA 125486

**BLA ACKNOWLEDGEMENT**

Genentech, Inc.  
Attention: Michelle H. Rohrer, Ph.D.  
Vice President, Regulatory Affairs  
1 DNA Way  
South San Francisco, CA 94080-4990

Dear Dr. Rohrer:

We have received your Biologics License Application (BLA) submitted under section 351(a) of the Public Health Service Act (PHS Act) for the following:

**Name of Biological Product:** obinutuzumab

**Date of Application:** April 22, 2013

**Date of Receipt:** April 22, 2013

**Our Secondary Tracking Number (STN):** BLA 125486

**Proposed Use:** For the treatment of patients with previously untreated chronic lymphocytic leukemia

If you have not already done so, promptly submit the content of labeling [21 CFR 601.14(b)] in structured product labeling (SPL) format as described at <http://www.fda.gov/oc/datacouncil/spl.html>. Failure to submit the content of labeling in SPL format may result in a refusal-to-file action. The content of labeling must conform to the format and content requirements of 21 CFR 201.56-57.

You are also responsible for complying with the applicable provisions of sections 402(i) and 402(j) of the Public Health Service Act (PHS Act) [42 USC §§ 282 (i) and (j)], which was amended by Title VIII of the Food and Drug Administration Amendments Act of 2007 (FDAAA) (Public Law No. 110-85, 121 Stat. 904).

The BLA Submission Tracking Number provided above should be cited at the top of the first page of all submissions to this application. Send all submissions, electronic or paper, including those sent by overnight mail or courier, to the following address:

Reference ID: 3303097

Food and Drug Administration  
Center for Drug Evaluation and Research  
Division of Hematology Products  
5901-B Ammendale Road  
Beltsville, MD 20705-1266

All regulatory documents submitted in paper should be three-hole punched on the left side of the page and bound. The left margin should be at least three-fourths of an inch to assure text is not obscured in the fastened area. Standard paper size (8-1/2 by 11 inches) should be used; however, it may occasionally be necessary to use individual pages larger than standard paper size. Non-standard, large pages should be folded and mounted to allow the page to be opened for review without disassembling the jacket and refolded without damage when the volume is shelved. Shipping unbound documents may result in the loss of portions of the submission or an unnecessary delay in processing which could have an adverse impact on the review of the submission.

Secure email between CDER and applicants is useful for informal communications when confidential information may be included in the message (for example, trade secrets or patient information). If you have not already established secure email with the FDA and would like to set it up, send an email request to [SecureEmail@fda.hhs.gov](mailto:SecureEmail@fda.hhs.gov). Please note that secure email may not be used for formal regulatory submissions to applications.

If you have any questions, call me at (301) 796-3907.

Sincerely,

*{See appended electronic signature page}*

Tyree Newman  
Regulatory Health Project Manager  
Division of Hematology Products  
Office of Hematology and Oncology Products  
Center for Drug Evaluation and Research

-----  
**This is a representation of an electronic record that was signed electronically and this page is the manifestation of the electronic signature.**  
-----

/s/  
-----

TYREE L NEWMAN  
05/02/2013

Reference ID: 3303097

# **Attachment G**

**Power of Attorney from Genentech, Inc., to  
Practitioners**

Docket No.: 146392023400  
Client Ref. No.: 23437-US1

**IN THE UNITED STATES PATENT AND TRADEMARK OFFICE**

In re Patent of: Umaña *et al.*

Patent No.: 6,602,684

Issued: August 5, 2003

Application No: 09/294,584

For: GLYCOSYLATION ENGINEERING OF  
ANTIBODIES FOR IMPROVING ANTIBODY-  
DEPENDENT CELLULAR CYTOTOXICITY-  
Application for § 156 Patent Term Extension

Attorney Docket No: 146392023400

Assignee: Roche Glycart AG

Unit: Office of Patent Legal  
Administration

Mail Stop Hatch-Waxman PTE  
Commissioner for Patents  
P.O. Box 1450  
Alexandria, VA 22313-1450

**AUTHORIZATION AND POWER OF ATTORNEY TO FILE APPLICATION FOR  
EXTENSION OF PATENT TERM UNDER 35 U.S.C. § 156**

As an authorized representative of Genentech, Inc., I hereby authorize Genentech, Inc.'s counsel, Morrison & Foerster LLP, to file and prosecute a patent term extension application under 35 U.S.C. § 156 for U.S. Patent 6,602,684 ("the '684 Patent"). Genentech, Inc., exclusive licensee of the '684 Patent, is authorized to act as the agent of Roche Glycart AG, owner of the entire right, title and interest in the '684 Patent, with respect to submission of this patent term extension application. Accordingly, Genentech, Inc., appoints practitioners associated with Customer Number 25226 to file and prosecute the application for patent term extension for the '684 Patent and to transact all business in the United States Patent and Trademark Office connected with this patent term extension application. Please direct all correspondence regarding this application for



Patent No.: 6,602,684

Docket No.: 146392023400  
Client Ref. No.: 23437-US1

patent term extension to Morrison & Foerster LLP, 755 Page Mill Road, Palo Alto, CA 94304-1018. The correspondence address for the '684 Patent is to be unchanged for all other purposes.

Date December 12, 2013

Respectfully submitted,

By Irene Pleasure

Name: Irene Pleasure <sup>ELS</sup>

Title: Head of Patents, Senior Director

Phone: 650-225-1000

# **Attachment H**

**Letter from FDA to Genentech, Inc.,  
acknowledging receipt of IND**



DEPARTMENT OF HEALTH &amp; HUMAN SERVICES

Public Health Service

Food and Drug Administration  
Rockville, MD 20857

IND 104405

**IND ACKNOWLEDGEMENT**

Genentech, Inc.  
 Attention: Todd W. Rich, M.D.  
 Vice President, Development Regulatory Affairs, Medical Communications,  
 Drug Safety and Development Quality and Compliance  
 1 DNA Way  
 South San Francisco, CA 94080-4990

Dear Dr. Rich:

We acknowledge receipt of your Investigational New Drug Application (IND) submitted under section 505(i) of the Federal Food, Drug, and Cosmetic Act (FDCA). Please note the following identifying data:

**IND NUMBER ASSIGNED:** 104405**SPONSOR:** Genentech, Inc.**PRODUCT NAMES:** Human Monoclonal Antibody to CD20 (RO5072759)**DATE OF SUBMISSION:** February 6, 2009**DATE OF RECEIPT:** February 9, 2009

You may not initiate studies in humans until 30 days after the date of receipt shown above unless we notify you sooner that you may proceed. If, on or before March 11, 2009, we identify deficiencies in the IND that require correction before human studies begin or that require restriction of human studies, we will immediately notify you verbally or in writing that (1) clinical studies may not be initiated under this IND ("clinical hold") or (2) certain restrictions apply to clinical studies under this IND ("partial clinical hold"). If we place your human studies on clinical hold, you will be notified in writing of the reasons and the information necessary to correct the deficiencies. In the event of such notification, you must not initiate or you must restrict such studies until you have submitted information to correct the deficiencies, and we have subsequently notified you that the information you submitted is satisfactory.

It has not been our policy to object to a sponsor, upon receipt of this acknowledgement letter, either obtaining supplies of the investigational drug or shipping it to investigators listed in the IND. However, if the drug is shipped to investigators, they should be reminded that studies may not begin under the IND until 30 days after the IND receipt date or later if the IND is placed on clinical hold.

As sponsor of this IND, you are responsible for compliance with the FDCA (21U.S.C. §§ 301 et. seq.) as well as the implementing regulations [Title 21 of the Code of Federal Regulations (CFR)]. A searchable version of these regulations is available at <http://www.accessdata.fda.gov/scripts/cdrh/cfdocs/cfcfr/CFRSearch.cfm>. Your responsibilities include (1) reporting any unexpected fatal or life-threatening adverse experiences associated with use of the drug by telephone or fax no later than 7 calendar days after initial receipt of the information [21 CFR 312.32(c)(2)]; (2) reporting any serious, unexpected adverse experiences, as well as results from animal studies that suggest significant clinical risk, in writing to this Division and to all investigators within 15 calendar days after initial receipt of this information [21 CFR 312.32(c)(1)]; and (3) submitting annual progress reports within 60 days of the anniversary of the date that the IND went into effect (the date clinical studies were permitted to begin) [21 CFR 312.33]. You are also responsible for complying with the applicable provisions of section 402(i) and (j) of the Public Health Service Act (PHS Act) (42 USC §§ 282 (i) and (j)), which was amended by Title VIII of the Food and Drug Administration Amendments Act of 2007 (FDAAA) (Public Law No. 110-85, 121 Stat. 904).

Prior to use of each new lot of the investigational biologic in clinical studies, submit the lot number, the results of all tests performed on the lot, and the specifications when established (i.e., the range of acceptable results).

We remind you that you may not charge for this investigational drug without prior written approval of FDA.

All laboratory or animal studies intended to support the safety of this product should be conducted in compliance with the regulations for "Good Laboratory Practice for Nonclinical Laboratory Studies" (21 CFR Part 58). If such studies have not been conducted in compliance with these regulations, provide a statement describing in detail all differences between the practices used and those required in the regulations.

Item 7a of form FDA 1571 requests that either an "environmental assessment," or a "claim for categorical exclusion" from the requirements for environmental assessment, be included in the IND. If you did not include a response to this item with your application, please submit one. Information of environmental assessments is available in the guidance *Environmental Assessment of Human Drugs and Biologics*. This document is available at <http://www.fda.gov/cder/guidance/1730fnl.pdf>.

Cite the IND number listed above at the top of the first page of any communications concerning this application. Each submission to this IND must be provided in triplicate (original plus two copies). Please include three originals of all illustrations that do not reproduce well. Send all submissions, electronic or paper, including those sent by overnight mail or courier, to the following address:

Food and Drug Administration  
Center for Drug Evaluation and Research  
Division of Biologics Oncology Products  
Therapeutic Biological Products Document Room  
5901-B Ammendale Road  
Beltsville, MD 20705-1266

All regulatory documents submitted in paper should be three-hole punched on the left side of the page and bound. The left margin should be at least three-fourths of an inch to assure text is not obscured in the fastened area. Standard paper size (8-1/2 by 11 inches) should be used; however, it may occasionally be necessary to use individual pages larger than standard paper size. Non-standard, large pages should be folded and mounted to allow the page to be opened for review without disassembling the jacket and refolded without damage when the volume is shelved. Shipping unbound documents may result in the loss of portions of the submission or an unnecessary delay in processing which could have an adverse impact on the review of the submission. For additional information, see <http://www.fda.gov/cder/ddms/binders.htm>.

If you have any questions, concerning this IND call me at (301)796-0704.

Sincerely,

*{See appended electronic signature page}*

Gina M. Davis, MT  
Division of Biologics Oncology Products  
Office Oncology Drug Products  
Center for Drug Evaluation and Research

Linked Applications

Sponsor Name

Drug Name / Subject

IND 104405

Genetech Inc.

RO572759

-----  
**This is a representation of an electronic record that was signed electronically and this page is the manifestation of the electronic signature.**  
-----

/s/

-----  
GINA M DAVIS  
02/17/2009

# **Attachment I**

**Obinutuzumab BLA, Section 3.2.S.1.2  
Structure, redacted**



[REDACTED]

Obinutuzumab is a humanized monoclonal antibody based on a human IgG<sub>1</sub> ( $\kappa$ ) framework. The recombinant antibody is produced in Chinese hamster ovary (CHO) cells and consists of two heavy chains and two light chains with inter- and intra-chain disulfide bonds that are typical of IgG<sub>1</sub> antibodies.

[REDACTED]

[REDACTED]

[REDACTED]

- [REDACTED]
- [REDACTED]
- [REDACTED]
- [REDACTED]
- [REDACTED]

[REDACTED]

[REDACTED]

[REDACTED]

[REDACTED]

- [REDACTED]
- [REDACTED]



# **Attachment J**

**Klein *et al.*, *mAbs*, 2013, 5(1):22-33**

# Epitope interactions of monoclonal antibodies targeting CD20 and their relationship to functional properties

Christian Klein,<sup>1,\*</sup> Alfred Lammens,<sup>2</sup> Wolfgang Schäfer,<sup>4</sup> Guy Georges,<sup>4</sup> Manfred Schwaiger,<sup>3</sup> Ekkehard Mössner,<sup>1</sup> Karl-Peter Hopfner,<sup>2</sup> Pablo Umaña<sup>1</sup> and Gerhard Niederfellner<sup>3</sup>

<sup>1</sup>Discovery Oncology; Pharma Research and Early Development (pRED); Roche Glycart AG; Schlieren, Switzerland; <sup>2</sup>Department of Chemistry and Biochemistry; Gene Center; Ludwig-Maximilians University Munich; Munich, Germany; <sup>3</sup>Discovery Oncology; Pharma Research and Early Development (pRED); Roche Diagnostics GmbH; Penzberg, Germany; <sup>4</sup>Large Molecule Research; Pharma Research and Early Development (pRED); Roche Diagnostics GmbH; Penzberg, Germany

**Keywords:** Rituximab, obinutuzumab, ofatumumab, GA101, structure, type I, type II, non-Hodgkin lymphoma, immunotherapy, leukemia

**Abbreviations:** ADCC, antibody-dependent cellular cytotoxicity; ADCP, antibody-dependent cellular phagocytosis; CDC, complement-dependent cytotoxicity; CDR, complementarity-determining region; CLL, chronic lymphocytic leukemia; DLBCL, diffuse large B cell lymphoma; FcγR, Fcγ receptor; FL, follicular lymphoma; Ig, immunoglobulin; NHL, non-Hodgkin lymphoma; MS, multiple sclerosis

Several novel anti-CD20 monoclonal antibodies are currently in development with the aim of improving the treatment of B cell malignancies. Mutagenesis and epitope mapping studies have revealed differences between the CD20 epitopes recognized by these antibodies. Recently, X-ray crystallography studies confirmed that the Type I CD20 antibody rituximab and the Type II CD20 antibody obinutuzumab (GA101) differ fundamentally in their interaction with CD20 despite recognizing a partially overlapping epitope on CD20. The Type I CD20 antibodies rituximab and ofatumumab are known to bind to different epitopes. The differences suggest that the biological properties of these antibodies are not solely determined by their core epitope sequences, but also depend on other factors, such as the elbow hinge angle, the orientation of the bound antibody and differential effects mediated by the Fc region of the antibody. Taken together, these factors may explain differences in the preclinical properties and clinical efficacy of anti-CD20 antibodies.

## Introduction

CD20 is a transmembrane cellular protein that has been validated as a therapeutic target for treatment of B cell malignancies<sup>1</sup> (Fig. 1A). CD20 is highly expressed by over 95% of B cell lymphocytes throughout their development, from the pre-B cell stage until their final differentiation into plasma cells, but is absent on the hematopoietic stem cell.<sup>2</sup> Moreover, CD20 is believed to exist predominantly as a tetramer on the cell surface. It is also largely believed to be not usually shed or internalized

upon antibody binding, meaning that therapeutic antibodies may be expected to recruit immune effector cells and mediate sustained immunologic activity.<sup>3</sup> The physiological function of CD20 remains unclear,<sup>1</sup> although evidence suggested that it may be involved in calcium signaling downstream of B cell antigen receptor activation.<sup>4</sup>

Rituximab (MabThera<sup>®</sup>; Rituxan<sup>®</sup>, Roche/Genentech/Biogen IDEC) was the first monoclonal antibody to be approved for the treatment of lymphoma, and it has changed the treatment of non-Hodgkin lymphoma (NHL) and chronic lymphocytic leukemia (CLL),<sup>5</sup> particularly in combination with chemotherapy where it has been shown to improve survival compared with chemotherapy alone.<sup>6–10</sup> More recently, the use of rituximab in maintenance therapy has been shown to further improve outcomes in patients with follicular lymphoma (FL).<sup>11–16</sup> This has established rituximab's position as a standard-of-care therapy in the treatment of NHL and CLL.<sup>17–19</sup> Other anti-CD20 antibodies have been introduced into use, including ofatumumab (Arzerra<sup>®</sup>; Genmab/GlaxoSmithKline), which is a human antibody approved for refractory CLL,<sup>20,21</sup> and tositumomab (Bexxar<sup>®</sup>, GlaxoSmithKline) and ibritumomab tiuxetan (Zevalin<sup>®</sup>, Spectrum), which are murine antibodies used clinically as radioimmunoconjugates.<sup>22</sup> Ongoing research aims to develop novel anti-CD20 antibodies with improved properties and greater clinical efficacy. Critical to this process is a better understanding of the mechanisms by which anti-CD20 antibodies act and the relative contributions of different modes of action to clinical efficacy.

After binding to CD20-positive cells, antibodies are thought to trigger at least three different effector functions: (programmed) cell death (also termed as direct cell death or apoptosis), antibody-dependent cellular cytotoxicity (ADCC) or phagocytosis (ADCP) and complement-dependent cytotoxicity (CDC).<sup>3,23</sup> Anti-CD20 antibodies are categorized as

\*Correspondence to: Christian Klein; Email: christian.klein.ck1@roche.com  
Submitted: 09/30/12; Revised: 10/31/12; Accepted: 11/03/12  
<http://dx.doi.org/10.4161/mabs.22771>

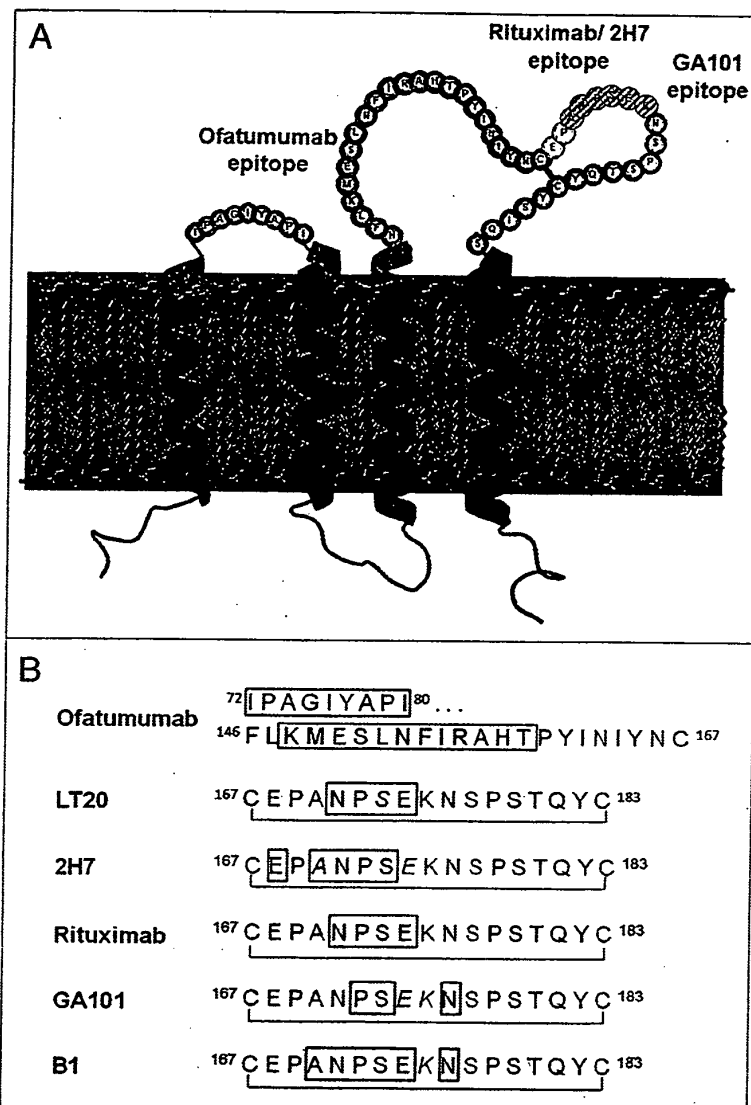


**Figure 1. (A)** The structure and topology of CD20 and the epitopes recognized by rituximab, ofatumumab and GA101. **(B)** Sequence alignment of CD20 epitopes recognized by CD20 antibodies based on published information. Core epitope residues are boxed in light blue. For 2F2 (ofatumumab), core epitope assignment is based on published work from Teeling et al. 46. For residues labeled in blue experimental evidence suggests a role in 2F2 binding. For the other antibodies, the following coloring scheme has been applied based on Pepscan results and FACS binding data of amino acid exchange mutants: green, almost any exchange tolerated at this position; brown, non-conservative exchange tested and not tolerated at this position; orange, conservative exchange tested and tolerated at this position; red, also conservative exchanges not tolerated at this position; black, position has not yet been evaluated. Italic font indicates that Pepscan and FACS-binding results are discordant. Since the FACS binding results better reflect the native protein context, the coloring in such instances was based on the FACS binding data.

Type I or Type II according to their mode of CD20 binding and their primary mechanism for killing CD20-positive cells<sup>24-29</sup> (Table 1).

This review article will focus on the application of anti-CD20 monoclonal antibodies to B cell malignancies; however, it should be noted that some of the antibodies discussed in this review have also been approved<sup>30</sup> or are being investigated<sup>31</sup> in the treatment of non-cancer indications (e.g., multiple sclerosis, rheumatoid arthritis, systemic lupus erythematosus).

### Type I and Type II CD20 Antibodies and their Effector Functions

Most existing anti-CD20 antibodies, including rituximab, veltuzumab, ocrelizumab and ofatumumab, are categorized as Type I (Table 2). These antibodies are characterized by their ability to induce a translocation of CD20 into large lipid microdomains or 'lipid rafts' within the plasma membrane upon binding.<sup>26,32,33</sup> This clustering process enhances the recruitment and activation of complement, and hence Type I antibodies exert potent CDC.<sup>25,26</sup> However, the contribution of complement activation to the depletion of B cells *in vivo* remains unclear.<sup>3,34</sup> Another characteristic feature of Type I antibodies is that B cells can be bound by twice as many Type I antibodies compared with Type II antibodies,<sup>27,35</sup> most likely due to different binding geometries. The biological significance of this is unknown, but it has been hypothesized that the 2:1 stoichiometry could be explained by Type I antibodies binding between two CD20 tetramers, thereby crosslinking tetramers with two antibodies bound per tetramer, whereas Type II antibodies may bind within a tetramer, resulting in only one antibody bound per CD20 tetramer<sup>29,36</sup> (Fig. 2). In line with this, the two known Type II anti-CD20 antibodies tositumomab (or B1) and obinutuzumab (GA101) (Table 2), do not induce accumulation of CD20 upon antibody binding in insoluble lipid rafts and show relatively little CDC activity.<sup>25,27</sup> On the other hand, Type II antibodies are more potent than Type I antibodies in inducing homotypic adhesion and direct cell death.<sup>24,25,27</sup> Although this form of cell death was initially described as apoptosis, recent studies have demonstrated that it is a non-apoptotic form of direct cell death that follows an actin-dependent enhancement of cell-to-cell contact, the rupturing of lysosomes

within the cytoplasm<sup>28,37,38</sup> and the generation of reactive oxygen species, but does not show the classical hallmarks of apoptosis such as DNA laddering or caspase dependence.<sup>39</sup>

The ADCC and ADCP activity of anti-CD20 antibodies is mediated by the interaction of their Fc region with FcγRIIIa and is not affected by the Type I or Type II character of the antibody. FcγRIIIa is expressed on various immune effector cells, most prominently macrophages/monocytes and natural killer cells. FcγRIIIa crosslinking by binding to CD20 on target cells stimulates release of lytic enzymes by the effector cells and induces cell killing or promotes the phagocytosis of the target CD20 positive cell.<sup>3</sup> Two variants of FcγRIIIa have been identified in humans: a predominant lower affinity form with a phenylalanine at position 158 (FcγRIIIa-158F) and a higher affinity form with valine at this position (FcγRIIIa-158V).<sup>40-42</sup> The binding of the Fc region of antibodies to FcγRIIIa is dependent on interactions between the carbohydrate moieties of both the FcγRIIIa and antibody.<sup>43</sup> Notably, ADCC activity does not differ between Type I and Type II anti-CD20 antibodies,<sup>3</sup> but antibodies such as GA101 have been engineered for enhanced affinity for FcγRIIIa leading to an increased ability to bind and recruit effector cells and hence a higher ADCC level.<sup>27,44</sup> The contribution of ADCC to the clinical activity of antibodies remains to be established. However, the expression of the higher affinity FcγRIIIa-158V genotype in lymphoma patients has been shown to be associated with an improved response to rituximab (mono-) therapy,<sup>40,45</sup> suggesting that enhanced FcγRIIIa affinity may confer a clinical advantage.

Recently, Beers and colleagues<sup>46</sup> demonstrated an increased potency in depleting B cells from human CD20 transgenic mice of Type II antibodies compared with Type I antibodies. They attributed much of this disparity to the Type I antibody-mediated internalization of CD20 by B cells leading to reduced recruitment of macrophages (ADCP) and degradation of CD20/antibody complexes. The authors also noted that the type of disease affected the degree of internalization, with most cases of CLL and mantle cell lymphoma showing rapid CD20 internalization; this was in contrast to FL and DLBCL cells, which were more resistant to CD20 loss. The internalization process was promoted by the inhibitory FcγRIIb on target B cells and investigations have suggested that rituximab can crosslink CD20 and FcγRIIb on the same cell (in cis), whereas Type II antibodies do not appear to have this function<sup>47</sup> (Fig. 3).

Anti-CD20 antibodies possess complementarity-determining regions (CDR) that bind to a specific epitope on the antigen. Mutational analyses and peptide scanning studies have revealed differences between antibodies in their CD20 epitopes.<sup>29,48,49</sup> Recently, three-dimensional crystallographic representations of several antibodies in complex with CD20 confirmed fundamental differences in their interactions with CD20 (Fig. 4) [rituximab,<sup>50</sup> C2H7 (ocrelizumab),<sup>51</sup> ofatumumab,<sup>52</sup> GA101].

Structurally, CD20 comprises four hydrophobic membrane-spanning domains, two extracellular loops (one of approximately 44 amino acids and a smaller one of approximately seven amino acids), and intracellular N- and C-terminal regions (Fig. 1A). The intracellular regions of CD20 can undergo phosphorylation upon antibody binding, thereby mediating cellular signaling.<sup>1</sup>

**Table 1.** Characteristics of Type I and II antibodies

Type I antibodies	Type II antibodies
Class I epitope	Class II epitope
Localize CD20 to lipid rafts	Do not localize CD20 to lipid rafts
High CDC	Low CDC
ADCC activity	ADCC activity
Full binding capacity	Half binding capacity
Weak homotypic aggregation	Homotypic aggregation
Cell death induction	Stronger cell death induction
Rituximab, ocrelizumab (2H7), ofatumumab (2F2)	GA101, tositumomab (B1)

ADCC, antibody-dependent cellular cytotoxicity; CDC, complement-dependent cytotoxicity; mAb, monoclonal antibody.

Most of the epitopes involved in antibody recognition are located within the larger extracellular loop. Recently, Niederfellner and colleagues<sup>29</sup> mapped the epitopes recognized by anti-CD20 antibodies. They showed that, despite recognizing an overlapping epitope on the large extracellular loop of CD20, Type II antibodies bind in a different orientation than Type I antibodies. For example, the core epitope of GA101 (a Type II antibody) is formed by residues 172–178, whereas the Type I antibody rituximab targets the more N-terminally comprising residues 168–175, with 170–173 contributing most essentially. For binding of Type II antibodies, asparagine 176 (N176) is a critical residue (Fig. 1B), whereas this residue does not seem to make any contacts with CD20-bound Type I antibodies, as exemplified by the crystal structure of rituximab (Fig. 5). The crystal structure of the GA101–CD20 epitope peptide complex confirmed that the shift in the core epitope resulted in a fundamentally different orientation of GA101 with respect to CD20. Based upon the currently available data, we have generated a model of rituximab and GA101 bound to CD20 (Fig. 6). Ofatumumab, another Type I antibody, binds to both the large and small CD20 extracellular loops,<sup>48,52</sup> as discussed below.

### Type I CD20 Antibodies

**Rituximab.** Rituximab is a Type I chimeric (human–mouse) immunoglobulin (Ig)G1 anti-CD20 antibody. The CD20 epitope recognized by rituximab and other mouse-derived antibodies spans amino acid residues 168–175 of the CD20 protein, with the ANPS motif at residues 170–173 on the large extracellular loop appearing to be of critical importance<sup>29,33,48,50,53</sup> (Fig. 1B). These key residues have been shown to form a network of hydrogen bonds with residues of the surrounding CDR loops.<sup>51</sup> The particular importance of the alanine residue at position 170 (A170) and the proline residue at position 172 (P172) was shown by site-directed mutagenesis studies taking advantage of the fact that rituximab binds only human, but not mouse, CD20. Introducing the <sup>170</sup>ANP<sup>172</sup> motif into mouse CD20 conferred binding of rituximab. The importance of the <sup>170</sup>ANPS<sup>173</sup> region for rituximab binding in humans has also been established by the screening of libraries of phage-displayed peptides with different

**Table 2.** Characteristics of selected anti-CD20 monoclonal antibodies

Names	Development status (Indication)	Description	Type I or II	Epitope
Rituximab	Approved (NHL, DLBCL, CLL) Phase 3 (MCL, DLBCL)	Chimeric IgG1	I	<ul style="list-style-type: none"> <li>Large extracellular loop</li> <li>• Core epitope: <sup>170</sup>ANPS<sup>173</sup> region<sup>33</sup></li> <li>• <sup>182</sup>YCYSI<sup>185</sup>: contributes to conformational stability<sup>49</sup></li> <li>• WPXWLE: functional significance unclear<sup>43</sup></li> <li>• Contact region: positions 165–182<sup>48</sup></li> </ul>
Ofatumumab (2F2; HuMax-CD20)	Approved (CLL) Phase 2 (DLBCL)	Human IgG1	I	<ul style="list-style-type: none"> <li>Large extracellular loop</li> <li>• Core epitope: FLKMESLNFIHAHT region<sup>48</sup></li> <li>• T159K, N163D and N166D residues critical, mostly likely for conformational stability<sup>48</sup></li> <li>Small extracellular loop</li> <li>• A74T, I76A and Y77S residues<sup>76</sup></li> </ul>
Veltuzumab (IMMU-06; hA20)	Phase 2 (NHL)	Humanized IgG1κ	I	Largely identical to rituximab (above) <sup>84</sup>
Ocaratuzumab (AME-D, AME-133)	Phase 2 (NHL)	Humanized IgG1 with Fab/Fc engineered to improve CD20 and FcγRIIIa affinity	I	Largely identical to rituximab (above) <sup>85</sup>
Ocrelizumab	Phase 3 (MS)	Humanized IgG1 (2H7-based)	I	<ul style="list-style-type: none"> <li>Large extracellular loop</li> <li>• Core epitope: <sup>170</sup>ANPS<sup>173</sup> <sup>51</sup></li> <li>• P168 and P170 contribute to binding<sup>51</sup></li> <li>• Contact region: positions 165–180<sup>48</sup></li> </ul>
PRO131921 (rhuMab v114)	Discontinued	Humanized IgG1 (2H7-based) Fc engineered to improve FcγRIIIa affinity	I	Same as 2H7/ocrelizumab <sup>51</sup>
TRU-015	Discontinued	Single-chain CD20-targeting protein derived from 2H7 and with a human IgG1 hinge	I	Same as 2H7/ocrelizumab <sup>51</sup>
Ibritumomab tiuxetan (Zevalin)	Approved (FL)	Murine IgG1κ	I	Same as rituximab (above) <sup>61</sup>
Tositumomab (Bexxar)	Approved Orphan status in FL	Murine IgG2αλ	II	<ul style="list-style-type: none"> <li>Large extracellular loop</li> <li>• Core epitope: <sup>170</sup>ANPS<sup>173</sup> <sup>33</sup></li> <li>• Contact region: positions 170–182<sup>48</sup></li> </ul>
Obinutuzumab GA101	Phase 3 (DLBCL, NHL, CLL, refractory)	Humanized IgG1κ	II	<ul style="list-style-type: none"> <li>Large extracellular loop</li> <li>• Core epitope: 172–176 region<sup>29</sup></li> </ul>
hOUBM3/6	Preclinical	Humanized IgG1κ	Unclear	<ul style="list-style-type: none"> <li>Large extracellular loop</li> <li>• ES, RAHT and INIYN<sup>75</sup></li> <li>• Not <sup>170</sup>A or P<sup>172</sup> <sup>75</sup></li> </ul>

CLL, chronic lymphocytic leukemia; DLBCL, diffuse large B cell lymphoma; FL, follicular lymphoma; Ig, immunoglobulin; MCL, mantle cell lymphoma; NHL, non-Hodgkin's lymphoma

sequences<sup>53</sup> where P172 was found to have a particular importance, since rituximab binds the human ANPS sequence but not the corresponding murine SNSS sequence.<sup>53</sup> Furthermore, mutation of the alanine and proline at positions 170 and 172 in human CD20 to serine was shown to abolish rituximab binding.<sup>33,48</sup> Asparagine 171 (N171) was also found to be a key residue for rituximab binding as any amino acid replacement at this position, except histidine, resulted in a substantial loss of binding affinity to peptides representing the extracellular CD20 loop.<sup>29</sup>

Phage-peptide screening also suggested that a second region of the epitope, <sup>182</sup>YCYSI<sup>186</sup>, contributes to the binding of rituximab through conformational stabilization.<sup>49</sup> Furthermore, when Perosa and colleagues screened phage-display peptide libraries containing a repertoire of sequences of random 7- or 12-amino acid peptides they found that, while cyclic peptides mimicking the CD20 epitope were dependent on the <sup>170</sup>ANPS<sup>173</sup> motif, linear mimics that also bound rituximab required a different motif—WPxWLE—that does not correspond to any sequence present in CD20 itself.<sup>53,54</sup> While the WPxWLE motif appears to share some rituximab contact points with <sup>170</sup>ANPS<sup>173</sup>, these regions are conformationally different and have been proposed as distinct epitopes.<sup>54</sup> However, the functional role and significance of the WPxWLE sequence is unclear.

Mutagenesis studies can identify residues affecting antibody binding, but cannot define the contact sites between the CD20 epitope and the antibody. The structure of the rituximab:epitope complex has been determined by co-crystallizing a synthetic peptide mimic of the extracellular loop epitope of CD20 (residues 163–187) in complex with the antigen-binding fragment of rituximab.<sup>50</sup> The bound CD20 peptide forms a cyclic conformation owing to a disulfide bond between two cysteine residues, C167 and C183. This structure comprises a short N-terminal coil (residues 167–171), a <sub>3</sub><sub>10</sub> helix (residues 172–174), a small loop (residues 175–177) and a short C-terminal  $\alpha$ -helix (residues 178–184). The key <sup>170</sup>ANPS<sup>173</sup> motif is embedded in a cyclic, four-region pocket formed by the CDRs of the rituximab antibody (Fig. 5). Residues of the <sup>170</sup>ANPS<sup>173</sup> motif bind to CDR residues via numerous hydrogen bonds and van der Waals contacts. In accordance with evidence that P172 has a critical role in antibody binding, this residue is deeply buried in the CD20/Ab interface and forms additional hydrophobic and hydrophilic contacts with residues at the bottom of the CDR pocket that are likely to be important in maintaining

the conformational stability of the epitope-antibody complex.<sup>50</sup> The <sup>182</sup>YCYSI<sup>186</sup> region at the C-terminus of the large extracellular loop of CD20 also appears to play a role in rituximab binding,<sup>49</sup> most likely through the formation of the disulfide bond that induces the cyclic conformation of the epitope<sup>50</sup> loop necessary for the binding of CD20 to rituximab.<sup>55</sup> Abrogating the internal disulfide bridge (C167-C183) of the large extracellular

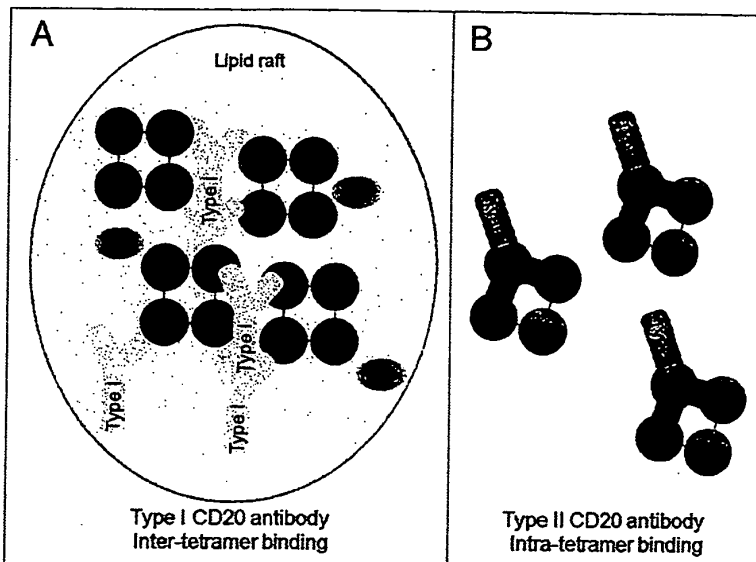


**Figure 2.** Hypothetical model for the 2:1 binding ratio of Type I and Type II CD20 antibodies binding to CD20 (tetramers, depicted in red). An explanation to explain the 2:1 binding stoichiometry between Type I and Type II CD20 antibodies is to assume that (A) Type I antibodies bind between CD20 tetramer (inter-tetramer, depicted in red) resulting in accumulation in lipid rafts together with Fc $\gamma$ R1b (gray oval). In contrast Type II (B) antibodies may bind within one tetramer (intra-tetramer).

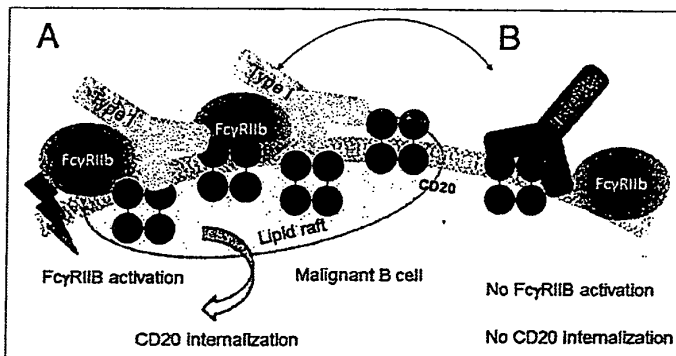


**Figure 3.** Hypothetical model for CD20 binding of Type I and Type II CD20 antibodies explaining the impact of Fc $\gamma$ R1b on internalization. (A) Type I antibodies such as rituximab may bind to CD20 in a conformation that allows simultaneous binding to Fc $\gamma$ R1b and subsequent signaling followed by internalization in lipid rafts. (B) Type II antibodies such as GA101 may bind in a conformation that does not allow simultaneous binding to Fc $\gamma$ R1b; thus resulting in reduced internalization.

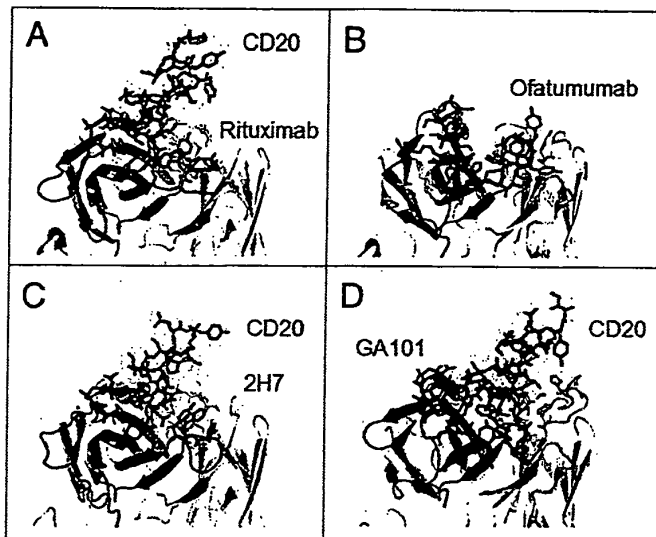


**Figure 4.** Published crystal structures of CD20 antibodies. (A) rituximab-CD20 complex,<sup>48</sup> (B) ofatumumab (no co-crystal structure is available),<sup>50</sup> (C) 2H7-CD20 complex,<sup>49</sup> and (D) GA101-CD20 complex.<sup>29</sup> The heavy chain is colored in darker shades, the peptides derived from CD20 are colored in red where appropriate.

loop seems to completely destabilize the CD20 protein, since expression of a CD20 variant with a C167S exchange is barely detectable by western blot analysis after transient transfection of HEK293 cells.<sup>29</sup>

The knowledge of the CD20 epitope was used to design rituximab variants in which point mutations were inserted into the CDR to improve the binding characteristics of the antibody.<sup>56</sup> Rituximab variants that bound to CD20 with enhanced avidity, or with a reduced off-rate, did not show improved activity in terms of CDC, complement fixation or rafting. However, a variant with three mutational changes (H57DE/H102YK/L93NR/) was shown to mediate enhanced avidity-dependent ADCC and cell death.<sup>56</sup>

In principle, genetic mutations in the rituximab epitope could reduce the binding and efficacy of the antibody, but clinical data in patients with DLBCL suggest that epitope mutations are very rare (0.4% of 264 patients at diagnosis and one of 15 patients at relapse) and are not an important cause of failure of treatment with rituximab in combination with conventional chemotherapy.<sup>27</sup>

**Veltuzumab.** Veltuzumab (IMMU-106; ha20, Immunomedics, Nycomed) is a humanized IgG1κ Type I antibody in Phase 2 development for treatment of relapsed or refractory NHL and autoimmune diseases<sup>58</sup> (Table 2). Veltuzumab has CDRs largely identical to those of rituximab with the exception of one residue, suggesting that it binds to the same epitope.<sup>59</sup> Veltuzumab competes for CD20 binding with rituximab and shows similar specificity, avidity and in vitro activity.<sup>58,59</sup>

**AME-133v.** AME-133v (Ocaratuzumab, LY2469298, MENTRIK) is a humanized IgG1 Type I antibody in Phase 2 development. AME-133v is an optimized version of rituximab

with a Fab region engineered to improve CD20-binding affinity. AME-133v has a ca. 13- to 20-fold greater binding affinity for CD20 than rituximab.<sup>60</sup> The Fc region has been modified to improve affinity for FcγRIIIa-158F and -158V genotypes. As a result, AME-133v shows greater in vitro activation of natural killer cells and 5- to 7-fold more potent ADCC than rituximab.<sup>44,60</sup> AME-133v recognizes the same epitope as rituximab.

**Ibritumomab.** Ibritumomab, a murine IgG1κ Type I antibody, is the antibody from which rituximab was derived and hence targets the same epitope as rituximab.<sup>61</sup> A radiolabeled form of the antibody, 90Y-ibritumomab tiuxetan (Zevalin, Spectrum), is used in the treatment of indolent NHL<sup>62-64</sup> and as consolidation therapy following induction.<sup>65,66</sup>

**Ocrelizumab.** Ocrelizumab (PRO70769, Roche/Genentech) is a humanized anti-CD20 IgG1 Type I antibody that has been evaluated in a Phase 1/2 study in patients with relapsed/refractory FL and is currently in development for the treatment of multiple sclerosis.<sup>67</sup> Compared with rituximab, ocrelizumab shows lower CDC activity but greater ADCC activity and enhanced binding to the low-affinity FcγRIIIa variant.<sup>67</sup> Ocrelizumab is based on the murine Type I IgG2b antibody 2H7. The CDR loops of 2H7 are structurally

similar to those of rituximab. Among the four CDR loops that interact with CD20, only one (H3) differs substantially from the rituximab counterpart in terms of residue sequence and conformation.<sup>51</sup> 2H7 was first thought to recognize exactly the same epitope as rituximab. Early studies confirmed that residues A170 and P172 of CD20 are necessary for 2H7 binding, but suggested that they are not sufficient alone. Rather, the <sup>162</sup>INxxN<sup>166</sup> motif also appeared to be necessary for full binding of 2H7 in the presence of A170/P172, possibly because these residues may stabilize the conformation of the 2H7:CD20 complex. Mutation of the QTSK motif present in murine CD20 to <sup>156</sup>RAHT<sup>59</sup> (as present in human CD20) also improved the binding of 2H7, but was not necessary for full binding. In addition, 2H7 appears to only bind the oligomeric form of CD20 (e.g., tetramers).<sup>33</sup> Subsequent peptide scanning studies demonstrated that the core contact regions for 2H7 (CD20 positions 165–180) and rituximab (CD20 positions 165–182) are almost identical.<sup>48</sup> Crystallography has confirmed that the CDR loops of 2H7, like those of rituximab, form a deep pocket enclosing the critical <sup>170</sup>ANPS<sup>173</sup> epitope motif of CD20.<sup>51</sup> The P168 and P170 residues of 2H7 also form hydrogen bonds with CD20, while P175, which occurs in both 2H7 and rituximab, forms a hydrophilic interaction with CD20 that is oriented differently in the 2H7-CD20 and rituximab-CD20 complexes. As with rituximab, the cyclic conformation of the 2H7-CD20 complex is maintained by the disulfide bond of the peptide. The different structure of the H3 loop of 2H7, as compared with rituximab, alters the topology of the complex. These differences result in fewer binding interactions for 2H7, and hence a lower binding affinity, compared with rituximab.<sup>51</sup>

**PRO131921.** PRO131921 (rhuMab v114, Genentech) is a humanized IgG1 anti-CD20 antibody that was studied in two

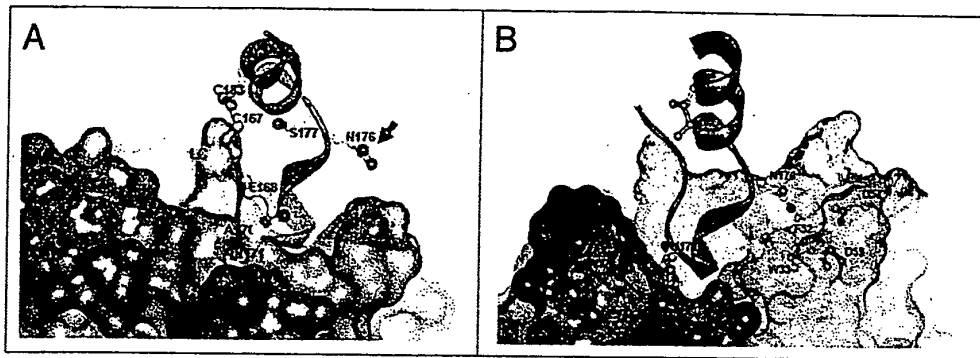


**Figure 5.** Comparison of (A) rituximab (Type I) and (B) GA101 (Type II) crystal structures in complex with CD20 peptide.<sup>29</sup> While for rituximab N171 is deeply immersed and N176 has no contacts with the rituximab CDRs, N171 is not deeply immersed in the the GA101 CDRs and vice versa N176 makes contacts to residues F52/D57/D59 of GA101 supporting the C-terminal shift of the GA101 epitope.

Phase 1 clinical trials, one for CLL and one for NHL. PRO131921 is derived from 2H7, but carries a modified Fc region with enhanced affinity for FcγRIIIa.<sup>68</sup> PRO131921 interacts with the same epitope as ocrelizumab.<sup>69</sup> Clinical development has been discontinued.<sup>70</sup>

**TRU-015.** TRU-015 is a single-chain CD20-targeting protein that was derived from 2H7 and has a human IgG1 hinge that binds to the same epitope of 2H7.<sup>51</sup> TRU-015 was described to show reduced CDC activity but more in vitro and in vivo properties compared with rituximab.<sup>71</sup> Clinical development was discontinued.

**Ofatumumab.** Ofatumumab is a human IgG1 Type I antibody that is approved for the treatment of patients with CLL refractory to fludarabine and alemtuzumab.<sup>20,21</sup> Ofatumumab is being studied in patients with lymphomas either as a single agent or in combination with chemotherapy.<sup>58,72-74</sup>

Like rituximab, ofatumumab shows Type I anti-CD20 activity, including CD20 rafting and CDC activity,<sup>35,75</sup> but binding studies suggest that ofatumumab recognizes an epitope different from that of rituximab. While the binding of rituximab is prevented by mutation of the A170/P172 residues, site-directed mutagenesis has shown that such mutations in the large extracellular loop of CD20 do not affect the binding of ofatumumab. Rather, the replacement of asparagine at position 163 (N163) or 166 (N166) with aspartic acid reduced ofatumumab binding by 50–75%. A triple mutant with mutations T159K, N163D and N166D did not bind ofatumumab at all.<sup>48,76</sup> None of these single mutations affected rituximab binding, although the triple mutant showed slightly decreased binding. Peptide scanning analyses confirmed that ofatumumab (together with the four other human IgG1 or IgGM antibodies tested) does not recognize the A170/P172 motif. Instead, these human antibodies recognize a particular region in the large extracellular loop (<sup>146</sup>FLK MES LNF IRA HTP<sup>160</sup>) that is N-terminal to A170 and P172 (Figs. 1B and 4B). This region does not include the N163 and N166 residues shown by mutagenesis studies to be necessary for

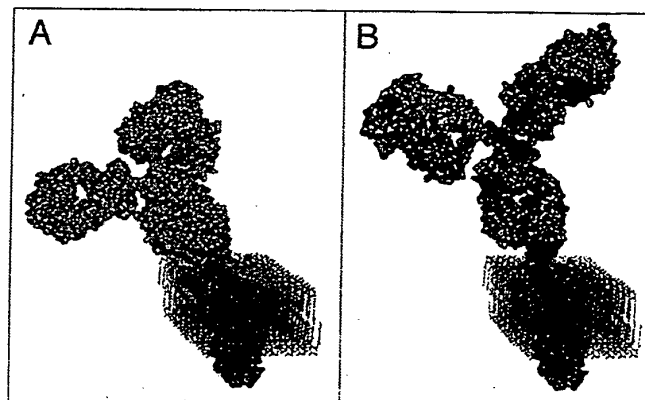


**Figure 6.** Three-dimensional models of (A) rituximab and (B) GA101. GA101 binds to the same binding epitope region of CD20 as rituximab, but in a different binding orientation. The molecular models were created by combining known structural data with the current knowledge and general understanding of antibody structure and membrane protein topology. The CD20 membrane protein model was created by combining the structural fragments of the crystallized CD20 antibody binding epitope and the transmembrane part of the HER2 receptor as a typical example of a membrane spanning molecule with known 3D information, and CD20 topology information.

ofatumumab binding, suggesting that these residues indirectly contribute to the stability of the epitope rather than forming part of the binding site itself.<sup>48</sup>

Peptide scanning and mutagenesis studies have revealed that the small extracellular loop of CD20 also contributes to the binding of ofatumumab. Binding of ofatumumab was almost completely prevented by the replacement of the entire small loop with an alternative sequence or by the insertion of three mutations (A74T, I76A and Y77S) in the loop. Neither the loop replacement nor these mutations affected the binding of rituximab.<sup>76</sup> These data confirm that ofatumumab recognizes an epitope distinct from that of rituximab, which comprises discontinuous



sequences across both the large and small extracellular loops of CD20 (Fig. 1A).

According to crystallography, the region of the ofatumumab molecule that binds with CD20 comprises six CDR loops, which form a deep pocket. Around the periphery of the pocket are hydrophobic residues (Y32, W94, W53, I58, Y60, Y102 and Y105) and at the bottom of the pocket is a positively charged residue (R91).<sup>52</sup> It should be noted that the crystal structure of the Fab fragment of ofatumumab was determined in the absence of CD20<sup>52</sup> (Fig. 4B). The hydrophobic pocket formed by the CDRs of ofatumumab is thought to interact with hydrophobic residues on both the large and small extracellular loops of CD20, and possibly with the cell membrane itself. The negatively charged N-terminal E150 residue of the large extracellular loop of CD20 is thought to interact with the positively charged R91 residue at the bottom of the CDR pocket of ofatumumab.

The binding of ofatumumab to the large and small extracellular loop of CD20 was hypothesized to position ofatumumab closer to the surface of the CD20 cell membrane than antibodies binding the large loop. This could be expected to facilitate the deposition of activated complement on the cell surface and hence the amplification of the complement response.<sup>77</sup> However, the impact of this is unclear as the CD20 extracellular loop is very small compared with the size of an antibody so that the antibody-binding domain of CD20 is already membrane-proximal. In addition to the difference in binding sites between ofatumumab and rituximab, studies have suggested that ofatumumab dissociates more slowly from the cell surface than rituximab<sup>35</sup> and exhibits greater CDC activity than rituximab in various B cell lines.<sup>35,48,75,77</sup> Furthermore, CDC by ofatumumab was found to be less dependent on the cell-surface density of CD20 than CDC by rituximab.<sup>48</sup> The differential action of ofatumumab on the complement has been supported by direct visualization of complement-mediated cell killing obtained using spinning-disk confocal microscopy.<sup>77</sup> Compared with rituximab, ofatumumab has been shown to be more active in both the deposition of complement and in causing morphologic effects induced by the membrane attack complexes of complement, namely blebbing (the formation of bulges in the cell membrane) and the creation of long, thin 'streamer' structures that extend from the cell membrane. Other data, however, have suggested that the preclinical activity of ofatumumab and rituximab are similar, demonstrating comparable levels of CDC, ADCC, whole blood B cell depletion and antitumor activity in preclinical assays and models.<sup>78</sup>

**Hu8E4.** Hu8E4 is a humanized Type I antibody incorporating CDRs from the mouse IgG2 anti-CD20 antibody, 8E4, grafted onto human light and heavy framework chains. Compared with rituximab, hu8E4 showed similar levels of ADCC and direct cell death against human lymphoma cells *in vitro*, but greater CDC and greater antitumor activity in lymphoma models in mice.<sup>79</sup> The epitope recognized by Hu8E4 is not currently known.

**Ublituximab.** Ublituximab (LFB-R603, LFP) is a chimeric glyco-engineered anti-CD20 antibody with enhanced FcγRIII affinity (as compared with rituximab) that acts via enhanced induction of ADCC. The CD20 epitope of ublituximab is unknown. Preclinical studies imply that ublituximab can disrupt

NF-κB/Snail/RKIP/PTEN/AKT signaling in B cell NHL cell lines that are resistant to chemotherapy and immunochemotherapy.<sup>80</sup> Ublituximab is currently in a Phase 1/2 clinical study in CLL.

## Type II CD20 Antibodies

**Tositumomab.** Radiolabeled 131I-tositumomab (Bexxar, GlaxoSmithKline), a murine IgG2aλ antibody, known as B1 in the scientific literature, is used clinically in extensively pretreated patients with NHL.<sup>81</sup> The activity of tositumomab is mainly achieved through its radioisotope rather than its antibody type.<sup>82</sup> The non-radioactive parental antibody B1, however, is the prototypic Type II CD20 antibody that displays all typical features of a Type II anti-CD20 activity, i.e., it binds B cells at approximately half the density of Type I antibodies and induces homotypic aggregation and cell death, but not rafting.<sup>33,35,37</sup> In transgenic mice expressing human CD20, tositumomab depleted normal B cells (both circulating and within lymphoid tissues) for significantly longer than rituximab,<sup>34</sup> although there was no difference in the CD20 binding affinities or biological half-lives of the antibody. Mutational studies showed that the <sup>170</sup>ANP<sup>172</sup> epitope motif of CD20 is critical to full binding of tositumomab, just as for rituximab.<sup>33</sup> Peptide scanning studies have confirmed that tositumomab shares most of the core contact region (positions 170–182) used by rituximab.<sup>48</sup> Importantly, both Type II antibodies, B1 and GA101, do not tolerate well substitutions of N176, while all Type I antibodies tested do (Fig. 1B).

**GA101.** GA101 (obinutuzumab, Roche) is a Type II, glyco-engineered, humanized IgG1κ anti-CD20 antibody derived from the murine antibody Bly-1<sup>27</sup> (Table 2). GA101 is in Phase 2 and 3 clinical trials for the treatment of patients with NHL and CLL.

GA101 shows biological activity characteristic of a Type II anti-CD20 antibody. It binds to the surface of the CD20 cell at a lower density than rituximab, and unlike Type I antibodies, GA101 does not induce rafting of CD20 and shows low CDC activity. GA101 triggers pronounced homotypic adhesion of lymphoma cells and high levels of direct cell killing activity that is superior to that of rituximab and tositumomab.<sup>27</sup> GA101 was significantly more effective than rituximab in depleting B cells in whole blood samples from healthy donors (n = 10) and from an individual with CLL.<sup>27</sup> GA101 also showed greater inhibition of tumor growth than rituximab, including complete tumor remission in xenograft models of human DLBCL and improved survival in a model of advanced, disseminated mantle cell lymphoma. GA101 and rituximab showed similar activity in depleting B cells from peripheral blood in cynomolgus monkeys, but GA101 was more effective in depleting B cells in spleen and lymph nodes.<sup>27</sup>

In addition to the antibody type, these characteristics also result from two unique, engineered features of the GA101 molecule, namely a non-fucosylated Fc portion and a modified elbow hinge region.<sup>27,29</sup> GA101 has been glyco-engineered to produce a non-fucosylated Fc region that substantially enhances the affinity of this antibody for both the FcγRIIIa-158F and FcγRIIIa-158V variants. This modification leads to an increased ability to

bind and recruit effector cells and hence to an increased ADCC activity against lymphoma cells compared with rituximab.<sup>27</sup> The elbow hinge region of GA101 between the variable region and the first constant domain was modified during the humanization process. A valine residue present in the parental murine B-1y1 antibody at Kabat position 11 was replaced by leucine present in B-1y1. This mutation widens the elbow angle for GA101 by almost 30° compared with rituximab and 2H7 as determined by X-ray structure analysis.<sup>29</sup> Mutagenesis experiments indicate that this mutation enhances its Type II antibody characteristics, including the increased direct cell death induction.<sup>27</sup> By mutating the Kabat 11 position, direct cell death induction can be switched on and off, although the CDRs of the antibody remain unchanged and binding to CD20 per se is retained.<sup>27</sup>

Positional mapping has confirmed that the epitopes of GA101 and rituximab overlap;<sup>29</sup> however, the GA101 epitope is shifted toward the C-terminus of CD20, with N176 contributing to binding of Type II but not of Type I antibodies (Fig. 5). The core of the GA101 epitope consists of an extended region, <sup>170</sup>ANP SEK NSP<sup>178</sup>, rather than the <sup>170</sup>ANPS<sup>173</sup> motif that is critical to rituximab binding.<sup>29</sup>

The relative roles of these residues in GA101 binding has been confirmed by crystallography (Figs. 4D and 5). N171 forms hydrogen bonds with GA101 but is not essential for binding. P172 and S173 both contribute to the binding of GA101, while residues at position 174–176 (<sup>174</sup>EKN<sup>176</sup>) form an extensive network of hydrogen bonds with the CDR of GA101.<sup>29</sup> Unlike ofatumumab,<sup>48,52</sup> GA101 does not appear to directly interact with the small extracellular loop of CD20 or the region preceding the larger loop.<sup>29</sup> However, Pepsan analyses indicate that residues from positions 142–160 affect GA101 binding, suggesting that they might indirectly stabilize the epitope conformation (unpublished observations).

The extended binding site sequence of GA101 may explain its high binding affinity for CD20. Moreover, GA101 binds CD20 with a different topology compared with other antibodies owing both to its unique epitope and elbow angle (Figs. 4D and 6). Rituximab and 2H7 bind to CD20 in positions oriented toward the core of the epitope. In comparison, the bound GA101 is rotated 90° clockwise around its middle axis and tilted about 70° toward the C-terminus of the peptide.<sup>29</sup> This topologic difference may explain several differences observed between the arrangement and conformation of rituximab–CD20 and GA101–CD20 complexes. According to protein tomography analysis, GA101 often binds monovalently to CD20, whereas rituximab binds the peptide mostly bivalently. This may favor intra- rather than inter-tetramer binding<sup>36</sup> (Fig. 2). Electron densities observed in protein tomography suggest that GA101 appears to bind to CD20 tetramers, while rituximab also binds to large CD20 complexes consisting of network-like structures of unidentified proteins.<sup>29</sup> The latter might represent higher order signaling complexes assembled in lipid rafts, e.g., the tetraspanin network. It is thought that the different geometry of the antibody–CD20 complexes may, in part, explain the differences in preclinical and clinical activity.

We believe that the differences in CD20 internalization and FcγRIIb dependence reported by other groups<sup>45,52</sup> might be

related to differences in the orientation of the antibodies after binding to CD20. Recent work with TNFR agonistic antibodies including CD40 and DR5 antibodies has shown that binding to CD40 and FcγRIIb in cis is required to mediate potent CD40 or DR5 activation.<sup>83–85</sup> We propose that Type I CD20 antibodies bind to CD20 on B cells in a conformation that allows simultaneous binding to FcγRIIb on the same cell (in cis) resulting in crosslinking, FcγRIIb co-activation and CD20 co-internalization upon binding potentially in lipid rafts. Vice versa, the biological effects could be explained by the different binding conformation of Type II CD20 antibodies that might prevent simultaneous binding in cis to FcγRIIb, which precludes FcγRIIb crosslinking and CD20 co-internalization (Fig. 3).

### Other Antibodies

hOUM3 and hOUbM6. hOUBM3 and hOUBM6 are humanized versions of the murine antibodies 1k1782 and 1k1791 that were previously identified as having properties and epitope specificities different from rituximab and ibritumomab.<sup>83</sup> In preclinical studies, variants of hOUBM6 showed higher CDC levels, similar or higher ADCC levels and similar depletion of leukemia and lymphoma cells compared with rituximab.<sup>75</sup>

Residues A170 and P172 of CD20 are not essential for binding of hOUBM3 and hOUBM6, suggesting that the epitope for these antibodies indeed differs from that of rituximab. According to the limited available data, the epitope for hOUBM6 includes the motifs <sup>287</sup>ES<sup>288</sup>, <sup>156</sup>RAHT<sup>159</sup> and <sup>162</sup>INIYN<sup>166</sup>.<sup>75</sup> Researchers reporting preclinical studies of a series of hOUBM3 and hOUBM6 variants recently proposed a classification scheme based on the affinity (measured by the dissociation constant) and the epitope of antibodies, rather than biological effects as used to categorize Type I and II anti-CD20 antibodies.<sup>75</sup> The affinity was correlated with potential to induce direct cell death, allowing antibodies to be defined into Group A and Group B antibodies. Group A antibodies (hOUBM3, hOUBM6 clones with lower  $K_d$  and ofatumumab) exhibited high affinity and did not induce direct cell death in lymphoma cells. Group B antibodies (i.e., rituximab and hOUBM6 clones with high  $K_d$ ) had lower affinity and induced apoptosis. The researchers proposed that antibodies with lower affinity might induce direct cell death more efficiently by binding simultaneously to two CD20 dimers, cross-linking them and bringing them into close proximity with each other. The authors further subcategorized antibodies according to the similarity with ibritumomab, the murine version of rituximab. Thus, antibodies with a non-ibritumomab-like epitope profile included hOUBM3, hOUBM6 and ofatumumab, and those with an ibritumomab-like profile were rituximab and 2H7. The relationship between these affinity/ $K_d$  and epitope categories and the conventional Type I and II categories of anti-CD20 antibody remains to be established.

### Conclusions

Characterization of anti-CD20 antibodies epitope specificity has revealed variations that may contribute to differences in the effects caused by these molecules. The relationship between the

epitope and the biological effect is not always clear and there is no apparent link between epitope and antibody type. For example, ofatumumab and rituximab are both classified as Type I antibodies and yet they recognize different CD20 epitopes. Conversely, tositumomab shows Type II activity but targets an epitope similar to one recognized by rituximab, so subtle differences in the interaction of anti-CD20 antibodies with their target can profoundly change the biological outcome.

These differences may affect the orientation of the antibodies in complex with their respective CD20 peptides, but other factors like the elbow-hinge angle and Fc effects also play a role. GA101 and rituximab, for example, bind CD20 in different orientations, even though their epitopes are largely shared. This appears to result in different overall conformations of bivalently bound CD20 complexes. The relative contribution of these factors to preclinical and clinical efficacy remains to be established. In general, it is not advisable to select therapeutic antibody candidates solely based on binding affinity and epitope binning data without testing them also in a functional biological assay, as demonstrated

by the substantially different biological effects of rituximab and GA101 with only subtle differences in their epitopes.

Further studies are required to determine whether differences in molecular and preclinical pharmacology translate into differences in clinical outcomes. Phase 3 head-to-head trials comparing GA101 or ofatumumab, with rituximab are currently recruiting and should help in optimization of existing antibody use and development of future treatments.

#### Potential Conflicts of interest

C.K., E.M. and P.U. are employees of Roche Glycart AG, W.S., G.G., M.S. and G.N. are employees of Roche Diagnostics GmbH, all other authors do not have a conflict of interest to declare. Writing support was provided by Zoe Crossman, Health Interactions, UK and Rachel Edwards, Prism Ideas, UK.

#### Acknowledgments

We thank all members and contributors in the GA101 preclinical team and the GA101 global life cycle team.

#### References

- Cragg MS, Walshe CA, Ivanov AO, Glennie MJ. The biology of CD20 and its potential as a target for mAb therapy. *Curr Dir Autoimmun* 2005; 8:140-74; PMID:15564720; <http://dx.doi.org/10.1159/000082102>
- Stashenko P, Nadler LM, Hardy R, Schlossman SE. Characterization of a human B lymphocyte-specific antigen. *J Immunol* 1980; 125:1678-85; PMID:6157744
- Glennie MJ, French RR, Cragg MS, Taylor RP. Mechanisms of killing by anti-CD20 monoclonal antibodies. *Mol Immunol* 2007; 44:3823-37; PMID:17768100; <http://dx.doi.org/10.1016/j.molimm.2007.06.151>
- Polyak MJ, Li H, Shariat N, Deans JP. CD20 homologs physically associate with the B cell antigen receptor. Dissociation upon receptor engagement and recruitment of phosphoproteins and calmodulin-binding proteins. *J Biol Chem* 2008; 283:18545-52; PMID:18474602; <http://dx.doi.org/10.1074/jbc.M800784200>
- Keating GM. Rituximab: a review of its use in chronic lymphocytic leukaemia, low-grade or follicular lymphoma and diffuse large B-cell lymphoma. *Drugs* 2010; 70:1445-76; PMID:20614951; <http://dx.doi.org/10.2165/11201110-000000000-00000>
- Marcus R, Imrie K, Belch A, Cunningham D, Flores E, Catalano J, et al. CVP chemotherapy plus rituximab compared with CVP as first-line treatment for advanced follicular lymphoma. *Blood* 2005; 105:1417-23; PMID:15494430; <http://dx.doi.org/10.1182/blood-2004-08-3175>
- Forstpointner R, Dreyling M, Repp R, Hermann S, Hänel A, Metzner B, et al; German Low-Grade Lymphoma Study Group. The addition of rituximab to a combination of fludarabine, cyclophosphamide, mitoxantrone (FCM) significantly increases the response rate and prolongs survival as compared with FCM alone in patients with relapsed and refractory follicular and mantle cell lymphomas: results of a prospective randomized study of the German Low-Grade Lymphoma Study Group. *Blood* 2004; 104:3064-71; PMID:15284112; <http://dx.doi.org/10.1182/blood-2004-04-1323>
- Hiddemann W, Kneba M, Dreyling M, Schmitz N, Lengfelder E, Schmits R, et al. Frontline therapy with rituximab added to the combination of cyclophosphamide, doxorubicin, vincristine, and prednisone (CHOP) significantly improves the outcome for patients with advanced-stage follicular lymphoma compared with therapy with CHOP alone: results of a prospective randomized study of the German Low-Grade Lymphoma Study Group. *Blood* 2005; 106:3725-32; PMID:16123223; <http://dx.doi.org/10.1182/blood-2005-01-0016>
- van Oers MH, Klasa R, Marcus RE, Wolf M, Kimby E, Gascoyne RD, et al. Rituximab maintenance improves clinical outcome of relapsed/resistant follicular non-Hodgkin lymphoma in patients both with and without rituximab during induction: results of a prospective randomized phase 3 intergroup trial. *Blood* 2006; 108:3295-301; PMID:16873669; <http://dx.doi.org/10.1182/blood-2006-05-021113>
- Herold M, Pasold R, Strock S, Nesser S, Niederwieser D, Neubauer A, et al. Results of a prospective randomised open label phase III study comparing rituximab plus mitoxantrone, chlorambucil, prednisolone chemotherapy (R-MCP) versus MCP alone in untreated advanced indolent non-Hodgkin's lymphoma (NHL) and mantle-cell-lymphoma (MCL). *Blood* 2004; 104:584
- Fowler, NH. Role of maintenance rituximab (rituxan) therapy in the treatment of follicular lymphoma. *PT* 2011; 36:590-8
- Salles G, Seymour JF, Offner F, López-Guillermo A, Belada D, Xerri L, et al. Rituximab maintenance for 2 years in patients with high tumour burden follicular lymphoma responding to rituximab plus chemotherapy (PRIMA): a phase 3, randomised controlled trial. *Lancet* 2011; 377:42-51; PMID:21176949; [http://dx.doi.org/10.1016/S0140-6736\(10\)62175-7](http://dx.doi.org/10.1016/S0140-6736(10)62175-7)
- van Oers MH, Van Glabbeke M, Giurgea L, Klasa R, Marcus RE, Wolf M, et al. Rituximab maintenance treatment of relapsed/resistant follicular non-Hodgkin's lymphoma: long-term outcome of the EORTC 20981 phase III randomized intergroup study. *J Clin Oncol* 2010; 28:2853-8; PMID:20439641; <http://dx.doi.org/10.1200/JCO.2009.26.5827>
- Forstpointner R, Unterhalt M, Dreyling M, Böck HP, Repp R, Wandt H, et al; German Low Grade Lymphoma Study Group (GLSG). Maintenance therapy with rituximab leads to a significant prolongation of response duration after salvage therapy with a combination of rituximab, fludarabine, cyclophosphamide, and mitoxantrone (R-FCM) in patients with recurring and refractory follicular and mantle cell lymphomas: Results of a prospective randomized study of the German Low Grade Lymphoma Study Group (GLSG). *Blood* 2006; 108:4003-8; PMID:16946304; <http://dx.doi.org/10.1182/blood-2006-04-016725>
- Marinelli G, Schmitz SF, Utiger U, Cemy T, Hess U, Bassi S, et al. Long-term follow-up of patients with follicular lymphoma receiving single-agent rituximab at two different schedules in trial SAKK 35/98. *J Clin Oncol* 2010; 28:4480-4; PMID:20697092; <http://dx.doi.org/10.1200/JCO.2010.28.4786>
- Vidal L, Gaferi-Gvili A, Leibovici L, Shpilberg O. Rituximab as maintenance therapy for patients with follicular lymphoma. *Cochrane Database Syst Rev* 2009; CD006552; PMID:19370640
- Eichhorst B, Dreyling M, Robak T, Monselet E, Hallek M; ESMO Guidelines Working Group. Chronic lymphocytic leukemia: ESMO Clinical Practice Guidelines for diagnosis, treatment and follow-up. *Ann Oncol* 2011; 22(Suppl 6):vi50-4; PMID:21908504; <http://dx.doi.org/10.1093/annonc/mdr377>
- Tilly H, Dreyling M; ESMO Guidelines Working Group. Diffuse large B-cell non-Hodgkin's lymphoma: ESMO Clinical Practice Guidelines for diagnosis, treatment and follow-up. *Ann Oncol* 2010; 21(Suppl 5):v172-4; PMID:20555073; <http://dx.doi.org/10.1093/annonc/mdq203>
- Dreyling M, Ghielmini M, Marcus R, Salles G, Vitolo U; ESMO Guidelines Working Group. Newly diagnosed and relapsed follicular lymphoma: ESMO Clinical Practice Guidelines for diagnosis, treatment and follow-up. *Ann Oncol* 2011; 22(Suppl 6):vi59-63; PMID:21908506; <http://dx.doi.org/10.1093/annonc/mdr388>
- Lemery SJ, Zhang JZ, Rothmann MD, Yang J, Earp JC, Zhao H, et al. U.S. Food and Drug Administration approval: ofatumumab for the treatment of patients with chronic lymphocytic leukemia refractory to fludarabine and alemtuzumab. *Clin Cancer Res* 2010; 16:4331-8; PMID:20601446; <http://dx.doi.org/10.1158/1078-0432.CCR-10-0570>

21. Wienda WG, Kipps TJ, Mayer J, Stiglbauer S, Williams CD, Hellmann A, et al.; Hx-CD20-406 Study Investigators. Ofatumumab as single-agent CD20 immunotherapy in fludarabine-refractory chronic lymphocytic leukemia. *J Clin Oncol* 2010; 28:1749-55; PMID:20194866; <http://dx.doi.org/10.1200/JCO.2009.25.3187>
22. Illidge T, Morschhauser F. Radioimmunotherapy in follicular lymphoma. *Best Pract Res Clin Haematol* 2011; 24:279-93; PMID:21658624; <http://dx.doi.org/10.1016/j.bcha.2011.03.005>
23. Lim SH, Beers SA, French RR, Johnson PW, Glennie MJ, Cragg MS. Anti-CD20 monoclonal antibodies: historical and future perspectives. *Haematologica* 2010; 95:135-43; PMID:19773256; <http://dx.doi.org/10.3324/haematol.2008.001628>
24. Chan HT, Hughes D, French RR, Tutt AL, Walshe CA, Teeling JL, et al. CD20-induced lymphoma cell death is independent of both caspases and its redistribution into Triton X-100 insoluble membrane rafts. *Cancer Res* 2003; 63:5480-9; PMID:14500384
25. Cragg MS, Glennie MJ. Antibody specificity controls in vivo effector mechanisms of anti-CD20 reagents. *Blood* 2004; 103:2738-43; PMID:14551143; <http://dx.doi.org/10.1182/blood-2003-06-2031>
26. Cragg MS, Morgan SM, Chan HT, Morgan BP, Filarov AV, Johnson PW, et al. Complement-mediated lysis by anti-CD20 mAb correlates with segregation into lipid rafts. *Blood* 2003; 101:1045-52; PMID:12393541; <http://dx.doi.org/10.1182/blood-2002-06-1761>
27. Mössner E, Brinker P, Moser S, Püntener U, Schmidt C, Herter S, et al. Increasing the efficacy of CD20 antibody therapy through the engineering of a new type II anti-CD20 antibody with enhanced direct and immune effector cell-mediated B-cell cytotoxicity. *Blood* 2010; 115:4393-402; PMID:20194898; <http://dx.doi.org/10.1182/blood-2009-06-225979>
28. Alduaij W, Ivanov A, Honeychurch J, Cheadle EJ, Potluri S, Lim SH, et al. Novel type II anti-CD20 monoclonal antibody (GA101) evokes homotypic adhesion and actin-dependent, lysosome-mediated cell death in B-cell malignancies. *Blood* 2011; 117:4519-29; PMID:21378274; <http://dx.doi.org/10.1182/blood-2010-07-296913>
29. Niederfellner G, Lammens A, Mundigl O, Georges GJ, Schaefer W, Schwaiger M, et al. Epitope characterization and crystal structure of GA101 provide insights into the molecular basis for type I/II distinction of CD20 antibodies. *Blood* 2011; 118:358-67; PMID:21444918; <http://dx.doi.org/10.1182/blood-2010-09-305847>
30. MabThera SmPC. June 2012. Available at: [http://www.ema.europa.eu/docs/en\\_GB/document\\_library/EPAR\\_-\\_Product\\_Information/human/000165/WC500025821.pdf](http://www.ema.europa.eu/docs/en_GB/document_library/EPAR_-_Product_Information/human/000165/WC500025821.pdf). Accessed October 2012
31. Clinical trials information is available at: <http://www.clinicaltrials.gov>. Accessed October 2012
32. Deans JP, Robbins SM, Polyak MJ, Savage JA. Rapid redistribution of CD20 to a low density detergent-insoluble membrane compartment. *J Biol Chem* 1998; 273:344-8; PMID:9417086; <http://dx.doi.org/10.1074/jbc.273.1.344>
33. Polyak MJ, Deans JP. Alanine-170 and proline-172 are critical determinants for extracellular CD20 epitopes; heterogeneity in the fine specificity of CD20 monoclonal antibodies is defined by additional requirements imposed by both amino acid sequence and quaternary structure. *Blood* 2002; 99:3256-62; PMID:11964291; <http://dx.doi.org/10.1182/blood.V99.9.3256>
34. Beers SA, Chan CH, James S, French RR, Artfield KE, Brennan CM, et al. Type II (rosinomab) anti-CD20 monoclonal antibody outperforms type I (rituximab-like) reagents in B-cell depletion regardless of complement activation. *Blood* 2008; 112:4170-7; PMID:18583569; <http://dx.doi.org/10.1182/blood-2008-04-149161>
35. Teeling JL, French RR, Cragg MS, van den Brakel J, Pluyter M, Huang H, et al. Characterization of new human CD20 monoclonal antibodies with potent cytolytic activity against non-Hodgkin lymphomas. *Blood* 2004; 104:1793-800; PMID:15172969; <http://dx.doi.org/10.1182/blood-2004-01-0039>
36. Cragg MS. CD20 antibodies: doing the time warp. *Blood* 2011; 118:219-20; PMID:21757627; <http://dx.doi.org/10.1182/blood-2011-04-346700>
37. Ivanov A, Beers SA, Walshe CA, Honeychurch J, Alduaij W, Cox KL, et al. Monoclonal antibodies directed to CD20 and HLA-DR can elicit homotypic adhesion followed by lysosome-mediated cell death in human lymphoma and leukemia cells. *J Clin Invest* 2009; 119:2143-59; PMID:19620786
38. Jak M, van Bochove G, Klein C, Umans J, Eldering E, Van Oers MHJ. CD40 stimulation sensitizes CLL cells to CD20-triggered cell death by rituximab and GA101 via a different mechanism. *Blood* 2011; 118:5178-88
39. Honeychurch J, Alduaij W, Azizyan M, Cheadle EJ, Pelicano H, Ivanov A, et al. Antibody-induced non-apoptotic cell death in human lymphoma and leukemia cells is mediated through a novel reactive oxygen species-dependent pathway. *Blood* 2012; 119:3523-33; PMID:22354003; <http://dx.doi.org/10.1182/blood-2011-12-395541>
40. Carton G, Dacheux L, Salles G, Solal-Celigny P, Bardos P, Colombat P, et al. Therapeutic activity of humanized anti-CD20 monoclonal antibody and polymorphism in IgG Fc receptor FcγRIIIa gene. *Blood* 2002; 99:754-8; PMID:11806974; <http://dx.doi.org/10.1182/blood.V99.3.754>
41. Carton G, Watier H, Golay J, Solal-Celigny P. From the bench to the bedside: ways to improve rituximab efficacy. *Blood* 2004; 104:2635-42; PMID:15226177; <http://dx.doi.org/10.1182/blood-2004-03-1110>
42. Koene HR, Kleijer M, Algra J, Roos D, von dem Borne AE, de Haas M. FcγRIIIa-158V/F polymorphism influences the binding of IgG by natural killer cell FcγRIIIa, independently of the FcγRIIIa-48L/R/H phenotype. *Blood* 1997; 90:1109-14; PMID:9242542
43. Ferrara C, Stuart F, Sondermann P, Brinker P, Umaña P. The carbohydrate at FcγRIIIa Asn-162. An element required for high affinity binding to non-fucosylated IgG glycoforms. *J Biol Chem* 2006; 281:5032-6; PMID:16330541; <http://dx.doi.org/10.1074/jbc.M510171200>
44. Bowles JA, Wang SY, Link BK, Allan B, Beuerlein G, Campbell MA, et al. Anti-CD20 monoclonal antibody with enhanced affinity for CD16 activates NK cells at lower concentrations and more effectively than rituximab. *Blood* 2006; 108:2648-54; PMID:16825493; <http://dx.doi.org/10.1182/blood-2006-04-020057>
45. Weng WK, Levy R. Two immunoglobulin G fragment C receptor polymorphisms independently predict response to rituximab in patients with follicular lymphoma. *J Clin Oncol* 2003; 21:3940-7; PMID:12975461; <http://dx.doi.org/10.1200/JCO.2003.05.013>
46. Beers SA, French RR, Chan HT, Lim SH, Jarrett TC, Vidal RM, et al. Antigenic modulation limits the efficacy of anti-CD20 antibodies: implications for antibody selection. *Blood* 2010; 115:5191-201; PMID:20223920; <http://dx.doi.org/10.1182/blood-2010-01-263533>
47. Lim SH, Vaughan AT, Ashton-Key M, Williams EL, Dixon SV, Chan HT, et al. FcγRIIIb on target B cells promotes rituximab internalization and reduces clinical efficacy. *Blood* 2011; 118:2530-40; PMID:21768293; <http://dx.doi.org/10.1182/blood-2011-01-330357>
48. Teeling JL, Macleus WJ, Wiegman LJ, van den Brakel JH, Beers SA, French RR, et al. The biological activity of human CD20 monoclonal antibodies is linked to unique epitopes on CD20. *J Immunol* 2006; 177:362-71; PMID:16785532
49. Binder M, Otto F, Mertelsmann R, Veelken H, Treppel M. The epitope recognized by rituximab. *Blood* 2006; 108:1975-8; PMID:16705086; <http://dx.doi.org/10.1182/blood-2006-04-014639>
50. Du J, Wang H, Zhong C, Peng B, Zhang M, Li B, et al. Structural basis for recognition of CD20 by therapeutic antibody Rituximab. *J Biol Chem* 2007; 282:15073-80; PMID:17395584; <http://dx.doi.org/10.1074/jbc.M701654200>
51. Du J, Wang H, Zhong C, Peng B, Zhang M, Li B, et al. Crystal structure of chimeric antibody C2H7 Fab in complex with a CD20 peptide. *Mol Immunol* 2008; 45:2861-8; PMID:18346788; <http://dx.doi.org/10.1016/j.molimm.2008.01.034>
52. Du J, Yang H, Guo Y, Ding J. Structure of the Fab fragment of therapeutic antibody Ofatumumab provides insights into the recognition mechanism with CD20. *Mol Immunol* 2009; 46:2419-23; PMID:19472037; <http://dx.doi.org/10.1016/j.molimm.2009.04.009>
53. Perosa F, Favoino E, Caragnano MA, Dammacco F. Generation of biologically active linear and cyclic peptides has revealed a unique fine specificity of rituximab and its possible cross-reactivity with acid sphingomyelinase-like phosphodiesterase 3b precursor. *Blood* 2006; 107:1070-7; PMID:16223774; <http://dx.doi.org/10.1182/blood-2005-04-1769>
54. Perosa F, Favoino E, Vicenti C, Guameria A, Raccanelli V, De Pinto V, et al. Two structurally different rituximab-specific CD20 mimotope peptides reveal that rituximab recognizes two different CD20-associated epitopes. *J Immunol* 2009; 182:416-23; PMID:19109173
55. Ernst JA, Li H, Kim HS, Nakamura GR, Yansura DG, Vandlen RL. Isolation and characterization of the B-cell marker CD20. *Biochemistry* 2005; 44:15150-8; PMID:16285718; <http://dx.doi.org/10.1021/bi0511078>
56. Li B, Zhao L, Guo H, Wang C, Zhang X, Wu L, et al. Characterization of a rituximab variant with potent antitumor activity against rituximab-resistant B-cell lymphoma. *Blood* 2009; 114:5007-15; PMID:19828699; <http://dx.doi.org/10.1182/blood-2009-06-225474>
57. Johnson NA, Leach S, Woolcock B, deLeeuw RJ, Bashashati A, Sehn LH, et al. CD20 mutations involving the rituximab epitope are rare in diffuse large B-cell lymphomas and are not a significant cause of R-CHOP failure. *Haematologica* 2009; 94:423-7; PMID:19211644; <http://dx.doi.org/10.3324/haematol.2008.001024>
58. Morschhauser F, Leonard JP, Fayad L, Coiffier B, Petillon MO, Coleman M, et al. Humanized anti-CD20 antibody, velinuzumab, in refractory/recurrent non-Hodgkin's lymphoma: phase I/II results. *J Clin Oncol* 2009; 27:3346-53; PMID:19451441; <http://dx.doi.org/10.1200/JCO.2008.19.9117>
59. Goldenberg DM, Rossi EA, Stein R, Cardillo TM, Czuczman MS, Hernandez-Ilizaliturri FJ, et al. Properties and structure-function relationships of velinuzumab (hA20), a humanized anti-CD20 monoclonal antibody. *Blood* 2009; 113:1062-70; PMID:18941114; <http://dx.doi.org/10.1182/blood-2008-07-168146>
60. Forero-Torres A, de Vos S, Pohlman BL, Pashkevich M, Cronier DM, Dang NH, et al. Results of a phase I study of AME-133v (LY2469298), an Fc-engineered humanized monoclonal anti-CD20 antibody, in FcγRIIIa genotyped patients with previously treated follicular lymphoma. *Clin Cancer Res* 2012; 18:1395-403; PMID:22223529; <http://dx.doi.org/10.1158/1078-0432.CCR-11-0850>
61. Gordon LI, Molina A, Witzig T, Emmanouilides C, Raubitschek A, Darif M, et al. Durable responses after ibritumomab tiuxetan radioimmunotherapy for CD20+ B-cell lymphoma: long-term follow-up of a phase 1/2 study. *Blood* 2004; 103:4429-31; PMID:15016644; <http://dx.doi.org/10.1182/blood-2003-11-3883>

62. Witzig TE, White CA, Wiseman GA, Gordon LI, Emmanouilides C, Raubitschek A, et al. Phase I/II trial of IDEC-Y2B8 radioimmunotherapy for treatment of relapsed or refractory CD20(+) B-cell non-Hodgkin's lymphoma. *J Clin Oncol* 1999; 17:3793-803; PMID:10577851
63. Witzig TE, Gordon LI, Cabanillas F, Czuczman MS, Emmanouilides C, Joyce R, et al. Randomized controlled trial of yttrium-90-labeled ibritumomab tiuxetan radioimmunotherapy versus rituximab immunotherapy for patients with relapsed or refractory low-grade, follicular, or transformed B-cell non-Hodgkin's lymphoma. *J Clin Oncol* 2002; 20:2453-63; PMID:12011122; <http://dx.doi.org/10.1200/JCO.2002.11.076>
64. Wiseman GA, Gordon LI, Mulani PS, Witzig TE, Spies S, Bartlett NL, et al. Ibritumomab tiuxetan radioimmunotherapy for patients with relapsed or refractory non-Hodgkin lymphoma and mild thrombocytopenia: a phase II multicenter trial. *Blood* 2002; 99:4336-42; PMID:12036859; <http://dx.doi.org/10.1182/blood.V99.12.4336>
65. Morschhauser F, Radford J, Van Hoof A, Vitolo U, Soubeyran P, Tilly H, et al. Phase III trial of consolidation therapy with yttrium-90-ibritumomab tiuxetan compared with no additional therapy after first remission in advanced follicular lymphoma. *J Clin Oncol* 2008; 26:5156-64; PMID:18854568; <http://dx.doi.org/10.1200/JCO.2008.17.2015>
66. Hainsworth JD, Spigel DR, Markus TM, Shipley D, Thompson D, Rotman R, et al. Rituximab plus short-duration chemotherapy followed by Yttrium-90 Ibritumomab tiuxetan as first-line treatment for patients with follicular non-Hodgkin lymphoma: a phase II trial of the Sarah Cannon Oncology Research Consortium. *Clin Lymphoma Myeloma* 2009; 9:223-8; PMID:19525191; <http://dx.doi.org/10.3816/CLM.2009.n.044>
67. Morschhauser F, Marlon P, Vitolo U, Lindén O, Seymour JF, Crump M, et al. Results of a phase II study of ocrelizumab, a fully humanized anti-CD20 mAb, in patients with relapsed/refractory follicular lymphoma. *Ann Oncol* 2010; 21:1870-6; PMID:20157180; <http://dx.doi.org/10.1093/annonc/mdq027>
68. Sikder MA, Friedberg JW. Beyond rituximab: The future of monoclonal antibodies in B-cell non-Hodgkin lymphoma. *Curr Hematol Malig Rep* 2008; 3:187-93; PMID:20425465; <http://dx.doi.org/10.1007/s11899-008-0027-5>
69. Shields RL, Namenuk AK, Hong K, Meng YG, Rae J, Briggs J, et al. High resolution mapping of the binding site on human IgG1 for Fc gamma RI, Fc gamma RII, Fc gamma RIII, and FcRn and design of IgG1 variants with improved binding to the Fc gamma R. *J Biol Chem* 2001; 276:6591-604; PMID:11096108; <http://dx.doi.org/10.1074/jbc.M009483200>
70. Friedberg JW, Vose JM, Kahl BS, Brunvand MW, Goy A, Kasamon YL, et al. A phase I study of PRO131921, a novel anti-CD20 monoclonal antibody in patients with relapsed/refractory CD20+ indolent NHL: Correlation between clinical responses and AUC pharmacokinetics. *Blood* 2009; 114:3742
71. Hayden-Ledbetter MS, Cerveny CG, Espling E, Brady WA, Grosmaire LS, Tan P, et al. CD20-directed small modular immunopharmaceutical, TRU-015, depletes normal and malignant B cells. *Clin Cancer Res* 2009; 15:2739-46; PMID:19351771; <http://dx.doi.org/10.1158/1078-0432.CCR-08-1694>
72. Czuczman MS, Fayad L, Delwail V, Cartron G, Jacobsen E, Kuliczkowski K, et al.; 405 Study Investigators. Ofatumumab monotherapy in rituximab-refractory follicular lymphoma: results from a multicenter study. *Blood* 2012; 119:3698-704; PMID:22389254; <http://dx.doi.org/10.1182/blood-2011-09-378323>
73. Czuczman MS, Hess G, Gadeberg OV, Pedersen LM, Goldstein N, Gupta I, et al.; 409 Study Investigators. Chemoimmunotherapy with ofatumumab in combination with CHOP in previously untreated follicular lymphoma. *Br J Haematol* 2012; 157:438-45; PMID:22409295; <http://dx.doi.org/10.1111/j.1365-2141.2012.09086.x>
74. Hagenbeek A, Plesner T, Johnson P, Pedersen L, Walewski J, Hellman A, et al. HuMax-CD20, a novel fully human anti-CD20 monoclonal antibody: Results of a phase I/II trial in relapsed or refractory follicular non-Hodgkin's lymphoma. *Blood* 2005; 106:Abstract 4760
75. Uchiyama S, Suzuki Y, Onake K, Yokoyama M, Ohta M, Aikawa S, et al. Development of novel humanized anti-CD20 antibodies based on affinity constant and epitope. *Cancer Sci* 2010; 101:201-9; PMID:19930155; <http://dx.doi.org/10.1111/j.1349-7006.2009.01392.x>
76. Engelbers P, Beurskens F, Mackus W, Bakker J, Vink T, Tiebout A, et al. Ofatumumab targets a conformational membrane-proximal epitope which contains amino acids located in the small and large loops of CD20. *Haematologica* 2010; 95:46
77. Beum PV, Lindorfer MA, Beurskens F, Stukenberg PT, Lohhorst HM, Pawluczko AW, et al. Complement activation on B lymphocytes opsonized with rituximab or ofatumumab produces substantial changes in membrane structure preceding cell lysis. *J Immunol* 2008; 181:822-32; PMID:18566448
78. Herter S, Waldhauer I, Oz T, Hering F, Lang S, Nicolini V, et al. Superior Efficacy of the Novel Type II, Glycoengineered CD20 Antibody GA101 vs. the Type I CD20 Antibodies Rituximab and Ofatumumab. *Blood* 2010; 116:3925
79. Wu L, Wang C, Zhang D, Zhang X, Qian W, Zhao L, et al. Characterization of a humanized anti-CD20 antibody with potent antitumor activity against B-cell lymphoma. *Cancer Lett* 2010; 292:208-14; PMID:20056316; <http://dx.doi.org/10.1016/j.canlet.2009.12.004>
80. Baritaki S, Militello L, Mahaponte G, Spandidos DA, Salcedo M, Bonavida B. The anti-CD20 mAb LFB-R603 interrupts the dysregulated NF- $\kappa$ B/Snail/RKIP/PTEN resistance loop in B-NHL cells: role in sensitization to TRAIL apoptosis. *Int J Oncol* 2011; 38:1683-94; PMID:21455568
81. Kaminski MS, Zelenetz AD, Press OW, Saleh M, Leonard J, Fehrenbacher L, et al. Pivotal study of iodine I 131 tositumomab for chemotherapy-refractory low-grade or transformed low-grade B-cell non-Hodgkin's lymphomas. *J Clin Oncol* 2001; 19:3918-28; PMID:11579112
82. Davis TA, Kaminski MS, Leonard JP, Hsu FJ, Wilkinson M, Zelenetz A, et al. The radioisotope contributes significantly to the activity of radioimmunotherapy. *Clin Cancer Res* 2004; 10:7792-8; PMID:15585610; <http://dx.doi.org/10.1158/1078-0432.CCR-04-0756>
83. Nishida M, Usuda S, Okabe M, Miyakoda H, Komatsu M, Haraoka H, et al. Characterization of novel murine anti-CD20 monoclonal antibodies and their comparison to 2B8 and c2B8 (rituximab). *Int J Oncol* 2007; 31:29-40; PMID:17549402
84. Stein R, Qu Z, Chen S, Rosario A, Shi V, Hayes M, et al. Characterization of a new humanized anti-CD20 monoclonal antibody, IMMU-106, and its use in combination with the humanized anti-CD22 antibody, epratuzumab, for the therapy of non-Hodgkin's lymphoma. *Clin Cancer Res* 2004; 10:2868-78; PMID:15102696; <http://dx.doi.org/10.1158/1078-0432.CCR-03-0493>
85. Forero-Torres A, de Vos S, Pohlman BL, Pashkevich M, Cronier DM, Dang NH, et al. Results of a phase I study of AME-133v (LY2469298), an Fc-engineered humanized monoclonal anti-CD20 antibody, in Fc $\gamma$ RIIIa-genotyped patients with previously treated follicular lymphoma. *Clin Cancer Res* 2012; 18:1395-403; PMID:22223529; <http://dx.doi.org/10.1158/1078-0432.CCR-11-0850>

# **Attachment K**

**Mössner *et al.*, *Blood*, 2010, 115:4393-4402**

# blood

2010 115: 4393-4402  
Prepublished online March 1, 2010;  
doi:10.1182/blood-2009-06-225979

## **Increasing the efficacy of CD20 antibody therapy through the engineering of a new type II anti-CD20 antibody with enhanced direct and immune effector cell-mediated B-cell cytotoxicity**

Ekkehard Mössner, Peter Brünker, Samuel Moser, Ursula Püntener, Carla Schmidt, Sylvia Herter, Roger Grau, Christian Gerdes, Adam Nopora, Erwin van Puijenbroek, Claudia Ferrara, Peter Sondermann, Christiane Jäger, Pamela Strein, Georg Fertig, Thomas Friess, Christine Schüll, Sabine Bauer, Joseph Dal Porto, Christopher Del Nagro, Karim Dabbagh, Martin J. S. Dyer, Sibrand Poppema, Christian Klein and Pablo Umaña

---

Updated information and services can be found at:  
<http://bloodjournal.hematologylibrary.org/content/115/22/4393.full.html>

Articles on similar topics can be found in the following Blood collections  
Immunobiology (4924 articles)  
Lymphoid Neoplasia (1303 articles)

---

Information about reproducing this article in parts or in its entirety may be found online at:  
[http://bloodjournal.hematologylibrary.org/site/misc/rights.xhtml#repub\\_requests](http://bloodjournal.hematologylibrary.org/site/misc/rights.xhtml#repub_requests)

Information about ordering reprints may be found online at:  
<http://bloodjournal.hematologylibrary.org/site/misc/rights.xhtml#reprints>

Information about subscriptions and ASH membership may be found online at:  
<http://bloodjournal.hematologylibrary.org/site/subscriptions/index.xhtml>

Blood (print ISSN 0006-4971, online ISSN 1528-0020), is published weekly by the American Society of Hematology, 2021 L St, NW, Suite 900, Washington DC 20036.  
Copyright 2011 by The American Society of Hematology; all rights reserved.



## Increasing the efficacy of CD20 antibody therapy through the engineering of a new type II anti-CD20 antibody with enhanced direct and immune effector cell-mediated B-cell cytotoxicity

Ekkehard Mössner,<sup>1</sup> Peter Brünker,<sup>1</sup> Samuel Moser,<sup>1</sup> Ursula Püntener,<sup>1</sup> Carla Schmidt,<sup>1</sup> Sylvia Herter,<sup>1</sup> Roger Grau,<sup>1</sup> Christian Gerdes,<sup>1</sup> Adam Nopora,<sup>1</sup> Erwin van Puijenbroek,<sup>1</sup> Claudia Ferrara,<sup>1</sup> Peter Sondermann,<sup>1</sup> Christiane Jäger,<sup>1</sup> Pamela Strein,<sup>2</sup> Georg Fertig,<sup>2</sup> Thomas Friess,<sup>2</sup> Christine Schüll,<sup>2</sup> Sabine Bauer,<sup>2</sup> Joseph Dal Porto,<sup>3</sup> Christopher Del Nagro,<sup>3</sup> Karim Dabbagh,<sup>3</sup> Martin J. S. Dyer,<sup>4</sup> Sibrand Poppema,<sup>5</sup> Christian Klein,<sup>1</sup> and Pablo Umaña<sup>1</sup>

<sup>1</sup>GlycArt Biotechnology AG, Schlieren, Switzerland; <sup>2</sup>Discovery Oncology, Roche Diagnostics GmbH, Penzberg, Germany; <sup>3</sup>Discovery Inflammation, Roche Glycart, Palo Alto, CA; <sup>4</sup>MRC Toxicology Unit, University of Leicester, Leicester, United Kingdom; and <sup>5</sup>Medical Center, University of Groningen, Groningen, The Netherlands

**CD20 is an important target for the treatment of B-cell malignancies, including non-Hodgkin lymphoma as well as autoimmune disorders. B-cell depletion therapy using monoclonal antibodies against CD20, such as rituximab, has revolutionized the treatment of these disorders, greatly improving overall survival in patients. Here, we report the development of GA101 as the first Fc-engineered,**

**type II humanized IgG1 antibody against CD20. Relative to rituximab, GA101 has increased direct and immune effector cell-mediated cytotoxicity and exhibits superior activity in cellular assays and whole blood B-cell depletion assays. In human lymphoma xenograft models, GA101 exhibits superior antitumor activity, resulting in the induction of complete tumor remission and increased overall survival.**

**In nonhuman primates, GA101 demonstrates superior B cell-depleting activity in lymphoid tissue, including in lymph nodes and spleen. Taken together, these results provide compelling evidence for the development of GA101 as a promising new therapy for the treatment of B-cell disorders. (*Blood*. 2010;115(22):4393-4402)**

### Introduction

Rituximab, a type I chimeric IgG1 anti-CD20 antibody, has revolutionized the management and treatment of B-cell malignancies, increasing the median overall survival of patients with many of these diseases.<sup>1</sup> In combination with chemotherapy, it has significantly improved response rates and progression-free and overall survival of patients with diffuse large B-cell lymphoma (DLBCL) or follicular lymphoma.<sup>1,2</sup> Rituximab treatment has also benefited patients with other diseases amenable to B-cell depletion therapy, including B-cell chronic lymphocytic leukemia (B-CLL) and rheumatoid arthritis.<sup>2,3</sup> Nevertheless, relapse is a common occurrence, for example, in B-CLL, and there remains a need for treatments that delay the onset of relapse without increasing toxicity.<sup>1</sup> To this end, various therapeutic approaches are being explored, including new chemotherapies, small molecules, antibody-drug conjugates, and the use of alternative B-cell targets. However, in contrast to the situation with rituximab, the clinical benefit of these therapies remains to be demonstrated. In addition, many of these agents exhibit poor safety and tolerability profiles or necessitate the use of more complex treatment regimens.

Thus far, CD20 has been the most effective unconjugated antibody target for the treatment of B-cell malignancies. An alternative and complementary approach is to generate new unconjugated CD20 antibodies with enhanced functional activities that may lead to superior efficacy. Three types of functional activities of anti-CD20 antibodies have been described: signaling in target cells on CD20 binding leading to growth inhibition

and (nonclassic) apoptosis (referred to as “direct cell death”), complement-dependent cytotoxicity (CDC), and antibody-dependent cellular cytotoxicity (ADCC) mediated by cells displaying Fcγ receptors (FcγRs), such as FcγRIIIa-expressing NK cells and macrophages.<sup>4,5</sup>

Anti-CD20 antibodies with different functions may be generated either (1) by selecting antibodies that bind to a different CD20 epitope, which bind in an alternative mode or with changed affinity, resulting in altered intensity or type of functional mechanism; or (2) by engineering the Fc region of the antibody to enhance immune effector functions. The epitope and/or binding mode have been shown to dictate 2 major types of CD20 antibody effector function profiles, termed type I or type II.<sup>5-7</sup> Although both types I and II antibodies bind bivalently to CD20, they form distinct complexes with CD20, as inferred from the fact that the B-cell surface can accommodate approximately double the number of type I antibodies compared with type II. Type I antibodies stabilize CD20 on lipid rafts, leading to stronger C1q binding and potent induction of CDC. However, this binding mode triggers only low levels of direct cell death. In contrast, type II antibodies do not stabilize CD20 in lipid rafts and thus exhibit reduced binding to C1q and lower levels of CDC, but they potently induce direct cell death.<sup>5</sup> The majority of CD20 antibodies, including rituximab, veltuzumab,<sup>8</sup> ocrelizumab,<sup>9</sup> and ofatumumab,<sup>10</sup> are of type I, whereas the prototype type II antibody is the murine antibody B1 (tositumomab).<sup>11</sup>

Submitted June 5, 2009; accepted January 10, 2010. Prepublished online as *Blood* First Edition paper, March 1, 2010; DOI 10.1182/blood-2009-06-225979.

The publication costs of this article were defrayed in part by page charge

payment. Therefore, and solely to indicate this fact, this article is hereby marked “advertisement” in accordance with 18 USC section 1734.

© 2010 by The American Society of Hematology



The Fc region of rituximab plays a critical role in triggering the cellular events that lead to B-cell elimination *in vivo*.<sup>7,12,13</sup> This region of the molecule can interact with complement protein C1q and FcγRs to trigger CDC and ADCC, respectively. Direct cell death mediated by rituximab does not involve the Fc region directly but could potentially be enhanced by Fc-mediated crosslinking via the C1q complex and FcγRs.<sup>5</sup> Alternative type I CD20 antibodies have been generated, including ofatumumab,<sup>14,15</sup> AME-133,<sup>16</sup> and a hexavalent anti-CD20 antibody.<sup>17</sup> However, superior maximal efficacy over rituximab, that is, efficacy at the saturation point of the dose-response curve, has not been shown for any of these antibodies, and their clinical efficacy compared with rituximab remains to be demonstrated.

Our aim was to engineer a novel unconjugated agent against CD20 that displayed enhanced activity. To this end, we report the first Fc-engineered type II CD20 humanized IgG1 antibody, GA101. This manuscript describes the engineering of the variable and Fc regions of GA101 and presents its *in vitro* and *in vivo* activity profiles.

## Methods

### Antibodies

The murine anti-CD20 antibody H299 (B1) was obtained from Beckman Coulter. Because of its aggregate content, the monomeric fraction was isolated using size exclusion chromatography. Commercial-grade rituximab was obtained from Hoffmann La Roche. GA101 was humanized by grafting the complementarity-determining region sequences from the murine antibody B-1y1 onto the following human frameworks: the VH1-10 plus the JH4 human germline sequences, and the VK-2-40 plus the JK4 human germline sequences, for the heavy and light chains, respectively. GA101 was expressed from stable Chinese hamster ovary (CHO) K1 cell lines engineered to constitutively overexpress the heavy and light chains of GA101 as well as recombinant wild-type β-1,4-N-acetyl-glucosaminyltransferase III and wild-type Golgi α-mannosidase II,<sup>18-21</sup> using the glutamine synthetase expression system (Lonza Biologics). GA101 was produced using a fed-batch fermentation process using the engineered CHO cells in a chemically defined animal component-free medium and was subsequently purified by protein A and ion-exchange chromatographic techniques. The identity and monomer content (> 98%) of the isolate were analytically confirmed. Fab' and F(ab)'<sub>2</sub> fragments of GA101 and rituximab were generated via digestion with papain or pepsin, respectively, according to standard procedures.

### NHL cell lines

Cell lines were obtained from DSMZ or ATCC; WSU-DLCL2 from Wayne State University, Detroit, MI; and OCI-LY cell lines from the Ontario Cancer Institute, Toronto, ON; and cultured according to the standard protocol recommendations.

### Scatchard plot analysis

Aliquots of  $2 \times 10^5$  SU-DHL4 cells were seeded into V-bottom plates, and Eu-labeled antibodies were added in different concentrations. Cells were washed, and the pellet was resuspended in enhancer solution, transferred into a black 96-well plate, and placed onto a shaker for 10 minutes. Release of coupled Eu was analyzed on a BMG PheraStar reader (ex337/em615).

### Annexin V/PI FACS assay

Phosphatidylserine (PS) exposure and cell death were assayed by flow cytometric analysis (FACScan, BD Biosciences) of annexin V (ie, Annexin-V-FLOUS Staining Kit; Roche Applied Science) and propidium iodide (PI)-stained cells. Simultaneous application of PI or 7-amino-actinomycin D as a DNA stain enabled the discrimination between live and dead cells. In

general,  $3 \times 10^5$  cells were seeded into 24-well plates and were either untreated (control) or treated with 10 μg/mL isotype control or antibody for 24 to 72 hours. Annexin V/PI staining was performed according to the manufacturer's instructions.

For CD40 stimulation of hCD20 cells from transgenic mice, red blood cells (RBCs) were removed by hypotonic ammonium-chloride-potassium (ACK) lysis, and untouched splenic B cells were purified by anti-CD43-mediated depletion of non-B cells (MACS). B cells were incubated in conditioned complete RPMI 1640 medium containing 10% fetal bovine serum for 2 hours (with or without 10 μg/mL mitogenic stimulation) and either anti-CD40 (BD Biosciences PharMingen) or anti-IgM Fab2 (Jackson ImmunoResearch Laboratories) antibodies. This was followed by 36 hours of anti-CD20 stimulation (GA101 or rituximab 10 μg/mL). As positive controls for the induction of cell death, the following agents were used: 100nM staurosporine (Sigma-Aldrich) for mitochondrial-mediated apoptosis, or 1 μg/mL anti-CD95 Fas (BD Biosciences PharMingen) for the extrinsic induction of apoptosis.

### FACS analysis of binding stoichiometry

To compare the binding mode of type I and type II antibodies, fluorescence-activated cell sorter (FACS) binding curves were generated by direct immunofluorescence using Cy5-conjugated rituximab and GA101, respectively. A total of  $5 \times 10^5$  cells per sample were stained for 30 minutes at 4°C in a final volume of 200 μL and washed in culture medium. PI staining was used to identify and exclude dead cells. Measurements were performed using the FACSArray (BD Biosciences); PI fluorescence levels were quantified using Far Red A and Cy5 using the Red-A settings.

### Western blot analysis of Triton X-100-soluble proteins

Aliquots of  $5 \times 10^6$  Ramos cells per sample were incubated at 37°C for 30 minutes in complete culture medium either alone or supplemented with 10 μg/mL antibody or 10 μg/mL isotype control. After centrifugation at 500g for 10 minutes, cells were treated on ice with 200 μL of lysis buffer consisting of 1% Triton X-100 in Tris-buffered saline (50mM Tris-HCl, 150mM NaCl, pH 7.5), 1mM ethylenediaminetetraacetic acid, 1mM phenylmethylsulfonyl fluoride, and 1mM Na<sub>3</sub>VO<sub>4</sub> plus a cocktail of protease inhibitors. Cells were left on ice for 30 minutes to lyse and centrifuged at 15 000g for 20 minutes (detergent-insoluble pellet). Samples were run on 4% to 12% Bis-Tris gels and transferred onto polyvinylidene difluoride membranes. Anti-Lyn (sc-15) rabbit monoclonal and anti-CD71 (transferrin receptor, sc-32272) mouse monoclonal antibodies were purchased from Santa Cruz Biotechnology. Mouse anti-human CD20 detection antibody for Western blotting was obtained from Dako North America (clone L26).

### Immunofluorescence

Colocalization of CD20 antibodies with cholera toxin subunit B (CTB) on Ramos cells was visualized using the Vybrant Lipid Raft Labeling Kit (Invitrogen) according to the manufacturer's instructions using confocal microscopy. CTB binds to the pentasaccharide chain of plasma membrane ganglioside GM1, which selectively partitions into membrane microdomains called "lipid rafts."

### CDC assay

Cells were plated in AIM-V medium at a density of 50 000 cells/well into flat-bottom 96-well plates. Diluted antibody was added 10 minutes before addition of the serum/complement preparation to the cells, and the suspension kept at room temperature. Rabbit serum (rabbit complement MA; Cederlane Labs) was diluted in 1 mL of cytotoxicity medium plus 2 mL AIM-V to the final concentration and added to the cell suspension, and incubated for 2 hours at 37°C/5%CO<sub>2</sub>. Release of LDH activity (Roche Applied Science) into the supernatant was used as a readout, relative to maximum lysis (0.66% Triton X-100) and spontaneous lysis levels (without antibody).

### ADCC assay

Raji cells were collected, washed, and resuspended in culture medium, stained with freshly prepared calcein AM (Invitrogen) at 37°C for 30 minutes, and plated on a round-bottom 96-well plate (at a density of 30 000 cells/well). The respective antibody dilution was added and incubated for 10 minutes before contact with human effector cells (peripheral blood mononuclear cells [PBMCs]). Effector and target cells at a ratio of 25:1 were cocultured for 4 hours. The retention of calcein in the remaining live cells was used as a readout as previously described.<sup>20</sup>

### Autologous whole blood B-cell depletion assay

Blood from healthy volunteer donors was collected and an aliquot placed into FACS tubes. Subsequently, 20  $\mu$ L of antibody dilution was added, and the tubes were mixed gently and incubated at 37°C for 24 hours in a humidified cell incubator. A 50- $\mu$ L aliquot of the blood was stained with anti-CD45 (lymphocyte population), anti-CD3 (T cells), and anti-CD19 (B cells). FACS lysis solution (BD Biosciences) was added to deplete erythrocytes and fix cells before analysis with a flow cytometer. Results were evaluated by displaying 20 000 cells in the CD45-positive lymphocyte gate. CD3-positive T cells and CD19-positive B-cell populations were gated. Evaluation of relative B-cell depletion was performed using the B-/T-cell ratio with the antibody-untreated samples set as 100% B cells (equivalent to 0% B-cell depletion). B-/T-cell ratio = number of B cells/number of T cells; percentage of B-cell depletion =  $100 - [(100/\text{B-/T-cell ratio in sample without antibody}) \times (\text{B-/T-cell ratio in sample containing antibody})]$ .

In cases where the B-/T-cell ratio could not be applied because the studied agent (alemtuzumab) not only depleted B cells but also T cells, B-cell depletion was determined based on absolute B-cell numbers quantified using TruCount tubes (BD Biosciences) containing a mixture of anti-CD3-fluorescein isothiocyanate (BD Biosciences), anti-CD19-phycoerythrin (BD Biosciences), and anti-CD45-phycoerythrin-Cy5 (BD Biosciences; 10  $\mu$ L each). After 15 minutes of incubation at room temperature in the dark, 300  $\mu$ L of BD FACSLysis Solution (BD Biosciences) was added. The samples were measured using a FACSCalibur machine (Software BD CellQuestPro). Estimation of relative B-cell depletion was performed based on the absolute B-cell counts. The B-cell numbers obtained with the antibody-untreated samples were set as 100% B cells (equivalent to 0% B-cell depletion).

### NHL xenograft studies in SCID beige mice

Female SCID beige mice, 4 to 5 weeks of age at arrival, were maintained under specific pathogen-free conditions according to guidelines. The experimental study protocol was reviewed and approved by the Roche Group ethical committee. Continuous health monitoring was carried out on a regular basis. Animals were monitored daily for clinical symptoms and detection of adverse effects. Throughout the experimental period, the body weight of animals was recorded twice weekly, and tumor volume was measured by caliper after staging. Three weeks after cell transplantation with established subcutaneous SU-DHL4 tumors (250 mm<sup>3</sup>), animals were randomized into treatment groups of 10 animals each and treated with 1, 10, and 30 mg/kg of the respective antibody (every 7 days, 3 times, intravenously).

For the second-line treatment study, animals with established subcutaneous SU-DHL4 xenografts were treated with first-line rituximab (30 mg/kg, every 7 days, intravenously) as a single agent (days 22-35). Animals with xenografts progressing after first-line rituximab treatment (750 mm<sup>3</sup>) were subsequently randomized and reassigned to the following treatment groups of 10 animals each with weekly dosing (from days 35-60) with the following agents: vehicle, rituximab (30 mg/kg every 7 days), or GA101 (30 mg/kg every 7 days).

For the disseminated Z138 model,  $10 \times 10^6$  Z138 MCL cells were injected intravenously per animal into the tail vein in 200  $\mu$ L of Aim V cell culture medium (Invitrogen). Treatment was initiated in a blinded fashion 29 days after intravenous injection of tumor cells followed by a weekly application of 10 mg/kg GA101 (every 7 days, 6 times, intraperitoneally).

Treatment began at the day of randomization approximately 4 weeks after cell transplantation with 10 animals per group. Antibodies and the corresponding vehicle as a single agent were given intraperitoneally at a dose of 10 mg/kg. Animals were monitored daily for clinical symptoms and detection of adverse effects. Study endpoints were visible disease, including scruffy fur, impaired locomotion, and hind leg paralysis.

### Analysis of B-cell depletion in cynomolgus monkeys (*Macaca fascicularis*)

The efficacy of GA101 in depleting B cells in cynomolgus monkeys was compared with that of rituximab in groups of 3 animals each. GA101 (2  $\times$  10 and 30 mg/kg) was compared with rituximab (2  $\times$  10 mg/kg) and vehicle after 2 intravenous doses administered on days 0 and 7 to male and female cynomolgus monkeys (n = 3 per group; 1 female, 2 males). The experimental study protocol was reviewed and approved by the Roche Group ethical committee. Total leukocytes from sodium heparin-collected peripheral blood were isolated by Ficoll buffy coat preparation. Residual RBCs were removed using a buffered ammonium chloride lysing solution. Lymph node and spleen tissue samples were weighed and then homogenized into single-cell suspension, lysed of residual RBCs, and filtered of debris. The resulting leukocyte cell preparations were washed and resuspended in an appropriate volume of Dulbecco phosphate-buffered saline supplemented with 1% fetal bovine serum. Absolute cell numbers for a given cell population were determined as the percentage of total leukocytes (based on cytometric surface marker detection) and the total cell counts of the sample corrected for volume or weight of starting material.

## Results

### Engineering of novel antibody variable regions and characterization of the type II CD20 antibody, GA101

GA101 was derived by humanization and further engineering of the parental murine IgG1- $\kappa$  antibody B-ly1.<sup>22</sup> This antibody mediates a degree of homotypic aggregation, a characteristic of type II antibodies, and did not stabilize CD20 in Triton X-100-resistant lipid rafts as it would have been expected for a classic type II antibody.<sup>11</sup> cDNAs encoding variable heavy (VH) and light (VL) chain regions were cloned from the B-ly1 hybridoma, and their complementarity-determining regions were grafted onto human VH and VL acceptor frameworks.<sup>23</sup> Different human frameworks were tested, and the resulting humanized antibody variants were compared for CD20 binding in human lymphoma cells. Those variants with complete identity to the human germline VH and VL framework sequences and with high binding affinity to human CD20 were selected for further analysis, including GA101. The affinity ( $K_D$  value) of GA101 for human CD20 was determined to be approximately 4.0nM according to Scatchard analysis of binding experiments using SU-DHL4 non-Hodgkin lymphoma (NHL) cells and labeled GA101, whereas a  $K_D$  value of approximately 4.5nM was obtained for rituximab. Binding experiments using Cy5-labeled GA101 and rituximab revealed that both antibodies compete for binding to B-cell CD20 and that GA101 recognizes a distinct but overlapping epitope compared with rituximab (manuscript in preparation).<sup>24</sup>

Because our goal was to obtain a functional type II, humanized CD20 antibody, the resulting variants were further screened for their ability to induce direct cell death in human B-cell lymphoma cells in vitro. Effective antibody variants were identified using the annexin V/PI assay, some of which showed a large gain of function compared with the parental murine B-ly1 antibody. The most significant structural distinction between high- and low-activity variants was a sequence alteration in the elbow-hinge region, an

area known to affect the flexibility of the Fab' and F(ab)'2 domains.<sup>25</sup> The more active variants, including GA101, harbored a human germline VH framework 1 with a valine residue at Kabat position 11 instead of the leucine present in the murine donor antibody. Figure 1 shows the results of the annexin V/PI assay for GA101 compared with rituximab. GA101 treatment resulted in higher PS exposure and cell death compared with rituximab (Figure 1A). To test whether this activity required the modified elbow-hinge residue, a GA101-variant was generated with the key residue on Kabat position 11 remutated back to the original leucine. This variant displayed a large loss of activity and decreased cell death induction to levels similar to rituximab (Figure 1B), despite maintaining its high binding affinity for CD20.

Further analysis of GA101 revealed that it exhibited characteristics typical of a type II antibody<sup>6,7,26,27</sup> (Figure 2). Figure 2A through D shows the results of GA101 characterization using various assays compared with the type I antibody rituximab. At saturating antibody concentrations, GA101 bound to B cells at levels approximately half those of rituximab (Figure 2A). Unlike GA101, rituximab stabilizes CD20 molecules into Triton X-100-resistant lipid rafts on the surface of B cells (Figure 2B-C). Type I antibody-CD20 complexes on lipid rafts bind more strongly to C1q, leading to higher levels of CDC compared with type II antibodies.<sup>7</sup> Consistent with this, GA101 displays reduced CDC relative to rituximab (Figure 2D). Typical of type II CD20 antibodies, GA101 induced stronger homotypic aggregation of B cells in vitro (Figure 2E). Interestingly, mutating the elbow-hinge valine of GA101 back to the parental murine leucine residue leads

to partial loss of its type II characteristics, as seen by increased maximal binding to B cells, higher CDC activity, reduced homotypic B-cell aggregation, and decreased induction of direct cell death (data not shown).

We further investigated the type II character of GA101 by comparing it with B1, the murine prototype type II CD20 antibody that has so far demonstrated the most pronounced in vitro direct cell death-inducing activity among type I and type II CD20 antibodies of the IgG isotype<sup>6,28</sup> (Figure 3). GA101 exhibited more pronounced type II in vitro characteristics compared with B1, with respect to direct cell death induction in Z138 MCL cells (Figure 3A). As described previously for B1,<sup>6,7,28</sup> this activity was mediated by the F(ab)'2 but not the Fab' antibody fragment of GA101, and could not be blocked by caspase inhibitors (data not shown). The superior ability of GA101 in inducing direct cell death and PS exposure was also observed in a panel of NHL cell lines of different origin (Figure 3B). In addition, GA101 showed superior growth inhibition of B-cell lymphoma cell lines, as tested in Raji and SUDHL-4 cells (data not shown). Lymphoma cells as well as normal human peripheral blood B cells were sensitive to GA101 when incubated with GA101 in the absence of plasma and of immune effector cells in vitro (Figure 3C). Finally, manipulation of the activation status of B cells using standard mitogens, such as anti-IgM and anti-CD40 antibodies, resulted in increased sensitivity to GA101 of B cells from human CD20 transgenic mice (Figure 3D).

#### Fc engineering and Fcγ receptor-dependent functions

In addition to an engineered variable region conferring type II CD20 binding, GA101 also harbors a glycoengineered Fc segment. Glycoengineering was accomplished by producing the antibody in CHO cells, which overexpressed the recombinant glycosylation enzymes β-1,4-N-acetyl-glucosaminyltransferase III and Golgi α-mannosidase II, leading to accumulation of antibody glycoforms containing bisected, complex, nonfucosylated oligosaccharides attached to asparagine 297 in the Fc region.<sup>29,30</sup> The glycoengineered antibody binds with increased affinity to FcγRIIIa, an activating Fc receptor displayed by immune effectors, such as NK cells and macrophages.<sup>29</sup>

Two dimorphic variants at position 158 of human FcγRIIIa are known: a more common, lower-affinity form containing phenylalanine (FcγRIIIa-158F) and another variant with a valine residue at the same position. GA101 and rituximab were compared by surface plasmon resonance for their binding affinity to these 2 variants of human FcγRIIIa. GA101 bound with higher affinity to both FcγRIIIa-158V and -158F ( $K_D$  of 55 and 270nM, respectively), compared with rituximab ( $K_D$  of 660 and 2000nM, respectively). Increased binding affinity of GA101 to FcγRIIIa translated into an increased induction of ADCC relative to rituximab, as demonstrated in vitro in ADCC assays using Raji lymphoma cells as targets and human PBMCs as effectors (Figure 4A). Both ADCC potency and efficacy were higher with GA101, and this was also maintained in the presence of an excess of nonspecific human IgG at physiologic concentrations, as present in human blood; under these conditions, rituximab showed no activity whereas that of GA101 was only partially inhibited, presumably because of the enhanced FcR binding (Figure 4B).

As a type II antibody, GA101 displays reduced CDC compared with type I antibodies. It was therefore of interest to compare the total B cell-depleting activity of GA101 in whole blood to better mimic in vivo conditions. The assay incorporated both FcγR-displaying effector cells, including NK cells, monocytes, and

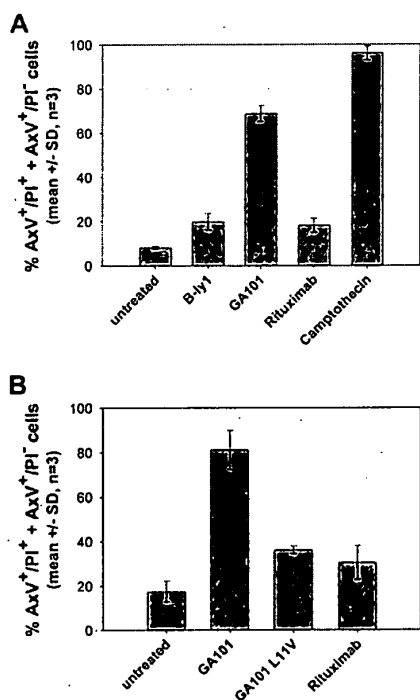
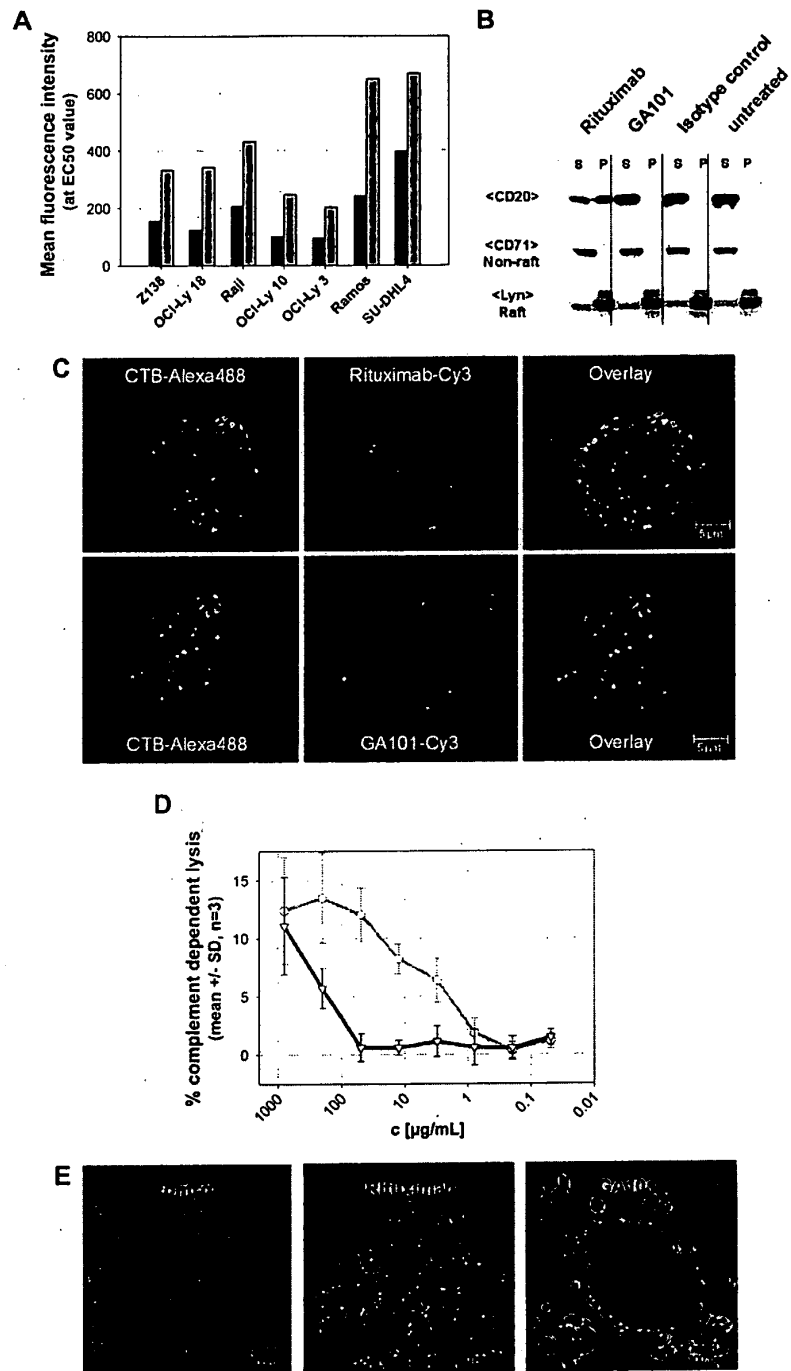


**Figure 1.** GA101 induces superior PS exposure and cell death induction compared with rituximab in the annexin V/PI FACS assay. Z138 NHL cells were seeded and treated with 10 μg/mL GA101 or rituximab for 24 hours. The graphs depict the mean percentage of total annexin V-positive, PI-negative (AnnV<sup>+</sup>) cells and annexin V/PI double-positive cells (AnnV<sup>+</sup>/PI<sup>+</sup>; n = 3). (A) Cell death induction by GA101 compared with B-ly1, camptothecin, and the type I anti-CD20 antibody rituximab. (B) Cell death induction by GA101 can be reduced to the level of rituximab by reintroducing the L11V mutation in the elbow-hinge region of the antibody.

**Figure 2. GA101 exhibits characteristics typical of a type II anti-CD20 antibody.** (A) Fluorescence intensity at the EC<sub>50</sub> value (half-maximal binding) of GA101 compared with rituximab. Titration of a panel of NHL cell lines with Cy-5-labeled GA101 (■) shows that only half the amount of antibody is bound to CD20 on the cells, compared with Cy-5 labeled rituximab (□) at the EC<sub>50</sub> concentration. (B) GA101 does not mobilize CD20 into lipid rafts. On binding of GA101 to CD20 in Ramos cells, CD20 is mainly found in the Triton X-100-soluble fraction (S) and not in the Triton X-100-insoluble pellet (P) representing lipid rafts (top row). In contrast, binding of rituximab resulted in the distribution of CD20 into the Triton X-100-insoluble pellet fraction (S; top row). The distribution of Lyn as a typical lipid raft marker and CD71 as a nonlipid raft marker is not affected (bottom 2 rows). (C) Confocal microscopy: Ramos cells were stained for 30 minutes at 37°C with Cy-3-labeled rituximab or GA101 (red fluorescence, middle panel) and costained with the Alexa 488-labeled lipid raft marker cholera toxin subunit B (CTB-Alexa 488, green fluorescence, left panel), which binds to the membrane ganglioside GM1 in lipid rafts. The overlay (right panel) confirms that rituximab binding to CD20 results in accumulation of CD20 clusters in lipid rafts as shown by colocalization with CTB-Alexa 488 (yellow fluorescence), whereas CD20 molecules do not redistribute to lipid rafts on binding of GA101 and do not colocalize with CTB-Alexa 488. Pictures were captured with a Leica TCS SP2 confocal microscope with an HCX PL APO CS 63.0×/1.32 OIL UV objective (numeric aperture 1.32) in glycerol and acquired with Leica Confocal Software Version 2.61. Image manipulation was performed with Metamorph Version 7.0r3 and Jasc Paint Shop Pro. (D) CDC assays (LDH release) with Z138 mantle cell lymphoma cells. In the presence of physiologic concentrations of human unspecific IgG (10 mg/mL RedImmune), the type II anti-CD20 antibody GA101 (black) mediates greatly reduced CDC induction compared with rituximab (gray; n = 3). (E) GA101 induces rapid and pronounced homotypic aggregation of SU-DHL4 cells, whereas rituximab induces only a weak aggregation. Pictures were taken 24 hours after the addition of antibody. Pictures were captured with a Zeiss Axiovert 135 microscope with a Zeiss Fluor 5×/0.25 objective (numeric aperture 0.25) in RPMI 1640, 10% FCS, 2mM L-Glutamin on non fixed Ramos cells and a Cool SNAP K4 camera (Visitron Systems GmbH). Image acquisition and manipulation were performed with Metamorph Version 7.0r3 and Jasc Paint Shop Pro.



neutrophils and human complement. The sum of immune effector functions, such as ADCC and antibody-mediated cellular phagocytosis, CDC, and effector (cell)-independent mechanisms, such as direct cell death induction, could thus be measured. GA101 was significantly more potent than rituximab at depleting B cells in whole blood from 10 healthy donors. Representative results are shown in Figure 4C. Compared with rituximab, GA101 exhibited 10- to 25-fold greater potency and was 1.5- to 2.5-fold more

effective in terms of absolute B-cell depletion. The efficacy of whole blood B-cell depletion by GA101 was significantly higher (~ *P* < .001) than that of rituximab in all samples tested. These findings were confirmed using malignant B cells from a chronic lymphocytic leukemia (B-CLL) patient (Figure 4D). In the latter case, the majority of cells in the assay were target B cells, and GA101 was also superior to the CD52 antibody alemtuzumab at depleting B-CLL cells. In addition, GA101 showed superior

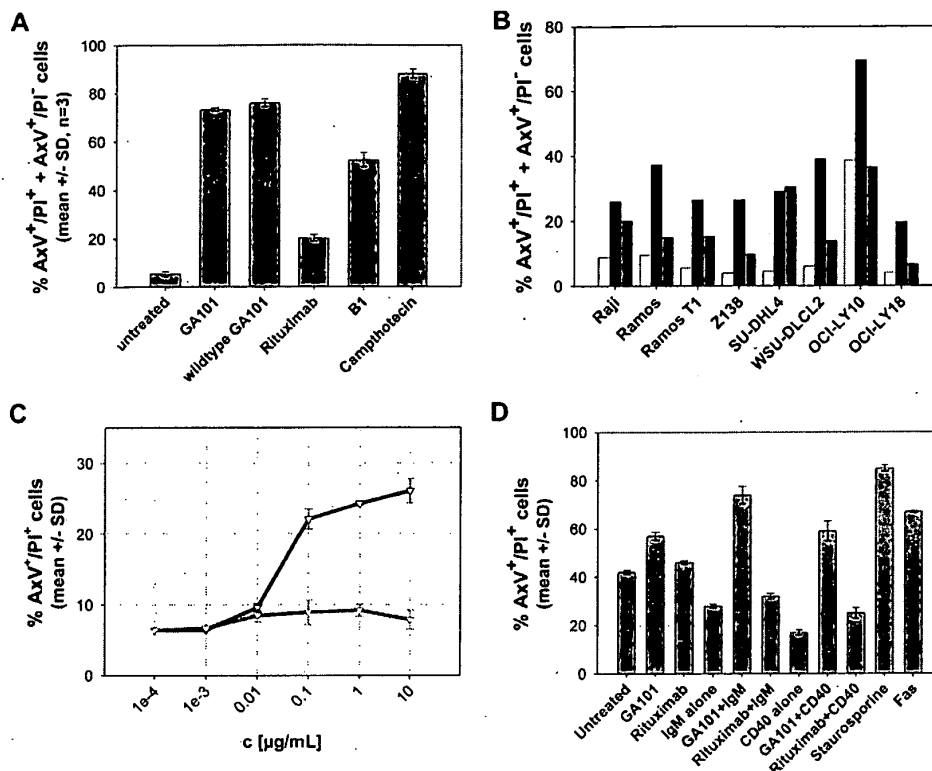


**Figure 3. The type II anti-CD20 antibody GA101 mediates superior direct cell death induction in normal and malignant B cells.** (A) GA101 induces PS exposure and cell death in the annexin V/PI FACS assay at levels superior to those induced by the type II anti-CD20 antibody B1 and rituximab. Z138 NHL cells were seeded and treated with 10 μg/mL GA101, nonglycoengineered GA101 (wt GA101), B1, rituximab, or camptothecin as control for 24 hours. The graph shows the mean percentage of total annexin V-positive cells, that is, annexin V/PI double-positive (AxV<sup>+</sup>/PI<sup>+</sup>) and annexin V-positive, PI-negative cells (AxV<sup>+</sup>/PI<sup>-</sup>; n = 3). (B) NHL cells were seeded and either left untreated (□) or treated with 10 μg/mL GA101 (■) or rituximab (▨), respectively, for 72 hours. The graph shows the percentage of total annexin V-positive cells for a cell line panel of 3 Burkitt lymphoma, 4 DLBCL, and 1 MCL cell lines from 1 representative experiment. (C) GA101 (black curve) induces increased cell death compared with rituximab in purified human nonmalignant B cells isolated from 2 healthy donors (gray curve), as measured by annexin V/PI double-positive staining at 36 hours. All measurements were performed in duplicate; the mean of replicate samples from multiple donors (n = 2) and SD are shown. (D) Murine purified B cells from human CD20 transgenic mice were treated as indicated for 36 hours ex vivo with GA101 or rituximab either with or without prior mitogenic stimulation by IgM or CD40L, and cell death induction was measured by annexin V/PI staining as described in "Annexin V/PI FACS assay." Two animals were used per stimulation. All measurements were performed in duplicate; the mean of replicate samples from multiple animals (n = 2) and SD are shown.

efficacy in this assay compared with a glycoengineered variant of rituximab (data not shown).

**Efficacy in human lymphoma xenograft models**

GA101 demonstrated in vivo efficacy superior to rituximab in various human lymphoma xenograft models. Both antibodies were first compared in a staged, aggressive DLBCL model using human SUDHL-4 cells subcutaneously injected in SCID beige mice. Therapy began when tumors were established and rapidly growing. Rituximab inhibited tumor growth more effectively at 10 mg/kg versus 1 mg/kg; however, the higher dose of 30 mg/kg did not result in increased efficacy of rituximab, and tumor regression was not observed at any dose. In contrast, GA101 showed a dose-dependent increase in efficacy in the range of 1 to 30 mg/kg and resulted in complete tumor regression in all animals and lasting tumor eradication in 9 of 10 animals at the highest dose of 30 mg/kg and in 1 of 10 animals at a dose of 10 mg/kg (Figure 5A).

A more aggressive, second-line therapy setting was also tested using the SUDHL-4 DLBCL model. All animals received weekly first-line treatment with rituximab at a dose of 30 mg/kg. When the tumors reached a prespecified size of approximately 750 mm<sup>3</sup>, animals were randomized into 3 groups for second-line treatment with rituximab

(30 mg/kg), GA101 (30 mg/kg), or vehicle. Tumors continued to grow rapidly in the rituximab- and vehicle-treated groups, whereas GA101 treatment was able to control tumor growth (Figure 5B). Notably, GA101 treatment resulted in tumor stasis in the presence of rituximab (> 300 μg/mL in plasma), which competes with GA101 for CD20 binding. The superior efficacy of GA101 was further demonstrated in an advanced, disseminated mantle cell lymphoma model using Z138 MCL cells in SCID beige mice (Figure 5C). GA101 treatment demonstrated superior efficacy both in terms of median and overall survival compared with rituximab (Figure 5C).

**In vivo depletion of normal B cells in peripheral blood and in lymphoid organs**

GA101 exhibited potent B cell-depleting activity in nonhuman primates, both in peripheral blood as well as in lymphoid tissue B cells (Figure 6). Cynomolgus monkeys were treated on days 1 and 8 with rituximab (10 mg/kg), GA101 (one group at 10 mg/kg and another at 30 mg/kg), or vehicle control. Both antibodies efficiently depleted B cells from peripheral blood (Figure 6A); however, B-cell depletion by GA101 was greater in spleen, and particularly in lymph nodes, where B-cell depletion is typically more problematic (Figure 6B-C). Preliminary data suggest that memory B cells and long-lived plasma cells are

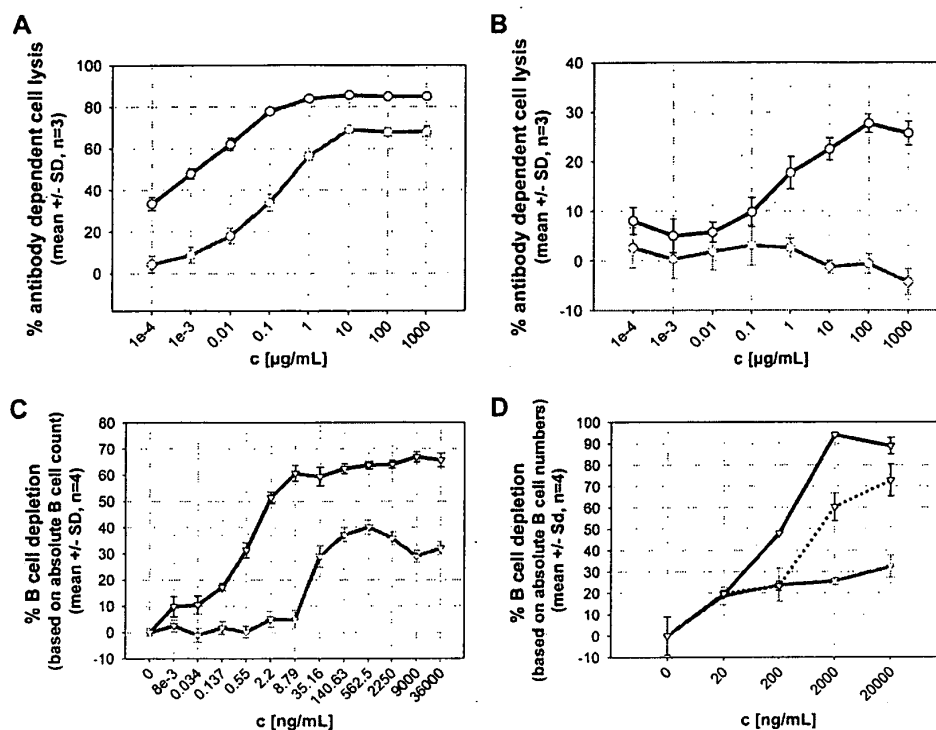


**Figure 4. Superior ADCC and B cell-depleting activities of GA101 compared with rituximab.** GA101 exhibits a more potent ADCC-inducing ability than rituximab, both in the presence and absence of nonspecific human IgG. Representative ADCC assay with Raji cells as target cells and NK cells from human PBMCs (F/V 158) as effector cells (calcein release, E/T ratio = 20:1) in the absence (A) and presence (B) of physiologic concentrations of nonspecific human IgG (20 mg/mL RedMune; n = 3). In the absence of nonspecific IgG, GA101 (black) was approximately 35-fold more potent in terms of EC<sub>50</sub> values than rituximab (gray) at inducing ADCC. In the presence of nonspecific IgG, GA101 (black) still exhibited significant ADCC-inducing activity, whereas that of rituximab (gray) was completely abolished. (C) Enhanced B cell-depletion activity of GA101, as demonstrated in a whole blood B cell-depletion assay with whole blood from a healthy donor (CD16 genotype F158/F158). Representative results for the depletion of CD19-positive B cells are depicted here. GA101 (black) was approximately 25-fold more potent in terms of EC<sub>50</sub> values and 1.9-fold more effective (in terms of absolute B-cell depletion) compared with rituximab (gray). Evaluation of relative B-cell depletion was performed using the B-/T-cell ratio set to 0% for untreated control samples (n = 4). (D) Representative whole blood B cell-depletion assay with whole blood from a B-CLL patient. GA101 (black) was more effective at depleting B cells compared with rituximab (gray) and the CD52 antibody alemtuzumab (dotted line). Because alemtuzumab also depletes T cells, the evaluation of relative B-cell depletion was performed based on the absolute B-cell counts. The B-cell numbers were then set to 100% for maximal depletion, and results were compared between the antibodies (n = 4).

spared from depletion, thus leaving humoral immunity and memory intact (data not shown).

## Discussion

The use of monoclonal anti-CD20 antibodies, such as rituximab for the treatment of B-cell malignancies, has greatly improved overall patient survival. Our goal was to refine and augment the efficacy of CD20 antibody therapy by engineering a novel CD20 antibody with enhanced B cell-depleting activity. Here, we describe the generation and characterization of GA101, the first Fc-engineered type II CD20 antibody to be brought to clinical development.<sup>30</sup> Although type II antibodies exhibit lower C1q binding and CDC compared with type I, our aim was to capitalize both on the direct and immune effector cell-mediated induction of B-cell death mediated by type II antibodies and further enhance the latter via Fc engineering while retaining its type II B-cell signaling properties. Here, we compare the *in vitro* and *in vivo* properties of GA101 to those of rituximab, a well-characterized type I antibody, and demonstrate the superior *in vivo* efficacy of the unconjugated CD20 type II IgG1 antibody GA101 versus rituximab.

The efficacy of GA101 was superior to that of rituximab in all parameters tested in this study. GA101 exhibited enhanced B cell-depleting properties in the lymphoid organs of cynomolgus mon-

keys, and in aggressive human B-cell lymphoma xenograft models. In addition to increased effects on B cells, an Fc-engineered type II anti-CD20 antibody may provide further advantages over type I antibodies. First, the complement-related effects characteristic of type I antibodies may have only limited efficacy *in vivo* because of overexpression of complement-resistance factors on target cells and to *in vivo* depletion of complement proteins.<sup>4</sup> Second, C1q binding to the type I antibody Fc region interferes with FcγR binding and may decrease ADCC.<sup>31</sup> Finally, it has been recently reported that type II anti-CD20 antibody complexes persist for longer periods of time on the B-cell surface compared with type I,<sup>32</sup> increasing the accessibility of the Fc region to immune effector cells at the target site *in vivo*, which may result in increased levels of ADCC.

An additional factor that contributes to the increased ADCC induction by GA101 is the higher binding affinity of the antibody to FcγRIIIa receptors achieved via Fc glycoengineering. The relevance of Fc-FcγRIIIa binding affinity has been demonstrated in various retrospective pharmacogenomic studies, which show a correlation between a genetic dimorphism affecting the affinity of human FcγRIIIa therapeutic IgG1 antibodies and the response rates and progression-free survival after antibody therapy. Approximately 15% of patients are homozygous for a high-affinity form of the receptor, displaying a valine residue at position 158, whereas the rest of the population carries the allele coding for a low-affinity receptor variant with a phenylalanine residue in that position.<sup>4</sup>

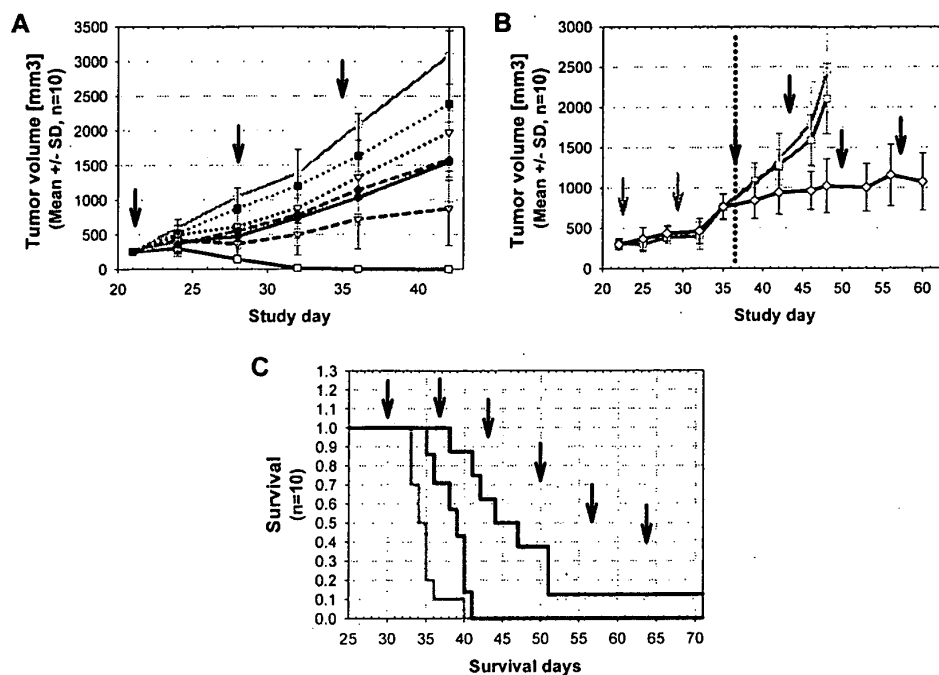


**Figure 5. Superior antitumor efficacy of GA101 compared with rituximab in human lymphoma xenograft models.** (A) Established subcutaneous SU-DHL4 (DLBCL) tumors (250 mm<sup>3</sup>; n = 10 per group) were treated with 1 mg/kg (dotted lines), 10 mg/kg (short dashed lines), and 30 mg/kg (solid lines) GA101 (every 7 days, 3 times, intravenously; black) compared with identical doses of rituximab (dark gray) and vehicle control (light gray). GA101 treatment resulted in a dose-dependent inhibition of tumor growth that was superior to that of rituximab. A total of 10 of 10 mice showed complete tumor remission and 9 of 10 mice showed long-term survival (> 90 days; cure) after treatment with 30 mg/kg GA101; and 1 of 10 mice showed complete tumor remission after treatment with 10 mg/kg GA101. In the rituximab-treated groups, no complete tumor remission was observed. Data are mean  $\pm$  SD. (B) Established subcutaneous SU-DHL4 xenografts (n = 10 per group) were treated with rituximab (30 mg/kg every 7 days, intravenously) as single-agent first-line therapy (days 22-35). Xenografts progressing under first-line rituximab treatment (30 mg/kg every 7 days) were subsequently randomized and reassigned to the following treatment groups with weekly dosing (from days 35-60): vehicle (gray curve), rituximab (30 mg/kg every 7 days; dark gray curve), or GA101 (30 mg/kg every 7 days; black curve). SU-DHL4 tumor progression (advanced xenografts; 750 mm<sup>3</sup>) was effectively controlled through the use of GA101 as a second-line therapy, whereas rituximab treated-tumors remained refractory. (C) Treatment of the aggressive orthotopic disseminated Z138 (MCL) model was initiated 29 days after intravenous injection of tumor cells (n = 10 per group). Treatment with 10 mg/kg GA101 (every 7 days, 6 times, intravenously; black line) resulted in increased overall and median survival, compared with 10 mg/kg rituximab treatment (dark gray line;  $P < .008$ ) and vehicle control (light gray line). † indicates the treatment time points.

Rituximab therapy of follicular lymphoma patients homozygous for the high-affinity allele is associated with significantly higher response rates and progression-free survival.<sup>33,34</sup> Similar studies have found the same correlation for other IgG1 antibodies, including trastuzumab in the treatment of metastatic breast cancer<sup>35</sup> and cetuximab in the therapy of colorectal carcinoma patients.<sup>36</sup> Here, we demonstrate that GA101 binds to both Fc $\gamma$ RIIIa variants with an affinity higher than that of rituximab for the high-affinity receptor isoform.

In summary, we have developed a new, Fc-glycoengineered type II anti-CD20 antibody with in vivo efficacy superior to that of rituximab, a widely used type I anti-CD20 therapeutic antibody with clearly demonstrated clinical benefits for patients with various B-cell malignancies. Several properties of GA101 may contribute to its higher in vivo efficacy. First, GA101 exerts stronger direct B-cell death induction. Although similar observations have been reported for B1, the prototype type II CD20 antibody,<sup>6,28</sup> GA101 exhibits more pronounced induction of direct cell death compared with B1. However, the molecular mechanism underlying caspase-independent cell death induction on binding of GA101 to CD20 remains to be elucidated. Similar effects have been described for other antibodies that target lymphocytic antigens, such as HLA-DR,<sup>37</sup> CD47,<sup>38</sup> and CD37.<sup>39</sup> In addition to direct cell death, the observed increase in PS exposure may facilitate phagocytosis of targeted cells.<sup>40</sup> GA101 also exhibits increased Fc $\gamma$ RIIIa-binding affinities, resulting in increased ADCC and higher B cell-depleting

activity in whole blood. The less pronounced down-modulation of CD20 by type II antibodies<sup>32</sup> may facilitate this activity.

Experiments to elucidate the contributions of these different biologic functions to the superior in vivo efficacy of GA101 are ongoing. Studies using nonglycoengineered GA101 suggest that its striking in vivo potency in subcutaneous xenograft models can be attributed primarily to the type II CD20 binding mode. Relative to murine model systems, an additional contribution of enhanced ADCC mediated by NK cells is possible in humans. Although different effector functions may be dominant depending on the nature of the target, we are encouraged by the superior efficacy of GA101 in all ex vivo and in vivo models studied to date.

In conclusion, our results provide preclinical evidence for GA101 as a potential new therapy for the treatment of B-cell disorders. This novel type II anti-CD20 antibody may provide a valuable treatment alternative for those disorders amenable to B-cell depletion therapy. A phase 1/2 clinical trial of GA101 for the treatment of patients with relapsed/refractory CD20-positive B-cell malignancies has recently yielded encouraging preliminary safety and efficacy results in this difficult-to-treat patient population.<sup>30</sup> Because of its superior B cell-depleting activity in lymphoid tissues, GA101 may provide an effective treatment alternative for autoimmune diseases, such as rheumatoid arthritis, systemic lupus erythematosus, or immune thrombocytopenic purpura, where rituximab has shown some benefit.

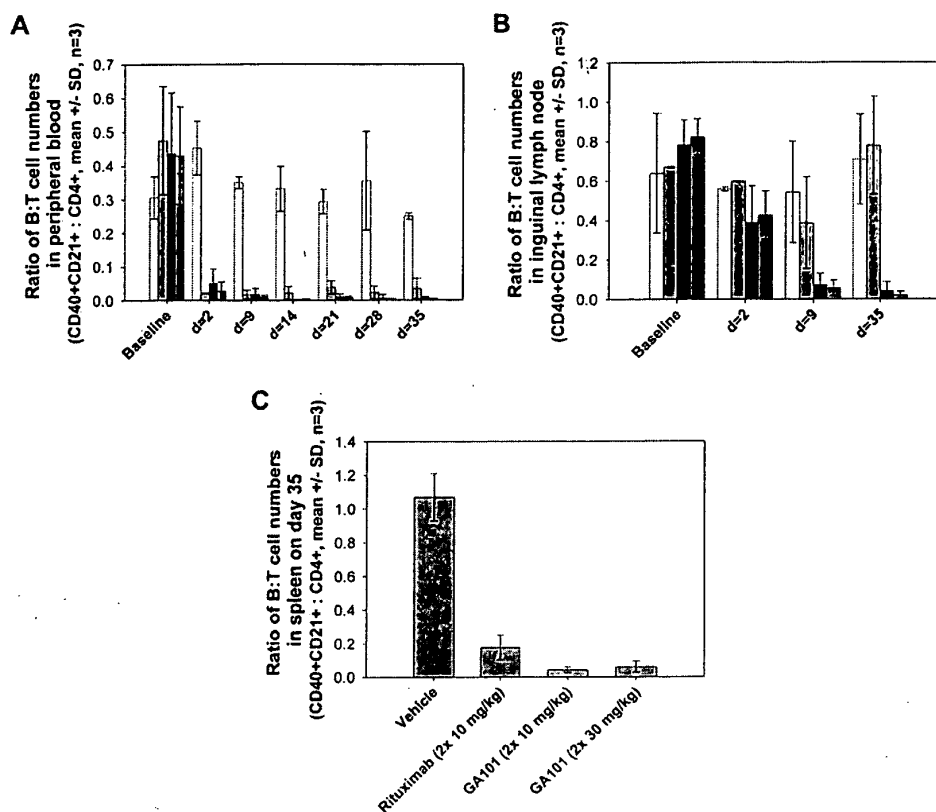


**Figure 6. Superior B-cell depletion in cynomolgus monkeys with GA101 treatment compared with rituximab.** The efficacy of GA101 at depleting B cells in cynomolgus monkeys was compared with that of rituximab in groups of 3 animals. GA101 ( $2 \times 10$  mg/kg, ■, and 30 mg/kg, ▨) was compared with rituximab ( $2 \times 10$  mg/kg, □) and vehicle (□) after 2 intravenous doses administered on days 0 and 7 to male and female cynomolgus monkeys ( $n = 3$  per group; 1 female, 2 males). Peripheral blood and lymph node B-cell numbers were evaluated at baseline (day  $-7$ ) and on the indicated days by flow cytometric analysis. B-cell numbers were evaluated in the spleens of the treated animals on day 35. (A) Mean B-cell numbers expressed as B-/T-cell ratios in peripheral blood of cynomolgus monkeys treated with GA101 and rituximab. (B) Mean B-cell numbers expressed as B-/T-cell ratios in the lymph nodes of cynomolgus monkeys treated with GA101 and rituximab. (C) Mean B-cell numbers expressed as B-/T-cell ratios in the spleens of cynomolgus monkeys treated with GA101 and rituximab on day 35. GA101 treatment resulted in statistically superior depletion of total B cells from lymph nodes, compared with rituximab, from days 9 to 35, with a decrease in B-cell numbers of more than 95%. Data are mean  $\pm$  SD.

## Acknowledgments

The authors thank all coworkers contributing to the identification and characterization of GA101 as well as the members of the GA101 project team.

## Authorship

Contribution: E.M., P.B., S.M., U.P., C. Schmidt, S.H., R.G., C.G., A.N., E.v.P., C.F., P. Sonderrmann, C.J., P. Strein, G.F., T.F., C. Schüll, S.B., J.D.P., C.D.N., and K.D. designed and performed research and analyzed data; M.J.S.D. designed research, contrib-

uted vital reagents, and analyzed data; S.P. contributed a vital new reagent; and C.K. and P.U. designed the research, analyzed the data, and wrote the article.

Conflict-of-interest disclosure: E.M., P.B., U.P., C. Schmidt, R.G., C.G., A.N., E.v.P., S.M., C.F., P. Sonderrmann, and P.U. are employees of GlycArt Biotechnology AG (a member of Roche Glycart AG); P. Strein, G.F., T.F., C. Schüll, S.B., and C.K. are employees of Roche Diagnostics GmbH; J.D.P., C.D.N., and K.D. are employees of Inflammation Discovery, Roche Glycart AG. The remaining authors declare no competing financial interests.

Correspondence: Pablo Umaña, Roche Glycart Biotechnology AG, Wagistrasse 18, CH-8952 Schlieren-Zürich, Switzerland; e-mail: pablo.umana@roche.com.

## References

- Tilly H, Zelenetz A. Treatment of follicular lymphoma: current status. *Leuk Lymphoma*. 2008; 49(suppl 1):7-17.
- Cvetković RS, Perry CM. Rituximab: a review of its use in non-Hodgkin's lymphoma and chronic lymphocytic leukaemia. *Drugs*. 2006;66(6):791-820.
- Gürcan HM, Keskin DB, Stern JN, Nitzberg MA, Shekhani H, Ahmed AR. A review of the current use of rituximab in autoimmune diseases. *Int Immunopharmacol*. 2009;9(1):10-25.
- Cartron G, Watier H, Golay J, Sola-Celigny P. From the bench to the bedside: ways to improve rituximab efficacy. *Blood*. 2004;104(9):2635-2642.
- Glennie MJ, French RR, Cragg MS, Taylor RP. Mechanisms of killing by anti-CD20 monoclonal antibodies. *Mol Immunol*. 2007;44(16):3823-3837.
- Chan HT, Hughes D, French RR, et al. CD20-induced lymphoma cell death is independent of both caspases and its redistribution into Triton X-100-insoluble membrane rafts. *Cancer Res*. 2003;63(17):5480-5489.
- Cragg MS, Glennie MJ. Antibody specificity controls in vivo effector mechanisms of anti-CD20 reagents. *Blood*. 2004;103(7):2738-2743.



8. Morschhauser F, Leonard JP, Fayad L, et al. Humanized anti-CD20 antibody, veltuzumab, in refractory/recurrent non-Hodgkin's lymphoma: phase I/II results. *J Clin Oncol*. 2009;27(20):3346-3353.
9. Genovese MC, Kaine JL, Lowenstein MB, et al. Ocrelizumab, a humanized anti-CD20 monoclonal antibody, in the treatment of patients with rheumatoid arthritis: a phase I/II randomized, blinded, placebo-controlled, dose-ranging study. *Arthritis Rheum*. 2008;58(9):2652-2661.
10. Hagenbeek A, Gadeberg O, Johnson P, et al. First clinical use of ofatumumab, a novel fully human anti-CD20 monoclonal antibody in relapsed or refractory follicular lymphoma: results of a phase 1/2 trial. *Blood*. 2008;111(12):5486-5495.
11. Beers SA, Chan CH, James S, et al. Type II (tositumomab) anti-CD20 monoclonal antibody outperforms type I (rituximab-like) reagents in B-cell depletion regardless of complement activation. *Blood*. 2008;112(10):4170-4177.
12. Clynes RA, Towers TL, Presta LG, Ravetch JV. Inhibitory Fc receptors modulate in vivo cytotoxicity against tumor targets. *Nat Med*. 2000;6(4):443-446.
13. Reff ME, Carner K, Chambers KS, et al. Depletion of B cells in vivo by a chimeric mouse human monoclonal antibody to CD20. *Blood*. 1994;83(2):435-445.
14. Teeling JL, French RR, Cragg MS, et al. Characterization of new human CD20 monoclonal antibodies with potent cytolytic activity against non-Hodgkin lymphomas. *Blood*. 2004;104(6):1793-1800.
15. Teeling JL, Mackus WJ, Wiegman LJ, et al. The biological activity of human CD20 monoclonal antibodies is linked to unique epitopes on CD20. *J Immunol*. 2006;177(1):362-371.
16. Bowles JA, Wang SY, Link BK, et al. Anti-CD20 monoclonal antibody with enhanced affinity for CD16 activates NK cells at lower concentrations and more effectively than rituximab. *Blood*. 2006;108(8):2648-2654.
17. Rossi EA, Goldenberg DM, Cardillo TM, Stein R, Wang Y, Chang CH. Novel designs of multivalent anti-CD20 humanized antibodies as improved lymphoma therapeutics. *Cancer Res*. 2008;68(20):8384-8392.
18. Brunker P, Sondermann P, Umana P. Glycoengineered therapeutic antibodies. In: Little M, ed. *Recombinant Antibodies for Immunotherapy*. New York, NY: Cambridge University Press; 2009:144-156.
19. Ferrara C, Brunker P, Suter T, Moser S, Puntener U, Umana P. Modulation of therapeutic antibody effector functions by glycosylation engineering: influence of Golgi enzyme localization domain and co-expression of heterologous beta1, 4-N-acetylglucosaminyltransferase III and Golgi alpha-mannosidase II. *Biotechnol Bioeng*. 2006;93(5):851-861.
20. Umana P, Brunker P, Ferrara C, Suter T, Puntener U, Moessner E. Antigen binding molecules with increased Fc receptor binding affinity and effector function. International Patent Application 2005;WO 2005/044859 A2.
21. Umana P, Jean-Mairet J, Bailey JE, Bailey MS. Glycosylation engineering of antibodies for improving antibody-dependent cellular cytotoxicity. U.S. Patent 2009; 7,517,870 B2.
22. Poppema S, Visser L. *Biotech Bull*. 1987;3:131-139.
23. Riechmann L, Clark M, Waldmann H, Winter G. Reshaping human antibodies for therapy. *Nature*. 1988;332(6162):323-327.
24. Binder M, Otto F, Martelsmann R, Veelken H, Trepel M. The epitope recognized by rituximab. *Blood*. 2006;108(6):1975-1978.
25. Stanfield RL, Zemla A, Wilson IA, Rupp B. Antibody elbow angles are influenced by their light chain class. *J Mol Biol*. 2006;357(5):1566-1574.
26. Cragg MS, Morgan SM, Chan HT, et al. Complement-mediated lysis by anti-CD20 mAb correlates with segregation into lipid rafts. *Blood*. 2003;101(3):1045-1052.
27. Deans JP, Li H, Polyak MJ. CD20-mediated apoptosis: signalling through lipid rafts. *Immunology*. 2002;107(2):176-182.
28. Cardarelli PM, Quinn M, Buckman D, et al. Binding to CD20 by anti-B1 antibody or F(ab')<sub>2</sub> is sufficient for induction of apoptosis in B-cell lines. *Cancer Immunol Immunother*. 2002;51(1):15-24.
29. Ferrara C, Stuart F, Sondermann P, Brunker P, Umana P. The carbohydrate at Fc gammaRIIIa Asn-162: an element required for high affinity binding to non-fucosylated IgG glycoforms. *J Biol Chem*. 2006;281(8):5032-5036.
30. Salles G, Morschhauser F, Cartron G, et al. A phase I/II study of RO5072759 (GA101) in patients with relapsed/refractory CD20+ malignant disease. *Blood*. 2008;112:Abstract 234.
31. Wang SY, Raclia E, Taylor RP, Weiner GJ. NK-cell activation and antibody-dependent cellular cytotoxicity induced by rituximab-coated target cells is inhibited by the C3b component of complement. *Blood*. 2008;111(3):1456-1463.
32. Beers SA, French RR, Chan CH, et al. Antigenic modulation limits the efficacy of anti-CD20 antibodies: implications for antibody selection [published online ahead of print March 16, 2010]. *Blood*. doi:10.1182/blood-2010-01-263533.
33. Cartron G, Dacheux L, Salles G, et al. Therapeutic activity of humanized anti-CD20 monoclonal antibody and polymorphism in IgG Fc receptor Fc gammaRIIIa gene. *Blood*. 2002;99(3):754-758.
34. Weng WK, Levy R. Two immunoglobulin G fragment C receptor polymorphisms independently predict response to rituximab in patients with follicular lymphoma. *J Clin Oncol*. 2003;21(21):3940-3947.
35. Musolino A, Naldi N, Bortesi B, et al. Immunoglobulin G fragment C receptor polymorphisms and clinical efficacy of trastuzumab-based therapy in patients with HER-2/neu-positive metastatic breast cancer. *J Clin Oncol*. 2008;26(11):1789-1796.
36. Bibeau F, Lopez-Crapez E, Di Fiore F, et al. Impact of Fc gammaRIIIa-Fc gammaRIIIa polymorphisms and KRAS mutations on the clinical outcome of patients with metastatic colorectal cancer treated with cetuximab plus irinotecan. *J Clin Oncol*. 2009;27(7):1122-1129.
37. Nagy ZA, Hubner B, Lohning C, et al. Fully human, HLA-DR-specific monoclonal antibodies efficiently induce programmed death of malignant lymphoid cells. *Nat Med*. 2002;8(8):801-807.
38. Barbier S, Chatre L, Bras M, et al. Caspase-independent type III programmed cell death in chronic lymphocytic leukemia: the key role of the F-actin cytoskeleton. *Haematologica*. 2009;94(4):507-517.
39. Zhao X, Lapalombella R, Joshi T, et al. Targeting CD37-positive lymphoid malignancies with a novel engineered small modular immunopharmaceutical. *Blood*. 2007;110(7):2569-2577.
40. Ravichandran KS, Lorenz U. Engulfment of apoptotic cells: signals for a good meal. *Nat Rev Immunol*. 2007;7(12):964-974.

# **Attachment L**

**Obinutuzumab BLA, Section 3.2.S.2.3  
Source, History, and Generation, redacted**



[REDACTED]

[REDACTED] the antibody genes were co-transfected together with genes encoding N-acetylglucosaminyltransferase III (GnTIII) and  $\alpha$ -mannosidase II (ManII) in order to engineer the oligosaccharide structure attached to the antibody [REDACTED]. The resulting antibody features a significantly increased Fc $\gamma$ RIIIa binding mediated by a modified glycosylation pattern which is related to enhanced antibody-dependent cell-mediated cytotoxicity (ADCC).

[REDACTED]

# **Attachment M**

**Obinutuzumab BLA, Section 3.2.S.2.2 Cell  
Culture and Harvest, redacted**



[REDACTED]

[REDACTED]

[REDACTED]

[REDACTED]

[REDACTED]

The production culture is harvested [REDACTED] followed by filters to remove cell debris. The cell-free harvested cell culture fluid is [REDACTED] filtered prior to purification of obinutuzumab.

[REDACTED]

[REDACTED]

# **Attachment N**

**Ferrara *et al.*, *J. Biol. Chem.*, 2006,  
281(8):5032-5036**

# The Carbohydrate at FcγRIIIa Asn-162 AN ELEMENT REQUIRED FOR HIGH AFFINITY BINDING TO NON-FUCOSYLATED IgG GLYCOFORMS\*

Received for publication, September 15, 2005, and in revised form, December 2, 2005. Published, JBC Papers in Press, December 5, 2005, DOI 10.1074/jbc.M510171200

Claudia Ferrara<sup>‡§</sup>, Fiona Stuart<sup>‡</sup>, Peter Sondermann<sup>‡</sup>, Peter Brünker<sup>‡</sup>, and Pablo Umaña<sup>†1</sup>

From the <sup>‡</sup>GLYCART Biotechnology AG (Roche Group), Wagistrasse 18, CH-8952 Schlieren, Switzerland and the <sup>§</sup>Institute of Biotechnology, ETH Zürich, CH-8093 Zürich, Switzerland

FcγRIIIa plays a prominent role in the elimination of tumor cells by antibody-based cancer therapies. Non-fucosylated bisected IgGs bind this receptor with increased affinity and trigger FcγRIII-mediated effector functions more efficiently than native, fucosylated antibodies. In this study the contribution of the carbohydrates of both binding partners to the strength of the complex was analyzed. Glycoengineering of the antibody increased affinity for two polymorphic forms of soluble human FcγRIIIa (by up to 50-fold) but did not affect binding to the inhibitory FcγRIIb receptor. While the absence of carbohydrate at FcγRIIIa's Asn-162 increased affinity for native IgG, presumably due to the removal of steric hindrance caused by the bulky sugars, it unexpectedly reduced affinity for glycoengineered (GE) antibodies by over one order of magnitude, bringing the affinity down to the same level as for native IgG. We conclude that the high affinity between GE antibodies and FcγRIII is mediated by productive interactions formed between the receptor carbohydrate attached at Asn-162 and regions of the Fc that are only accessible when it is nonfucosylated. As FcγRIIIa and FcγRIIb are the only human Fcγ receptors glycosylated at this position, the proposed interactions explain the observed selective affinity increase of GE antibodies for only these receptors. Furthermore, we predict from our structural model that only one of the two Fc-fucose residues needs to be absent for increased binding affinity toward FcγRIII. This information can be exploited for the design of new antibodies with altered Fc receptor binding affinity and enhanced therapeutic potential.

Antibodies provide a link between the humoral and the cellular immune system with IgG<sup>2</sup> being the most abundant serum immunoglobulin. While the Fab regions of the antibody recognize antigens, the Fc part interacts with membrane-bound Fcγ receptors (FcγRs) that are differentially expressed by all immune competent cells. Receptor cross-linking by a multivalent antigen-antibody complex triggers degranulation, cytolysis or phagocytosis of the target cell, and transcriptional activation of cytokine-encoding genes (1).

Recently, the importance of the activating receptor FcγRIIIa for the *in vivo* elimination of tumor cells in humans has been demonstrated. In follicular non-Hodgkin's lymphoma patients, a relationship was discovered between the FcγRIIIa genotype and clinical and molecular responses to rituximab, an anti-CD20 chimeric antibody used against

hematological malignancies (2). The authors demonstrated that the efficacy of rituximab was higher in patients homozygous for the "high affinity" FcγRIIIa, characterized by a valine at position 158 (FcγRIIIa[Val-158]), than in patients heterozygous or homozygous for the "low affinity" FcγRIIIa, which has a phenylalanine residue at this position (FcγRIIIa[Phe-158]) and has lower affinity for IgG (3). Increased survival of lymphoma patients that mount an anti-tumor humoral response after anti-idiotypic vaccination has also been correlated with homozygosity for FcγRIIIa[Val-158] (4).

The above observations imply a crucial role for FcγRIIIa in the elimination of tumor cells and support the idea that therapeutic monoclonal antibodies (mAbs) with increased affinity for FcγRIIIa will have improved biological activity. One route to increase the affinity of monoclonal antibodies toward FcγRIIIa and consequently to enhance their effector functions is manipulation of their carbohydrate moiety (5–7). The *N*-glycosylation of the Fc fragment at Asn-297 in both Cγ2 domains is crucial to the affinity for all FcγRs (8, 9) and is required to elicit proper effector functions (10, 11). It is comprised of a conserved pentasaccharide structure with variable addition of fucose and outer arm sugars (12). The *N*-glycosylation pattern of mAbs can be manipulated by engineering the glycosylation pathway of the production cell line using enzyme activities that lead to naturally occurring carbohydrates. Umaña and co-workers (5, 7) reported the production of glycoengineered (GE) antibodies, which feature high proportions of bisected, non-fucosylated oligosaccharides, improved affinity for FcγRIIIa and enhanced antibody-dependent cellular cytotoxicity. Antibodies with increased binding to FcγRIIIa have also been obtained using a cell line which is unable to add fucose residues to *N*-linked oligosaccharides (6, 13).

Little information is available on the influence of FcγRIIIa carbohydrates on the affinity for IgG. The crystal structure of unglycosylated FcγRIII in complex with the Fc fragment of human (h) IgG1 indicates that a carbohydrate moiety attached at Asn-162 of FcγRIII would point into the central cavity within the Fc fragment (14), where the rigid core glycans attached to IgG-Asn-297 are also located (15). In the present study, binding of glycosylated soluble (s) hFcγRIIIa variants to distinct antibody glycovariants was evaluated by surface plasmon resonance (SPR) and in a cellular system to dissect the interaction between IgG1 and glycosylated FcγRIIIa on a molecular level.

## EXPERIMENTAL PROCEDURES

**Cell Lines, Expression Vectors, and Antibodies**—HEK293-EBNA cells were a kind gift from Rene Fischer (Laboratory of Organic Chemistry, Zürich, Switzerland). Additional cell lines used in this study were Jurkat cells (human lymphoblastic T cell, ATCC number TIB-152) and FcγRIIIa[Val-158]- and FcγRIIIa[Val-158/Gln-162]-expressing Jurkat cell lines, generated as described previously (7). The cells were cultivated according to the instructions of the supplier. DNA encoding the

\* The costs of publication of this article were defrayed in part by the payment of page charges. This article must therefore be hereby marked "advertisement" in accordance with 18 U.S.C. Section 1734 solely to indicate this fact.

<sup>1</sup> To whom correspondence should be addressed. Tel: 41-44-755-6161; Fax: 41-44-755-61-60; E-mail: pablo.umana@roche.com.

<sup>2</sup> The abbreviations used are: IgG, immunoglobulin G; GE, glycoengineered; Fuc, fucose; GnT-III, β1,4-*N*-acetylglucosaminyltransferase III; FcγR, Fcγ receptor; mAb, monoclonal antibody; SPR, surface plasmon resonance; h, human; s, soluble; m, mouse.

## High Affinity IgG Binding by FcγRIIIa

shFcγRIIIa[Val-158] and shFcγRIIIa[Phe-158] variants were fused after residue 191 to a hexahistidine tag (NH<sub>2</sub>-MRTEDL... GYQG(H<sub>6</sub>)-COOH, numbering is based on the mature protein) using PCR as described (16). Asn-162 of shFcγRIIIa[Val-158] was exchanged for Gln by PCR. All expression vectors contained the replication origin oriP from the Epstein-Barr virus for expression in HEK293-EBNA cells. GE and native anti-CD20 antibodies were produced in HEK-293 EBNA cells and characterized by standard methods. Neutral oligosaccharide profiles for the antibodies were analyzed by mass spectrometry (Autoflex, Bruker Daltonics GmbH, Faellanden, Switzerland) in positive ion mode (17).

**Production and Purification of Recombinant shFcγRIIIa Receptors**—The shFcγRIIIa variants were produced by transient expression in HEK-293-EBNA cells (18) and purified using a HiTrap Chelating HP column (Amersham Biosciences, Otelfingen, Switzerland) and a size exclusion chromatography step with HBS-EP buffer (0.01 M HEPES, pH 7.4, 0.15 M NaCl, 3 mM EDTA, 0.005% Surfactant P20). Human sFcγRIIb and mouse (m) sFcγRIIb were produced and purified as described (19). The concentration of proteins was determined as described (20).

**SPR**—SPR experiments were performed on a Biacore3000 with HBS-EP as running buffer (Biacore, Freiburg, Germany). Direct coupling of around 1,000 resonance units of human IgG glycovariants was performed on a CM5 chip using the standard amine coupling kit (Biacore). Different concentrations of soluble FcγRs were passed with a flow rate of 10 μl/min through the flow cells. Increasing the flow rate did not influence the binding curves. Bulk refractive index differences were corrected for by subtracting the response obtained on flowing sample over a bovine serum albumin-coupled surface. The steady state response was used to obtain the dissociation constant *K<sub>D</sub>* by non-linear curve fitting of the Langmuir binding isotherm. Kinetic constants were obtained using the BIAevaluation program curve-fitting facility (v3.0, Biacore), to fit rate equations for 1:1 Langmuir binding by numerical integration.

**Binding of IgG to FcγRIIIa-expressing Cells**—The experiment was conducted as described previously (7). Briefly, hFcγRIIIa-expressing Jurkat cells were incubated with IgG variants in phosphate-buffered saline, 0.1% bovine serum albumin. After two washes with phosphate-buffered saline, 0.1% bovine serum albumin, antibody binding was detected by incubating with 1:200 fluorescein isothiocyanate-conjugated goat anti-human F(ab')<sub>2</sub>, F(ab')<sub>2</sub> fragments (Jackson ImmunoResearch, West Grove, PA) (16). The fluorescence intensity of the bound antibody variants was determined on a FACS Calibur (BD Biosciences, Allschwil, Switzerland).

**Modeling**—We visualized the interaction of the Fc fragment derived from native IgG and the FcγRIII glycans after creating a carbohydrate *in silico*, attached at the position Asn-162 of the receptor. The glycan unit was modeled on to the crystal structure of FcγRIII in complex with Fc-IgG (Protein Data Bank code 1e4k). The interaction between FcγRIII and IgG was modeled by directing the Fc-linked pentasaccharide core to the fucose residue of oligosaccharide linked to the Fc-Asn-297. The model was not energy minimized and only created to visualize the proposed binding mode.

### RESULTS

**Biochemical Characterization of Soluble hFcγRIIIa Receptors and Antibody Glycovariants**—ShFcγRIIIa[Val-158], shFcγRIIIa[Phe-158], and shFcγRIIIa[Val-158/Gln-162] were expressed in HEK293-EBNA cells and purified to homogeneity. The purified shFcγRIIIa[Val-158] and [Phe-158] migrate as broad bands in the apparent molecular weight range of 40–50 kDa when subjected to reducing SDS-PAGE. The apparent molecular weight is slightly lower for the mutant shFcγRIIIa[Val-

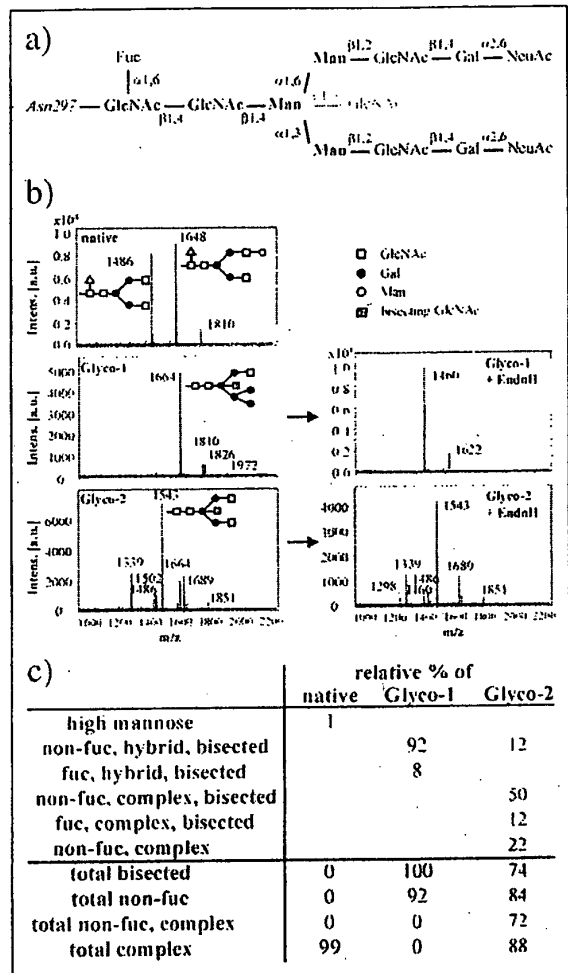


**FIGURE 1.** Oligosaccharide characterization of GE and native antibodies. *a*, carbohydrate moiety attached to Asn-297 of human IgG1-Fc. The sugars in bold define the pentasaccharide core; the addition of the other sugar residues is variable. The bisecting β1,4-linked GlcNAc residue is introduced by GnT-III. *b*, MALDI-MS spectra of neutral oligosaccharides released from native and GE antibodies. The *m/z* value corresponds to the sodium-associated oligosaccharide ion. To confirm the carbohydrate type the antibodies were treated with endoglycosidase H, which hydrolyzes hybrid but not complex glycans. *c*, oligosaccharide distributions of the IgG glycovariants used in this study.

158/Gln-162] (data not shown). This can be explained by the elimination of the carbohydrates linked to Asn-162. Upon enzymatic *N*-deglycosylation all three receptor variants migrate identically in the apparent molecular weight range of 25–30 kDa and feature three bands as observed previously for the membrane form of *N*-deglycosylated hFcγRIII (21, 22). This heterogeneous pattern may result from the presence of *O*-linked carbohydrates.

The native antibody glycosylation pattern is characterized by biantennary, fucosylated complex oligosaccharides (Fig. 1, *b* and *c*), heterogeneous with respect to terminal galactose content. GE-hIgG1 antibodies were produced in a cell line overexpressing β1,4-*N*-acetylglucosaminyltransferase III (GnT-III), an enzyme catalyzing the addition of a bisecting GlcNAc (Fig. 1*a*) to the β-mannose of the core. Two different GE antibody variants were generated; Glyco-1 was produced by



## High Affinity IgG Binding by FcγRIIIa

**TABLE 1**  
Summary of affinity constants determined by equilibrium and kinetic analysis  
Data are the average of two experiments. ND = not determined.

IgG1	Fcγ receptor	$k_{on}$ $\times 10^5 \mu\text{M}^{-1} \text{s}^{-1}$	$k_{off}$ $\times 10^{-3} \text{s}^{-1}$	$K_D$	
				Kinetic $\mu\text{M}$	Steady state
Native	shFcγRIIIa[Val-158]	ND <sup>a</sup>	ND <sup>a</sup>	ND <sup>a</sup>	0.75 ± 0.08
Glyco-1	shFcγRIIIa[Val-158]	2.4 ± 0.01	5.8 ± 0.01	0.024 ± <0.001	ND
Glyco-2	shFcγRIIIa[Val-158]	3.2 ± 0.01	5.1 ± 0.01	0.016 ± <0.001	0.015 ± <0.001 <sup>b</sup>
Native	shFcγRIIIa[Phe-158]	ND <sup>a</sup>	ND <sup>a</sup>	ND <sup>a</sup>	5.0 ± 0.59
Glyco-1	shFcγRIIIa[Phe-158]	1.6 ± 0.09	32 ± 0.1	0.20 ± 0.001	0.27 ± 0.02
Glyco-2	shFcγRIIIa[Phe-158]	2.3 ± 0.01	29 ± 0.1	0.13 ± 0.001	0.18 ± 0.02
Native	shFcγRIIIa[Val-158/Gln-162]	5.9 ± 0.05	90 ± 0.4	0.16 ± 0.001	0.24 ± 0.03
Glyco-1	shFcγRIIIa[Val-158/Gln-162]	4.7 ± 0.02	89 ± 0.5	0.19 ± 0.001	0.30 ± 0.02
Glyco-2	shFcγRIIIa[Val-158/Gln-162]	8.1 ± 0.06	72 ± 0.3	0.09 ± 0.001	0.20 ± 0.02
Native	shFcγRIIb	ND <sup>a</sup>	ND <sup>a</sup>	ND <sup>a</sup>	2.4 ± 0.21
Glyco-1	shFcγRIIb	ND <sup>a</sup>	ND <sup>a</sup>	ND <sup>a</sup>	2.4 ± 0.10
Glyco-2	shFcγRIIb	ND <sup>a</sup>	ND <sup>a</sup>	ND <sup>a</sup>	1.6 ± 0.10
Native	smFcγRIIb	ND <sup>a</sup>	ND <sup>a</sup>	ND <sup>a</sup>	0.44 ± 0.03
Glyco-1	smFcγRIIb	ND <sup>a</sup>	ND <sup>a</sup>	ND <sup>a</sup>	0.69 ± 0.03
Glyco-2	smFcγRIIb	ND <sup>a</sup>	ND <sup>a</sup>	ND <sup>a</sup>	0.46 ± 0.03

<sup>a</sup> Kinetic too fast for exact determination.

<sup>b</sup> No duplicate.

overexpression of GnT-III alone and Glyco-2 by co-expression of GnT-III and recombinant Man-II (Ref. 7 and Fig. 1b). Both Glyco-1 and Glyco-2 feature high proportions of bisected, non-fucosylated oligosaccharides (92 and 84%, respectively; Fig. 1c). We have previously shown that both forms give similar increases in affinity for FcγRIIIa and increased antibody-dependent cellular cytotoxicity relative to native hIgG1 but differ in their reactivity in complement-dependent cytotoxicity assays (7).

**IgG Oligosaccharide Modifications Lead to Antibodies with Increased Affinity for shFcγRIIIa**—The interaction of antibody glycovariants with shFcγRIIIa variants ([Val-158], [Phe-158], and [Val-158/Gln-162]) shFcγRIIb and smFcγRIIb was analyzed by SPR. Binding of shFcγRIIIa[Val-158] to the GE antibodies was up to 50-fold stronger than to the native antibody ( $K_D$ (Glyco-2) 0.015  $\mu\text{M}$  versus  $K_D$ (native) 0.75  $\mu\text{M}$ , Table 1). The low affinity polymorphic form of the receptor, shFcγRIIIa[Phe-158], also bound to the GE antibodies with significantly higher affinity than to the native antibody ( $K_D$ (Glyco-1) 0.27  $\mu\text{M}$  (18-fold),  $K_D$ (Glyco-2) 0.18  $\mu\text{M}$  (27-fold),  $K_D$ (native) 5  $\mu\text{M}$  (Table 1)).

Although the dissociation of both receptor variants from native IgG was too fast to enable a direct determination of kinetic constants for these interactions, overlaying the experimental data clearly shows that a major effect of glycoengineering the antibodies is decreased dissociation from the receptors (Fig. 2a). To estimate dissociation rates from native IgG dissociation curves were simulated using different rate constants and compared with the experimental data (data not shown). These calculations indicated that the entire increase in affinity upon glycoengineering could be accounted for by decreased dissociation rate constant ( $k_{off}$ ).

The association rate constants ( $k_{on}$  values) of the two polymorphic forms of shFcγRIIIa for GE antibodies were similar, but the dissociation rate of shFcγRIIIa[Phe-158] was significantly faster and largely accounts for the lower affinity of this receptor (Table 1).

The affinity of the antibodies for human and murine FcγRIIb was also measured. GE and native IgGs bound the human inhibitory receptor shFcγRIIb with similar affinity ( $K_D$  = 1.6–2.4  $\mu\text{M}$ , Table 1). For the murine version of this receptor the affinity for human IgG1 was also unaltered by antibody glycoengineering, but surprisingly was 3.4–5.5 times that of the human FcγRIIb receptor (Table 1). The dissociation constant ( $K_D$ ) for the interaction of the native antibody with

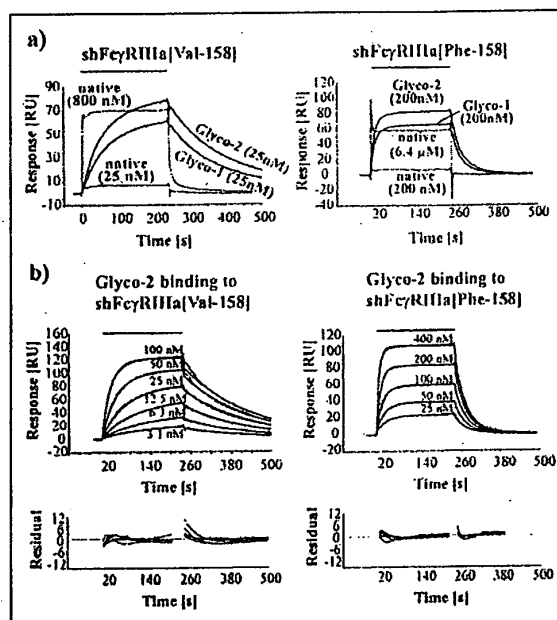


**FIGURE 2.** Binding of shFcγRIIIa[Val-158] or shFcγRIIIa[Phe-158] to immobilized IgG glycovariants. The association phase is represented by a solid bar above the curves. The concentrations shown are those of the receptors. *a*, overlay of sensograms of the binding events for shFcγRIIIa[Val-158] and shFcγRIIIa[Phe-158] respectively. To compare binding within a similar response range, sensograms obtained using high concentrations of receptor on the native antibody surface were also included. All sensograms were normalized to the immobilization level. *b*, kinetic analysis for shFcγRIIIa[Val-158] or shFcγRIIIa[Phe-158] binding to Glyco-2. Fitted curves and residual errors (below) were derived by non-linear curve fitting.

sh/mFcγRIIb could only be determined by steady state analysis (Table 1) because the equilibrium was attained too quickly for a kinetic evaluation (Fig. 2a).

**FcγRIIIa Glycosylation Regulates Binding to Antibody Glycovariants**—A mutant form of hFcγRIIIa that is not glycosylated at Asn-162 (shFcγRIIIa[Val-158/Gln-162]) was used to analyze the influence of

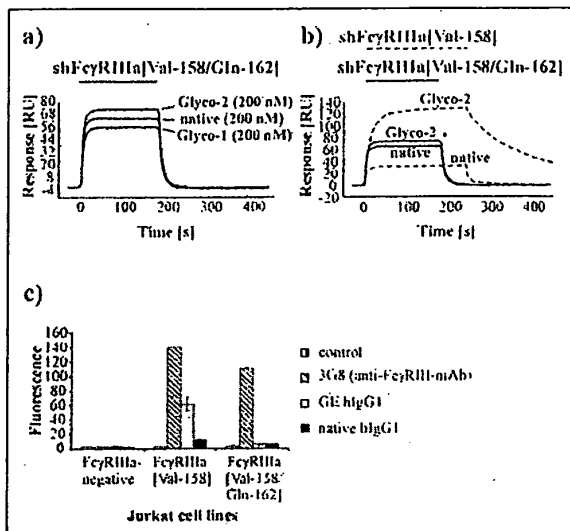


**FIGURE 3.** Binding of IgG glycovariants to hFcγRIIIa[Val-158] or hFcγRIIIa[Val-158/Gln-162]. **a**, overlay of sensograms for binding of 200 nM shFcγRIIIa[Val-158/Gln-162]. The association phase is represented by a solid bar above the curves. **b**, overlay of sensograms for binding of 200 nM shFcγRIIIa[Val-158] or 200 nM shFcγRIIIa[Val-158/Gln-162] to native IgG1 or Glyco-2 IgG1. All sensograms were normalized to the immobilization level. **c**, binding of IgG to hFcγRIIIa[Val-158]- and hFcγRIIIa[Val-158/Gln-162]-expressing or FcγRIIIa-negative Jurkat cells. FcγRIIIa binding was measured by cytometry in arbitrary units. mAb 3G8 was used to control the FcγRIIIa expression level.

the receptor's carbohydrate on complex formation with IgG. Interestingly, upon removal of *N*-glycosylation at Asn-162, native IgG showed a 3-fold increase ( $K_D = 0.24$  versus  $0.75 \mu\text{M}$ ) in affinity for the receptor, whereas GE antibodies showed an over 13-fold decrease in affinity (Table 1). For binding to GE antibodies, removal of the receptor glycosylation site resulted in an almost 2-fold increase in  $k_{on}$  but an over 14-fold increase in  $k_{off}$  (Table 1). Steady state and kinetically determined  $K_D$  values differed by 1.6–2.2-fold for binding of shFcγRIIIa[Val-158/Gln-162] to the antibodies. This discrepancy most likely results from a high error in fitting the very fast dissociation phase.

The SPR-based results were corroborated using Jurkat cells expressing membrane bound FcγRIIIa, which represents a natural environment for FcγRIIIa expression (23). We used the anti-FcγRIII mAb 3G8, which does not discriminate between FcγRIIIa[Val-158] and FcγRIIIa[Val-158/Gln-162] (24), to monitor FcγRIII expression in these cell lines. In this experiment GE antibodies bound FcγRIIIa[Val-158] better than the native antibody (Fig. 3c). Binding to FcγRIIIa[Val-158/Gln-162] was, however, significantly reduced for all IgG variants, including native IgG (Fig. 3c). The very fast dissociation rate constants found in the SPR experiment for binding of FcγRIIIa[Val-158/Gln-162] to all three IgG variants could explain the lower binding in the cellular assay.

## DISCUSSION

**Kinetic Analysis of the FcγRIIIa/IgG Interaction**—Overall our measured  $K_D$  values for the interaction of IgG1 with glycosylated FcγRIIIa agree with those previously published by Okazaki *et al.* (25). These authors concluded that the affinity increase of the non-fucosylated (GE) antibody is predominantly caused by an increase in  $k_{on}$ . In contrast, although we could not quantify  $k_{on}$  and  $k_{off}$  for binding to native IgG due to the high velocity of the reaction, comparison of the binding curves for native and GE antibodies clearly shows significantly faster dissociation

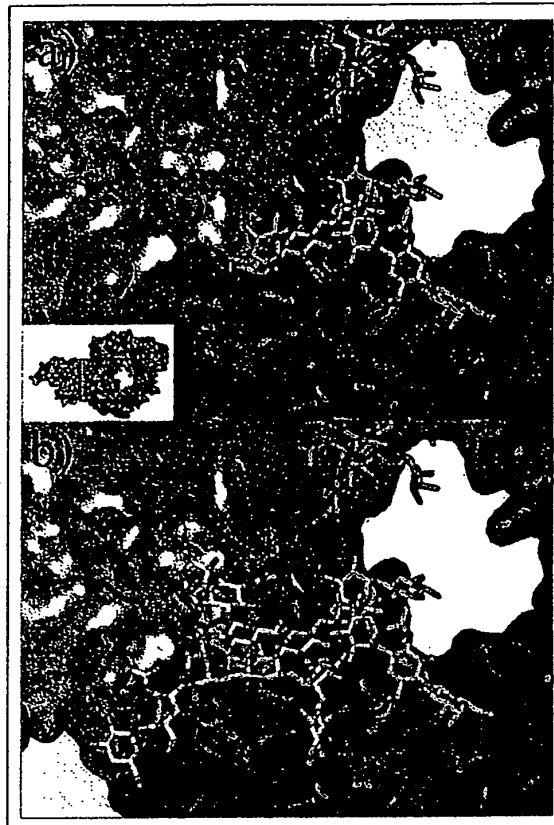


**FIGURE 4.** The proposed interaction of glycosylated FcγRIII with the Fc fragment of IgG. **a**, clipping of the crystal structure of FcγRIII in complex with the Fc fragment of native (fucosylated) IgG (Protein Data Bank code 1e4k) shown in the inset marked by a rectangle. The two chains of the Fc fragment are depicted as red and blue and the unglycosylated FcγRIII as green surface with Asn-162 in yellow. The glycans attached to the Fc are shown as ball and sticks and colored accordingly. The central fucose residue linked to the carbohydrate of the blue Fc fragment chain is colored red. **b**, model of the interaction between a glycosylated FcγRIII and the (non-fucosylated) Fc fragment of GE-IgG. As the fucose is not present within GE-IgG, the carbohydrates attached at Asn-162 of the receptor can thoroughly interact with the GE-IgG. The figure was created using the program PYMOL ([www.delanoscientific.com](http://www.delanoscientific.com)).

of the receptor variants from native IgG (Fig. 2a). We conclude that upon antibody glycoengineering either new interactions between the binding partners are formed or the present ones are improved. Importantly, we showed that glycoengineered antibodies bind with significantly higher affinity to the more common low affinity variant of FcγRIIIa than native antibodies do to the less common high affinity variant of the receptor. This gives the hope of improving anti-cancer antibody therapies for people with this allelic variant.

**The Glycosylation of FcγRIIIa at Asn-162 Modulates Binding to Antibodies**—FcγRIIIa of mammalian origin is a highly glycosylated protein with five *N*-linked glycosylation sites. From the crystal structure of IgG1-Fc in complex with unglycosylated FcγRIII (14), glycosylation at Asn-162 in FcγRIII has been hypothesized to reduce affinity for native IgG1 due to steric hindrance exerted by the hFcγRIIIa[Asn-162] carbohydrate moiety. This has been confirmed with the appropriate glycosylation mutant of FcγRIII, while removal of carbohydrates at the other four *N*-glycosylation sites did not affect affinity for native IgG (24).

## High Affinity IgG Binding by FcγRIIIa

To further investigate the importance of glycosylation of IgG and FcγRIIIa for their interaction, a mutant version of the high affinity receptor which is unglycosylated at position 162 (shFcγRIIIa[Val-158/Gln-162]) was constructed. As expected, removal of the carbohydrate at Asn-162 of the receptor increased binding affinity for the native antibody (3-fold, Table 1). On the other hand, removal of the FcγRIIIa's carbohydrate at Asn-162 unexpectedly led to reduced binding affinity for GE antibodies by over an order of magnitude, bringing the affinity down to the level observed for the native antibody. The data were corroborated in a cellular assay system, where GE antibodies bound significantly better to hFcγRIIIa[Val-158] than to hFcγRIIIa[Val-158/Gln-162]-expressing cells (Fig. 3c).

In summary, two requirements have to be met for high affinity interaction between GE IgG and FcγRIII; a carbohydrate has to be attached at FcγRIII's Asn-162, and productive contacts of this receptor carbohydrate with the IgG-Fc can only be made if the latter is non-fucosylated. Based on these results we propose a model in which the Asn-162-linked carbohydrate of FcγRIII contacts a region of the IgG-Fc where a fucose residue is attached in native antibodies. This fucose residue protrudes from the continuous surface of the Fc into open space and may prohibit a close approach of the Fc receptor carbohydrate core, thereby precluding additional productive interactions (Fig. 4). It should be noted that a complete overlap with the mentioned Fc region is attained by a receptor carbohydrate with as few three monosaccharide units (Fig. 4). Furthermore, the model predicts that only one of the two Fc-fucose residues needs to be absent for increased binding affinity toward FcγRIII.

In a recent study Okazaki *et al.* (25) proposed that non-fucosylated antibodies bind FcγRIIIa with increased affinity as a result of a newly formed bond between Tyr-296 of the Fc and Lys-128 of the FcγRIIIa. However, we found that the increased affinity of non-fucosylated antibodies depends on glycosylation of the receptor which implies that an IgG-Fc[Tyr-296]/FcγRIIIa[Lys-128] bond is insignificant to the affinity between GE antibodies and FcγRIIIa.

FcγRIIIa and FcγRIIIb forms are the only forms of the human FcγRs that possess N-glycosylation sites within the binding region to IgG. We therefore conclude that affinity for IgG will be influenced by receptor glycosylation only for these two FcγRs. Comparison of the amino acid sequences of FcγRIII from other species indicates that the N-glycosylation site Asn-162 is shared by FcγRIII from macaca, cat, cow, and pig, whereas it is lacking in the known rat and mouse FcγRIII. Recently mouse (CD16-2) and rat (GenBank™ accession number AY219230) genes with high homology to the human FcγRIII and which encode proteins containing the Asn-162 glycosylation site were identified (26), and functional expression of the murine protein was recently reported (27). The presence of a FcγRIIIa-Asn-162 glycosylation site may enable the immune system to tune the affinity toward FcγRIII by differential FcγRIII glycosylation (21) and by modulation of the fucose content of IgG.

*The Immunological Balance between Activating and Inhibitory FcγRs*—It has been proposed that an improvement in the ratio of activating to inhibitory signals should enhance the efficacy of therapeutic antibodies (28). In the current study, the inhibitory shFcγRIIb receptor was found to have a similar affinity for native and GE antibodies (Table 1). The inhibitory receptors shFcγRIIb from mouse and human are not glycosylated at Asn-162. The lack of discrimination for GE antibodies displayed by FcγRIIb is consistent with glycosylation of activating FcγRIII at Asn-162 being essential for increased binding to non-fucosy-

lated IgGs and suggests that these GE antibodies could show enhanced therapeutic efficacy.

The finding that murine FcγRII has significantly higher affinity than human FcγRIIb for both native and GE hIgG1 may be important for the correct interpretation of *in vivo* experiments using mouse models. Enhanced binding to the inhibitory receptor in a mouse model may result in a different threshold of the immune response than that observed in humans.

## CONCLUSION

We demonstrated the importance of the carbohydrate moieties of both FcγRIII and IgG for their interaction. Our data provide further insight into the complex formation and identified an important interaction between the Asn-162 carbohydrate of FcγRIII and the Fc of non-fucosylated IgG glycoforms. This finding should allow the design of new antibody variants that make further productive interactions with the carbohydrate of FcγRIIIa, which may impact on future therapies with monoclonal antibodies.

## REFERENCES

- Deo, Y. M., Graziano, R. F., Repp, R., and van de Winkel, J. G. (1997) *Immunol. Today* 18, 127–135
- Cartron, G., Dacheux, L., Salles, G., Solal-Celigny, P., Bardos, P., Colombat, P., and Watier, H. (2002) *Blood* 99, 754–758
- Koene, H. R., Kleijer, M., Algra, J., Roos, D., von dem Borne, A. F., and de Haas, M. (1997) *Blood* 90, 1109–1114
- Weng, W. K., Czerwinski, D., Timmerman, J., Hsu, F. J., and Levy, R. (2004) *J. Clin. Oncol.* 22, 4717–4724
- Umaña, P., Jean-Mairet, J., Moudry, R., Amstutz, H., and Bailey, J. E. (1999) *Nat. Biotechnol.* 17, 176–180
- Shields, R. L., Lai, J., Keck, R., O'Connell, L. Y., Hong, K., Meng, Y. G., Weikert, S. H., and Presta, L. G. (2002) *J. Biol. Chem.* 277, 26733–26740
- Ferrara, C., Brünker, P., Suter, T., Moser, S., Püntener, U., and Umaña, P. (2006) *Biotechnol. Bioeng.*, in press
- Tao, M. H., and Morrison, S. L. (1989) *J. Immunol.* 143, 2595–2601
- Mimura, Y., Sondermann, P., Ghirlando, R., Lund, J., Young, S. P., Goodall, M., and Jefferis, R. (2001) *J. Biol. Chem.* 276, 45539–45547
- Wright, A., and Morrison, S. L. (1994) *J. Exp. Med.* 180, 1087–1096
- Sarmay, G., Lund, J., Rozsnyay, Z., Gergely, J., and Jefferis, R. (1992) *Mol. Immunol.* 29, 633–639
- Jefferis, R., Lund, J., and Pound, J. D. (1998) *Immunol. Rev.* 163, 59–76
- Shinkawa, T., Nakamura, K., Yamane, N., Shoji-Hosaka, E., Kanda, Y., Sakurada, M., Uchida, K., Anazawa, H., Satoh, M., Yamasaki, M., Hanai, N., and Shitara, K. (2003) *J. Biol. Chem.* 278, 3466–3473
- Sondermann, P., Huber, R., Oosthuizen, V., and Jacob, U. (2000) *Nature* 406, 267–273
- Huber, R., Deisenhofer, J., Colman, P. M., Matsushima, M., and Palm, W. (1976) *Nature* 264, 415–420
- Shields, R. L., Namenuk, A. K., Hong, K., Meng, Y. G., Rae, J., Briggs, J., Xie, D., Lai, J., Stadler, A., Li, B., Fox, J. A., and Presta, L. G. (2001) *J. Biol. Chem.* 276, 6591–6604
- Papac, D. I., Briggs, J. B., Chin, E. T., and Jones, A. J. (1998) *Glycobiology* 8, 445–454
- Jordan, M., Schallhorn, A., and Wurm, F. M. (1996) *Nucleic Acids Res.* 24, 596–601
- Sondermann, P., and Jacob, U. (1999) *Biol. Chem.* 380, 717–721
- Gill, S. C., and von Hippel, P. H. (1989) *Anal. Biochem.* 182, 319–326
- Edeberg, J. C., and Kimberly, R. P. (1997) *J. Immunol.* 158, 3849–3857
- Ravetch, J. V., and Perussia, B. (1989) *J. Exp. Med.* 170, 481–497
- Braakman, E., van de Winkel, J. G., van Krimpen, B. A., Jansz, M., and Bolhuis, R. L. (1992) *Cell Immunol.* 143, 97–107
- Drescher, B., Witte, T., and Schmidt, R. E. (2003) *Immunology* 110, 335–340
- Okazaki, A., Shoji-Hosaka, E., Nakamura, K., Wakitani, M., Uchida, K., Kakita, S., Tsumoto, K., Kumagai, I., and Shitara, K. (2004) *J. Mol. Biol.* 336, 1239–1249
- Mechetina, L. V., Najakshin, A. M., Alabyev, B. Y., Chikavev, N. A., and Taranin, A. V. (2002) *Immunogenetics* 54, 463–468
- Nimmerjahn, F., Bruhns, P., Horiuchi, K., and Ravetch, J. V. (2005) *Immunity* 23, 41–51
- Clynes, R. A., Towers, T. L., Presta, L. G., and Ravetch, J. V. (2000) *Nat. Med.* 6, 443–446

# **Attachment O**

**Ferarra et al., Biotechnology and  
Bioengineering, 2006, 93(5):851-61**

# Modulation of Therapeutic Antibody Effector Functions by Glycosylation Engineering: Influence of Golgi Enzyme Localization Domain and Co-Expression of Heterologous $\beta$ 1,4-*N*-acetylglucosaminyltransferase III and Golgi $\alpha$ -mannosidase II

Claudia Ferrara,<sup>1,2</sup> Peter Brünker,<sup>1</sup> Tobias Suter,<sup>1</sup> Samuel Moser,<sup>1</sup> Ursula Püntener,<sup>1</sup> Pablo Umaña<sup>1</sup>

<sup>1</sup>GLYCART biotechnology AG, Wagistrasse 18, CH-8952 Schlieren, Switzerland; telephone: +41 044 755 61 61; fax: +41 044 755 61 60; e-mail: pablo.umana@glycart.com

<sup>2</sup>Institute of Biotechnology, ETH Zürich, Zürich, Switzerland

Received 21 April 2005; accepted 10 October 2005

Published online 24 January 2006 in Wiley InterScience (www.interscience.wiley.com). DOI: 10.1002/bit.20777

**Abstract:** The effector functions elicited by IgG antibodies strongly depend on the carbohydrate moiety linked to the Fc region of the protein. Therefore several approaches have been developed to rationally manipulate these glycans and improve the biological functions of the antibody. Overexpression of recombinant  $\beta$ 1,4-*N*-acetylglucosaminyltransferase III (GnT-III) in production cell lines leads to antibodies enriched in bisected oligosaccharides. Moreover, GnT-III overexpression leads to increases in non-fucosylated and hybrid oligosaccharides. Such antibody glycovariants have increased antibody-dependent cellular cytotoxicity (ADCC). To explore a further variable besides overexpression of GnT-III, we exchanged the localization domain of GnT-III with that of other Golgi-resident enzymes. Our results indicate that chimeric GnT-III can compete even more efficiently against the endogenous core  $\alpha$ 1,6-fucosyltransferase ( $\alpha$ 1,6-FucT) and Golgi  $\alpha$ -mannosidase II (ManII) leading to higher proportions of bisected non-fucosylated hybrid glycans ("Glyco-1" antibody). The co-expression of GnT-III and ManII led to a similar degree of non-fucosylation as that obtained for Glyco-1, but the majority of the oligosaccharides linked to this antibody ("Glyco-2") are of the complex type. These glycovariants feature strongly increased ADCC activity compared to the unmodified antibody, while Glyco-1 (hybrid-rich) features reduced complement-dependent cytotoxicity (CDC) compared to Glyco-2 or unmodified antibody. We show that apart from GnT-III overexpression, engineering of GnT-III localization is a versatile tool to modulate the biological activities of antibodies relevant for their therapeutic application.

© 2006 Wiley Periodicals, Inc.

Tobias Suter's present address is Section of Clinical Immunology, University Hospital, CH-8044 Zürich, Switzerland.

Correspondence to: P. Umaña

**Keywords:** glycosylation engineering; antibody-dependent cellular cytotoxicity (ADCC); complement-dependent cytotoxicity (CDC); therapeutic IgG; chimeric GnT-III

## INTRODUCTION

Antibodies of the IgG class have proven to be useful anti-cancer therapeutics (Carter, 2001). Their high specificity for an antigen, for targeting a cancerous cell, and the simultaneous recruitment of immune effector cells, by binding to Fc $\gamma$  receptors (Fc $\gamma$ Rs) via their Fc region, make them a powerful tool for immunotherapies. This linker function of the antibodies results in the elimination of the cancerous cell by cell-mediated effector functions, such as antibody-dependent cellular cytotoxicity (ADCC).

Many therapeutic antibodies depend on Fc-mediated effector functions and it was concluded that they require a higher *in vivo* efficacy to increase their potential as therapeutic drugs. The recruitment of Fc $\gamma$ R-expressing cells relies on an efficient binding to the Fc region of IgG (Dall'Ozzo et al., 2004). The affinity of this interaction can be improved by amino acid mutations of the polypeptide (Shields et al., 2001), which bear the risk of immunogenicity. On the other hand the presence of specific oligosaccharide structures linked to the Cy2 domain of the Fc fragment was reported to affect the biological activity of the antibody (Jefferis et al., 1998; Lively et al., 1995; Wright and Morrison, 1997) by influencing the interaction with Fc $\gamma$ Rs (Tao and Morrison, 1989). In this context, modification of the carbohydrate moiety associated to the Fc region of IgG has proven to be a successful approach to

enhance ADCC (Shields et al., 2002; Shinkawa et al., 2003; Umaña et al., 1999).

Recombinant DNA-based glyco-engineering for increased antibody effector function was first achieved by over-expression of heterologous  $\beta$ 1,4-*N*-acetylglucosaminyltransferase III (GnT-III), in antibody-producing cells (Umaña et al., 1999). GnT-III catalyzes the addition of a bisecting *N*-acetylglucosamine (GlcNAc) to *N*-linked oligosaccharides, as long as they have been modified by *N*-acetylglucosaminyltransferase I (GnT-I) and have not been modified by  $\beta$ 1,4 galactosyltransferase (GalT). Therefore, any non-galactosylated hybrid or complex oligosaccharide, whether fucosylated or not, can be modified by GnT-III. However, once GnT-III adds a bisecting GlcNAc to an oligosaccharide, other central reactions of the biosynthetic pathway such as core-fucosylation and conversion of hybrid to complex glycans are blocked (Schachter, 1986). This gives GnT-III a high degree of control over the glycosylation process in the Golgi apparatus. Overexpression of GnT-III in antibody-producing cells results in the formation of bisected, non-fucosylated oligosaccharides linked to the antibodies that mediate increased ADCC (Shields et al., 2002; Shinkawa et al., 2003; Umaña et al., 1999).

Previously, we have shown that the GnT-III expression level has a large impact on the relative levels of complex and hybrid, fucosylated, or non-fucosylated oligosaccharides (Umaña et al., 1999). Besides the expression level, the Golgi localization domain of GnT-III, which controls its spatial distribution relative to other enzymes, is another variable influencing the impact of GnT-III on the glycosylation pathway (Nilsson et al., 1996). Here we explore the localization variable by fusing the catalytic domain of GnT-III to the localization domain (cytoplasmic, transmembrane, and stem region) of other Golgi-resident enzymes of the *N*-glycosylation pathway. The resulting chimeric proteins were expressed in antibody-producing cells to engineer the antibody glycosylation pattern and the associated antibody effector functions.

## MATERIALS AND METHODS

### Construction of Expression Vectors

The DNA for the variable heavy (VH) and variable light (VL) chain of the anti-CD20 antibody was assembled by polymerase chain reaction (PCR) on the basis of the published sequence of the murine C2B8 antibody (Kobayashi et al., 1997; Reff et al., 1994). The IgG1 constant regions were amplified from a human leukocyte cDNA library (BD Biosciences, Allschwil, Switzerland). The rat *GnT-III* gene was amplified using specific primers from a rat kidney cDNA library (BD Biosciences) and a sequence coding for a C-terminal c-myc-epitope tag was added. The construction of the GnT-III-chimeric genes was performed by subsequent overlapping PCR reactions. The DNA fragments coding for the localization domains (cytoplasmic, transmembrane, and stem regions) of human GnT-I (102 amino acids), ManII

(100 amino acids), GnT-II (103 amino acids), and  $\alpha$ 1,6-fucosyltransferase ( $\alpha$ 1,6-FucT) (101 amino acids) were amplified from different material of human origin using the specific primers. The gene coding for Golgi  $\alpha$ -mannosidase II was amplified by PCR from human DNA using specific primers. The gene coding for the human *N*-acetylglucosaminyltransferase II (GnT-II) was amplified from pGnTII (RG002551, Invitrogen AG, Basel, Switzerland) by PCR using specific primers. The construction of the catalytically inactive GnT-III<sup>ManII</sup> (iGnT-III<sup>ManII</sup>) was performed as described (Ihara et al., 2002). The construction of two mutant GnT-III<sup>mutManII</sup> was accomplished by site-directed PCR mutagenesis, where the mutations R60Q, R73N, L79S, and E81S (GnT-III<sup>mutManII(4aa)</sup>) or R73N, L79S, and E81S (GnT-III<sup>mutManII(3aa)</sup>) were introduced into ManII (Nilsson et al., 1996). All expression vectors were combined with an origin of replication from the Epstein Barr virus (oriP) for episomal vector replication and maintenance in cells producing the Epstein Barr virus nuclear antigen (EBNA). Expression of the protein was confirmed by Western blot detection of GnT-III C-terminal c-myc tag.

For the generation of the Fc $\gamma$ RIIIa-expressing CHO cell line, an expression vector for Fc $\gamma$ RIIIa-Val158  $\alpha$ -chain,  $\gamma$ -chain, and the gene conferring puromycin resistance was constructed. The cDNAs coding for the Fc $\gamma$ RIIIa and the  $\gamma$ -chain were amplified from a healthy donor using specific primers. Genotyping for the Fc $\gamma$ RIIIa-Val/Phe158 and Fc $\gamma$ RIIc polymorphisms were performed as described (Koene et al., 1997; Metes et al., 2001).

### Production and Purification of Glyco-Engineered Anti-CD20 Antibodies in HEK293-EBNA Cells

HEK293-EBNA cells, a kind gift from Rene Fischer (Laboratory of Organic Chemistry, ETH Zürich, Switzerland), were grown as adherent monolayer cultures using DMEM culture medium supplemented with 10% FCS (Invitrogen AG) and were transfected essentially as described by Jordan et al. (1996). HEK293-EBNA cells were used as a transient expression system where the episomal replication of the expression vectors allowed high antibody titres and high expression levels of the glycosylation enzymes. Glyco-engineered antibodies were produced by co-transfection of the cells with two plasmids coding for antibody and chimeric GnT-III, at a ratio of 4:1, respectively, while for unmodified antibody the plasmids coding for the carbohydrate-modifying enzymes were omitted. For the combination of the chimeric GnT-III<sup>ManII</sup> and ManII, cells were co-transfected with three expression vectors coding for antibody, GnT-III<sup>ManII</sup> and ManII at a ratio of 3:1:1. The same ratio was used for the combination of GnT-III and ManII, and for that of ManII/GnT-III and GnT-II. At day 5 post-transfection, supernatant was harvested and monoclonal antibody purified using two sequential chromatographic steps as described (Umaña et al., 1999), followed by size exclusion chromatography (HiLoad<sup>TM</sup> 16/60 Superdex<sup>TM</sup> 200 column, Amersham Biosciences, Otelfingen, Switzerland).

### Oligosaccharide Analysis

Oligosaccharides were enzymatically released from the antibodies by *N*-Glycosidase digestion (PNGaseF, EC 3.5.1.52, QA-Bio, San Mateo, CA) at 0.05 mU/ $\mu$ g protein in 2 mM Tris, pH7 for 3 h at 37°C. A fraction of the PNGaseF-treated sample was subsequently digested with Endoglycosidase H (EndoH, EC 3.2.1.96, Roche, Basel, Switzerland) at 0.8 mU/ $\mu$ g protein and incubated for 3 h at 37°C. The released oligosaccharides were incubated in mild acid (150 mM acetic acid) prior to purification through a cation exchange resin (AG50W-X8 resin, hydrogen form, 100–200 mesh, BioRad, Reinach, Switzerland) packed into a micro-bio-spin chromatography column (BioRad) as described (Papac et al., 1998). The oligosaccharide samples were then analyzed with sDHB as matrix (Papac et al., 1998) using an Autoflex MALDI/TOF (Bruker Daltonics, Faellanden, Switzerland) in positive ion mode. For the assignment of an oligosaccharide structure to each peak, Endoglycosidase H was used due to its specificity. It digests most hybrid and high mannose, but not complex oligosaccharides. A refined oligosaccharide analysis was necessary to distinguish between bisected hybrid and complex (*m/z* 1,339 and 1,502) and their fucosylated versions (*m/z* 1,648 and 1,810), as both structures are not digested by EndoH. For this purpose, EndoH analysis was combined with *in vitro* galactosylation of the whole antibody performed as described (Raju et al., 2001). The aim was to distinguish between hybrid or complex oligosaccharides by making use of the fact that hybrid oligosaccharides can be galactosylated only at one terminal GlcNAc residue.

### Binding of Monomeric IgG1 Glycovariants to Natural Killer (NK) Cells and Fc $\gamma$ RIIIa-Expressing CHO Cell Line

Human NK cells were isolated from freshly isolated peripheral blood mononuclear cells (PBMC) applying a negative selection enriching for CD16- and CD56-positive cells (MACS system, Miltenyi Biotec GmbH, Bergisch Gladbach, Germany). The purity determined by CD56 expression was between 88% and 95%. Freshly isolated NK cells were incubated in PBS without calcium and magnesium ions ( $3 \times 10^5$  cells/mL) for 20 min at 37°C to remove NK cell-associated IgG. Cells were incubated at  $10^6$  cells/mL at different concentrations of anti-CD20 antibody (0, 0.1, 0.3, 1, 3, 10  $\mu$ g/mL) in PBS, 0.1% BSA. After two washes with PBS, 0.1% BSA antibody, binding was detected by incubating with 1:200 FITC-conjugated F(ab')<sub>2</sub> goat anti-human, F(ab')<sub>2</sub> specific IgG (Jackson ImmunoResearch, West Grove, PA), and anti-human CD56-PE (BD Biosciences, Shields et al., 2002). The anti-Fc $\gamma$ RIIIa 3G8 F(ab')<sub>2</sub> fragments (Ansell, Bayport, MN) were added at a concentration of 10  $\mu$ g/mL to compete binding of antibody glycovariants (3  $\mu$ g/mL). Fluorescence intensity was determined for CD56-positive cells on a FACSCalibur (BD Biosciences) and refers to the geometric mean measured for different antibody concentrations, from which the

geometric mean of cells incubated without primary antibody was subtracted.

CHO cells were transfected by electroporation (280 V, 950  $\mu$ F, 0.4 cm) with an expression vector coding for the Fc $\gamma$ RIIIa-Val158  $\alpha$ -chain and the  $\gamma$ -chain. Transfectants were selected by addition of 6  $\mu$ g/mL puromycin and stable clones were analyzed by FACS using 10  $\mu$ L FITC-conjugated anti-Fc $\gamma$ RIII 3G8 monoclonal antibody (BD Biosciences) for  $10^6$  cells. Binding of IgG1 to Fc $\gamma$ RIIIa-Val158-expressing CHO cells was performed analogously to the NK cell binding described above by omitting CD56-staining.

### Biological Activity of Anti-CD20 Monoclonal Antibody Glycovariants

#### Antibody-Dependent Cellular Cytotoxicity (ADCC) Assay

CD20-positive Raji cells (DMEM, 10% FCS, 1% Glutamax, Invitrogen AG) were labeled with the fluorescent dye Calcein AM for 20 min, according to the manufacturer's instruction (Molecular Probes, Leiden, The Netherlands). Antibodies were serially diluted in AIM-V (Invitrogen AG) and incubated with the target cells for 10 min at room temperature prior to the addition of effector cells. PBMCs were prepared from a donor heterozygous for Fc $\gamma$ RIIIa-Val/Phe158 and lacking Fc $\gamma$ RIIc expression using Histopaque-1077 (Sigma-Aldrich, Buchs, Switzerland) following the manufacturer's instructions. PBMCs were added to the wells at an effector to target ratio of 25:1. After 4 h incubation at 37°C, the cells were spun down, washed twice with PBS without calcium and magnesium ions, and lysed by addition of 50 mM borate, 0.1% Triton X-100 solution. The content of the wells was subsequently transferred to a 96-well black flat-bottomed plate. Retention of the fluorescent dye by intact target cells was measured with a fluorometer (485 nm excitation, 520 nm emission, FLUOstar Optima, BMG Labtechnologies, Inc., Durham, NC). Specific lysis was calculated relative to the total lysis control, resulting from incubating the target cells with 1% Triton X-100. Percentage of specific antibody-mediated cytotoxicity was calculated as follows:

$$\% \text{ cytotoxicity} = \frac{(\text{Fluorescence at concentration } x - \text{Fluorescence of spontaneous release})}{(\text{Fluorescence maximal release} - \text{Fluorescence spontaneous release})} \times 100$$

Each antibody dilution was analyzed in quadruplicate.

#### Complement-Dependent Cytotoxicity (CDC) Assay

CD20 positive human B lymphoblastoid SKW 6.4 cells (DMEM, 10% FCS, 1% Glutamax, Invitrogen AG) were incubated with increasing concentrations of antibody for 10 min at room temperature prior to the addition of normal human serum (NHS, Fc $\gamma$ RIIIa-Val158 and Fc $\gamma$ RIIc homozygous donor), prepared from the blood of healthy

volunteers, as source of complement. The blood was allowed to coagulate for 1 h at room temperature and then centrifuged at 1,200g for 20 min. The serum was diluted threefold with AIM-V and added to the wells to obtain a final concentration of 20% NHS. The assay plates were incubated for 2 h at 37°C. Maximal release was determined by incubating the cells in the presence of 1% Triton X-100. Relative cytotoxicity was determined using the AlamarBlue™ Assay (Serotec, Inc., Düsseldorf, Germany). Fluorescence was monitored on a fluorometer (540 nm excitation, 590 nm emission, FLUOstar Optima, BMG Labtechnologies, Inc.). Each antibody concentration was measured in quadruplicate.

#### Whole Blood B Cell Depletion Assay

Four hundred ninety microliters heparinized blood from a healthy FcγRIIIA-Val/Phe158 and FcγRIIC negative donor, were incubated at 37°C with 10 μL PBS or 50-fold concentrated antibody glycovariants (final concentrations of 0.1, 1, 10, 100, 1,000 ng/mL). After 24 h 50 μL blood were stained with a mixture of anti-CD19-PE, anti-CD3-FITC, and anti-CD45-CyChrome (BD Biosciences) for 15 min at room temperature. Before analysis, 500 μL PBS containing 2% FCS and 5 mM EDTA were added to the tubes. The CD3-FITC and CD19-PE fluorescence of the blood samples were flowcytometrically analyzed by gating on all CD45-positive cells. B cell-depletion was determined by plotting the ratio of CD19-positive B cells to CD3-positive T cells. Each antibody concentration was analyzed in triplicate.

## RESULTS

### Generation of Anti-CD20 Antibody Glycovariants Achieved by Co-Expression of GnT-III or Chimeric GnT-III Proteins

Modulation of antibody glycosylation was achieved by co-expression of the genes coding for antibody and chimeric GnT-III proteins in HEK293-EBNA cells. In the chimeric proteins, the localization domain of GnT-III was replaced with those of various other Golgi-resident enzymes of the N-linked glycosylation pathway (Fig. 1A). The oligosaccharide profiles obtained for the expressed antibodies indicate a significant impact of the enzyme localization on the outcome of the glycosylation process (Fig. 2A, Table I). The expression of GnT-III leads to antibodies with high proportions of bisected oligosaccharides, which can be fucosylated or non-fucosylated and of the complex or hybrid type. The assignment of these structures to the peaks was confirmed by digestion with EndoH, an enzyme digesting high mannose and most hybrid, but not complex oligosaccharides. Thus, peaks at *m/z* 1,664 and 1,810 shift to 1,460, and those at 1,826 and 1,972 to 1,622, confirming the increase in bisected, non-fucosylated hybrid (*m/z* 1,664 and 1,826) and their fucosylated versions (*m/z* 1,810 and 1,972) upon recombinant expression of GnT-III (Fig. 2A and B). The use of the localization domain of GnT-I,

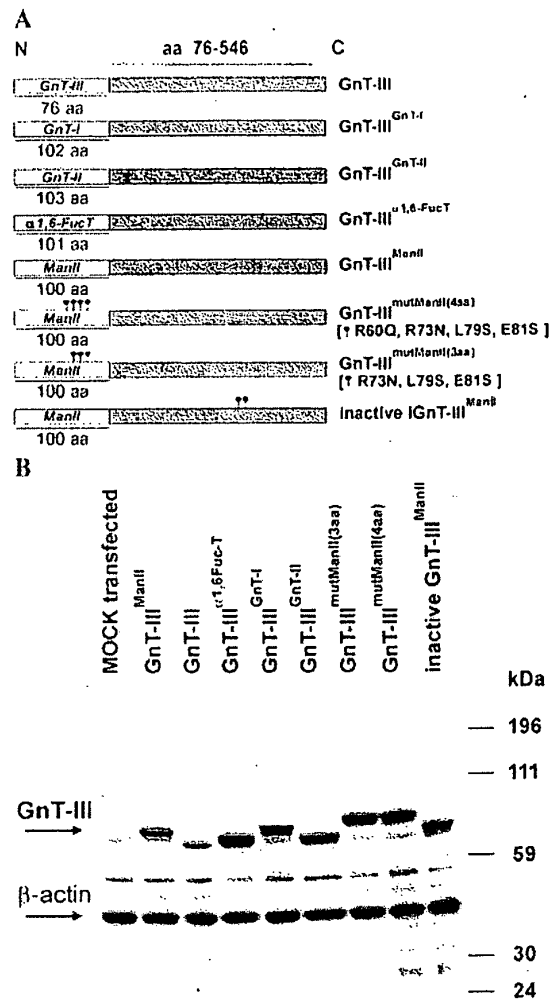


**Figure 1.** A: β1,4-N-acetylglucosaminyltransferase III (GnT-III) chimeric proteins. GnT-III with different localization domains were constructed by fusing the catalytic domain of GnT-III (gray) to the localization domain CTS (white), consisting of cytoplasmic tail, transmembrane domain, and stem region of other Golgi-resident enzymes. The length of the respective regions is indicated. In the last three constructs single amino acid substitutions are indicated. B: Western blot detection of GnT-III. Fifteen micrograms of cell lysates were separated on a 4–12% NU-PAGE gel (Invitrogen AG, Basel, Switzerland) and electroblotted to nitrocellulose membrane. Detection of GnT-III was performed via its C-terminal c-myc tag, while β-actin detection served as an internal control for the amount of loaded extracts (Abcam Ltd, Cambridge, UK).

α1,6-FucT, GnT-II, or ManII, instead of that of GnT-III results in a further increase in the proportion of bisected non-fucosylated hybrid oligosaccharides (mainly *m/z* 1,664) linked to the secreted antibody. Among these chimeric proteins, GnT-III fused to the localization domain of ManII (GnT-III<sup>ManII</sup>) leads to the highest content of these carbohydrates (Table I, Fig. 2A).





To assess if the localization domain of ManII itself and not the enzymatic activity of the catalytic domain of GnT-III accounts for any of the oligosaccharide modifications, a catalytically inactive iGnT-III<sup>ManII</sup> chimeric protein was prepared by replacing residues Asp321 and Asp323 of GnT-III by alanine residues (Ihara et al., 2002) (Fig. 1A). The spectrum of the glycans modified by the inactive chimeric protein indicates that the catalytic domain of GnT-III is mainly responsible for the oligosaccharide profile of the GnT-III<sup>ManII</sup>-modified antibody. The reason for the minor increase in the fraction of complex non-fucosylated oligosaccharides needs further investigation (Table I). To ascertain if a different expression level of the enzymes may account for the differences in the oligosaccharide patterns, the expression of GnT-III was quantified by Western blot analysis via a C-terminal c-myc tag (Fig. 1B). Both GnT-III<sup>ManII</sup> and GnT-III showed a slightly reduced expression compared to those of the other GnT-III chimeric proteins.

We also evaluated the hypothesis that the existence of relatively well organized functional glycosylation reaction subcompartments within the medial and trans Golgi cisternae may account for the glycosylation profiles derived from the chimeric GnT-III proteins. Given that pairs of charged amino acid residues in the stem regions of GnT-I and ManII have been postulated as critical for oligomer formation between enzymes (Nilsson et al., 1996), it was investigated if such a pairing could account for the GnT-III<sup>ManII</sup>-derived antibody glycosylation profile. Therefore the amino acid mutations R73N, L79S, and E81S (GnT-III<sup>mutManII(3aa)</sup>) or R60Q, R73N, L79S, and E81S (GnT-III<sup>mutManII(4aa)</sup>) were introduced into the stem region of ManII (Fig. 1A). Both mutants were expressed in similar amounts (Fig. 1B) and yielded antibody glycovariants featuring substantially reduced proportions of bisected non-fucosylated oligosaccharides compared to the non-mutated GnT-III<sup>ManII</sup> (Table I).

Either GnT-III<sup>ManII</sup> or GnT-III was co-expressed with ManII to shift the biosynthetic pathway from hybrid to complex bisected oligosaccharides (Fig. 2B). The expression of both enzyme combinations lead to the generation of antibodies characterized by high proportions of complex type glycans lacking core-fucosylation, with the majority being bisected (Table I). In vitro galactosylation analysis confirmed that peaks at *m/z* 1,339 and 1,502, which were not digested by EndoH, could be assigned to non-fucosylated complex glycan structures, with only minor contribution of bisected non-fucosylated hybrid structures (Fig. 2, Table I). GnT-III<sup>ManII</sup> was also co-expressed with GnT-II, an enzyme that similarly to ManII directs the glycosylation pathway toward the formation of complex type glycans. This led to the accumulation of high mannose structures and a low proportion of bisected non-fucosylated oligosaccharides (data not shown), and this enzyme combination was not investigated further.

Two glyco-engineered antibodies, namely those produced either by transient co-expression with GnT-III<sup>ManII</sup> (termed "Glyco-1," bearing mainly hybrid non-fucosylated bisected glycans) or with GnT-III<sup>ManII</sup> and ManII ("Glyco-2," bearing

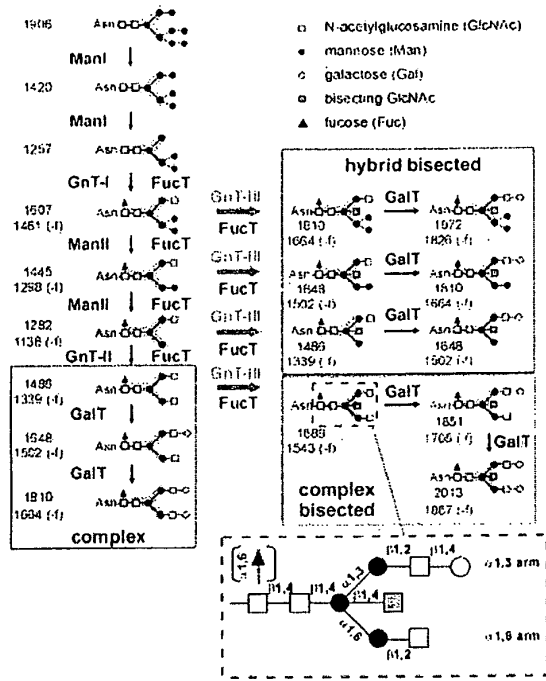


**Figure 3.** N-linked oligosaccharide biosynthetic pathway leading to complex or hybrid structures bearing a bisecting GlcNAc. The mass to charge (*m/z*) value of the sodium-associated oligosaccharide ion obtained by MALDI/TOF-MS analysis is indicated next to the corresponding oligosaccharide structure. The shaded monosaccharides belong to the core of the oligosaccharide, shared by all naturally occurring N-linked glycoforms, the presence of the other sugars is variable. A bisecting N-acetylglucosamine (GlcNAc; gray) can be  $\beta$ 1,4 linked to the core mannose by the enzyme GnT-III, as long as the oligosaccharide has been previously modified by GnT-I.  $\alpha$ 1,6-fucosyltransferase ( $\alpha$ 1,6-FucT) catalyses the addition of a fucose  $\alpha$ 1,6-linked to the GlcNAc residue attached to Asn, to any oligosaccharides that have not been modified by GnT-III or GalT. Complex and hybrid glycans structures are defined by the structure of the  $\alpha$ 1,6 arm. ManI, mannosidase I; GnT-I,  $\beta$ 1,2-N-acetylglucosaminyltransferase I; ManII, Golgi  $\alpha$ -mannosidase II; GnT-II,  $\beta$ 1,2-N-acetylglucosaminyltransferase II; GalT,  $\beta$ 1,4-galactosyltransferase (GalT); GnT-III,  $\beta$ 1,4-N-acetylglucosaminyltransferase III;  $\alpha$ 1,6-FucT, core  $\alpha$ 1,6-fucosyltransferase.

mainly complex non-fucosylated bisected glycans) were examined for their affinity for Fc $\gamma$ R3A and compared either to the unmodified antibody or to an antibody glycovariant produced under the same conditions by transient co-expression of GnT-III ("Glyco-0") (Fig. 3).

### Fc $\gamma$ R3A Binding of Glyco-0, Glyco-1, and Glyco-2 Anti-CD20 Monoclonal Antibodies

Binding of glyco-engineered antibodies to Fc $\gamma$ R3A was evaluated on peripheral human natural killer (NK) cells, which are known to be important mediators of ADCC, and to constitutively express Fc $\gamma$ R3A. Binding to NK cells was performed by incubating the antibody glycovariants with freshly isolated NK cells from a donor who was genotyped as heterozygous for Fc $\gamma$ R3A-Val/Phe158 (Koene et al., 1997).

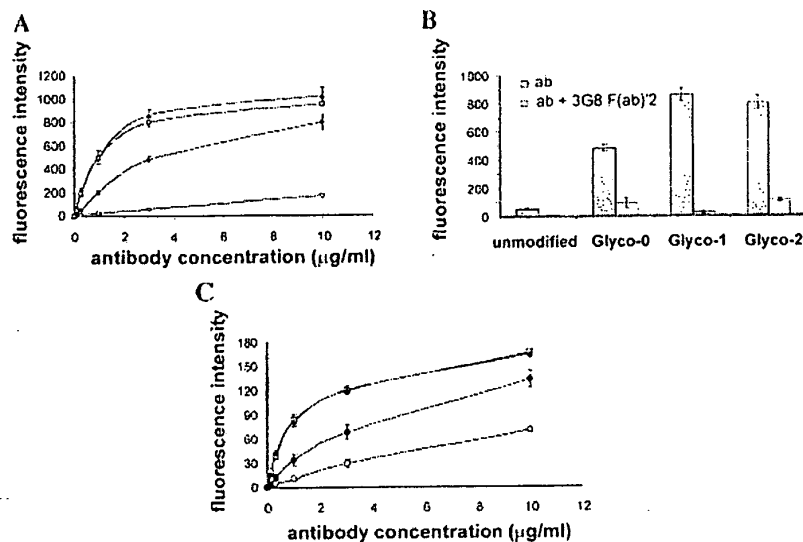


**Figure 4.** Fc $\gamma$ RIIIa binding of monomeric anti-CD20 glycovariant antibodies. Binding to purified NK cells from a donor heterozygous for Fc $\gamma$ RIIIA-Val/Phe 158 and negative for Fc $\gamma$ RIIC was evaluated. A: Binding of antibodies at concentrations ranging from 0.1 to 10  $\mu$ g/mL. B: Antibody binding (3  $\mu$ g/mL) to Fc $\gamma$ RIIIA was competed by addition of blocking anti-Fc $\gamma$ RIIIa 3G8 F(ab')<sub>2</sub> fragments (10  $\mu$ g/mL). C: Binding to a CHO cell line stably expressing human Fc $\gamma$ RIIIa-Val 158  $\alpha$ -chain and  $\gamma$ -chain was evaluated to confirm the dependence of antibody binding to Fc $\gamma$ RIIIa. All assays were performed in quadruplicate.  $\circ$ , unmodified;  $\bullet$ , Glyco-0;  $\blacktriangle$ , Glyco-1; and  $\square$ , Glyco-2 antibodies.

Both Glyco-1 and Glyco-2 bind with a considerably higher affinity to NK cells than unmodified antibody (Fig. 4A). Under the transient gene expression levels of this study, GnT-III co-expression leads to an antibody (Glyco-0) with a lower level of bisected non-fucosylated oligosaccharides with intermediate Fc $\gamma$ RIIIa binding affinity. Antibody binding to NK cells occurred exclusively via Fc $\gamma$ RIIIa as it could be outcompeted by the addition of blocking anti-Fc $\gamma$ RIIIa F(ab')<sub>2</sub> fragments (Fig. 4B). Similar results were obtained using a recombinant CHO cell line stably expressing the Fc $\gamma$ RIIIa-Val158  $\alpha$ -chain receptor (Fig. 4C).

#### Biological Activity of Glyco-1 and Glyco-2 Anti-CD20 Monoclonal Antibodies

In a next step we investigated whether increased Fc $\gamma$ RIIIa binding correlates with an improvement in the biological activity of the glyco-engineered antibodies, which are characterized by bisected non-fucosylated oligosaccharides. Both glycovariants mediate an enhanced ADCC against CD20-positive Raji cells, independently of the Fc-linked glycans being of complex or hybrid type (Fig. 5A).

Glyco-1 and Glyco-2 were also evaluated for complement-dependent cytotoxicity (CDC) against CD20-positive tumor cells SKW6.4 in the presence of human serum (Fig. 5B). Glyco-2, bearing complex oligosaccharides, performs similarly to the unmodified antibody in CDC. For Glyco-1, on the contrary, a reduction in CDC is observed, correlating with high proportion of hybrid oligosaccharides that are characteristic for this glycovariant.

To assess whether both ADCC and CDC can contribute to the elimination of target cells, we evaluated these glyco-engineered antibodies for B cell depletion in a whole blood assay (Fig. 5C). Glyco-1 and Glyco-2 anti-CD20 variants were over 100-fold more potent than unmodified anti-CD20 in depleting B cells, while no significant difference could be observed between the two glycovariants, indicating a minor contribution of CDC.

## DISCUSSION

### Chimeric GnT-III Proteins

GnT-III is an ideal enzyme to manipulate the *N*-glycosylation of expressed proteins (glyco-engineering), as it exerts a large degree of control over the glycosylation process by blocking the action of  $\alpha$ 1,6-FucT, ManII, and GnT-II (Schachter, 1986; Umaña et al., 1999). While natural human IgG in serum contains low percentages of bisected oligosaccharides in the Fc region (Wormald et al., 1997), up to 40% bisected glycans were observed for antibodies produced in YB2/0 rat myeloma cell line (Lifely et al., 1995). In the present study the impact of the localization domain of GnT-III on the antibody glycosylation profile was evaluated. We obtained antibodies with engineered carbohydrate moieties by co-expression of chimeric GnT-III proteins, composed of the catalytic domain of GnT-III fused to the localization domain of GnT-I,  $\alpha$ 1,6-FucT, GnT-II, or ManII (Fig. 1A). As for the GnT-III-derived antibody, the resulting glycovariants feature a bisecting *N*-acetylglucosamine (GlcNAc) residue on

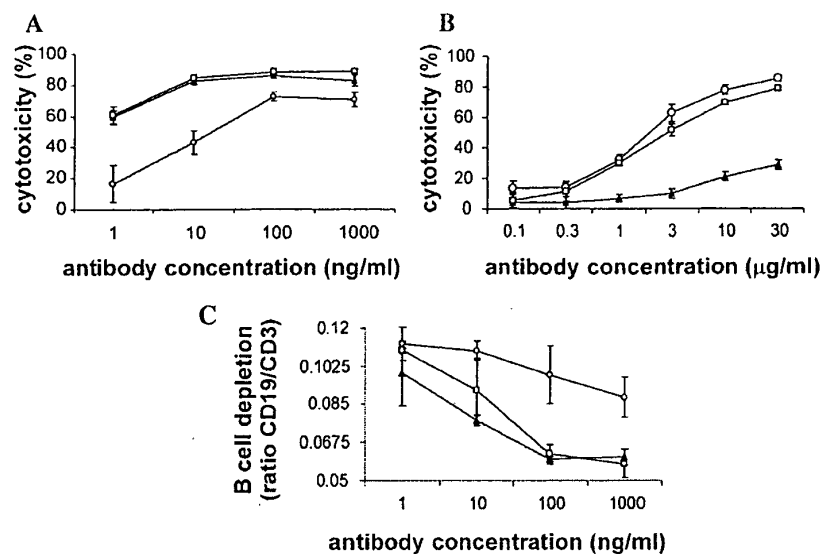


**Figure 5.** Biological activity assays of anti-CD20 antibody glycovariants. A: ADCC using PBMcs (FcγRIIIA-Val/Phe158, FcγRIIC negative donor) as effectors and human lymphoma Raji cells as targets. B: CDC against B lymphoblastoid SKW6.4 cells in the presence of human serum as a source of complement. C: B-cell depletion in whole blood (FcγRIIIA-Val/Phe158, FcγRIIC negative donor), which was calculated from the ratio of CD19-positive B cells to CD3-positive T cells as measured by FACS analysis. ○, unmodified; ▲, Glyco-1; and □, Glyco-2 antibodies.

almost all oligosaccharide structures, indicating that all chimeric GnT-III proteins were active (Table I, Fig. 2A). Relative to GnT-III-modified antibody, use of chimeric GnT-III led to an increase in the fractions of bisected non-fucosylated, and of bisected hybrid oligosaccharides, indicating a more efficient competition of the chimeric GnT-III against  $\alpha$ 1,6-FucT and ManII (Fig. 2A).

Among the chimeric GnT-III proteins, GnT-III<sup>ManII</sup> is the most efficient in the competition against the above-mentioned enzymes, leading to the antibody glycovariant with the highest proportion of bisected non-fucosylated hybrid oligosaccharides. Since the expression level of GnT-III<sup>ManII</sup> was not higher than for the other chimeric proteins or GnT-III, we propose that the higher efficiency of GnT-III<sup>ManII</sup> results either from a different distribution in Golgi compartments or from a different functional organization of enzymes within a compartment. This allows GnT-III to act immediately after GnT-I in the biosynthetic process, leading to higher levels of bisected, non-fucosylated hybrid oligosaccharides (Table I) relative to the other chimeric GnT-III proteins.

#### Influence of the ManII Stem Region Residues on the Glycosylation Pattern

The higher efficiency of the chimeric protein GnT-III<sup>GnT-I</sup>, compared to the unmodified GnT-III, for the synthesis of bisected hybrid and bisected non-fucosylated oligosaccharides can be explained by an earlier Golgi distribution, in the *cis*-to-*trans* direction of glycoprotein substrate transport, of GnT-I relative to GnT-III. The fine Golgi distributions of

GnT-I and ManII have been determined previously by quantitative immunoelectron microscopy (Rabouille et al., 1995). Both enzymes co-distribute along the Golgi, being localized mainly in the medial and *trans* cisternae (Dunphy et al., 1985; Rabouille et al., 1995; Velasco et al., 1993). The spatial distributions of  $\alpha$ 1,6-FucT and GnT-II have not yet been determined quantitatively, but rat GnT-III has been found predominantly in the *trans* Golgi cisternae (Umaña, 1998). This, however, does not explain why the chimeric GnT-III<sup>ManII</sup> is significantly more efficient than GnT-III<sup>GnT-I</sup> at synthesizing bisected, hybrid, and bisected, non-fucosylated oligosaccharides, since both GnT-I and ManII have identical spatial distributions along the Golgi subcompartments. Additionally, the slightly lower expression level of GnT-III<sup>ManII</sup> compared to those of the other chimeric GnT-III proteins, indicates that the antibody glycoprofile is not a result of an increased enzyme expression level (Fig. 1B), but a consequence of a more efficient processing of GnT-I-modified oligosaccharides, denoted here as "functional pairing" of GnT-III<sup>ManII</sup> with GnT-I.

To assess if this functional pairing relies on a physical interaction between the two enzymes, we evaluated GnT-III<sup>ManII</sup> mutants with amino acid substitutions in the localization domain of ManII which were reported to be critical determinants for the formation of hetero-oligomers of GnT-I and ManII (Nilsson et al., 1996). Although it has been suggested that these residues are not essential for incorporation into high molecular weight complexes of Golgi enzymes or even for Golgi localization (Opat et al., 2000), it is possible that they are involved in a finer pairing of the catalytic

domains during oligosaccharide biosynthesis. We observed a significant reduction in bisected non-fucosylated hybrid oligosaccharides with these mutants (Table I). Both GnT-III<sup>mutManII</sup> mutants were expressed at comparable levels as GnT-III<sup>ManII</sup>, excluding the expression level of the latter as being responsible for higher proportions of bisected non-fucosylated glycans (Fig. 1B). However, the exchanged residues do not seem to be the sole determinant of the resulting oligosaccharide product distribution, suggesting either additional contributions of the rest of the stem or catalytic regions to functional enzyme pairing, or an enrichment of these enzymes in subcompartments caused by different mechanisms. Evidence for pairing may possibly be obtained via co-immunoprecipitation and electron microscopy experiments. Another possible explanation may be a conformational change caused by the modified stem region, which may lead to a catalytic domain with increased activity. Our data suggest that by virtue of the ManII localization domain, a physical and/or a functional pairing takes place between the catalytic domains of the endogenous GnT-I and the recombinant GnT-III<sup>ManII</sup> chimeric protein.

#### Co-Expression of GnT-III<sup>ManII</sup> and ManII

With the described approach, we are able to modulate the glycosylation pattern of antibodies from fucosylated complex glycans to bisected non-fucosylated hybrid oligosaccharides by overexpressing GnT-III<sup>ManII</sup>. The co-expression of GnT-III<sup>ManII</sup> and ManII, or of GnT-III and ManII led to the formation of bisected non-fucosylated glycans of the complex type. ManII overexpression redirects the biosynthetic pathway causing the product shift from hybrid to complex carbohydrates (Fig. 2B, Table I). Although equally high levels of bisected non-fucosylated complex oligosaccharides can be synthesized by high level expression of GnT-III, the results presented here show that GnT-III<sup>ManII</sup> is more efficient at adding a bisecting GlcNAc residue to the GnT-I-processed oligosaccharides prior to the reactions catalyzed by ManII, GnT-II, and  $\alpha$ 1,6-FucT.

Similarly to ManII, GnT-II was co-expressed with GnT-III<sup>ManII</sup> with the intent of forming complex type glycans linked to the antibody. The resulting glycovariant had lower proportions of bisected non-fucosylated (37%) and complex (22%) glycans compared to the GnT-III<sup>ManII</sup>/ManII-derived antibody (data not shown). Moreover, a significant fraction of high mannose oligosaccharides characterized this glycovariant, suggesting an influence of the overexpression of GnT-II on the maturation process of high mannose glycans. Under these conditions, the enzyme seems to inhibit the GnT-I-mediated reaction (Table I) by unknown mechanisms. A similar phenomenon was reported for overexpression of  $\beta$ 1,4-GalT, which led to an enrichment of high mannose oligosaccharides on recombinantly co-expressed IFN- $\gamma$  (Fukuta et al., 2001). Although the cellular localization of GnT-II is yet to be discovered, high molecular weight complexes between GnT-I and GnT-II have been found in

Golgi extracts of mammalian cells (Opat et al., 2000). The formation of such complexes might be disturbed by GnT-II overexpression.

We could show that the formation of a desired carbohydrate profile can be achieved by the combination and overexpression of enzymes, although not all the potential enzymes are suitable for this purpose, indicating that the glycosylation process is governed by a well-balanced system of enzymes that needs further elucidation.

#### Biological Activity of Glyco-Engineered Antibodies

A high affinity to Fc $\gamma$ RIIIa is important for ADCC, which is mediated by unconjugated therapeutic antibodies in humans. This was deduced from pioneering pharmacogenomic studies evaluating the impact of the Fc $\gamma$ RIIIa polymorphisms on the activity of rituximab in lymphoma patients (Cartron et al., 2002). In that study, the objective response rates at 2/12 months were 100/90% for homozygous Fc $\gamma$ RIIIa-Val158 and 67/51% for Fc $\gamma$ RIIIa-Phe158 carriers, respectively. The superior response of the former seems to be the result of a significantly increased binding of the antibody to Fc $\gamma$ RIIIa-Val158 compared to Fc $\gamma$ RIIIa-Phe158 (Koene et al., 1997).

Glyco-1, featuring mainly bisected non-fucosylated hybrid glycans, and Glyco-2, bearing mainly bisected non-fucosylated complex carbohydrates, were examined for their binding to Fc $\gamma$ RIIIa and their reactivity in cytotoxicity assays. Both Glyco-1 and Glyco-2 have an increased affinity for Fc $\gamma$ RIIIa, which correlates with high proportions of bisected non-fucosylated oligosaccharides but seems independent of the glycans being of the hybrid or complex type. It has been reported that the absence of core fucose is responsible for an increased affinity to Fc $\gamma$ RIIIa (Shields et al., 2002). Moreover, the absence of core fucose but not the presence of galactose or bisecting GlcNAc was reported to be responsible for increased ADCC under the tested conditions (Shinkawa et al., 2003).

Both Glyco-1 and Glyco-2 mediate an increased ADCC to a similar extent compared to the unmodified antibody, but feature a different reactivity in CDC assays. While Glyco-2 acts similarly to the unmodified antibody, Glyco-1 displays a reduced CDC, suggesting a significant influence of the glycan type (complex vs. hybrid). The main difference between Glyco-1 and Glyco-2 is the structure of their carbohydrate  $\alpha$ 1,6-arm. In contrast to Glyco-1, carrying hybrid glycans with mannose residues  $\alpha$ 1,3- and  $\alpha$ 1,6-linked to the  $\alpha$ -6 arm. Glyco-2 and unmodified antibodies have mainly  $\beta$ 1,2-linked GlcNAc residues at this position (complex glycans), which may be followed by galactose. This carbohydrate arm is in close contact with the IgG-Cy2 domain polypeptide and may therefore influence domain conformations required for binding to C1q (Duncan and Winter, 1988; Huber et al., 1976; Idusogie et al., 2000). An even larger reduction in CDC was reported for antibodies featuring only high mannose oligosaccharides (Wright and Morrison, 1994).

The glyco-engineered antibodies also performed better than their unmodified counterparts in the depletion of B-cells in a whole blood assay, where both ADCC and CDC contribute to the elimination of target cells. The reduction in CDC activity, observed for Glyco-I, does not seem to affect our model of B-cell depletion in whole blood, suggesting that ADCC is the predominant mechanism in this assay. Moreover as first-dose-related side effects in vivo have been recently attributed to complement activation (van der Kolk et al., 2001; Winkler et al., 1999), Glyco-I may provide a tool to prevent these problems.

We could therefore demonstrate that apart from modulating glycosyltransferase expression levels, engineering of Golgi localization domains can also be exploited for the production of tailored glyco-engineered therapeutic antibodies with unique combinations of biological activities.

We would like to thank Rene Fischer (Laboratory of Organic Chemistry, ETH Zürich, Switzerland) for providing the HEK293-EBNA cell line and Patrik Buholzer, Christian Gerdes, Samuel Haldane, Saskia Karg, Julia Maria Martinez, Peter Sondermann, and Manuel Späni for assistance and useful comments on this manuscript.

## References

- Carter P. 2001. Improving the efficacy of antibody-based cancer therapies. *Nat Rev Cancer* 1:118–129.
- Cartron G, Dacheux L, Salles G, Solal-Celigny P, Bardos P, Colombat P, Watier H. 2002. Therapeutic activity of humanized anti-CD20 monoclonal antibody and polymorphism in IgG Fc receptor FcγRIIIa gene. *Blood* 99:754–758.
- Dall'Ozzo S, Tartas S, Paintaud G, Cartron G, Colombat P, Bardos P, Watier H, Thibault G. 2004. Rituximab-dependent cytotoxicity by natural killer cells: Influence of FCGR3A polymorphism on the concentration-effect relationship. *Cancer Res* 64:4664–4669.
- Duncan AR, Winter G. 1988. The binding site for C1q on IgG. *Nature* 332(6166):738–740.
- Dunphy WG, Brands R, Rothman JE. 1985. Attachment of terminal N-acetylglucosamine to asparagine-linked oligosaccharides occurs in central cisternae of the Golgi stack. *Cell* 40(2):463–472.
- Fukuta K, Abe R, Yokomatsu T, Minowa MT, Takeuchi M, Asanagi M, Makino T. 2001. The widespread effect of beta 1,4-galactosyltransferase on N-glycan processing. *Arch Biochem Biophys* 392(1):79–86.
- Hübler R, Deisenhofer J, Colman PM, Matsushima M, Palm W. 1976. Crystallographic structure studies of an IgG molecule and an Fc fragment. *Nature* 264(5585):415–420.
- Idusogie EE, Presta LG, Gazzano-Santoro H, Totpal K, Wong PY, Ultsch M, Meng YG, Mulkern MG. 2000. Mapping of the C1q binding site on rituxan, a chimeric antibody with a human IgG1 Fc. *J Immunol* 164(8):4178–4184.
- Ihara H, Ikeda Y, Koyota S, Endo T, Honke K, Taniguchi N. 2002. A catalytically inactive beta 1,4-N-acetylglucosaminyltransferase III (GnT-III) behaves as a dominant negative GnT-III inhibitor. *Eur J Biochem* 269:193–201.
- Jefferis R, Lund J, Pound JD. 1998. IgG-Fc-mediated effector functions: Molecular definition of interaction sites for effector ligands and the role of glycosylation. *Immunol Rev* 163:59–76.
- Jordan M, Schallhorn A, Wunn FM. 1996. Transfecting mammalian cells: Optimization of critical parameters affecting calcium-phosphate precipitate formation. *Nucleic Acids Res* 24:596–601.
- Kobayashi N, Soderlind E, Borrebaeck CA. 1997. Analysis of assembly of synthetic antibody fragments: Expression of functional scFv with predefined specificity. *Biotechniques* 23:500–503.
- Koene HR, Kleijer M, Algra J, Roos D, von dem Borne AE, de Haas M. 1997. Fc gammaRIIIa-158V/F polymorphism influences the binding of IgG by natural killer cell Fc gammaRIIIa, independently of the Fc gammaRIIIa-48L/R/H phenotype. *Blood* 90:1109–1114.
- Lifely MR, Hale C, Boyce S, Keen MJ, Phillips J. 1995. Glycosylation and biological activity of CAMPATH-1H expressed in different cell lines and grown under different culture conditions. *J Glycobiol* 5:813–822.
- Metes D, Gambotto AA, Nellis J, Ruscini A, Stewart-Akers AM, Morel PA, Rao AS. 2001. Identification of the CD32/FcγRIIc-Q13/STP13 polymorphism using an allele-specific restriction enzyme digestion assay. *J Immunol Methods* 258:85–95.
- Nilsson T, Rabouille C, Hui N, Watson R, Warren G. 1996. The role of the membrane-spanning domain and stalk region of N-acetylglucosaminyltransferase I in retention, kin recognition and structural maintenance of the Golgi apparatus in HeLa cells. *J Cell Sci* 109(Pt 7):1975–1989.
- Opat AS, Houghton F, Gleeson PA. 2000. Medial Golgi but not late Golgi glycosyltransferases exist as high molecular weight complexes. Role of luminal domain in complex formation and localization. *J Biol Chem* 275:11836–11845.
- Papac DJ, Briggs JB, Chin ET, Jones AJ. 1998. A high-throughput microscale method to release N-linked oligosaccharides from glycoproteins for matrix-assisted laser desorption/ionization time-of-flight mass spectrometric analysis. *Glycobiology* 8:445–454.
- Rabouille C, Hui N, Hunte F, Kieckbusch R, Berger EG, Warren G, Nilsson T. 1995. Mapping the distribution of Golgi enzymes involved in the construction of complex oligosaccharides. *J Cell Sci* 108(Pt 4):1617–1627.
- Raju TS, Briggs JB, Chamow SM, Winkler ME, Jones AJ. 2001. Glycoengineering of therapeutic glycoproteins: In vitro galactosylation and sialylation of glycoproteins with terminal N-acetylglucosamine and galactose residues. *Biochemistry* 40:8868–8876.
- Reff ME, Camer K, Chambers KS, Chinn PC, Leonard JE, Raab R, Newman RA, Hanna N, Anderson DR. 1994. Depletion of B cells in vivo by a chimeric mouse human monoclonal antibody to CD20. *Blood* 83:435–445.
- Schachter H. 1986. Biosynthetic controls that determine the branching and microheterogeneity of protein-bound oligosaccharides. *Biochem Cell Biol* 64:163–181.
- Shields RL, Namenuk AK, Hong K, Meng YG, Rae J, Briggs J, Xie D, Lai J, Stadlen A, Li B, Fox JA, Presta LG. 2001. High resolution mapping of the binding site on human IgG1 for Fc gamma RI, Fc gamma RII, Fc gamma RIII, and FcRn and design of IgG1 variants with improved binding to the Fc gamma R. *J Biol Chem* 276(9):6591–6604.
- Shields RL, Lai J, Keck R, O'Connell LY, Hong K, Meng YG, Weikert SH, Presta LG. 2002. Lack of fucose on human IgG1 N-linked oligosaccharide improves binding to human FcγRIII and antibody-dependent cellular cytotoxicity. *J Biol Chem* 277:26733–26740.
- Shinkawa T, Nakamura K, Yamane N, Shoji-Hosaka E, Kanda Y, Sankurata M, Uchida K, Anazawa H, Satoh M, Yamasaki M, Hanai N, Shitara K. 2003. The absence of fucose but not the presence of galactose or bisecting N-acetylglucosamine of human IgG1 complex-type oligosaccharides shows the critical role of enhancing antibody-dependent cellular cytotoxicity. *J Biol Chem* 278:3466–3473.
- Tao MH, Morrison SL. 1989. Studies of aglycosylated chimeric mouse-human IgG. Role of carbohydrate in the structure and effector functions mediated by the human IgG constant region. *J Immunol* 143:2595–2601.
- Umaña P. 1998. Engineering of protein glycosylation in chinese hamster ovary cells. Pasadena, CA: California Institute of Technology. 155p.
- Umaña P, Jean-Mairet J, Moudry R, Amstutz H, Bailey JE. 1999. Engineered glycoforms of an antineuroblastoma IgG1 with optimized antibody-dependent cellular cytotoxic activity. *Nat Biotechnol* 17:176–180.

- van der Kolk LE, Grillo-Lopez AJ, Baars JW, Hack CE, van Oers MH. 2001. Complement activation plays a key role in the side-effects of rituximab treatment. *Br J Haematol* 115:807-811.
- Velasco A, Hendricks L, Moremen KW, Tulsiani DR, Touster O, Farquhar MG. 1993. Cell type-dependent variations in the subcellular distribution of alpha-mannosidase I and II. *J Cell Biol* 122(1):39-51.
- Winkler U, Jensen M, Manzke O, Schulz H, Diehl V, Engert A. 1999. Cytokine-release syndrome in patients with B-cell chronic lymphocytic leukemia and high lymphocyte counts after treatment with an anti-CD20 monoclonal antibody (rituximab, IDEC-C2B8). *Blood* 94:2217-2224.
- Wormald MR, Rudd PM, Harvey DJ, Chang SC, Scragg IG, Dwek RA. 1997. Variations in oligosaccharide-protein interactions in immunoglobulin G determine the site-specific glycosylation profiles and modulate the dynamic motion of the Fc oligosaccharides. *Biochemistry* 36(6):1370-1380.
- Wright A, Morrison SL. 1994. Effect of altered CH2-associated carbohydrate structure on the functional properties and in vivo fate of chimeric mouse-human immunoglobulin G1. *J Exp Med* 180(3):1087-1096.
- Wright A, Morrison SL. 1997. Effect of glycosylation on antibody function: Implications for genetic engineering. *Trends Biotechnol* 15:26-32.

# **Attachment P**

**Obinutuzumab BLA,  
Section 3.4.2, redacted**





[REDACTED]

[REDACTED]	[REDACTED]	[REDACTED]	[REDACTED]
[REDACTED]	[REDACTED]	[REDACTED]	[REDACTED]
[REDACTED]	[REDACTED]	[REDACTED]	[REDACTED]
[REDACTED]	[REDACTED]	[REDACTED]	[REDACTED]
[REDACTED]	[REDACTED]	[REDACTED]	[REDACTED]

[REDACTED]

**3.4.2** [REDACTED]

The addition of a bisecting N-acetylglucosamine (bGlcNAc) by overexpression of GnTIII in obinutuzumab antagonizes the addition of core fucose by core  $\alpha$ -1,6-fucosyltransferase ( $\alpha$ -1,6-FucT), and thus, leads to an increase in core afucosylation and enhancement of ADCC bioactivity [REDACTED]

[REDACTED]

[REDACTED]

[REDACTED]	[REDACTED]	[REDACTED]	[REDACTED]
[REDACTED]	[REDACTED]	[REDACTED]	[REDACTED]
[REDACTED]	[REDACTED]	[REDACTED]	[REDACTED]
[REDACTED]	[REDACTED]	[REDACTED]	[REDACTED]
[REDACTED]	[REDACTED]	[REDACTED]	[REDACTED]

[REDACTED]

[REDACTED]

[REDACTED]

# **Attachment Q**

**Nagelkerken *et al.*, *J Immunol.*,  
2004, 173:993-999**



## FcR Interactions Do Not Play a Major Role in Inhibition of Experimental Autoimmune Encephalomyelitis by Anti-CD154 Monoclonal Antibodies

This information is current as of December 10, 2013.

Lex Nagelkerken, Inge Haspels, Wouter van Rijs, Bep Blauw, Janine L. Ferrant, Donna M. Hess, Ellen A. Garber, Fred R. Taylor and Linda C. Burkly

*J Immunol* 2004; 173:993-999; ;  
<http://www.jimmunol.org/content/173/2/993>

- 
- References** This article cites 37 articles, 18 of which you can access for free at:  
<http://www.jimmunol.org/content/173/2/993.full#ref-list-1>
- Subscriptions** Information about subscribing to *The Journal of Immunology* is online at:  
<http://jimmunol.org/subscriptions>
- Permissions** Submit copyright permission requests at:  
<http://www.aai.org/ji/copyright.html>
- Email Alerts** Receive free email-alerts when new articles cite this article. Sign up at:  
<http://jimmunol.org/cgi/alerts/etoc>

---

*The Journal of Immunology* is published twice each month by  
The American Association of Immunologists, Inc.,  
9650 Rockville Pike, Bethesda, MD 20814-3994.  
Copyright © 2004 by The American Association of  
Immunologists All rights reserved.  
Print ISSN: 0022-1767 Online ISSN: 1550-6606.



## FcR Interactions Do Not Play a Major Role in Inhibition of Experimental Autoimmune Encephalomyelitis by Anti-CD154 Monoclonal Antibodies

Lex Nagelkerken,<sup>1\*</sup> Inge Haspels,<sup>\*</sup> Wouter van Rijs,<sup>\*</sup> Bep Blauw,<sup>\*</sup> Janine L. Ferrant,<sup>†</sup> Donna M. Hess,<sup>†</sup> Ellen A. Garber,<sup>†</sup> Fred R. Taylor,<sup>†</sup> and Linda C. Burkly<sup>†</sup>

It has been demonstrated that anti-CD154 mAb treatment effectively inhibits the development of experimental autoimmune encephalomyelitis (EAE). However, although it appears to prevent the induction of Th1 cells and reactivation of encephalitogenic T cells within the CNS, little information is available regarding the involvement of alternative mechanisms, nor has the contribution of Fc effector mechanisms in this context been addressed. By contrast, efficacy of anti-CD154 mAbs in models of allotransplantation has been reported to involve long-term unresponsiveness, potentially via activation of T regulatory cells, and recently was reported to depend on Fc-dependent functions, such as activated T cell depletion through Fc $\gamma$ R or complement. In this study we demonstrate that anti-CD154 mAb treatment inhibits EAE development in SJL mice without apparent long-term unresponsiveness or active suppression of disease. To address whether the mechanism of inhibition of EAE by anti-CD154 mAb depends on its Fc effector interactions, we compared an anti-CD154 mAb with its aglycosyl counterpart with severely impaired Fc $\gamma$ R binding and reduced complement binding activity with regard to their ability to inhibit clinical signs of EAE and report that both forms of the Ab are similarly protective. This observation was largely confirmed by the extent of leukocyte infiltration of the CNS; however, mice treated with the aglycosyl form may display slightly more proteolipid protein 139–151-specific immune reactivity. It is concluded that FcR interactions do not play a major role in the protective effect of anti-CD154 mAb in the context of EAE, though they may contribute to the full abrogation of peripheral peptide-specific lymphocyte responses. *The Journal of Immunology*, 2004, 173: 993–999.

**T**he interaction between CD40 and CD154 plays a crucial role in the induction of B and T cell responses (1). It is well established that interactions between CD40 on APCs and CD154 on T cells results in the polarization of Th1 responses (2, 3). This is mainly due to the induction of IL-12 in the APC (3, 4).

Several studies have demonstrated that anti-CD154 mAbs inhibit such responses and are capable of blocking experimental diseases that are Th1-mediated. In the classical model of experimental autoimmune encephalomyelitis (EAE)<sup>2</sup> that can be induced in SJL mice by immunization with the dominant encephalitogenic epitope of proteolipid protein (PLP), i.e., PLP<sub>139–151</sub>, anti-CD154 was effective in inhibiting disease when administered during the induction phase (5) and this might be attributed to inhibition of T cell priming. However, it was also demonstrated that such Abs are effective in an adoptive transfer model of EAE, which suggests that CD40-CD154 interactions may play a role in the reactivation of encephalitogenic T cells in the CNS by microglia or that anti-CD154 blocks Th1 effector functions (6, 7). This hypothesis was

supported by the notion that human microglia are dependent on CD40-CD154 interactions for the induction of IL-12 (8), and by the diminished severity of disease in CD40-deficient mice as compared with wild-type mice after adoptive transfer of encephalitogenic T cells in one (9) but not another study (10). Anti-CD154 mAb treatment also has been shown to facilitate long-term graft survival in rodents (11) and non-human primates (12) and it has been suggested that this result may be due to the activation of regulatory T cells (13, 14). In addition, it is uncertain in this or other disease settings whether anti-CD154 mAb mediates part of its effect by depletion of CD154-positive targets via Fc-dependent mechanisms such as Ab-dependent cellular cytotoxicity and activation of the complement cascade. Interestingly, it was recently demonstrated that the induction of tolerance by anti-CD154 mAb in a murine model of islet cell transplantation depends on complement activation (15), and efficacy of anti-CD154 mAbs in a model of skin allotransplantation requires FcR or complement-mediated T cell depletion (16). FcRs may also enhance binding of an anti-CD154 mAb to its target by the formation of a scaffold of the mAb on the surface of FcR bearing cells or through the effects of FcR interactions on its localization in vivo.

We wished to determine whether the inhibition of EAE by anti-CD154 mAb was associated with long-term unresponsiveness or an active suppression mechanism and to what extent it was mediated by a mechanism that is dependent on Fc-dependent interactions of the Ab. To assess the latter, we used a form of anti-CD154 mAb in which Fc function is impaired by the elimination of the conserved N-linked glycosylation site in the CH2 domain of the Fc dimer. It is well established by in vitro studies that removal of the CH2 glycans alters the Fc structure such that Ab binding to FcRs and the complement protein C1q are significantly reduced (17–21).

<sup>1</sup>Division of Immunological and Infectious Diseases, The Netherlands Organization for Applied Scientific Research (TNO), Prevention and Health, Leiden, The Netherlands; and <sup>†</sup>Biogen, Cambridge, MA 02142

Received for publication July 31, 2003. Accepted for publication May 12, 2004.

The costs of publication of this article were defrayed in part by the payment of page charges. This article must therefore be hereby marked *advertisement* in accordance with 18 U.S.C. Section 1734 solely to indicate this fact.

<sup>1</sup> Address correspondence and reprint requests to Dr. Lex Nagelkerken, Division of Immunological and Infectious Diseases, The Netherlands Organization for Applied Scientific Research TNO, Prevention and Health, P.O. Box 2215, 2301 CE Leiden, The Netherlands. E-mail address: am.nagelkerken@pg.tno.nl

<sup>2</sup> Abbreviations used in this paper: EAE, experimental autoimmune encephalomyelitis; PLP, proteolipid protein; LSD, least significant difference; H chain, heavy chain; L chain, light chain; muMR1, murine MR1; Agly, aglycosyl.

Furthermore, *in vivo* studies have confirmed the reduction in effector function of the aglycosyl Abs (22–24). Importantly, it has also been shown that removal of glycans has little deleterious effect on other functional properties of Abs such as serum half-life and Ag binding activity (17, 19, 21, 25, 26).

We report that the mechanism underlying protection against EAE by anti-CD154 mAbs does not appear to involve long-term unresponsiveness or an active suppressor mechanism in this particular model. We also show that FcR interactions of the mAb do not play a major role with respect to clinical efficacy of anti-CD154 in EAE.

## Materials and Methods

### Preparation of mAbs

The variable domains of the heavy (H) chain and light (L) chain of the hamster anti-mouse CD154 mAb (MR1) were cloned by RT-PCR from total RNA from the hybridoma. Expression vectors for hamster/mouse chimeric mAb were constructed by engineering murine IgG2a or murine  $\kappa$  constant region cDNAs (derived from full-length cDNA clones of the H chain and L chain from the anti-human CD154 mAb 5c8) onto the variable domains of the H chain or L chain, respectively, using standard recombinant DNA techniques. Transiently expressed chimeric MR1 mAb, designated muMR1, was demonstrated to recapitulate the CD154 binding properties of the hamster mAb by flow cytometry and immunoprecipitation. The aglycosyl chimeric MR1, designated agly muMR1, was constructed by site-directed mutagenesis of the H chain to change the asparagine residue N297 (Kabat nomenclature (38)) in the Fc *N*-linked glycosylation site to a glutamine residue. Stable expression vectors containing CMV-immediate early (IE) promoter-driven tandem transcription cassettes for the Ig L chain and H chain and a glutamine synthetase gene as a selectable marker were constructed for both murine MR1 (muMR1) and agly muMR1 IgG2a and  $\kappa$  mAbs. The expression vectors were transfected into NSO cells and stable clones were isolated by selection in glutamine-free medium.

muMR1 and agly muMR1 were affinity-purified from bioreactor cell supernatants on protein A-Sepharose followed by size exclusion chromatography on Sephacryl 300 to remove aggregates. Chromatography resins were purchased from Amersham Pharmacia Biotech (Piscataway, NJ). The mAbs were shown to be >95% pure by SDS-PAGE, and endotoxin analysis ensured safeness of these reagents for *in vivo* use. The murine IgG2a isotype control mAb, P1.17 (American Type Culture Collection no. TIB-10) was protein A-purified from ascites at Protos Immunoresearch (Burlingame, CA) under contract by Biogen (Cambridge, MA).

### Characterization of chimeric mAbs

As summarized in Table I, separate studies demonstrated that muMR1 and agly muMR1 have the same relative affinity for cell surface murine CD154 based on a competitive binding assay *in vitro* and the same pharmacokinetic half-life *in vivo*. Agly muMR1 does not bind to murine Fc $\gamma$ R<sup>1</sup> cells at concentrations as high as 400  $\mu$ g/ml whereas the EC<sub>50</sub> for muMR1 was 10  $\mu$ g/ml in this assay, and agly muMR1 had a 2-fold decreased binding capacity for human C1q.<sup>3</sup> Although murine C1q was not available for comparable binding studies in our hands, this reduction in C1q binding activity in an aglycosylated mouse IgG2a mAb is consistent with that previously reported (18).

### Induction of EAE and treatment with anti-CD154

Female SJL mice (10–12 wk of age; Harlan Breeders, Gannat, France) were immunized s.c. with 50  $\mu$ g of PLP<sub>139–151</sub> emulsified in IFA supplemented with 1 mg/ml *Mycobacterium tuberculosis* H37 Ra (Difco, Detroit, MI). Three days later, mice were injected i.v. with 10<sup>9</sup> heat-killed *Bordetella pertussis* organisms (Rijksinstituut voor Volksgezondheid en Milieu, Bilthoven, The Netherlands). Development of EAE was monitored by daily assessment of bodyweight and a disability score. This score ranges from 0: no symptoms, 0.5: partial loss of tail tonus, 1: complete loss of tail tonus, 2: limb weakness, 2.5: partial paresis, 3: complete paralysis of hind limbs, 3.5: complete paralysis from diaphragm and hind limbs, incontinence, 4: moribund, to 5: death due to EAE.

Table I. Characterization of chimeric MR1 mAbs

	muMR1	Agly muMR1
CD154 binding <sup>a</sup> (IC <sub>50</sub> )	0.77 $\mu$ g/ml	0.87 $\mu$ g/ml
Half-life <sup>b</sup>	8.5 d	8.5 d
Fc $\gamma$ R binding <sup>c</sup> (EC <sub>50</sub> )	10 $\mu$ g/ml	No binding at 400 $\mu$ g/ml
C1q binding <sup>d</sup> (relative)	1	0.5

<sup>a</sup> The chimeric mAbs compete with hamster MR1 for binding to murine CD154<sup>+</sup> cells in FACS assay.

<sup>b</sup> The chimeric mAbs have the same half-life in BALB/c mice after a single 100  $\mu$ g dose.

<sup>c</sup> Glycosylated muMR1 binds to murine FcR<sup>1</sup> cells whereas the aglycosyl form does not.

<sup>d</sup> Agly muMR1 has decreased human C1q binding ability compared with the glycosylated form.

Mice were treated (i.p.) on day 0, 2, and 4 with 200  $\mu$ g (or less where indicated) of muMR1, agly muMR1, or the murine IgG2a isotype control P1.17. Where indicated mice were re-immunized on day 80 with 50  $\mu$ g of PLP<sub>139–151</sub> emulsified in complete H37 Ra adjuvant.

In one experiment spleen cells were collected 7 days after treatment with these three dosages of 200  $\mu$ g of the Abs (two mice per Ab), in conjunction with immunization with 50  $\mu$ g of PLP<sub>139–151</sub> emulsified in complete H37 Ra adjuvant (no *B. pertussis*). After lysing the erythrocytes spleen cells were injected i.v. (20  $\times$  10<sup>6</sup> cells/recipient), 1 day before active EAE induction with 50  $\mu$ g of PLP<sub>139–151</sub> emulsified in complete H37 Ra adjuvant, followed by i.v. injection of *B. pertussis* 3 days later.

All of these studies were performed with the approval of the Animal Ethical Committee and in compliance with Dutch governmental regulations on Animal Experimentation. This approval has been filed in the protocol numbers DEC 803 and DEC 1257.

### Histology

Brain tissue and spinal cord of each individual mouse was fixed in 10% formalin and embedded in paraffin. From each individual mouse three spinal cord sections (4  $\mu$ m) and six sections of cerebellum separated by 100  $\mu$ m were stained with hematoxylin. The area of each section was measured by morphometry and the number of infiltrating mononuclear cells per section was counted. For each individual mouse the mean number of infiltrating cells per square millimeter tissue was determined. Results are expressed as group means.

### Lymphocyte culture

Lymph node cells were isolated from inguinal, axillary and brachial lymph nodes. Cells were suspended in RPMI 1640 containing 100 U/ml penicillin, 100  $\mu$ g/ml streptomycin, 50  $\mu$ M 2-ME, 2 mM L-glutamine, and 5% FCS (Life Technologies, Gaithersburg, MD). Lymph node cells (3  $\times$  10<sup>5</sup> per well) were cultured (four replicate-wells per culture condition) in 200  $\mu$ l in 96-well flat-bottom microtiter plates (Costar, Cambridge, MA) and stimulated with 0, 3, 10, or 30  $\mu$ g/ml PLP<sub>139–151</sub>. Replicate plates were incubated to enable kinetics of proliferation. Cells were labeled on day 3, 4, and 5 with 0.5  $\mu$ Ci [<sup>3</sup>H]-labeled TdR (2 Ci/mmol; Radiochemical Center, Amersham, Buckinghamshire, U.K.) for 6 h and harvested onto glass fiber filters. Incorporated label was counted using a Wallac Trilux 1450 Microbeta liquid scintillation counter (PerkinElmer Life Science, Turku, Finland).

### Antibodies

Sera of individual mice were collected on day 58. PLP<sub>139–151</sub>-specific IgG1, IgG2a, and IgG2b were measured as previously described (27). Pooled serum from mice with EAE was used as an external standard, defined as containing 10,000 arbitrary units of peptide-specific IgG subclass Ab per milliliter. Results are expressed as arbitrary units per milliliter. Ab levels in sera of unimmunized mice are below the detection limit of the assay.

### Statistical analysis

Results of multiple group comparisons were analyzed by one-way ANOVA, followed by posthoc analysis using the Fisher least significant difference (LSD) test. *p* values <0.05 were regarded significant. Where indicated the Mann-Whitney *U* test was applied to compare muMR1 and agly muMR1 with the isotype control P1.17 at a 3  $\times$  200  $\mu$ g dosage.

<sup>3</sup> J. Ferrant, C. Benjamin, A. Cutler, S. Kalled, Y.-M. Hsu, E. Garber, D. Hess, R. Shapiro, N. Kenyon, D. Harlan, et al. The contribution of Fc effector mechanisms in the efficacy of anti-CD154 immunotherapy depends on the nature of the immune challenge. Submitted for publication.

**Results**

*Influence of glycosylation of anti-CD154 on its ability to inhibit EAE*

Previous studies have demonstrated that anti-CD154 is very effective in the suppression of EAE. However, it is as yet unclear to what extent this inhibitory effect is mediated by mechanisms that are dependent on its Fc region, such as depletion of target cells via complement activation or Ab-dependent cell-mediated cytotoxicity. Because Fc effector functions are highly dependent on glycosylation of the Ab CH2 domain (22–24) an aglycosyl form of anti-CD154 mAb was engineered to address this issue. In a separate study it is shown that the aglycosyl form of a murinized anti-CD154 Ab (agly muMR1) has CD154 binding activity in vitro and a pharmacokinetic profile in vivo that are comparable with that of its glycosylated counterpart.<sup>3</sup> However, agly muMR1 is heavily impaired in terms of FcR binding and its ability to bind human C1q is 2-fold decreased (summarized in Table I). We compared muMR1 with its aglycosyl form with respect to their ability to inhibit the development of EAE in SJL mice induced by immunization (day 0) with 50 µg of PLP<sub>139–151</sub> emulsified in complete H37 Ra adjuvant. On days 0, 2, and 4 mice were treated with muMR1, agly muMR1, or isotype control Ab P1.17.

As shown in Fig. 1, both forms of anti-CD154 mAb were effective in inhibiting clinical signs of EAE during the entire follow-up period, when administered as three dosages of 200 µg. This result was evident from the mean cumulative EAE score (as indicated by *p* values in Fig. 1) and from the mean maximal EAE score (*p* < 0.0005 for both groups as compared with P1.17-treated mice; data not shown). In this respect the Abs were comparable with hamster MRI (data not shown).

Administration of lower dosages of these Abs resulted in less inhibition of disease as measured by the cumulative EAE score (Fig. 1). Although muMR1 appears to be slightly more effective than agly muMR1 at three dosages of 75 µg, all groups had a significantly lower maximal EAE score (all groups *p* < 0.0005 as compared with P1.17 with the exception of 3 × 25 µg muMR1, *p* < 0.05; data not shown). Therefore, these experiments did not

reveal major differences between the Abs with respect to their ability to inhibit EAE.

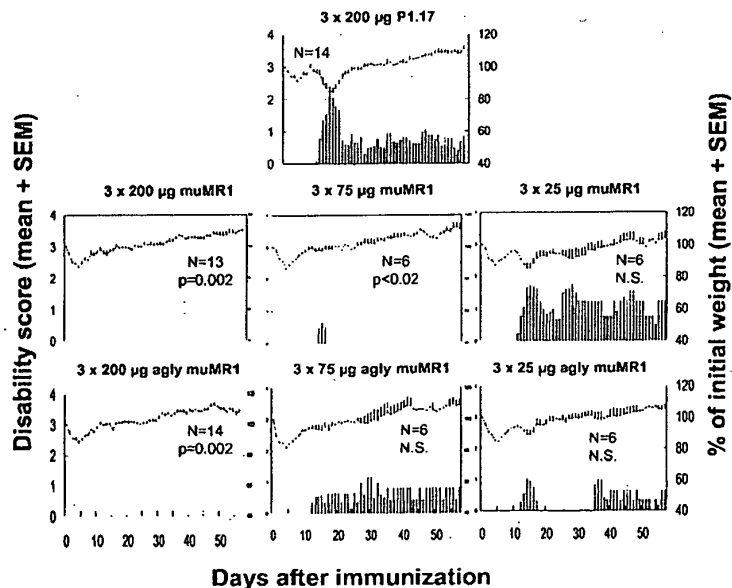
To assess whether the Abs differed in inhibiting the development of inflammatory infiltrates within the CNS, mice treated with different amounts of Ab were sacrificed on day 16, i.e., at the peak of disease activity in mice treated with the isotype control Ab. Cerebellum and spinal cord representing the major sites of inflammation were analyzed with regard to the number of infiltrating mononuclear cells. Our historical data show that mononuclear cell infiltrates are not detectable in the CNS 18 or 60 days after immunization with a non-encephalitogenic peptide (data not shown).

The results are shown in Fig. 2. We observed a dose-dependent decrease in infiltrates in mice treated with muMR1 or agly muMR1 and sacrificed on day 16, although simultaneous analysis of all groups by ANOVA did not indicate significant differences at this time point. However, a less stringent analysis comparing only the 3 × 200 µg groups by the Mann-Whitney *U* test revealed significantly less infiltrates in the cerebellum and the spinal cord for the highest dosage of either form of anti-CD154 as compared with P1.17, indicating that at this dosage both Abs inhibit infiltration. No significant differences were observed between the two anti-CD154 Abs with regard to their ability to suppress the development of inflammatory infiltrates within the CNS.

In addition, we evaluated the CNS tissues from 6 (low and intermediate dosages) to 14 mice (high dosage and controls) per group at the endpoint of this study (day 58). The majority of mice treated with P1.17 still had high numbers of inflammatory cells in cerebellum, whereas these numbers were 15-fold lower in spinal cord as compared with day 16. Mice treated with muMR1 or agly muMR1 revealed significantly less infiltrates in their cerebellum than P1.17 treated mice; the only difference between the two forms of anti-CD154 was found at a dosage of 3 × 25 µg in which muMR1 was not effective.

Thus, anti-CD154 has a slightly inhibitory effect on the infiltration of the CNS by mononuclear cells at day 16, apparently sufficient to inhibit clinical symptoms, and this is independent of glycosylation of its Fc part. Anti-CD154 inhibits mononuclear

**FIGURE 1.** Glycosylation is not essential for the inhibitory effect of anti-CD154 in EAE. Female SJL mice were subjected to EAE induction by immunization (s.c.) with 50 µg of PLP<sub>139–151</sub> in complete H37 Ra adjuvant (day 0). Mice received three injections (i.p.) of isotype control Ab P1.17, muMR1, or agly muMR1. Group size (*N*) and amount of Ab are indicated. Results show the development of disease in time in terms of mean disability and mean percentage of initial bodyweight. The cumulative scores (area under the curve) of each individual mouse was determined and included in statistical evaluation (ANOVA and posthoc LSD) of the data as compared with P1.17 treated mice. Values of *p* for the cumulative score are indicated. N.S., Not significant.



Downloaded from http://www.jimmunol.org/ at Incyte Corp on December 10, 2013

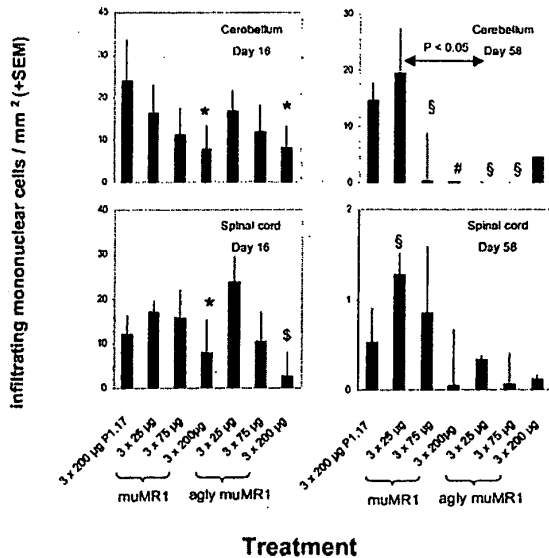


**FIGURE 2.** Glycosylation of anti-CD154 is not required for inhibition of CNS infiltration in EAE. Mice subjected to EAE induction with or without Ab treatment were sacrificed on day 16 ( $n = 11$ , left panels) or day 58 ( $n = 6-11$ , right panels). Cerebellum and spinal cord were evaluated with regard to the number of inflammatory cells, and statistical analysis was performed as described in *Materials and Methods*. Mann-Whitney  $U$  test: \*,  $p < 0.05$  and \$,  $p < 0.01$  as compared with P1.17-treated mice at day 16. ANOVA and posthoc LSD: \$,  $p = 0.05-0.1$  and #,  $p < 0.05$ , as compared with P1.17-treated mice at day 58. The arrow indicates a significant difference between muMR1 and agly muMR1 at a dosage of  $3 \times 25 \mu\text{g}$ .

infiltration significantly at day 58, and this effect is also independent of glycosylation of its Fc part. The significant, albeit weak effect of anti-CD154 mAbs at the early time point and significant effect at the later time point is consistent with previously published studies (7) showing that anti-CD154 does not eliminate early T cell entry into the CNS but rather inhibits retention/expansion of these cells within the target organ.

Altogether we conclude that FcR-mediated mechanisms do not play a major role in the inhibition of EAE by anti-CD154, although we cannot rule out a role for residual C1q binding.

#### *Effect of anti-CD154 treatment on peptide-specific T cell and B cell responses*

To further investigate whether there was subclinical activity in mice treated with muMR1 and agly muMR1 in the absence of signs of EAE, the activation state of their T cells was evaluated. Sixteen days after immunization, i.e., shortly after treatment with the Abs, we did not observe an effect of Ab treatment on T cell proliferation. As shown in Fig. 3A, lymph node cells from mice treated with  $3 \times 200 \mu\text{g}$  of muMR1 or agly muMR1 were comparable with lymph node cells from P1.17-treated mice regarding their ability to proliferate in response to PLP<sub>139-151</sub>. Also lower dosages of the Abs did not reveal significant differences (data not shown). When T cell proliferation was studied 60 days after immunization lymph node cells isolated from muMR1 or agly muMR1 treated mice showed significantly decreased T cell responses as compared with cells from P1.17 treated mice (Fig. 3B). The two forms of anti-CD154 did, however, not differ in their ability to inhibit peptide-specific T cell proliferation. In two other

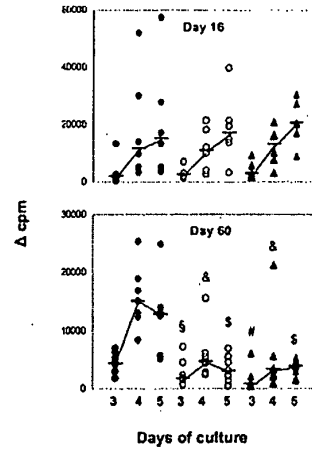


**FIGURE 3.** Effect of anti-CD154 on PLP<sub>139-151</sub> specific T cell proliferation. Lymph node cells from mice subjected to EAE induction and anti-CD154 treatment were collected 16 or 60 days after immunization. Cells derived from mice treated with  $3 \times 200 \mu\text{g}$  control Ab P1.17 (●), muMR1 (○), or agly muMR1 (▲) were stimulated with  $30 \mu\text{g/ml}$  PLP<sub>139-151</sub> as described in *Materials and Methods*. Proliferation was assessed after 3, 4, and 5 days of culture by [<sup>3</sup>H]thymidine incorporation. Symbols represent the response of individual mice; results are expressed as  $\Delta\text{cpm}$  obtained by subtraction of background proliferation. Statistical analysis was performed by ANOVA, followed by posthoc LSD: \$,  $p < 0.05$ ; #,  $p < 0.005$ ; &,  $p < 0.0001$ ; \$,  $p < 0.000001$ .

independent experiments, using group-wise pooled lymph node cells collected on day 58, one indicated that agly muMR1 may be less effective in suppression of T cell proliferation; these experiments also showed that the decreased ability of lymphocytes from anti-CD154 treated mice to proliferate was reflected by a decreased secretion of IFN- $\gamma$ , without evidence for an up-regulation of IL-4 or IL-10 (data not shown).

Our observations are in line with previous studies by Howard et al. (6, 7) who found that CD40-CD154 blockade does not affect early expansion of T cells but rather the development of Th1 effector cells, without the preferential expansion of Th2 cells.

This was further substantiated by the assessment of the subclass of PLP<sub>139-151</sub>-specific Abs in serum (Fig. 4). PLP<sub>139-151</sub>-specific Abs were undetectable in sera of nonimmunized mice (data not shown). Mice that had been treated with three dosages of  $200 \mu\text{g}$  muMR1 or agly muMR1 did not differ from P1.17 treated mice with regard to peptide-specific IgG1 Abs. However, both forms of anti-CD154 mAb resulted in lower levels of peptide-specific IgG2b. Whereas muMR1 treated mice showed a decrease in IgG2a Abs ( $p < 0.0001$ ), mice treated with three dosages of  $200 \mu\text{g}$  agly muMR1 showed only a trend toward a significant decrease ( $p = 0.098$ ). The lower dosages ( $3 \times 75 \mu\text{g}$  or  $3 \times 25 \mu\text{g}$ ) of either muMR1 or agly muMR1 were ineffective in the inhibition of these Ab responses (data not shown). These data further support the hypothesis that anti-CD154 mAb treatment suppresses the development of Th1 responses without the concomitant up-regulation of a Th2 response and indicate that possibly the aglycosyl form of the mAb is slightly less effective in inhibiting immune reactivity than the glycosylated anti-CD154 in EAE.

#### *No demonstrable long-term unresponsiveness or active suppression by anti-CD154 mAb treatment in EAE*

The efficacy of agly muMR1 in EAE demonstrates that FcR interactions do not play a major role in the inhibition by anti-CD154 in

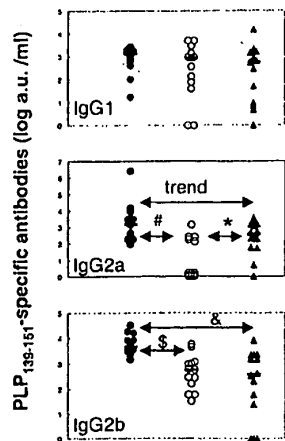


**FIGURE 4.** Anti-CD154 treatment inhibits the development of PLP<sub>139-151</sub>-specific IgG2a and IgG2b Abs. Mice received three injections (i.p.) of 200  $\mu$ g isotype control Ab P1.17 (●), muMRI (○), or agly muMRI (▲). PLP<sub>139-151</sub>-specific Abs present in sera collected on day 58 were assayed as described in *Materials and Methods*. Results are expressed as arbitrary units per milliliter. ANOVA was followed by posthoc LSD test: \*,  $p < 0.01$ ; \$,  $p < 0.001$ ; #,  $p < 0.0001$ ; and &,  $p < 0.00001$ .

this context. Anti-CD154 mAb treatment has been suggested to inhibit the rejection of an allogeneic transplant by the induction of regulatory T cells (13, 14) and at least one study indicated that CD154 blockade was sufficient (28). To investigate whether anti-CD154 inhibits EAE via the induction of an active suppressor mechanism, we assessed whether mice treated with muMRI or agly muMRI on days 0, 2, and 4 after EAE induction display a long-lasting resistance to disease. To ensure that levels of circulating Ab would be low enough and not further capable of mediating a direct inhibitory effect, mice were not re-immunized until 80 days after the first immunization and Ab treatments.

As can be concluded from Fig. 5, mice treated with muMRI or agly muMRI did not develop symptoms of disease after primary peptide immunization in contrast with mice treated with the isotype control P1.17. The muMRI or agly muMRI treated animals also did not develop clinical symptoms during the follow-up period of 80 days (data not shown). When mice were re-immunized with PLP<sub>139-151</sub> emulsified in complete H37 Ra adjuvant there was an increased severity of clinical symptoms in P1.17 treated animals. Mice that had been treated on days 0, 2, and 4 with either of the anti-CD154 forms developed EAE after rechallenge with a severity that was less than observed after reimmunization of P1.17 treated mice, though comparable with the first phase of EAE in P1.17-treated mice and to that normally found after EAE induction in untreated mice (data not shown). We therefore conclude that anti-CD154 mAb treatment did not result in complete or long-lasting unresponsiveness in this model system.

We also studied whether the transfer of  $20 \times 10^6$  spleen cells collected from mice, 1 wk after EAE induction and treatment with muMRI or agly muMRI, would render naive recipient mice resistant to subsequent active EAE induction. As shown in Fig. 5, neither spleen cells from muMRI-treated mice nor spleen cells from agly muMRI-treated mice were capable of transferring resistance against EAE. Therefore, we did not obtain evidence for an active suppression mechanism in this particular experimental setting.

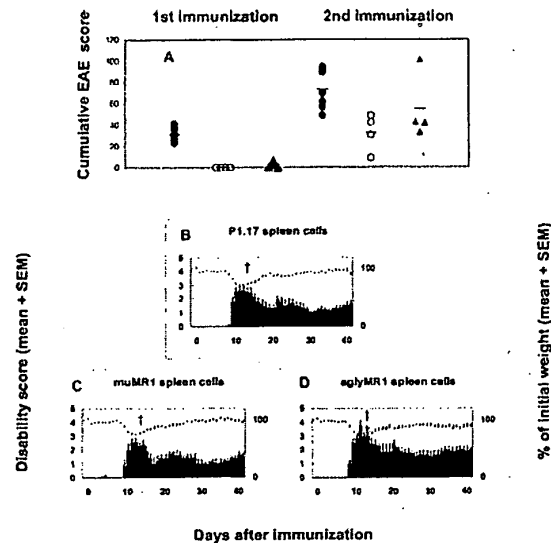


**FIGURE 5.** No demonstrable long-term unresponsiveness or active suppression of EAE by anti-CD154 mAb. *A*, No long-term protection to EAE by anti-CD154 treatment. Female SJL mice were subjected to EAE induction by immunization (s.c.) with 50  $\mu$ g of PLP<sub>139-151</sub> in complete H37 Ra adjuvant (day 0). Mice received three injections (i.p.) of 200  $\mu$ g isotype control Ab P1.17 (●,  $n = 8$ ), muMRI (○,  $n = 4$ ), or agly muMRI (▲,  $n = 4$ ). On day 80 EAE induction was repeated. The cumulative EAE score of each individual mouse, assessed during the first 31 days after each immunization is shown. *B-D*, Spleen cells from anti-CD154-treated mice do not transfer protection to EAE. Recipient mice ( $n = 6$  per group) were treated (i.v.) with  $20 \times 10^6$  spleen cells from donor mice, 1 day before active EAE induction. Donor spleen cells were isolated on day 7 from mice ( $n = 2$  per group) that had received three injections (i.p.) of 200  $\mu$ g isotype control Ab P1.17 (*B*), muMRI (*C*), or agly muMRI (*D*) on days 0, 2, and 4 after immunization with 50  $\mu$ g of PLP<sub>139-151</sub> in complete H37 Ra adjuvant (day 0). Each dagger marks a mouse that died as a consequence of EAE.

## Discussion

Previous studies have demonstrated that treatment with anti-CD154 mAb inhibits induction (5) and progression (6) of EAE and pointed to reduced T cell priming, Th1 differentiation or reactivation of previously activated T cells, preventing the development of Th1 effector cells (6, 7). However, it is unclear whether the inhibitory activities of the mAb in this disease context are dependent on Fc effector mechanisms, i.e., complement-mediated lysis, or FcR-dependent mechanisms such as Ab-dependent cytotoxicity, Fc/FcR-dependent distribution of the Ab to critical sites of immune activation, or scaffolding of the mAb by FcR thereby potentially increasing its avidity for CD154. In this report, we used a novel tool, an aglycosyl version of anti-CD154 mAb, to address the contribution of Fc function to the inhibitory activity of anti-CD154 mAb in murine EAE. We demonstrate for the first time that the mechanism of protection against clinical EAE is not dependent on FcR-mediated functions of the mAb, although anti-CD154-mediated effects on subclinical immune activity may be partly dependent on Fc interactions.

The role of the CD154 pathway in EAE, has previously been independently demonstrated by resistance of CD154 knockout and CD40 knockout mice to disease (29). These studies indicate that the lack of CD154-CD40 interactions is sufficient for protection, and suggest that mAb blocking of CD154-CD40 may be adequate for its therapeutic effects. However, the mechanism(s) whereby



Abs mediate therapeutic effects may be highly complex and involve secondary Fc-dependent mechanisms. For example, in transplant settings, partial or complete engraftment has been obtained in CD154 and CD40 knockout mice (30–34). However, a dependence on complement for mAb efficacy was recently demonstrated in an islet transplant model (15). In addition, there are other reports showing that treatment with an anti-CD154 mAb results in a better reduction in immune response than that found in the knockout mice (35, 36). In these instances, there must be additional activity of the mAb beyond CD154/CD40 blockade.

To obtain insight into the role of such mechanisms in the inhibitory effect of anti-CD154 on EAE we compared the efficacy of a murinized form of MR1 with its agly counterpart. As shown in this study these Abs did not show major differences with regard to their efficacy to inhibit clinical signs of EAE. However, we obtained evidence that the aglycosyl form may be less able to suppress PLP<sub>139–151</sub>-related immune reactivity in this model system. Although T cell PLP-reactivity at day 58 was comparably inhibited by muMR1 and agly muMR1 in two independent experiments, the inhibitory activity of agly muMR1 was somewhat reduced in one other; in addition, agly muMR1 was less effective in suppressing the development of PLP<sub>139–151</sub>-specific IgG2a Ab. In contrast, the 3 × 25 μg dosage agly muMR1 was actually more effective than muMR1 in limiting cerebellar inflammation at day 58. Thus, the glycosylated form may have an additional mechanism of action that enables it to limit the generation of peripheral T cell responses. Because our data also show that the anti-CD154 mAb treated mice are not protected from disease upon rechallenge, the glycosylated form of the mAb does not appear to significantly deplete peptide-specific T cells in this system. We speculate that Fc/FcR interactions of the mAb contribute to its blocking activity by altering its distribution or increasing its avidity for CD154 *in vivo*.

Interestingly, a study using an agly mutant of a humanized anti-CD154 mAb in non-human primates showed that it could inhibit the humoral immune response and was comparable in this respect with the glycosyl form, but had decreased efficacy in allograft rejection in cynomolgus monkeys.<sup>3</sup> Thus the contribution of Fc interactions in anti-CD154-mediated efficacy depends on the nature or magnitude of the immune response. Possibly, the use of CFA, which is required for the induction of EAE and the concomitant production of IL-12, is responsible for the somewhat diminished efficacy of agly muMR1 in the EAE setting. Thus our data substantiate the notion that the importance of Fc effector function for immune inhibition is dependent on the type of immune challenge.

Apart from the inhibition of T cell reactivity, anti-CD154 treatment might result in the development of a tolerizing or active suppressive mechanism. Although anti-CD154 treatment was associated with prolonged graft survival we did not obtain evidence that anti-CD154 treatment during EAE-induction resulted into long-term protection to EAE. In anti-CD154 treated mice the severity of EAE after re-immunization was comparable with the disease activity during first phase in P1.17-treated mice (or untreated mice, data not shown) and the increase in disease activity during the second phase in P1.17-treated mice. Also spleen cells isolated on day 7 after anti-CD154 treatment and EAE induction did not protect naive recipients from subsequent EAE induction. In a study by Howard et al. (37), T cells from anti-CD154-treated animals were shown to have retained their encephalitogenic capacity inasmuch as they aggravated EAE when cotransferred with suboptimal numbers of encephalitogenic Th1 blasts. These and our data do not provide support for the possibility that anti-CD154 treatment of EAE is associated with an active suppressor mechanism. At this stage the reason for the discrepancy between observations in the

transplantation models wherein anti-CD154 induces long-term graft acceptance, possibly through T regulatory activity, and in the EAE model in which it did not induce long-term unresponsiveness or active suppression, are uncertain. In the transplantation models alloantigen is present for a prolonged period of time and when these are recognized when other inflammatory signals have subsided, lack of appropriate costimulation may favor expansion of regulatory T cells and active suppression. In the EAE model described, it is likely that the encephalitogenic peptide will eventually disappear and with it a stimulus for regulatory T cells. Conversely, it should be taken into account that EAE induction occurred by immunization of the peptide in an emulsion with complete adjuvant, containing *M. tuberculosis* and by additional administration of heat-killed *B. pertussis* bacteria. Indeed, we have demonstrated that *B. pertussis* or pertussis toxin can abrogate tolerance induction in a setting in which tolerance to EAE (i.e., resistance to active induction of disease) is induced by immunization with a mannosylated form of the encephalitogenic peptide.<sup>4</sup> Most likely, in the classical EAE model T cell recognition occurs in the presence of costimulatory signals and in the context of ligation of Toll-like receptors. Therefore, additional studies are required to address the role of regulatory T cells in anti-CD154-mediated suppression of experimental autoimmune models that do not require strong adjuvants.

Anti-CD154 mAb is a promising tool in the treatment of a variety of immunological disorders. Understanding their mechanism of action is key to the development and optimization of safe and effective therapeutic candidates. Thromboembolic complications that occurred during the course of anti-CD154 human 5c8 clinical studies remain unexplained but could be related to FcR interactions. Our studies show that mice treated with agly MRI may develop some subclinical immune reactivity; however, this reactivity is insufficient to allow for the development of EAE. Thus the efficacy profile of the agly form of anti-CD154 mAb may be beneficial for dampening the T cell reactivity that is heightened in immune disorders without completely abrogating protective responses of the host to infectious agents.

### Acknowledgments

We acknowledge Renee Shapiro and Konrad Miatkowski of Biogen (Cambridge, MA) for excellent technical assistance.

### References

- Grewal, I.S., and R. A. Flavell. 1998. CD40 and CD154 in cell-mediated immunity. *Annu. Rev. Immunol.* 16:111.
- Stuber, E., W. Strober, and M. Neurath. 1996. Blocking the CD154-CD40 interaction *in vivo* specifically prevents the priming of T helper 1 cells through the inhibition of interleukin 12 secretion. *J. Exp. Med.* 183:693.
- Howland, K. C., L. J. Ausubel, C. A. London, and A. K. Abbas. 2000. The roles of CD28 and CD40 ligand in T cell activation and tolerance. *J. Immunol.* 164:4465.
- Koch, F., U. Stanzl, P. Jennewein, K. Janke, C. Heufler, E. Kampgen, N. Romani, and G. Schuler. 1996. High level IL-12 production by murine dendritic cells: upregulation via MHC class II and CD40 molecules and downregulation by IL-4 and IL-10. *J. Exp. Med.* 184:741.
- Gerritse, K., J. D. Laman, R. J. Noelle, A. Aruffo, J. A. Ledbetter, W. J. Boersma, and E. Claassen. 1996. CD40-CD40 ligand interactions in experimental allergic encephalomyelitis and multiple sclerosis. *Proc. Natl. Acad. Sci. USA* 93:2499.
- Howard, L. M., A. J. Miga, C. L. Vanderlugt, M. C. Dal Canto, J. D. Laman, R. J. Noelle, and S. D. Miller. 1999. Mechanisms of immunotherapeutic intervention by anti-CD154 (CD154) antibody in an animal model of multiple sclerosis. *J. Clin. Invest.* 103:281.
- Howard, L. M., and S. D. Miller. 2001. Autoimmune intervention by CD154 blockade prevents T cell retention and effector function in the target organ. *J. Immunol.* 166:1547.

<sup>4</sup> M. Luca, J. Kel, W. van Rijs, J.-W. Drijfhout, F. Koning and L. Nagelkerken. Mannosylated self-peptide induces tolerance to experimental autoimmune encephalomyelitis. *Submitted for publication.*

8. Becher, B., M. Blain, and J. P. Antel. 2000. CD40 engagement stimulates IL-12 p70 production by human microglial cells: basis for Th1 polarization in the CNS. *J. Neuroimmunol.* 102:44.
9. Becher, B., B. G. Durell, A. V. Miga, W. F. Hickey, and R. J. Noelle. 2001. The clinical course of experimental autoimmune encephalomyelitis and inflammation is controlled by the expression of CD40 within the central nervous system. *J. Exp. Med.* 193:967.
10. Mendel, I., and E. M. Shevach. 2002. Differentiated Th1 autoreactive effector cells can induce experimental autoimmune encephalomyelitis in the absence of IL-12 and CD40/CD154 interactions. *J. Neuroimmunol.* 122:63.
11. Honey, K., S. P. Cobbold, and H. Waldmann. 1999. CD40 ligand blockade induces CD4<sup>+</sup> T cell tolerance and linked suppression. *J. Immunol.* 163:4805.
12. Kirk, A. D., L. C. Burkly, D. S. Batty, R. E. Baumgartner, J. D. Berning, K. Buchanan, J. H. Fechner, R. L. Germond, R. L. Kampen, N. B. Patterson, et al. 1999. Treatment with humanized monoclonal antibody against CD154 prevents acute renal allograft rejection in nonhuman primates. *Nat. Med.* 5:686.
13. Taylor, P. A., T. M. Friedman, R. Korngold, R. J. Noelle, and B. R. Blazar. 2002. Tolerance induction of alloreactive T cells via ex vivo blockade of the CD40:CD154 costimulatory pathway results in the generation of a potent immune regulatory cell. *Blood* 99:4601.
14. Graca, L., K. Honey, E. Adams, S. P. Cobbold, and H. Waldmann. 2000. Anti-CD154 therapeutic antibodies induce infectious transplantation tolerance. *J. Immunol.* 165:4783.
15. Sanchez-Fueyo, A., C. Domenig, T. B. Strom, and X. X. Zheng. 2002. The complement dependent cytotoxicity (CDC) immune effector mechanism contributes to anti-CD154 induced immunosuppression. *Transplantation* 74:898.
16. Monk, N. J., R. E. G. Hargreaves, J. E. Marsh, C. A. Farrar, S. H. Sacks, M. Millrain, E. Simpson, J. Dyson, and S. Jurcevic. 2003. Fe-dependent depletion of activated T cells occurs through CD40L-specific antibody rather than costimulation blockade. *Nat. Med.* 9:1275.
17. Nose, M., and H. Wigzell. 1983. Biological significance of carbohydrate chains on monoclonal antibodies. *Proc. Natl. Acad. Sci. USA* 80:6632.
18. Leatherbarrow, R. J., T. W. Rademacher, R. A. Dwek, J. M. Woof, A. Clark, D. R. Burton, N. Richardson, and A. Feinstein. 1985. Effector functions of a monoclonal aglycosylated mouse IgG2a: binding and activation of complement component C1 and interaction with human monocyte Fc receptor. *Mol. Immunol.* 22:407.
19. Tao, M. H., and S. L. Morrison. 1989. Studies of aglycosylated chimeric mouse-human IgG: role of carbohydrate in the structure and effector functions mediated by the human IgG constant region. *J. Immunol.* 143:2595.
20. Lund, J., T. Tanaka, N. Takahashi, G. Sarmay, Y. Arata, and R. Jefferis. 1990. A protein structural change in aglycosylated IgG3 correlates with loss of huFcγRI and huFcγRIII binding and/or activation. *Mol. Immunol.* 27:1143.
21. Dorai, H., B. M. Mueller, R. A. Reisfeld, and S. D. Gillies. 1991. Aglycosylated chimeric mouse/human IgG1 antibody retains some effector function. *Hybridoma* 10:211.
22. Isaacs, J. D., M. R. Clark, J. Greenwood, and H. Waldmann. 1992. Therapy with monoclonal antibodies: an in vivo model for the assessment of therapeutic potential. *J. Immunol.* 148:3062.
23. Friend, P. J., G. Hale, L. Chatenoud, P. Rebello, J. Bradley, S. Thiru, J. M. Phillips, and H. Waldmann. 1999. Phase I study of an engineered aglycosylated humanized CD3 antibody in renal transplant rejection. *Transplantation* 68:1632.
24. Boyd, P. N., A. C. Lines, and A. K. Patel. 1995. The effect of the removal of sialic acid, galactose and total carbohydrate on the functional activity of Campath-1H. *Mol. Immunol.* 32:1311.
25. Hand, P. H., B. Calvo, D. Milenic, T. Yokota, M. Finch, P. Snoy, K. Garmestani, O. Gansow, J. Schlom, and S. V. Kashmiri. 1992. Comparative biological properties of a recombinant chimeric anti-carcinoma mAb and a recombinant aglycosylated variant. *Cancer Immunol. Immunother.* 35:165.
26. Hobbs, S. M., L. E. Jackson, J. Hoadley. 1992. Interaction of aglycosyl immunoglobulins with the IgG Fc transport receptor from neonatal rat gut: comparison of deglycosylation by tunicamycin treatment and genetic engineering. *Mol. Immunol.* 29:949.
27. Nagelkerken, L., B. Blauw, and B. M. Tielemans. 1997. IL-4 abrogates the inhibitory effect of IL-10 on the development of experimental allergic encephalomyelitis in SJL mice. *Int. Immunol.* 9:1243.
28. Jarvinen, L. Z., B. R. Blazar, O. A. Adeyi, T. B. Strom, and R. J. Noelle. 2003. CD154 on the surface of CD4<sup>+</sup>CD25<sup>+</sup> regulatory T cells contributes to skin transplant tolerance. *Transplantation* 76:1375.
29. Grewal, I. S., H. G. Foellmer, K. D. Grewal, J. Xu, F. Hardardottir, J. L. Baron, C. A. Janevay, and R. A. Flavell. 1996. Requirement for CD40 ligand in costimulation induction, T cell activation, and experimental allergic encephalomyelitis. *Science* 273:1864.
30. Shimizu, K., U. Schonbeck, F. Mach, P. Libby, and R. N. Mitchell. 2000. Host CD40 ligand deficiency induces long-term allograft survival and donor-specific tolerance in mouse cardiac transplantation but does not prevent graft arteriosclerosis. *J. Immunol.* 165:3506.
31. Kurtz, J., H. Ito, T. Wekerle, J. Shaffer, and M. Sykes. 2001. Mechanisms involved in the establishment of tolerance through costimulatory blockade and BMT: lack of requirement for CD40L-mediated signaling for tolerance or deletion of donor-reactive CD4<sup>+</sup> cells. *Am. J. Transplant.* 1:339.
32. Bingaman, A. W., J. Ha, M. M. Durham, S. Y. Waitze, C. Tucker-Burden, S. R. Cowan, T. C. Pearson, and C. P. Larsen. 2001. Analysis of the CD40 and CD28 pathways on alloimmune responses by CD4<sup>+</sup> T cells in vivo. *Transplantation* 72:1286.
33. Larsson, L. C., M. Corbascio, H. Widner, T. C. Pearson, C. P. Larsen, and H. Ekberg. 2002. Simultaneous inhibition of B7 and LFA-1 signaling prevents rejection of discordant neural xenografts in mice lacking CD154. *Xenotransplantation* 9:68.
34. Zhai, Y., X. D. Shen, F. Gao, A. J. Coito, B. A. Wasowska, A. Salama, I. Schmitt, R. W. Busuttil, M. H. Sayegh, and J. W. Kupiec-Weglinski. 2002. The CD154-CD40 T cell costimulation pathway is required for host sensitization of CD8<sup>+</sup> T cells by skin grafts via direct antigen presentation. *J. Immunol.* 169:1270.
35. Gorbachev, A. V., P. S. Heeger, and R. L. Fairchild. 2001. CD4<sup>+</sup> and CD8<sup>+</sup> T cell priming for contact hypersensitivity occurs independently of CD40-CD154 interactions. *J. Immunol.* 166:2323.
36. Taylor, P. A., C. J. Lees, H. Waldmann, R. J. Noelle, and B. R. Blazar. 2001. Requirements for the promotion of allogeneic engraftment by anti-CD154 (anti-CD40L) monoclonal antibody under nonmyeloablative conditions. *Blood* 98:467.
37. Howard, L. M., S. Ostrovidov, C. E. Smith, C. M. Dal Canto, and S. D. Miller. 2002. Normal Th1 development following long-term therapeutic blockade of CD154-CD40 in experimental autoimmune encephalomyelitis. *J. Clin. Invest.* 109:233.
38. Kabat, E. A., T. T. Wu, H. M. Perry, K. S. Gottesman, and C. Foeller. 1991. *Sequence of Proteins of Immunological Interest*, 3rd Ed., Vol. 1. National Institutes of Health, Bethesda.